

QA: QA

**Civilian Radioactive Waste Management System
Management and Operating Contractor**

**Integrated Site Model
Process Model Report**

TDR-NBS-GS-000002 REV 00

November 1999

Prepared for:

**U.S. Department of Energy
Yucca Mountain Site Characterization Office
P.O. Box 30307
North Las Vegas, Nevada 89036-0307**

Prepared by:

**TRW Environmental Safety Systems Inc.
1261 Town Center Drive
Las Vegas, Nevada 89144-6352**

**Under Contract Number
DE-AC08-91RW00134**

DISCLAIMER

This report was prepared as an account of work sponsored by an agency of the United States Government. Neither the United States Government nor any agency thereof, nor any of their employees, nor any of their contractors, subcontractors or their employees, makes any warranty, express or implied, or assumes any legal liability or responsibility for the accuracy, completeness, or any third party's use or the results of such use of any information, apparatus, product, or process disclosed, or represents that its use would not infringe privately owned rights. Reference herein to any specific commercial product, process, or service by trade name, trademark, manufacturer, or otherwise, does not necessarily constitute or imply its endorsement, recommendation, or favoring by the United States Government or any agency thereof or its contractors or subcontractors. The views and opinions of authors expressed herein do not necessarily state or reflect those of the United States Government or any agency thereof.

Civilian Radioactive Waste Management System
Management and Operating Contractor

Integrated Site Model
Process Model Report

TDR-NBS-GS-000002 REV 00

November 1999

Prepared by:



Thom Booth

11/18/99

Date

Checked by:

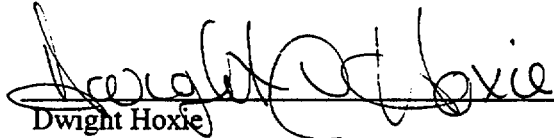


Gerald Nieder-Westermann

11/18/99

Date

Approved by:


Dwight Hoxie

11/18/99

Date

CONTENTS

	Page
ACRONYMS	xiii
1. INTRODUCTION	1-1
1.1 OBJECTIVES	1-1
1.1.1 Objectives of this Report	1-1
1.1.2 Purpose of the Model	1-2
1.2 SCOPE	1-2
1.3 QUALITY ASSURANCE	1-2
1.4 OVERVIEW OF THE INTEGRATED SITE MODEL AND ITS COMPONENT MODELS	1-2
1.4.1 Integrated Site Model	1-2
1.4.2 Geologic Framework Model	1-3
1.4.3 Rock Properties Model	1-7
1.4.4 Mineralogic Model	1-8
1.5 RELATIONSHIP TO OTHER PROCESS MODEL REPORTS AND PROJECT DOCUMENTS	1-8
2. EVOLUTION OF THE INTEGRATED SITE MODEL	2-1
2.1 PHILOSOPHY OF PMR DEVELOPMENT	2-1
2.2 INTEGRATED SITE MODEL DEVELOPMENT HISTORY	2-1
2.2.1 Geologic Framework Model	2-1
2.2.2 Rock Properties Model	2-2
2.2.3 Mineralogic Model	2-2
2.2.4 Integrated Site Model	2-3
3. INTEGRATED SITE MODEL	3-1
3.1 SUMMARY OF COMPONENT PARTS	3-1
3.2 GEOLOGIC FRAMEWORK MODEL	3-1
3.2.1 Introduction	3-1
3.2.2 Summary of Model Inputs and Model Software	3-1
3.2.3 Construction of the Model	3-3
3.2.4 Model Results	3-7
3.2.5 Model Uncertainties and Limitations	3-14
3.2.6 Alternative Interpretations	3-15
3.2.7 Model Validation	3-16
3.3 ROCK PROPERTIES MODEL	3-20
3.3.1 Introduction	3-20
3.3.2 Summary of Data Inputs and Model Software	3-20
3.3.3 Construction of the Model	3-21
3.3.4 Model Results	3-29
3.3.5 Model Uncertainties and Limitations	3-33
3.3.6 Alternative Interpretations	3-39
3.3.7 Model Validation	3-39

CONTENTS (Continued)

	Page
3.4 MINERALOGIC MODEL	3-40
3.4.1 Introduction.....	3-40
3.4.2 Summary of Data Inputs and Model Software	3-41
3.4.3 Construction of the Model	3-41
3.4.4 Model Results	3-45
3.4.5 Model Uncertainties and Limitations.....	3-50
3.4.6 Alternative Interpretations	3-50
3.4.7 Model Validation	3-50
4. RELATIONSHIP WITH THE NUCLEAR REGULATORY COMMISSION ISSUE RESOLUTION STATUS REPORTS.....	4-1
5. REFERENCES	5-1
5.1 DOCUMENTS CITED.....	5-1
5.2 CODES, STANDARDS, REGULATIONS, AND PROCEDURES.....	5-4

FIGURES

	Page
1-1. Interrelationships of Component Models, Integrated Site Model, and Downstream Uses.....	1F-1
1-2. Flow of Information From Data Collection Through the AMRs, PMRs, and TSPA and Into the Site Recommendation (SR) and Finally to the License Application (LA).....	1F-2
1-3. Area of Integrated Site Model, Showing Model Boundaries.....	1F-3
2-1. Locations of Boreholes, Exploratory Studies Facility, and Cross-Block Drift.....	2F-1
2-2. Surface Traces of Faults Modeled in GFM.....	2F-2
3-1. Locations of Measured Sections, Gravity Profiles, and Seismic Profiles.....	3F-1
3-2. Isochore Method.....	3F-2
3-3. Interpretive Constraints.....	3F-3
3-4. Locations of Post-Tiva Rock Units (Vertical View of GFM Model Area, as Defined in Figure 1-3).....	3F-4
3-5. Wedge of Post-Tiva Rocks in Solitario Canyon (View to North of Slice Through GFM).....	3F-5
3-6. Model-Isochore Map of Alluvium.....	3F-6
3-7. Model-Isochore Map of Tiva Canyon Tuff Crystal-Poor Member Vitric Zone Densely Welded Subzone (Tpcpv3).....	3F-7
3-8. Model-Isochore Map of Yucca Mountain Tuff (Tpy).....	3F-8
3-9. Model-Isochore Map of Pah Canyon Tuff (Tpp).....	3F-9
3-10. Model-Isochore Map of Paintbrush Tuff Nonwelded Unit (PTn).....	3F-10
3-11. Model-Isochore Map of Topopah Spring Tuff (Tpt).....	3F-11
3-12. Model-Isochore Map of Topopah Spring Tuff Crystal-Poor Member Vitric Zone Densely Welded Subzone (Tptpv3).....	3F-12
3-13. Model-Isochore Map of Repository Host Horizon (RHH).....	3F-13
3-14. Model-Isochore Map of Calico Hills Formation (Ta).....	3F-14
3-15. Model-Isochore Map of Prow Pass Tuff (Tcp).....	3F-15
3-16. Model-Isochore Map of Bullfrog Tuff (Tcb).....	3F-16
3-17. Model-Isochore Map of Tram Tuff (Tct).....	3F-17
3-18. Elevation Map of Top of Older Tertiary Units (Tund).....	3F-18
3-19. Elevation Map of Tertiary-Paleozoic Unconformity.....	3F-19
3-20. Model-Isochore Map of Repository Host Horizon Showing Less Constrained Areas.....	3F-20
3-21. SD-6 Comparison of Predicted Versus Actual Contact Depths (Measured at Unit Tops).....	3F-21
3-22. WT-24 Comparison of Predicted Versus Actual Contact Depths (Measured at Unit Tops).....	3F-22
3-23. Conceptual Probability Density Functions Representing the Uncertainty Associated With Various Unsampled Locations.....	3F-23
3-24. Conceptual Representation of a Monte Carlo Process Incorporating Geostatistical Simulation Techniques.....	3F-24

FIGURES (Continued)

	Page
3-25. Conceptual Illustration of the Construction and Use of Stratigraphic Coordinates.....	3F-25
3-26. Graphical Representation of the Quantile-Preserving Normal-Score Transform Process Using Cumulative Distribution Functions	3F-25
3-27. Scatterplot of Core Versus Petrophysically-Derived Bound-Water Content for 354 Depth-Matched Pairs of Samples	3F-26
3-28. Scatterplot of Total Hydrous-Phase Mineral Content Versus Adjusted Bound- Water Content for 334 Depth-Matched Pairs of Samples	3F-26
3-29. Indicator Variogram and Fitted Model Computed for Hydrous-Phase Mineral Alteration in the CHn Model Unit.....	3F-27
3-30. Indicator Variogram and Fitted Model Computed for Alteration in the Tcp Model Unit.....	3F-28
3-31. Logic Diagram for Postprocessing Porosity and Hydraulic Conductivity Simulations To Recognize Vitrophyre Rock Type	3F-29
3-32. Logic Diagram for Postprocessing Porosity and Alteration Indicator Simulations To Recognize Hydraulic Conductivity Dependence on Alteration State.....	3F-30
3-33. Perspective Diagrams Showing E-Type Model Matrix Porosity in the PTn Model Unit in Both Stratigraphic and Real-World Coordinates	3F-31
3-34. Cross-Sectional Views Showing E-Type Heterogeneity of Matrix Porosity in the PTn Model Unit in Stratigraphic Coordinates.....	3F-32
3-35. Cross-Sectional Views Showing E-Type Heterogeneity of Bulk Density in the PTn Model Unit in Stratigraphic Coordinates.....	3F-32
3-36. Cross-Sectional Views Showing E-Type Heterogeneity of Matrix-Saturated Hydraulic Conductivity in the PTn Model Unit in Stratigraphic Coordinates.....	3F-33
3-37. Perspective Diagrams Showing E-Type Matrix Porosity in the TSw Model Unit in Both Stratigraphic and Real-World Coordinates	3F-34
3-38. Cross-Sectional Views Showing E-Type Heterogeneity of Matrix Porosity in the TSw Model Unit in Stratigraphic Coordinates.....	3F-35
3-39. Perspective Diagrams Showing E-Type Lithophysal Porosity in the TSw Model Unit in Both Stratigraphic and Real-World Coordinates	3F-36
3-40. Cross-Sectional Views Showing E-Type Heterogeneity of Lithophysal Porosity in the TSw Model Unit in Stratigraphic Coordinates.....	3F-37
3-41. Cross-Sectional Views Showing E-Type Heterogeneity of Bulk Density in the TSw Model Unit in Stratigraphic Coordinates.....	3F-37
3-42. Cross-Sectional Views Showing E-Type Heterogeneity of Thermal Conductivity in the TSw Model Unit in Stratigraphic Coordinates.....	3F-38
3-43. Cross-Sectional Views Showing E-Type Heterogeneity of Matrix-Saturated Hydraulic Conductivity in the TSw Model Unit in Stratigraphic Coordinates.....	3F-38
3-44. Perspective Diagrams Showing E-Type Matrix Porosity in the CHn Model Unit in Both Stratigraphic and Real-World Coordinates	3F-39
3-45. Cross-Sectional Views Showing E-Type Heterogeneity of Matrix Porosity in the CHn Model Unit in Stratigraphic Coordinates.....	3F-40
3-46. Cross-Sectional Values Showing E-Type Heterogeneity of Bulk Density in the CHn Model Unit in Stratigraphic Coordinates.....	3F-40

FIGURES (Continued)

	Page
3-47. Block Diagram and Cross-Sectional Views Showing E-Type Heterogeneity of Matrix-Saturated Hydraulic Conductivity in the CHn Model Unit in Stratigraphic Coordinates.....	3F-41
3-48. Perspective Diagrams Showing E-Type Model Matrix Porosity in the Tcp Model Unit in Both Stratigraphic and Real World Coordinates.....	3F-42
3-49. Cross-Sectional Views Showing E-Type Heterogeneity of Matrix Porosity in the Tcp Model Unit in Stratigraphic Coordinates.....	3F-43
3-50. Cross-Sectional Views Showing E-Type Heterogeneity of Bulk Density in the Tcp Model Unit in Stratigraphic Coordinates.....	3F-43
3-51. Block Diagrams and Cross-Sectional Views Showing E-Type Heterogeneity of Matrix-Saturated Hydraulic Conductivity in the Tcp Model Unit in Stratigraphic Coordinates.....	3F-44
3-52. Uncertainty Model Showing E-Type Standard Deviation of Matrix Porosity in the PTn Model Unit.....	3F-45
3-53. Uncertainty Model Showing E-Type Standard Deviation of Matrix Porosity in the TSw Model Unit.....	3F-45
3-54. Uncertainty Model Showing E-Type Standard Deviation of Lithophysal Porosity in the TSw Model Unit.....	3F-46
3-55. Uncertainty Model Showing E-Type Standard Deviation of Matrix Porosity in the CHn Model Unit.....	3F-46
3-56. Uncertainty Model Showing E-Type Standard Deviation of Matrix Porosity in the Tcp Model Unit.....	3F-47
3-57. Locations of Boreholes Used in MM3.0.....	3F-48
3-58. Shaded Relief View of Tpcpv1, Nonwelded Subzone of Vitric Zone of Tiva Canyon Tuff.....	3F-49
3-59. North-South Cross Section Illustrating Sequence Used in MM3.0.....	3F-50
3-60. East-West Cross Section Illustrating Sequences Used in MM3.0.....	3F-50
3-61. Schematic Stratigraphic Column Showing Approximate Thicknesses of Units Listed in Table 1-1.....	3F-51
3-62. Map View of Volcanic Glass Distribution in the PTn Unit, Tpcpv1-Tptrv2 (Sequence 20) for Entire MM3.0.....	3F-52
3-63. Zeolite Distribution in North-South and East-West Cross-Sections Through Center of Potential Repository Block.....	3F-53
3-64. Zeolite Distribution in North-South Cross-Section Through Potential Repository Block and Above Water Table.....	3F-54
3-65. Zeolite Distribution in East-West Cross-Section Through Potential Repository Block and Above Water Table.....	3F-54
3-66. Zeolite Distribution in Map View of Upper Layer (Layer 14) of Calico Hills Formation (Tac, Sequence 11).....	3F-55
3-67. Zeolite Distribution in Map View of Middle-Upper Layer (Layer 13) of Calico Hills Formation (Tac, Sequence 11).....	3F-56
3-68. Zeolite Distribution in Map View of Middle-Lower Layer (Layer 12) of Calico Hills Formation (Tac, Sequence 11).....	3F-57

FIGURES (Continued)

	Page
3-69. Zeolite Distribution in Map View of Lower Layer (Layer 11) of Calico Hills Formation (Tac, Sequence 11)	3F-58
3-70. Zeolite Distribution in Map View of Bedded Tuff Below Calico Hills Formation (Tactb, Sequence 10).....	3F-59
3-71. Zeolite Distribution in Map View of Upper Vitric Zone of Prow Pass Tuff (Tcupv, Sequence 9).....	3F-60
3-72. Smectite + Illite Distribution in North-South Cross-Section Through Potential Repository Block.....	3F-61
3-73. Smectite + Illite Distribution in East-West Cross-Section Through Potential Repository Block.....	3F-61
3-74. Volcanic Glass Distribution in North-South Cross-Section Through Potential Repository Block.....	3F-62
3-75. Volcanic Glass Distribution in East-West Cross-Section Through Potential Repository Block.....	3F-62
3-76. Tridymite Distribution in North-South Cross-Section Through Potential Repository Block.....	3F-63
3-77. Tridymite Distribution in East-West Cross-Section Through Potential Repository Block	3F-63
3-78. Cristobalite + Opal-CT Distribution in North-South Cross-Section Through Potential Repository Block.....	3F-64
3-79. Cristobalite + Opal-CT Distribution in East-West Cross-Section Through Potential Repository Block.....	3F-64
3-80. Quartz Distribution in North-South Cross-Section Through Potential Repository Block	3F-65
3-81. Quartz Distribution in East-West Cross-Section Through Potential Repository Block	3F-65

TABLES

	Page
1-1. Correlation Chart for Model Stratigraphy.....	1-4
3-1. Predicted and Actual Stratigraphy for the ECRB Cross-Block Drift.....	3-19
3-2. Variogram Parameters for Spatial Continuity Model, Alteration in the CHn and Tep Model Units.....	3-28
3-3. Mineralogy of the Topopah Spring Tuff and Upper Calico Hills Formation	3-52

INTENTIONALLY LEFT BLANK

ACRONYMS

AMR	Analysis/Model Report
ECRB	Enhanced Characterization of the Repository Block
ESF	Exploratory Studies Facility
E-type	expected-value type
GFM	Geological Framework Model
GFM3.1	Geological Framework Model Version 3.1
ISM	Integrated Site Model
ISM3.1	Integrated Site Model Version 3.1
K_s	saturated hydraulic conductivity
KTI	Key Technical Issue
LA	License Application
MM	Mineralogic Model
MM3.0	Mineralogic Model Version 3.0
NRC	Nuclear Regulatory Commission
<i>pdf</i>	probability density function
PMR	Process Model Report
QA	quality assurance
r	correlation coefficient
RHH	Repository Host Horizon
RPM	Rock Properties Model
RPM3.1	Rock Properties Model Version 3.1
SR	Site Recommendation
SZ	saturated zone
3-D	three-dimensional
TSPA	Total System Performance Assessment
UZ	unsaturated zone
VWC	volumetric water content
XRD	x-ray diffraction
YMP	Yucca Mountain Site Characterization Project

INTENTIONALLY LEFT BLANK

1. INTRODUCTION

The Integrated Site Model (ISM) provides a framework for discussing the geologic features and properties of Yucca Mountain, which is being evaluated as a potential site for a geologic repository for the disposal of nuclear waste. The ISM is a static model that provides a three-dimensional (3-D), computer-based representation of site geology, selected hydrologic and rock properties, and mineralogic-characteristics data. The different types of data are represented in three separate model components of the ISM: the Geologic Framework Model (GFM), the Rock Properties Model (RPM), and the Mineralogic Model (MM). Functional summaries of the component models and their respective output are provided in Section 1.4. The ISM is important to the evaluation of the site because it provides 3-D portrayals of site geologic, rock property, and mineralogic characteristics and their spatial variabilities.

Each of the component models of the ISM considers different specific aspects of the site geologic setting, and the ISM represents an overall synthesis of the component model results. Each model was developed using unique methodologies and inputs, and the determination of the modeled units for each of the components is dependent on the requirements of that component. Therefore, while the ISM represents the integration of the rock properties and mineralogy into a geologic framework, the discussion of ISM construction and results is most appropriately presented in terms of the three separate components.

This Process Model Report (PMR) summarizes the individual component models of the ISM (the GFM, RPM, and MM) and describes how the three components are constructed and combined to form the ISM. A detailed description of each component model is provided in its respective Analysis/Model Report (AMR): the *Geologic Framework Model (GFM3.1) Analysis Model Report* (CRWMS M&O 1999a), the *Rock Properties Model (RPM3.1) Analysis Model Report* (CRWMS M&O 1999b), and the *Mineralogic Model (MM3.0) Analysis Model Report* (CRWMS M&O 1999c).

1.1 OBJECTIVES

1.1.1 Objectives of this Report

The objectives of this report are to document Version 3.1 of the ISM (ISM3.1) with regard to the data input methodologies used to construct the model, uncertainties and limitations of the modeling results, and model validation. This report summarizes the following:

- Sources of data input
- Methodologies used to construct the model components
- Modeling results, uncertainties, and limitations.

Assumptions that are specific to the ISM and its component models are listed in Sections 3.2.2.2, 3.3.2.2, and 3.4.2.2. Additional details of model assumptions can be found in Section 5 of the individual GFM, RPM, and MM AMRs (CRWMS M&O 1999a, 1999b, and 1999c, respectively).

1.1.2 Purpose of the Model

The principal purpose of the ISM is to provide a common framework of stratigraphy, rock properties, and mineralogy for subsequent process and performance assessment modeling. The subsequent processes predict groundwater flow and transport in the saturated and unsaturated zones (SZ and UZ) and are also used in thermal studies and Total System Performance Assessment (TSPA) studies.

1.2 SCOPE

This PMR describes how stratigraphic, geophysical, rock property, and mineralogic information was used to characterize variations in geologic properties of the site. This report provides the basis for development of the ISM and describes the interrelationship of its component models. Figure 1-1 shows the relationship of the component models and the ISM. The figure also shows the flow of information from the ISM PMR to subsequent users, including the UZ Flow and Transport Model, the SZ Flow and Transport Model, and repository design. The ISM does not directly support either TSPA or the major project milestones, such as the Site Recommendation (SR) and the License Application (LA). Rather, the information in the ISM feeds directly to subsequent processes, which then feed to the TSPA and, finally, the SR and LA. Figure 1-2 illustrates the flow of information from data acquisition into the ISM-supporting AMRs and the PMR, then to other PMRs, and finally into TSPA, the SR, and the LA.

1.3 QUALITY ASSURANCE

Pursuant to evaluations (CRWMS M&O 1999d, 1999e) performed in accordance with QAP-2-0, *Conduct of Activities*, it was determined that activities supporting development of the ISM, its component models, and their documentation are quality-affecting activities that are subject to the quality assurance (QA) requirements of the *Quality Assurance Requirements and Description* (DOE 1998a). The ISM was constructed by the Civilian Radioactive Waste Management System Management and Operating Contractor in accordance with QA procedures QAP-SIII-1, *Scientific Investigation Control*; QAP-SIII-3, *Scientific Notebooks* and AP-SIII.1Q, *Scientific Notebooks*; and QAP-SIII-2, *Review of Scientific Documents and Data*.

The ISM PMR was prepared in accordance with AP-3.11Q, *Technical Reports*, and reviewed in accordance with AP-2.14Q, *Review of Technical Products*. The QA procedures under which the component GFM, RPM, and MM were developed are identified in the respective AMRs and associated planning documents. The AMRs were prepared in accordance with AP-3.10Q, *Analyses and Models*.

1.4 OVERVIEW OF THE INTEGRATED SITE MODEL AND ITS COMPONENT MODELS

1.4.1 Integrated Site Model

The ISM merges the detailed project stratigraphy into model stratigraphic units for the primary subsequent models and repository design, including the UZ and SZ ground-water flow models and the radionuclide transport models. All of the models and the repository design, in turn, will be incorporated into the TSPA of the potential radioactive waste repository system to determine

the suitability of Yucca Mountain as a host for the repository. The ISM is based on three component models: the GFM, RPM, and MM. The GFM summarizes data that serve as a baseline for the geology of the Yucca Mountain site. It also provides the 3-D structure into which the mathematical simulations of rock properties (from the RPM) and mineral distributions (from the MM) are integrated to form the ISM. Figure 1-3 shows the boundaries of the ISM component models. Table 1-1 is a correlation chart of the stratigraphy used in the ISM.

The ISM is designed to apply to a variety of Yucca Mountain Site Characterization Project (YMP) interpretive and administrative needs, including the following:

- Repository design, ground-water flow, radionuclide transport models for the SZ and UZ
- Uncertainty assessment
- Document and presentation preparation
- Confirmatory test planning
- Management and analysis
- Public outreach
- Decision analysis.

1.4.2 Geologic Framework Model

The GFM is a 3-D interpretation of the geology surrounding the location of the potential repository. The area and volume represented by the GFM, as shown in Figure 1-3, are 170 square kilometers (65 square miles) and 771 cubic kilometers (185 cubic miles).

The GFM was constructed primarily from geologic map and borehole data. Additional information from measured stratigraphic sections, gravity profiles, and seismic profiles were also considered.

The boundaries of the GFM (shown in Figure 1-3) were chosen to encompass the most widely distributed set of exploratory boreholes (the "WT" series) and provide a geologic framework over the area of interest for hydrologic flow and radionuclide transport modeling through the UZ. The boundary coordinates in Nevada State Plane coordinates are N738,000 to N787,000 feet (N224,945 to N239,881 meters) and E547,000 to E584,000 feet (E166,728 to E178,005 meters). Nevada State Plane coordinates are also used in the figures of Sections 2 and 3. The depth of the model is constrained by the deepest contact in the model, the Tertiary-Paleozoic unconformity, which is as deep as 3,962 meters (13,000 feet) below the ground surface.

Table 1-1. Correlation Chart for Model Stratigraphy

Stratigraphic Unit					Abbreviation*	RHH*	Geologic Framework Model Unit	Rock Properties Model Unit	Mineralogic Model Unit
Group	Formation	Member	Zone	Subzone					
	Alluvium and Colluvium				Qal, Qc		Alluvium		
	Timber Mountain Group				Tm				
	Rainier Mesa Tuff				Tmr				
	Paintbrush Group				Tp				
				Post-tuff unit "x" bedded tuff	Tpbt6				
				Tuff unit "x" ^{nc}	Tpki (informal)				
				Pre-tuff unit "x" bedded tuff	Tpbt5				
	Tiva Canyon Tuff				Tpc				
	Crystal-Rich Member				Tpcr				
				Vitric zone	Tpcrv				
				Nonwelded subzone	Tpcrv3				
				Moderately welded subzone	Tpcrv2				
				Densely welded subzone	Tpcrv1				
				Nonlithophysal subzone	Tpcm				
				Subvitrophyre transition subzone	Tpcm4				
				Pumice-poor subzone	Tpcm3				
				Mixed pumice subzone	Tpcm2				
				Crystal transition subzone	Tpcm1				
				Lithophysal zone	Tpcrl				
				Crystal transition subzone	Tpcrl1				
	Crystal-Poor Member				Tpcp		Post-Tiva		
				Upper lithophysal zone	Tpcpul				
				Spherulite-rich subzone	Tpcpul1				
				Middle nonlithophysal zone	Tpcpmn				
				Upper subzone	Tpcpmn3				
				Lithophysal subzone	Tpcpmn2				
				Lower subzone	Tpcpmn1				
				Lower lithophysal zone	Tpcpll				
				Hackly-fractured subzone	Tpcpllh				
				Lower nonlithophysal zone	Tpcpln				
				Hackly subzone	Tpcplnh				
				Columnar subzone	Tpcplnc				
							Tpcp		Sequence 22 (Layer 26)
							TpcLD	Not modeled	Alluvium- Tpc_un

Table 1-2. Correlation Chart for Model Stratigraphy (Continued)

Stratigraphic Unit				Abbreviation ^a	RHH ^b	Geologic Framework Model Unit	Rock Properties Model Unit	Mineralogic Model Unit
Group	Formation	Member	Zone	Subzone				
				Vitric zone	Tpcpv			
				Densely welded subzone	Tpcpv3		Not modeled	Sequence 21 (Layer 25) Tpcpv3-Tpcpv2
				Moderately welded subzone	Tpcpv2			
				Nonwelded subzone	Tpcpv1			
				Pre-Tiva Canyon bedded tuff	Tpbt4			
				Yucca Mountain Tuff	Tpy			
				Pre-Yucca Mountain bedded tuff	Tpbt3			
				Pah Canyon Tuff	Tpp			
				Pre-Pah Canyon bedded tuff	Tpbt2			
				Topopah Spring Tuff	Tpt			
				Crystal-Rich Member	Tptr			
				Vitric zone	Tptrv		PTn	Sequence 20 (Layer 24) Tpcpv1-Tptrv2
				Nonwelded subzone	Tptrv3			
				Moderately welded subzone	Tptrv2			
				Densely welded subzone	Tptrv1			
				Nonlithophysal zone	Tptrn			Sequence 19 (Layer 23) Tptrv1
				Dense subzone	Tptrn3			
				Vapor-phase corroded subzone	Tptrn2			Sequence 18 (Layer 22) Tptrn-Tptf
				Crystal transition subzone	Tptrn1			
				Lithophysal zone	Tptrl			
				Crystal transition subzone	Tptrl1			
				Crystal-Poor Member	Tptp			Sequence 17 (Layer 21) Tptpul
				Lithic-rich zone	Tptpf or Tptrf			
				Upper lithophysal zone	Tptpul			Sequence 16 (Layer 20) Tptpmn
				Middle nonlithophysal zone	Tptpmn			
				Nonlithophysal subzone	Tptpmn3			
				Lithophysal bearing subzone	Tptpmn2			
				Nonlithophysal subzone	Tptpmn1			Sequence 15 (Layer 19) Tptpll
				Lower lithophysal zone	Tptpll			
				Lower nonlithophysal zone	Tptplin			Sequence 14 (Layer 18) Tptplin
				Vitric zone	Tptpv			
				Densely welded subzone	Tptpv3		TSw	Sequence 13 (Layers 16 & 17) Tptpv3-Tptpv2
				Moderately welded subzone	Tptpv2			
				Nonwelded subzone	Tptpv1			
				Pre-Topopah Spring bedded tuff	Tpbt1			Sequence 12 (Layer 15) Tptpv1-Tpbt1
				Calico Hills Formation	Ta			
				Bedded tuff	Tacbt			Sequence 11 ^a Tac (Layers 11-14) Sequence 10 (Layer 10) Tacbt

Table 1-3. Correlation Chart for Model Stratigraphy (Continued)

Stratigraphic Unit				Abbreviation ^a	RHH ^b	Geologic Framework Model Unit	Rock Properties Model Unit	Mineralogic Model Unit
Group	Formation	Member	Zone	Subzone				
Crater Flat Group					Tc			
	Prow Pass Tuff				Tcp			
			Prow Pass Tuff upper vitric nonwelded zone		(Tcpu) ^c			Sequence 9 (Layer 9) Tcpu
			Prow Pass Tuff upper crystalline nonwelded zone		(Tcpu) ^c			Sequence 8 (Layer 8) Tcpu-Tcplc
			Prow Pass Tuff moderately-densely welded zone		(Tcpcmd) ^c			
			Prow Pass Tuff lower crystalline nonwelded zone		(Tcplc) ^c			
			Prow Pass Tuff lower vitric nonwelded zone		(Tcplv) ^c			Sequence 7 (Layer 7) Tcplv-Tcbuv
			Pre-Prow Pass Tuff bedded tuff		(Tcpcb) ^c			
	Bullfrog Tuff				Tcb			
			Bullfrog Tuff upper vitric nonwelded zone		(Tcbuv) ^c			Sequence 6 (Layer 6) Tcbuv-Tcblc
			Bullfrog Tuff upper crystalline nonwelded zone		(Tcbuc) ^c			
			Bullfrog Tuff welded zone		(Tcbmd) ^c			
			Bullfrog Tuff lower crystalline nonwelded zone		(Tcblc) ^c			Sequence 5 (Layer 5) Tcblv-Tctuv
			Bullfrog Tuff lower vitric nonwelded zone		(Tcblv) ^c			
			Pre-Bullfrog Tuff bedded tuff		(Tcbbt) ^c			
	Tram Tuff				Tct			
			Tram Tuff upper vitric nonwelded zone		(Tctuv) ^c			Sequence 4 (Layer 4) Tctuc-Tctlc
			Tram Tuff upper crystalline nonwelded zone		(Tctuc) ^c			
			Tram Tuff moderately-densely welded zone		(Tctmd) ^c			
			Tram Tuff lower crystalline nonwelded zone		(Tctlc) ^c			Sequence 3 (Layer 3) Tctlv-Tctbt
			Tram Tuff lower vitric nonwelded zone		(Tctlv) ^c			
			Pre-Tram Tuff bedded tuff		(Tctbt) ^c			
			Lava and flow breccia (informal)		Tll			Sequence 2 (Layer 2) Tund
			Bedded tuff		Tllbt			
	Lithic Ridge Tuff				Tr			
			Bedded tuff		Trlbt			
			Lava and flow breccia (informal)		Tll2			
			Bedded tuff		Tllbt			
			Lava and flow breccia (informal)		Tll3			
			Bedded tuff		Tll3bt			
			Older tuffs (informal)		Tt			
			Unit a (informal)		Tta			
						Not modeled		

Table 1-4. Correlation Chart for Model Stratigraphy (Continued)

Stratigraphic Unit					Abbreviation ^a	RHH ^b	Geologic Framework Model Unit	Rock Properties Model Unit	Mineralogic Model Unit
Group	Formation	Member	Zone	Subzone					
				Unit b (informal)	Ttb		Tund	Not modeled	Sequence 2 (Layer 2) Tund
				Unit c (informal)	Ttc				
				Sedimentary rocks and calcified tuff (informal)	Tca				
				Tuff of Yucca Flat (informal)	Tyf				
Pre-Tertiary sedimentary rock							Paleozoic	Not modeled	Sequence 1 (Layer 1) Paleozoic ^h
				Lone Mountain Dolomite	Sim				
				Roberts Mountain Formation	Sm				

^aSource: CRWMS M&O 1999a.

^bSource: CRWMS M&O 1997, pp. 43-50; RHH = Repository Host Horizon

^cCorrelated with the rhyolite of Comb Peak (Buesch et al. 1996, Table 2).

^dIncludes rhyolite of Delirium Canyon north of Yucca Wash (Day et al. 1997).

^eFor the purposes of GFM3.1, each formation in the Crater Flat Group was subdivided into six zones based on the requirements of the users of the Geologic Framework Model. The subdivisions are upper vitric (uv), upper crystalline (uc), moderately to densely welded (md), lower crystalline (lc), lower vitric (lv), and bedded tuff (bt) (Buesch and Spengler 1999, pp. 62-64).

^fSequence 13 (Tptpv3-Tptpv2) is subdivided into 2 layers of equal thickness.

^gSequence 11 (Tac) is subdivided into 4 layers of equal thickness.

^hSequence 1 (Paleozoic) represents a bounding lower surface.

NOTE: Shaded rows indicate header lines for subdivided units.

1.4.3 Rock Properties Model

The RPM is a 3-D, conditional, Monte Carlo simulation model of bulk and hydrologic material properties for most of the rock units within the UZ at Yucca Mountain. The model divides its volume into four internally similar units, as indicated in Table 1-1, and is tied geometrically to the bounding surfaces of model units within the GFM. For all four units, the modeled material properties are:

- Matrix porosity
- Whole-rock bulk density
- Matrix-saturated hydraulic conductivity.

Additionally, the following material properties are modeled for the TSw model unit:

- Lithophysal porosity
- Whole-rock thermal conductivity.

There are three fundamentally different types of models included within the RPM. The first type is a suite of 50 simulated property models generated for each material property using conditional simulation techniques. The second type is the summary expectation (E-type or expected value) model for each rock property. These E-type models provide a single average value (based on the

50 individual simulations) at each node to represent the property values most likely to be encountered at each discretized location. The third model is also a summary-type model and provides the node-by-node standard deviation of the 50 individual simulated property models to provide users with an estimate of the associated geologic uncertainty.

1.4.4 Mineralogic Model

The MM is a weighted, inverse distance model that enables project personnel to estimate mineral abundance at any position, within any region, or within any stratigraphic unit in the model area. It is referenced to the stratigraphic framework defined in GFM3.1 and was developed from mineralogic data obtained from boreholes. The MM supports the analyses of hydrologic properties, radionuclide transport, mineral health hazards, repository performance, and repository design. Additional details can be found in the MM AMR (CRWMS M&O 1999c, Section 1).

1.5 RELATIONSHIP TO OTHER PROCESS MODEL REPORTS AND PROJECT DOCUMENTS

The ISM provides spatially distributed subsurface data and information to the UZ Flow and Transport Model, the SZ Flow and Transport Model, and to Repository Subsurface Design and other subsequent model and design activities. The information that ISM provides for repository design includes locations of contacts between geologic units, unit attitudes and thicknesses, fault locations and attitudes, distance above the water table, and petrophysical properties.

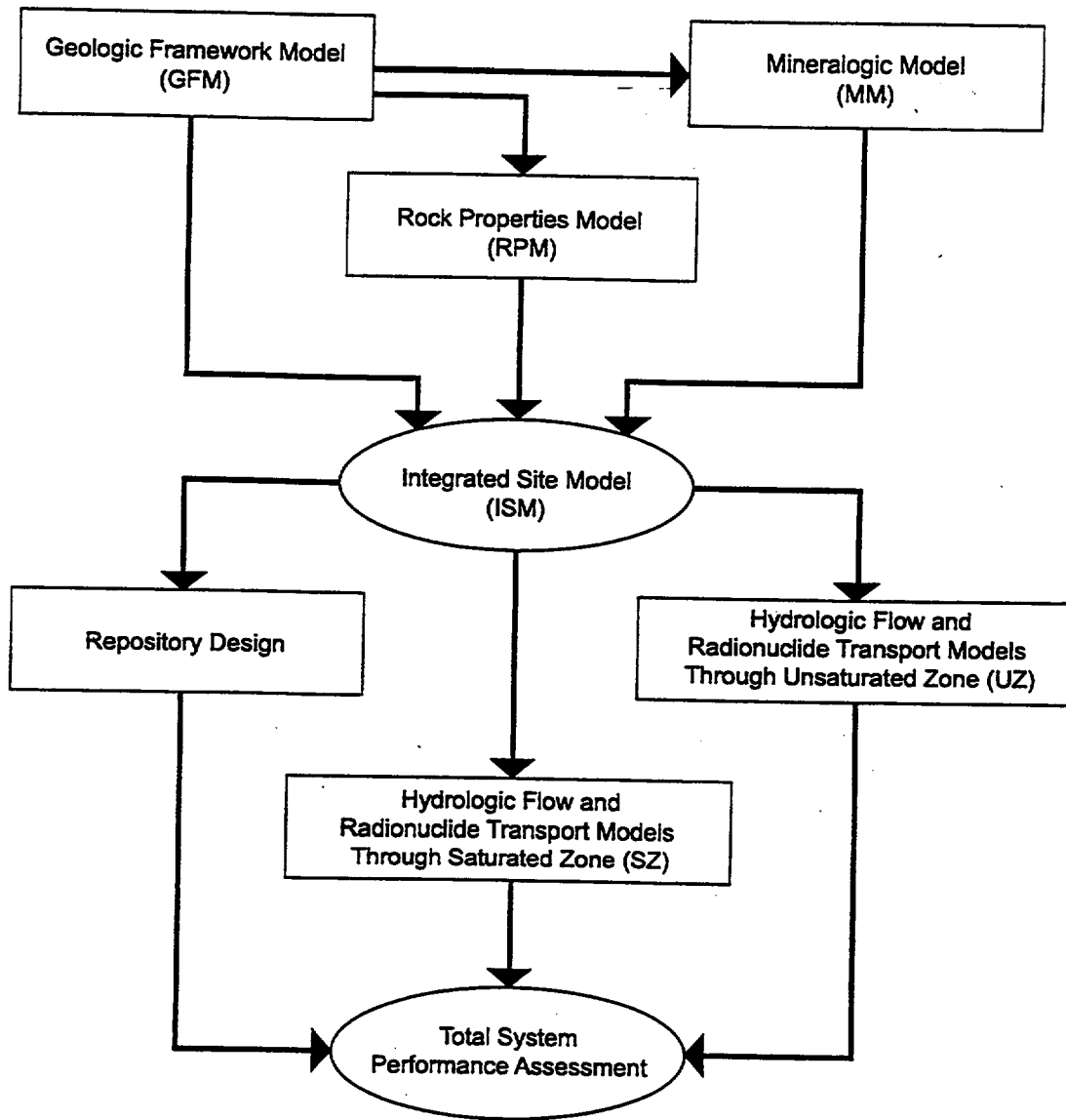


Figure 1-1. Interrelationships of Component Models, Integrated Site Model, and Downstream Uses (CRWMS M&O 1999a Figure 2)

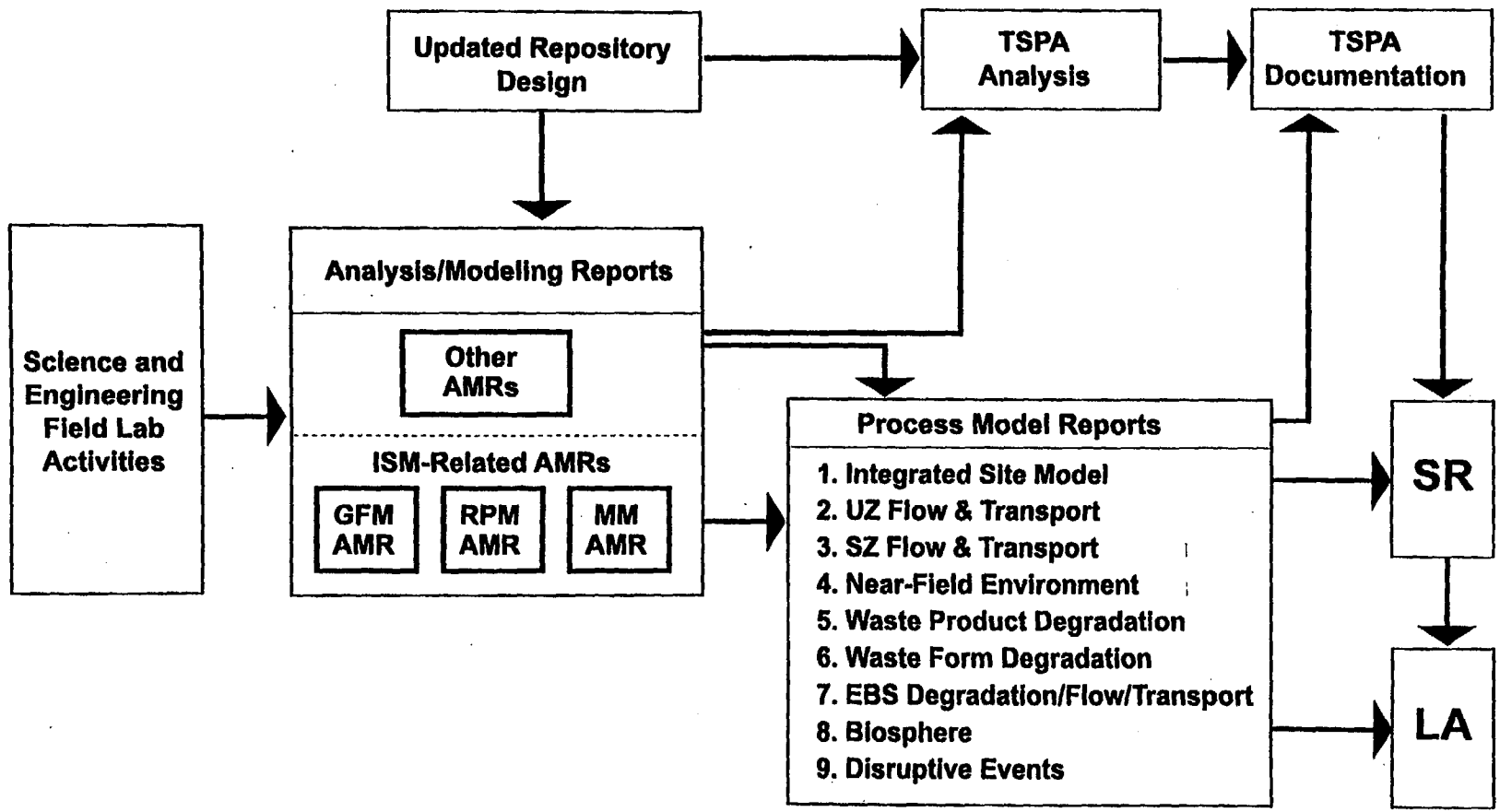


Figure 1-2. Flow of Information From Data Collection Through the AMRs, PMRs, and TSPA, and Into the Site Recommendation (SR) and Finally to the License Application (LA)

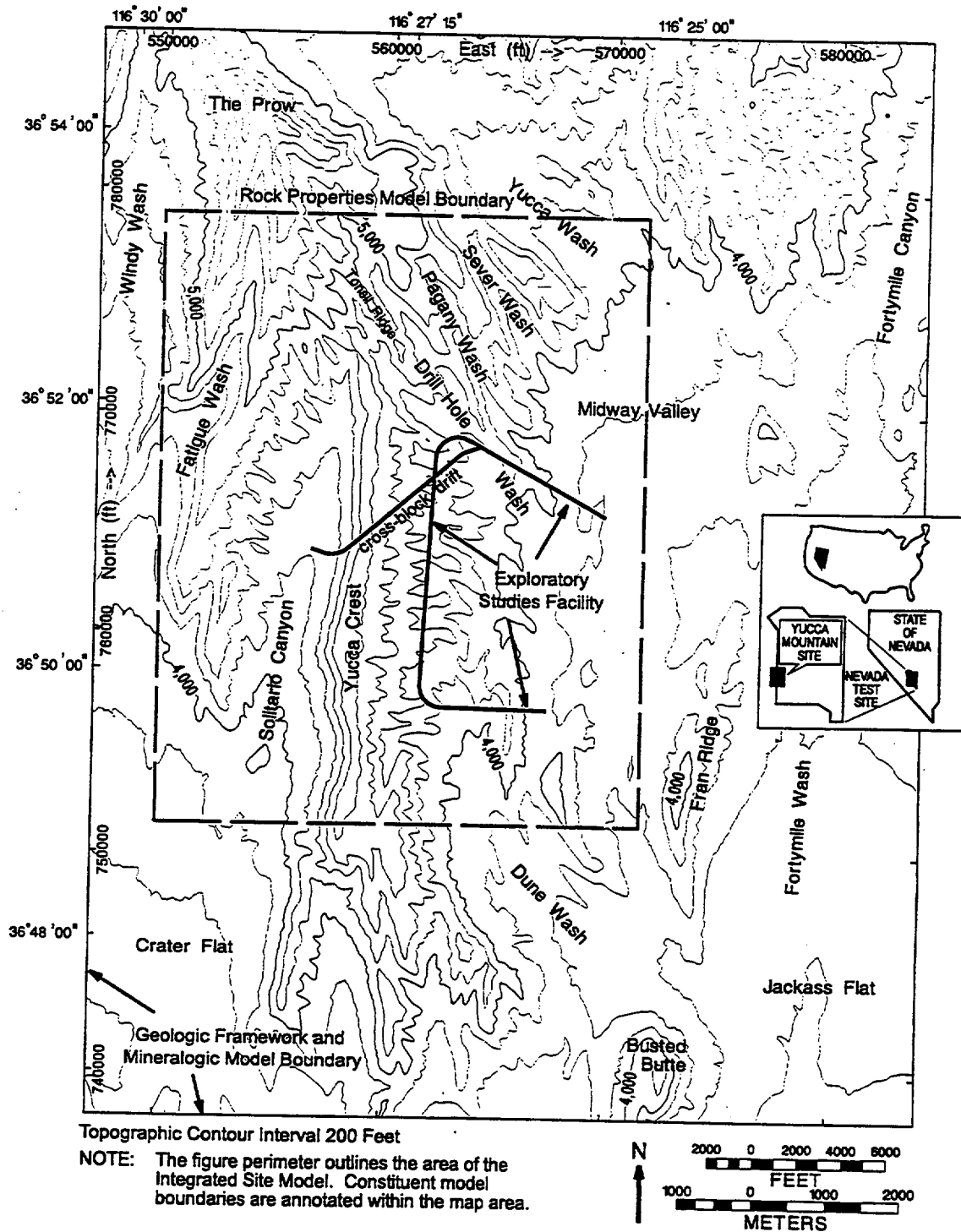


Figure 1-3. Area of Integrated Site Model, Showing Model Boundaries (CRWMS M&O 1999a, Figure 1)

INTENTIONALLY LEFT BLANK

2. EVOLUTION OF THE INTEGRATED SITE MODEL

2.1 PHILOSOPHY OF PMR DEVELOPMENT

The PMRs provide a summary and synthesis of their component AMRs. The PMRs identify, document, and describe the primary (major) processes and inputs to the TSPA SR. The PMRs provide the technical basis that supports the TSPA model. In this role, the PMRs identify, document, and describe the information needed to demonstrate postclosure performance. The development process ensures that each PMR provides transparency and traceability of data, information, and references related to its process model and support of TSPA.

2.2 INTEGRATED SITE MODEL DEVELOPMENT HISTORY

This section provides an overview of the development of the three ISM component models. Included are summaries of the versions of each model and the relevant changes in those versions.

2.2.1 Geologic Framework Model

As of the preparation of this report, GFM3.1 is the most current version of the model and is based on data from surface mapping, outcrop studies, boreholes, the Exploratory Studies Facility (ESF) and cross-block drift (Figure 2-1) data, and traces of the major known faults that transect the model domain (Figure 2-2). The following list summarizes the changes to the GFM as it evolved. Additional details can be found in the *Geologic Framework Model (GFM3.1) Analysis Model Report* (CRWMS M&O 1999a, Section 6.2).

- GFM1.0 was based on data from boreholes and regional geologic maps. All faults were portrayed as vertical.
- GFM1.0 to GFM2.0. GFM2.0 improved GFM1.0 by including dipping faults, and additional rock units.
- GFM2.0 to GFM3.0. The primary difference between GFM3.0 and GFM2.0 was use of the bedrock geologic map of the Yucca Mountain area (see Day et al. 1997), revised borehole information, and refined modeling methodologies. The number of rock layers modeled was also increased. The interim version, GFM2.1, was used as a testbed model to develop and test refined methods for GFM3.0 and GFM3.1.
- GFM3.0 to GFM3.1. GFM3.1 was constructed to incorporate new data from boreholes USW SD-6 (SD-6) and USW WT-24 (WT-24) and from the cross-block drift excavated during the Enhanced Characterization of the Repository Block (ECRB; see CRWMS M&O 1999a, Section 6.2.3). Figure 2-1 shows the locations of boreholes SD-6 and WT-24 and the ECRB cross-block drift. In addition, GFM3.1 includes one new fault, which is located at The Prow (Figure 2-2), and is designated *NW*. The new fault was included to properly model the Calico Hills Formation and Prow Pass Tuff outcrops.

GFM3.1 was also constructed with more curvature on the dominant faults to be consistent with cross sections published in Day et al. (1997) and to account for field relations showing rotated

hanging-wall strata as described in the *Geologic Framework Model (GFM3.1) Analysis Model Report* (CRWMS M&O 1999a, Section 6.2.3).

2.2.2 Rock Properties Model

As of the preparation of this report, RPM3.1 is the most current version of the RPM. The RPM2.0 was the first rock properties modeling effort. The "2.0" designation was assigned by the RPM's association with GFM2.0 as part of the ISM2.0 modeling effort; there was no RPM1.0. The following summarizes the changes between versions as the model evolved; additional details are presented in the *Rock Properties Model (RPM3.1) Analysis Model Report* (CRWMS M&O 1999b, Section 6.2).

From RPM2.0 to RPM3.1, four changes were made:

- Stratigraphic unit groupings were modified to better match mineralogic and properties data.
- The model area was reduced, resulting in an improved spatial distribution of borehole data in the remaining area.
- All of the petrophysically based porosity data were recomputed.
- The approach used to identify the spatial distribution of hydrous-phase mineral alteration was modified.

2.2.3 Mineralogic Model

As of the preparation of this report, MM3.0 is the most current version of the MM. The following list summarizes the changes that were made as the model evolved. Additional details are provided in the *Mineralogic Model (MM3.0) Analysis Model Report* (CRWMS M&O 1999c, Section 6.1).

- Preliminary MM. The initial model was developed in the stratigraphic framework adapted from GFM1.0.
- MM1.0. The stratigraphic framework was adapted from GFM2.0. New mineralogic data from boreholes USW H-3 (H-3), USW NRG-6 (NRG-6), USW NRG-7/7a (NRG-7a), USW SD-7 (SD-7), USW SD-9 (SD-9), USW SD-12 (SD-12), USW UZ-14 (UZ-14), and USW UZ-N32 (UZ-N32) were incorporated.
- MM1.1. New mineralogic data from borehole WT-24 were incorporated.
- MM2.0. The stratigraphic framework was adapted from GFM3.0. The grid resolution was refined from 244 to 61 meters (800 to 200 feet). Data from borehole USW H-6 (H-6) was incorporated with new data from boreholes SD-6, SD-7, SD-12, UE-25 UZ#16 (UZ#16), and WT-24. The number of modeled mineral classes was expanded from six to ten. Mineralogic modeling was conducted in stratigraphic coordinates (see

Section 3.4.3.2). The stratigraphic framework used for the MM was simplified from 31 to 22 sequences.

- MM3.0. The stratigraphic framework was adapted from GFM3.1. New data from boreholes SD-6 and WT-24 were included, and Sequence 13 (Tptpv3–Tptpv2) was subdivided into two layers. The area covered by the MM was expanded to include the same area as GFM3.1. The procedure for mineralogic modeling in stratigraphic coordinates was improved.

2.2.4 Integrated Site Model

The ISM does not have its own unique development history. The development histories of the GFM, RPM, and MM constitute the development history of the ISM.

INTENTIONALLY LEFT BLANK

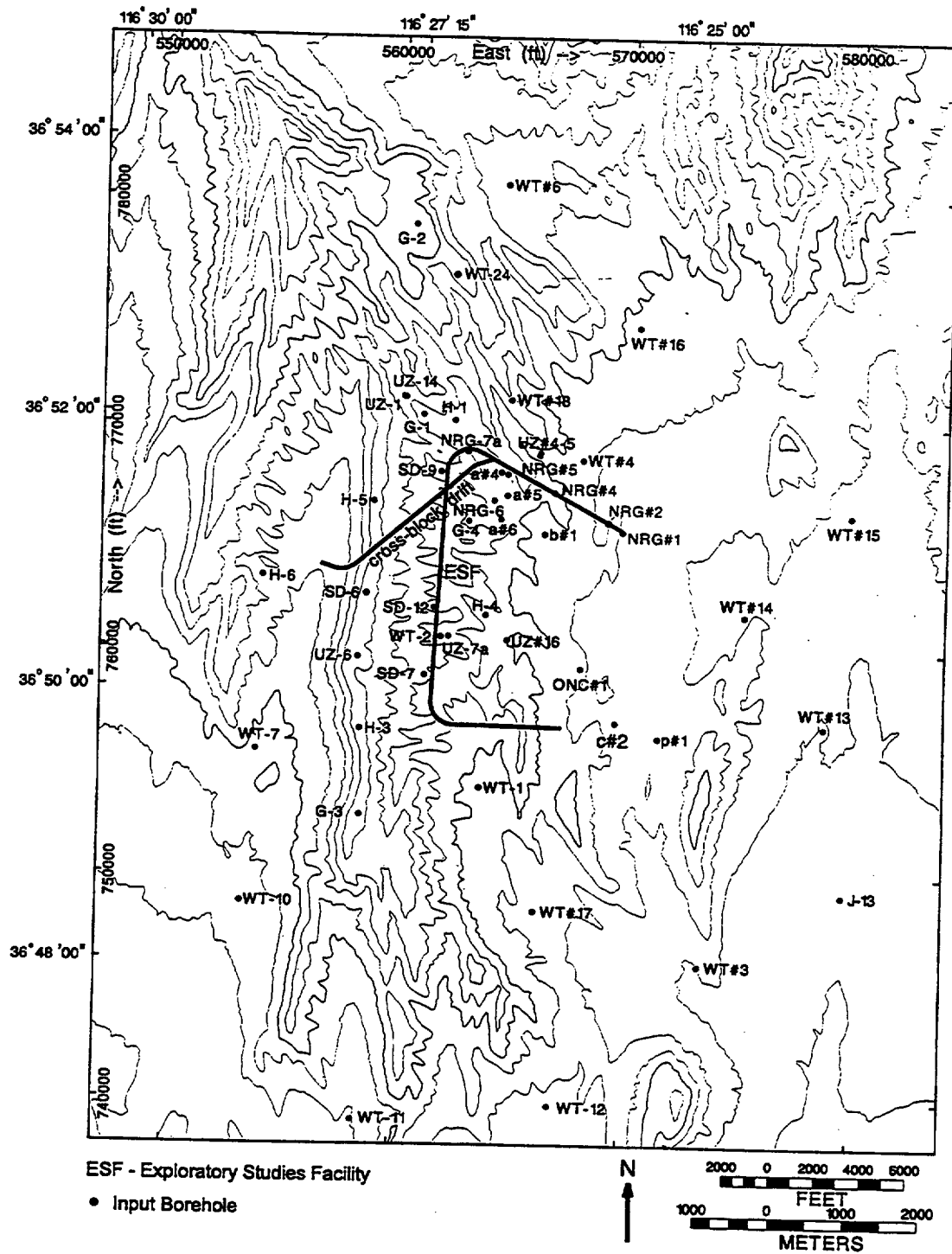
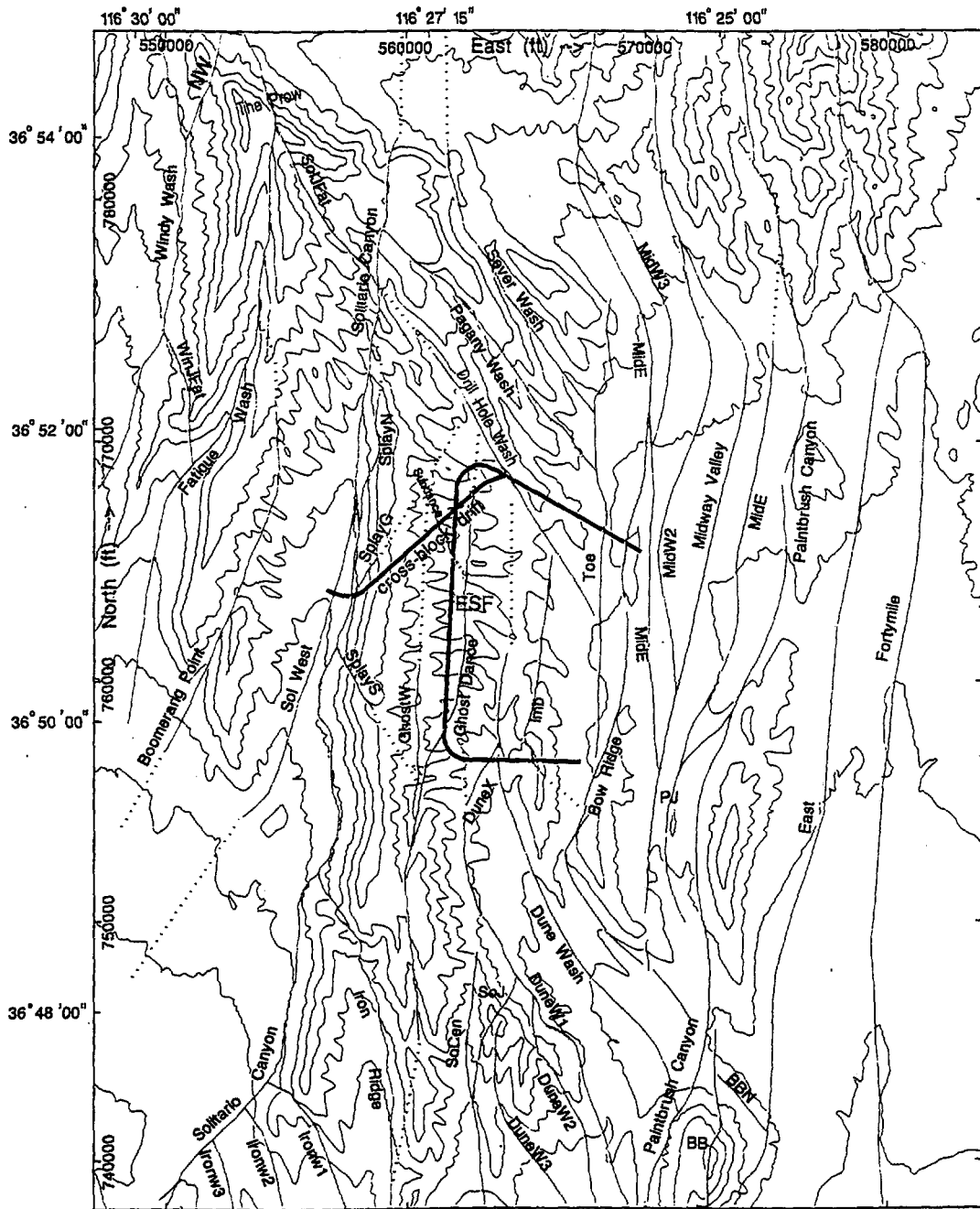
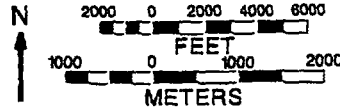


Figure 2-1. Locations of Boreholes, Exploratory Studies Facility, and Cross-Block Drift (CRWMS M&O 1999a, Figure 3)



ESF - Exploratory Studies Facility

— Fault Trace Inputs, dotted where fault is buried or extended



NOTE: Fault names shown here are for GFM modeling purposes only.

Figure 2-2. Surface Traces of Faults Modeled in GFM (CRWMS M&O 1999a, Figure 4)

3. INTEGRATED SITE MODEL

This section provides a general description of the three model components of the ISM, their construction (including inputs and methodologies), and the uncertainties and limitations of the output. Additional details about the individual models can be found in the respective AMRs (CRWMS M&O 1999a, 1999b, 1999c).

3.1 SUMMARY OF COMPONENT PARTS

Each component model of the ISM is discussed individually in the following sections:

- Section 3.2 – Geologic Framework Model (GFM)
- Section 3.3 – Rock Properties Model (RPM)
- Section 3.4 – Mineralogic Model (MM).

The discussions are divided to present the methods, software, data sets, and results that are unique to each component model. Because the models are complementary and do not overlap in content, the component models, when combined, depict the results of the ISM.

3.2 GEOLOGIC FRAMEWORK MODEL

This section provides a summary description of GFM3.1. A more detailed discussion can be found in the *Geologic Framework Model (GFM3.1) Analysis Model Report* (CRWMS M&O 1999a).

3.2.1 Introduction

The GFM is a description of the distributions of rock layers and faults in the subsurface of Yucca Mountain. It is the framework into which rock properties and mineralogic distributions are placed and, thus, serves as the framework of the ISM in terms of both construction and discussion.

The GFM was constructed as a volume model based on the additive application of individual geologic unit thicknesses. Isochores (unit thickness measured vertically) are the fundamental building blocks of the GFM; individual isochores are constructed primarily on the basis of borehole and surface geologic mapping data. Additionally, through the application of a conceptual model approach, consistent with known site geologic processes, interpretive constraints were applied to guide the shapes of the isochores.

The manner in which the GFM was constructed, and a summary of the results, is provided in the following subsections. The software QA documentation, planning documents, modeling implementation procedures, and scientific notebooks for the GFM are described in the *Geologic Framework Model (GFM3.1) Analysis Model Report* (CRWMS M&O 1999a, Sections 2 and 3).

3.2.2 Summary of Model Inputs and Model Software

This section summarizes the inputs and software used to construct the GFM. The qualification status of the software and data used in the construction of the GFM is documented in Sections 3

and 4, respectively, of the *Geologic Framework Model (GFM3.1) Analysis Model Report* (CRWMS M&O 1999a).

3.2.2.1 Inputs

Input data for the GFM are:

- Borehole lithostratigraphic contacts
- Maps of geology and topography
- Underground data from the ECRB cross-block drift and the ESF
- Measured stratigraphic sections.

The location of boreholes from which lithostratigraphic picks used as input into the GFM were taken are shown in Figure 2-1. A basic inclusion criterion for borehole data was correlation, the comparison and adjustment of all data to a common standard. In this case, the common standard was the geophysical logs because they are the most widely available data among the boreholes. All available borehole data were considered in determining the stratigraphic contacts, but the geophysical logs were used as the primary data set.

Interpretations from geophysical (gravity) data were used to infer structures beneath alluvium in Midway Valley. The input data and their data tracking numbers (DTNs) are identified in Section 4.1 of the *Geologic Framework Model (GFM3.1) Analysis Model Report* (CRWMS M&O 1999a).

With the exception of a fault modeled under Fortymile Wash, the fault traces modeled in the GFM are based on the bedrock geologic map of the Yucca Mountain area (Day et al. 1997). This map was superseded in the TDMS after its incorporation into the GFM. The newer version (Day et al. 1998) includes minor typographic changes, including omitting labels and line segments, which have no technical impact on the GFM. Fault offsets, where modeled, were also derived from the bedrock geologic map of the Yucca Mountain area (Day et al. 1997). An exception to this was a feature interpreted as a horst from gravity and magnetic profiles beneath Midway Valley. This structure has vertical displacements of 75 meters (246 feet) on the faults bounding the structure (Ponce and Langenheim 1994, p. 6).

Data from the ESF were used to constrain the elevation of the reference horizon (see Section 3.2.3.4) at the base of the Tiva Canyon Tuff. Only data for the elevation of this horizon were used as input to the GFM because the underground data do not provide thickness information for the modeled rock layers.

In addition to a series of qualified measured sections that were used as input into the GFM, a group of 44 non-qualified measured sections located primarily in and north of Yucca Wash provide qualitative data on stratigraphic thicknesses of the shallow units in the northern part of the model. They provide support to the conceptual model (discussed in Section 3.2.3.1), but were not used as direct input into the model.

Interpretations of seismic reflection profiles (Brocher et al. 1998, pp. 947–971) were used qualitatively to formulate 3-D fault geometries and interpret tilted strata. The seismic profiles

from this study are not sufficient to provide quantitative model input data because of noise and uncertainties regarding rock seismic velocity. Results of a gravity inversion study (Majer et al. 1998) were used for the Tertiary-Paleozoic unconformity. The locations of the seismic and gravity profiles are shown in Figure 3-1. This is described in greater detail in Section 6.3.1.10 of the *Geologic Framework Model (GFM3.1) Analysis Model Report* (CRWMS M&O 1999a).

3.2.2.2 Assumptions

In the context of this PMR, assumptions are those assertions that influence data or input parameters. For the GFM, an assumption was made regarding the appropriateness of the topographic grid input. This assumption is discussed in Sections 4.1 and 5 of the *Geologic Framework Model (GFM3.1) Analysis Model Report* (CRWMS M&O 1999a).

In addition to assumptions, the GFM used selected methodological premises upon which the model construction is founded. These are the isochore method and the application of the minimum tension algorithm. Details of the application of these assumptions and methodologies are provided in Section 3.2.3.

3.2.2.3 Software

The GFM was constructed with EARTHVISION Version 4.0 software (Dynamic Graphics of Alameda, California), which is designed for 3-D modeling. During construction of the model, the software was used as intended by its developers. Additional information on the software and its qualification can be found in the *Geologic Framework Model (GFM3.1) Analysis Model Report* (CRWMS M&O 1999a, Section 3).

3.2.3 Construction of the Model

This section describes the GFM in terms of its development, methodology, results, and uncertainties and limitations. The intent is to provide a relatively high-level conceptual description of the GFM modeling approach. The methodology is described in more detail in the *Geologic Framework Model (GFM3.1) Analysis Model Report* (CRWMS M&O 1999a, Section 6.3). The GFM was constructed in the following general steps:

1. Development of grid construction and contouring methodology
2. Construction of faults
3. Construction of reference horizons
4. Construction of model-isochores
5. Assembly of faults and rock layers
6. Assessment and iteration.

Table 1-1 presents the correlation between the stratigraphic units modeled in the GFM, the RPM, and the MM. The table includes the location of the potential RHH, which is the body of rock in which the potential repository, if built, would be excavated. It spans four lithostratigraphic zones (the lower part of the Ttpul, Ttpmn, Ttppl, and Ttppln) as defined in *Determination of Available Volume for Repository Siting: YMP.M03* (CRWMS M&O 1997, pp. 43-50). The model unit designated as RHHtop corresponds to a density log signature that defines the uppermost portion of the potential RHH.

The GFM stratigraphy was constructed by the thickness (or isochore) method. The isochore method involves building the model stratigraphy by beginning at a reference horizon (for instance, the surface at the base of the Tiva Canyon Tuff). From that reference horizon, the stratigraphic unit thicknesses (isochores) are added to build upward and subtracted to build downward until the complete stratigraphic column is represented. This concept is illustrated in Figure 3-2. This method was chosen for several reasons:

- In volcanic units, thickness tends to be systematically distributed over large areas. Reasonable estimates can be made based on an understanding of the underlying geologic processes.
- Because the volcanic strata at Yucca Mountain consist of many units that pinch out, are very thin, or have highly variable thicknesses (creating highly variable differences between the elevations of stratal tops and bottoms), the use of isochores prevents the top and bottom grids from intersecting unintentionally.
- Construction of stratigraphy by isochores results in fewer thickness anomalies than the construction of each surface as an elevation grid.

The drawback of the isochore method is the possible generation of unintended surface undulations; however, none of significance were noted in GFM3.1. Surfaces in the shadow zone, which develops beneath dipping faults as illustrated in Figure 3-2, were controlled by the use of reference horizons in the deeper units and building the isochores upward. The isochore maps included in this report may differ from true isochores because they may contain artifacts of the modeling process. For this reason, the maps are referred to as "model-isochores." A true isochore map would not include partial thicknesses caused by faulting, but the model-isochores do in cases where the fault is not included in the model.

3.2.3.1 Conceptual Model

As discussed in the following subsections, interpretive constraints were used to guide the shapes of model-isochores (thicknesses), which are the fundamental building blocks of the GFM. The conceptual model discussed below was used to formulate the interpretive constraints and consists of the guiding principles given below.

- Volcanogenic rocks generally become thinner as distance from the source increases.
- The major deposits in the subsurface at Yucca Mountain generally fill in pre-existing topography, so that the top of a formation may be more planar than the base.
- The top of a formation may have eroded after deposition.
- The lower vitric zones of the Topopah Spring and Tiva Canyon Tuffs blanketed pre-existing topography and began the process of filling in topographic lows.

- Topopah Spring Tuff lithophysal and nonlithophysal zones were produced by multiple processes and, although approximating a planar geometry, these zones may have irregular thickness distributions.

The conceptual model was applied to shape each model-isochore between and away from the locations of input data. Where suggested by the data, the conceptual model was applied to extrapolate away from unusually thick and thin intervals to provide an internally consistent volumetric representation.

3.2.3.2 Overview of GFM3.1 Methodology

The methodology for constructing GFM3.1 included a combination of mathematical grid construction (gridding) and the application of interpretive constraints in the form of augmenting contour segments (Figure 3-3). In this way, the model honors the measured data while allowing for interpretations in areas where data are sparse or where a grid generated by the model may be inconsistent with the conceptual model.

3.2.3.2.1 Grid Construction

A grid is a systematic array of points, or *nodes*. In three dimensions, a grid forms a surface. Topography is an example of a surface that can be represented by a grid. Gridding is the process of creating a surface (grid) across an area based on widely and variably spaced input data. Many methods (both mathematical and interpretive) are available for use in creating surfaces in a model. Examples include triangulation, hand contouring, linear interpolation, geostatistical methods, and various mathematical algorithms. The gridding method used in the GFM is based on a *minimum tension* mathematical algorithm that calculates a surface passing through the input data, and is an option in EARTHVISION. For every grid in the GFM, the minimum tension algorithm is constrained by field data (from boreholes, tunnels, measured sections, or the geologic map) and interpretive constraints in the form of contour segments (discussed in Section 6.3.2.2 of the *Geologic Framework Model (GFM3.1) Analysis Model Report (CRWMS M&O 1999a)*). Grid node spacing for all grids except topography is 61 by 61 meters (200 by 200 feet). The topographic grid spacing is 30 by 30 meters (100 by 100 feet) to accurately represent details of the ground surface.

In the GFM, the grids represent the geologic surfaces (reference horizons) or unit thicknesses (isochores) and are the fundamental building blocks of the model. Grids also are created to define fault planes. For fault planes and reference horizons, each node contains an elevation; for model-isochores, each node contains a thickness.

3.2.3.2.2 Interpretive Constraints

As illustrated in Figure 3-3, interpretive constraints, in the form of contour segments, were inserted into the model and were used to control the shapes of the grids to ensure appropriate adherence to the conceptual model. The reference horizon, fault, and model-isochore grids in the GFM were calculated using both field data and interpretive constraints. None of the grids represent a purely minimum tension interpretation of the field data.

The process for creating grids for faults, reference horizons, and model-isochores consisted of the following steps:

1. The input data were first gridded without any interpretive constraints. These results were analyzed to determine whether interpretive constraints were needed and to choose the most appropriate locations for their use.
2. The grid was then modified by introducing interpretive constraints and regriding.
3. The process was iterated until the grid represented the interpretation being applied by the modeler.

3.2.3.3 Construction of Faults

The initial step in fault construction was development of the criteria for fault inclusion. Due to the large number of faults in the modeled area and limitations in modeling technology, criteria were needed to select faults that can realistically be modeled. These criteria are based primarily on feedback from the users of previous model versions, but are also based on the importance of a fault to the GFM and models using the GFM. If no users of the model needed a fault, and omitting the fault did not adversely affect the GFM, the fault was not modeled. More stringent criteria were developed for the potential repository area to meet the requirements of repository design. The criteria for fault inclusion are listed in Section 6.1.2 of the *Geologic Framework Model (GFM3.1) Analysis Model Report* (CRWMS M&O 1999a).

For GFM3.0 (and GRM3.1), the locations of fault traces were established by the geologic map of the site area (Day et al. 1997). An additional fault was added beneath Fortymile Wash, as shown in Figure 2-2, to account for geometric relations between outcrop data and boreholes WT#13, WT#15, and J-13. Fault displacements were estimated from borehole data and the geologic map. An exception to this was a feature interpreted as a horst from gravity and magnetic profiles beneath Midway Valley. This feature has vertical displacements of 75 meters (246 feet) on the faults bounding the structure (Ponce and Langenheim 1994, p. 6). Fault displacements and geometries were modified during technical reviews of each model to incorporate feedback from YMP scientists.

Fault grids were constructed primarily with the use of data from the geologic map, boreholes, and tunnel intercepts. Interpretive constraints were imposed to create the proper dip of the fault plane. The grid was then recalculated with the use of the field data and interpretive constraints. The interpretive constraints were then modified as needed to produce model results that matched the geologic map (Day et al. 1997) and the conceptual model (described in Section 3.2.3.1).

3.2.3.4 Construction of Reference Horizons and Model-Isohores

In geologic modeling, a reference horizon is an elevation grid that establishes the strike and dip of the rock layers and the vertical displacement of rock layers along faults. The grid is constructed with the use of data from the geologic map, boreholes, and tunnels. Where the grid crosses a fault, the grid is displaced by an appropriate amount. Thicknesses (isochores) of other rock layers are then added to or subtracted from the reference horizon to create other rock units

and horizons in the model, as illustrated in Figure 3-2. The reference horizon and the model-isochores grids were constructed by the methods discussed in Section 3.2.3.2.

Reference horizons were constructed at the base of the Tiva Canyon Tuff Crystal-Poor Member Vitric Zone Nonwelded subzone (Tpcpv1), top of the Calico Hills Formation (Ta), and top of the older Tertiary unit (Tund) (Table 1-1).

3.2.3.5 Assembly of Faults and Rock Layers

The reference horizon grids, model-isochores grids, and fault grids were combined to produce the final model. Calculations were performed for this final combination in the EARTHVISION software to determine the intersections of faults and rock units; this information was stored with each grid. The final model consists of a grid for each rock unit in each fault block (the volume of rock between faults) and a grid for each fault.

To visually examine the model, a graphical construction called a "faces model" was created. The faces model uses the grids of reference horizons and faults to create a 3-D display in which rock layers and faults can be shown individually or in combination. Examples of the faces models are provided in Figures 3-4 and 3-5.

3.2.4 Model Results

The results of the GFM provide an interpretation of the spatial position and geometry of rock units and faults, and are summarized in the following subsections. Additional details of the results can be found in the *Geologic Framework Model (GFM3.1) Analysis Model Report* (CRWMS M&O 1999a, Section 6.4).

3.2.4.1 Interpretation of the Rock Units

This section describes the geometry and distribution of rock units in the GFM that are important for the ISM, RPM, and MM, as well as for the major direct and indirect users of the ISM (repository design and flow modeling through the UZ and the SZ). Geologic features described include each geologic formation, the Paintbrush Tuff (PTn) hydrological and thermal-mechanical unit, the undifferentiated older Tertiary unit (Tund), and the Tertiary-Paleozoic unconformity. Subunits of the formations that are particularly important for GFM uses are also described.

Regional stratigraphy and structure, deposition, origin, age, and lithology of the rock layers modeled in the GFM are discussed in the *Yucca Mountain Site Description* (CRWMS M&O 1998, Chapters 3.2 and 3.5).

3.2.4.1.1 Alluvium and Post-Tiva Units

Overview—The alluvium (Qal) and post-Tiva rock units (Table 1-1) in the GFM account for a very small amount of the total model volume (much less than 1 percent), and they occur outside the boundaries of the ESF.

Unit Geometry—The distribution of modeled alluvium, illustrated in Figure 3-6, is based on geologic mapping and borehole data, including data from many boreholes constructed to

measure infiltration rates through alluvium. The areal extent of alluvium is well constrained by geologic mapping; however, because some boreholes did not penetrate to bedrock, the modeled alluvial thickness is constrained by limited subsurface information. The map, therefore, should be considered to be more representative of a minimum alluvial thickness or an interpretation based on sparse data rather than of an absolute thickness.

As shown in map view (Figure 3-4), the post-Tiva rock units are only sparsely encountered in the modeled area. South of Yucca Wash, these units are typically preserved in wedges on the downthrown sides of faults. For example, in Figure 3-5, a wedge of the post-Tiva unit is shown on the downthrown side of the Solitario Canyon fault.

3.2.4.1.2 Tiva Canyon Tuff (Tpc)

Overview—In the GFM, the Tiva Canyon Tuff (Table 1-1) consists of the Crystal-Rich Member (Tpcr, grouped with post-Tiva rocks) and the Crystal-Poor Member (Tpcp), which is undivided in the GFM, except for the three basal vitric subzones (Tpcpv1, Tpcpv2, and Tpcpv3) and a low-density zone (TpcLD). The Tiva Canyon Tuff makes up most of the exposed bedrock in the modeled area (Figure 3-4). As a result, the Tiva Canyon Tuff is important in hydrologic studies of net infiltration into the UZ.

Unit Geometry—The Tiva Canyon Tuff is thickest in the center of the modeled area and thins to the east, west, and south. Because the top of the formation is eroded over most of the modeled area, a true thickness map cannot be produced. The crystal-poor densely welded vitric subzone (Tpcpv3) is present only in the southwestern part of the area and appears to be distributed as pods or in a web-like pattern (Figure 3-7).

3.2.4.1.3 Paintbrush Tuff Nonwelded Unit (PTn)

Overview—The PTn unit (defined in Table 1-1 in the Rock Properties Model Unit column) is a grouping of rock layers used in hydrologic and thermal-mechanical modeling. Stratigraphically, it consists of the stratigraphic units Tpcpv1, Tpb4, Tpy, Tpb3, Tpp, Tpb2, Tptrv3, and Tptrv2. Because the mostly nonwelded rock units of the PTn unit are distinct from the overlying and underlying welded units, the distribution and thickness of the PTn unit are important in hydrologic modeling.

Unit Geometry—The major formations of the PTn unit, the Yucca Mountain Tuff (Tpy) (Figure 3-8) and Pah Canyon Tuff (Tpp) (Figure 3-9), thicken to the north and northwest but are absent over the southern half of the modeled area. In the southern half of the modeled area, the PTn unit comprises bedded tuffs (Tpb2, Tpb3, and Tpb4) and the vitric units of the lower Tiva Canyon Tuff (Tpcpv1 and Tpcpv2) and the upper Topopah Spring Tuff (Tptrv2 and Tptrv3). In the vicinity of the ESF, the PTn unit is 23 to 76 meters (75 to 250 feet) thick and thickens rapidly to the north to a maximum of more than 168 meters (550 feet). A model-isochore map of this unit is shown in Figure 3-10.

3.2.4.1.4 Topopah Spring Tuff (Tpt)

Overview—The Topopah Spring Tuff encompasses the potential RHH (identified in Table 1-1) as well as lithologically distinct units used in modeling rock properties, mineralogy, and hydrologic

flow. The Topopah Spring Tuff is exposed locally in the northern, western, and southeastern parts of the modeled area, as can be seen in Figure 3-4.

The Topopah Spring Tuff is important for the repository design because it encompasses the potential RHH. The distributions and thicknesses of the densely welded vitric subzones of the Topopah Spring Tuff are important for hydrologic modeling because those subzones have very low porosities and affect hydrologic flow (DOE 1998b, p. 2-38). In addition, the distribution of the Topopah lower densely welded vitric subzone (Tptpv3) is important because it bounds the bottom of the potential RHH. The lithic-rich unit (referred to in the GFM as Tptf) is important for the geologic interpretation of the Topopah Spring Tuff because it provides information on the transition from crystal-poor to crystal-rich units.

Unit Geometry—The Topopah Spring Tuff reaches a maximum thickness of more than 366 meters (1,200 feet) along a northwest-southeast axis located across the vicinity of the ESF (Figure 3-11). The Topopah Spring Tuff thins rapidly toward the northeast, pinching out at the far northeastern corner of the modeled area (Day et al. 1997). To the southeast, the thickness is less than 229 meters (750 feet).

The crystal-rich densely welded vitric subzone (Tptrv1) near the top of the Topopah Spring Tuff is less than 3 meters (10 feet) thick over most of the modeled area, with isolated areas where it pinches out. The vitrophyre (crystal-poor, densely welded vitric subzone) near the bottom of the formation (Tptpv3) is much thicker, ranging from 7 to 35 meters (24 to 114 feet) over the vicinity of the ESF and from 0 to 35 meters (0 to 115 feet) over the total modeled area (Figure 3-12), though it pinches out in the northeastern corner of the modeled area. The thicknesses of both vitrophyre units vary by as much as 300 percent over distances as short as 610 meters (2,000 feet).

The potential RHH (identified in Table 1-1) includes model units RHHtop (representing the lower part of Tptpul), Tptpmn, Tptpll, and Tptpln, within the Topopah Spring Tuff. The thickness of this unit mimics that of the total Topopah Spring Tuff, in that it reaches a maximum thickness of more than 229 meters (750 feet) along the same northwest-southeast axis (Figure 3-13). The thickness of the unit ranges from about 168 to 229 meters (550 to 750 feet) in the vicinity of the ESF and decreases to less than 122 meters (400 feet) to the south. Model unit RHHtop was incorrectly constructed locally at the Prow (Figure 1-3) in the far northwestern corner of the modeled area. As a result, the potential RHH in Figure 3-13f is approximately 12 meters (40 feet) too thick in this small area, and appears thicker than the Topopah Spring Tuff (Tpt) in Figure 3-11. No impact is anticipated on users of the GFM because model unit RHHtop and remaining model units comprising the complete RHH are used for subsurface repository design in the vicinity of the ESF.

3.2.4.1.5 Calico Hills Formation (Ta)

Overview—Outcrops of the Calico Hills Formation occur in the northern part of the modeled area, as well as at one isolated exposure at Busted Butte near the southern boundary of the modeled area. The Calico Hills Formation is lithologically distinct from the overlying Topopah Spring Tuff.

The Calico Hills Formation is important for hydrologic and radionuclide transport modeling because it lies in the flow path between the potential repository and the water table. Over much of the modeled area, the formation has been altered to zeolites and clay, which may retard certain radionuclides (DOE 1998b, p. 2-19).

Unit Geometry—The Calico Hills Formation ranges in thickness from less than 30 meters (100 feet) in the south to more than 457 meters (1,500 feet) in the northeast (Figure 3-14). In the northeast, geologic map data provide only a minimum thickness because the base of the formation is not exposed. In the vicinity of the ESF, the formation thickness ranges from less than 12 meters (40 feet) to greater than 91 meters (300 feet).

3.2.4.1.6 Prow Pass Tuff (Tcp)

Overview—The Prow Pass Tuff is present beneath the entire modeled area, but is exposed at the surface in one small outcrop in the northwestern corner of the modeled area.

The Prow Pass Tuff is important for hydrologic and radionuclide transport modeling because, like the Calico Hills Formation, it lies in the flow path between the potential repository and the water table. It also has, in part, been altered to zeolites and clay, which may retard certain radionuclides (DOE 1998b, p. 2-20).

Unit Geometry—This formation is thickest along a north-south axis through the center of the modeled area, reaching a maximum observed thickness of 194 meters (636 feet) in borehole USW H-4 (H-4) (Figure 3-15). In the vicinity of the ESF, the formation ranges in thickness from less than 91 meters (300 feet) to more than 168 meters (550 feet). The formation pinches out several miles northeast of the modeled area according to geologic map data (Byers et al. 1976); however, the exact location at which the Prow Pass Tuff pinches out is unknown. Although not used as direct input, a regional interpretation (Carr et al. 1986, Fig. 15) shows the pinchout in a similar location.

3.2.4.1.7 Bullfrog Tuff (Tcb)

Overview—The Bullfrog Tuff is present beneath the entire modeled area and is the deepest stratigraphic unit exposed at the surface in the modeled area. It is exposed in one small outcrop in the far northwestern corner of the modeled area.

The Bullfrog Tuff is important for hydrologic and radionuclide transport modeling because part of it lies in the flow path between the potential repository and the water table. In addition, the Bullfrog Tuff has, in part, been altered to zeolites and clay, which may retard certain radionuclides (DOE 1998b, p. 2-20).

Unit Geometry—The Bullfrog Tuff is thickest in the southwestern part of the central modeled area, reaching a maximum thickness of 188 meters (618 feet) in borehole USW G-3 (G-3) (Figure 3-16). In the vicinity of the ESF, the formation ranges in thickness from 113 meters (370 feet) to 165 meters (540 feet). The formation pinches out several miles northeast of the modeled area according to geologic map data (Byers et al. 1976); however, the exact location at which the Bullfrog Tuff pinches out is unknown. Although not used as direct input, a regional interpretation (Carr, et al. 1986, Fig. 14) shows the pinchout in a similar location.

3.2.4.1.8 Tram Tuff (Tct)

Overview—The Tram Tuff is present beneath the entire modeled area, but is not exposed in any outcrop. The Tram Tuff is important for hydrologic and radionuclide transport modeling because part of it lies in the flow path between the potential repository and the water table. In addition, the Tram Tuff has, in part, been altered to zeolites and clay, which may retard certain radionuclides (DOE 1998b, p. 2-20).

Unit Geometry—In the GFM, the Tram Tuff is the thickest of the formations in the Crater Flat Group. It is thickest in a north-northeasterly trending axis over the central part of the modeled area (Figure 3-17), with a maximum thickness greater than 366 meters (1,200 feet) at borehole G-3. In the vicinity of the ESF, it ranges in thickness from about 198 meters (650 feet) to about 341 meters (1,120 feet). The formation pinches out several miles northeast of the modeled area according to geologic map data (Byers et al. 1976). Although not used as direct input, a regional interpretation (Carr, et al. 1986, Figure 11) shows a thickness of more than 250 meters (820 feet) in northern Crater Flat northwest of the modeled area. In the northwestern part of the modeled area, the thickness is constrained only by borehole USW G-2 (G-2). However, this borehole may be located on a buried structural high and may not be representative of the regional trend.

In Figure 3-17, the anomalously thin Tram Tuff at borehole UE-25 p#1 (p#1) (183 meters (601 feet)) is interpreted in this model to be due to faulting. The faulted thickness was used in the model so that all stratigraphic contacts would be honored. (This is true for all faulted contacts, not just for the contact in borehole p#1. If a hypothetical true thickness were used for the Tram Tuff in borehole p#1 and no fault explicitly modeled there, the model would not match the rest of the stratigraphic contacts in the borehole. The thickened Tram Tuff would have forced the other contacts to be out of place. (As described in Section 3.2.3.4, the model is built by thicknesses, not elevations.) No fault was included at this rock layer because no other information about the fault is available. An alternative interpretation is that this fault is the Paintbrush Canyon fault and the Tertiary-Paleozoic contact in borehole p#1 is not the Paintbrush Canyon Fault. In the absence of confirmatory data, the solution that was most consistent with the model construction was selected.

3.2.4.1.9 Older Tertiary Unit (Tund)

Overview—The Tertiary rock units older than the pre-Tram Tuff bedded tuff (Tctbt) are labeled as Tertiary undifferentiated (Tund) in the GFM. Although this unit represents the greatest share of the modeled volume, it is the least known of all the Tertiary units because few boreholes penetrate it.

The older Tertiary unit is important for hydrologic and radionuclide transport modeling because it lies in the flow path between the potential repository and the regional carbonate aquifer in the Paleozoic rocks below. It also makes up a large percentage of the SZ volume beneath Yucca Mountain.

Unit Geometry—The elevation map of the top of this unit is shown in Figure 3-18. The unit thickness was not modeled because it is believed to be entirely dependent on the configuration of

the Tertiary-Paleozoic unconformity. Because the Paleozoic surface was provided as an elevation grid, no model-isochore map (grid) was generated for Tund during the model construction.

3.2.4.1.10 Tertiary-Paleozoic Unconformity

The elevation of the Tertiary-Paleozoic unconformity is important for hydrologic modeling because it forms the top of the regional carbonate aquifer (Carr et al. 1986, p. 6). Alternative interpretations regarding the elevation of this surface are potentially important because of the range of vertical differences between the interpreted surfaces and consequent potential impacts on hydrologic and radionuclide transport modeling. These alternative interpretations are presented in Section 3.2.6. According to the GFM interpretation, which is based on gravity inversion data (Majer et al. 1998), the unconformity occurs 2,438 to 3,553 meters (8,000 to 11,000 feet) below the ESF.

Unit Geometry—The Tertiary-Paleozoic unconformity in the GFM includes vertical displacements along the modeled faults (Figure 3-19), which were not included in the gravity interpretation that served as the input for this model surface. Fault displacements on the Tertiary-Paleozoic unconformity were constructed by matching the vertical displacements of the shallower modeled units and displacing the gravity interpretation accordingly.

The unconformity forms a high ridge beneath Busted Butte and Fran Ridge in the southeastern model area, falling away to deeper levels to the north and west. At its deepest point in the northwest, the unconformity is 3,962 meters (13,000 feet) below ground surface in the GFM. At its shallowest point beneath Fran Ridge, it is 1,067 meters (3,500 feet) below ground surface. It was intersected at a depth of 1,244 meters (4,080 feet) in p#1, the one borehole that penetrates this surface. The deepening to the west can be explained by the combined down-to-the-west vertical displacement of several known north-trending Tertiary normal faults, but may also be enhanced by erosion and displacement on older, unknown faults. The deepening to the north may be a result of caldera deformation, deposition of the thick Tertiary volcanic pile, or older deformations.

3.2.4.2 Interpretation of Faults

This section discusses the interpretation of faults for the GFM. The following subsections discuss the particular features of the faults modeled in the GFM and summarize the results provided in the AMR (CRWMS M&O 1999a, Section 6.4.2).

3.2.4.2.1 Fault Curvature

In the GFM interpretation, the dominant faults were constructed as slightly curved (i.e., dip shallowing slightly with depth) in cross section. The faults could have been depicted with greater curvature; however, in practical terms, the uncertainty of fault geometries at depth outweighs any fine details that could be applied to the modeled faults.

3.2.4.2.2 Fault Patterns

The north-trending fault system (Figure 2-2) dominates the model. The largest of these faults are the Solitario Canyon and Paintbrush Canyon faults, both of which displace strata down to the west by more than 427 meters (1,400 feet). The Windy Wash fault is as large as these, but is present only in the far northwestern edge of the model. Other north-trending faults of note include the Fatigue Wash, Iron Ridge, and Bow Ridge faults, which form major topographic features within the site area. A system of faults beneath Midway Valley produces a series of small horst-graben bedrock structures now buried by alluvium (Day et al. 1997).

Prominent topographic features have also formed along-northwest-trending faults in the site area. A series of northwest-trending faults is present in the prominent drainages (Drill Hole, Pagany, and Sever Washes) in the north-central part of the area. The vertical displacements on these faults are small and, therefore, are not significant at the scale of the model. In the southern part of the area, Dune Wash contains a complex pattern of intersecting north- and northwest-trending faults including the Dune Wash fault, which has a maximum vertical displacement of more than 61 meters (200 feet). The mapped pattern of faults in Dune Wash is complex, so much so that only a few of these faults could be included in the GFM. The actual structure in Dune Wash is, therefore, more complex than represented in the GFM.

3.2.4.2.3 Features of Individual Faults

The Paintbrush Canyon fault (Figure 2-2) is the longest of the faults in the GFM and has the greatest Tertiary vertical displacement. The main strand of the fault passes along the west side of Fran Ridge. The Paintbrush Canyon fault reaches its maximum displacement of approximately 427 meters (1,400 feet) in the model area at the mouth of Dune Wash, where several faults intersect the Paintbrush Canyon fault and increase the total vertical displacement.

The Solitario Canyon fault is a scissor fault that changes dip direction at Tonsil Ridge from west-dipping in the south to east-dipping in the north. The location of Tonsil Ridge is indicated in Figure 1-3. As described in the *Geologic Framework Model (GFM3.1) Analysis Model Report* (CRWMS M&O 1999a, Section 6.2.2.6), this dip change was generalized in the GFM as a single surface. Therefore, interpretations from the model from Tonsil Ridge northward should take this generalization into account, however, the uncertainties regarding fault dips and locations at great depth are expected to outweigh the potential impacts of the generalization.

The Bow Ridge fault (Figure 2-2) is also a scissor fault, with its hinge point covered by alluvium located approximately at the mouth of Sever Wash. North of the hinge point, the Bow Ridge fault is called the "MidE" fault in the GFM (Figure 2-2).

Minor faults, such as the Ghost Dance, Abandoned Wash, and numerous faults around Dune Wash, appear to be secondary features that accommodated strain between the dominant faults. Their intersections with more dominant faults at depth are uncertain; however, the interpretation shown in the GFM is that the Dune Wash, Bow Ridge, and Midway Valley faults intersect the Paintbrush Canyon fault at depth. The Ghost Dance and Abandoned Wash faults do not intersect any major faults in the GFM, but could intersect these faults at deeper crustal levels.

3.2.4.2.4 Faulting and Deposition

In the GFM, model-isochores maps of the Paintbrush Group and older units do not show changes in thickness across faults, although some minor changes could be interpreted from the available data. Geologic map relations (Day et al. 1997) show that isolated thickness changes across faults in Solitario Canyon and Fatigue Wash are associated with pre-Tiva Canyon Tuff faulting. However, the greatest vertical displacements and tilting of the stratigraphic section appear to have occurred after the deposition of the Tiva Canyon Tuff (CRWMS M&O 1998, p. 3.3-3). Thickness changes across faults are, therefore, likely to be relatively small in the Paintbrush Group, but are probably more common than that indicated by currently available data.

3.2.5 Model Uncertainties and Limitations

For the GFM, uncertainty is an estimation of how closely the model matches the real world. The primary factor affecting uncertainty in the GFM is distance from the data points. Because borehole data are restricted in depth, uncertainty increases with vertical distance below the boreholes and in horizontal distance away from them. Likewise, interpretations regarding deeper rock units, which have fewer borehole penetrations, have more uncertainty associated with them than those associated with shallower rock units. Rock layers near the surface are constrained by the geologic map (Day et al. 1997). For example, Figure 3-20 shows the RHH model-isochores and labels the less constrained areas.

Because of the faulting and tilting of the rock layers in much of the modeled area and the sparseness of data, geostatistical techniques were not used to estimate uncertainty. Instead, methods that examine the modeling process were used to determine the amount of uncertainty associated with gridding, contouring, interpreting, and interpolating. The details of these methods are provided in the *Geologic Framework Model (GFM3.1) Analysis Model Report* (CRWMS M&O 1999a, Section 6.5 and Attachment II).

In summary, elevation uncertainty in the geologic model increases with distance from the data points and also is a function of geologic processes such as deposition, faulting, erosion, and postdepositional processes. Uncertainty in the thickness of individual units is a contributing factor to elevation uncertainty and is strongly influenced by the thickness range of a unit and the geologic processes that formed it. The most uncertain areas in the model are its four corners, the less constrained areas, and the volume deeper than the borehole penetrations. For locations between boreholes in the central part of the model (the constrained areas), model predictions and acceptable alternative interpretations would be expected to fall within the following maximum vertical ranges (the window of uncertainty):

- Surface to Tptrv1: ± 9 meters (30 feet)
- Tptrv1 to Tac (includes the potential RHH): ± 12 meters (40 feet)
- Base of Tac to Tctbt: ± 15 meters (50 feet).

In structurally complex areas (such as Dune Wash or Midway Valley) or in areas distant from boreholes, uncertainty can be estimated only qualitatively because of a lack of constraints.

Because each reference horizon and model-isochore in the GFM is an interpretation, each is non-unique, and other viable interpretations are possible. An expected window of uncertainty bounds all interpretations and predictions made by the GFM. It is implicitly recognized that alternative interpretations that fall within this window would also be considered valid and, therefore, changes to the GFM within the expected window of uncertainty would not be considered significant. A significant change to the GFM (or a significant alternative interpretation) would be one that exceeds the expected window of uncertainty.

Finally; it should be noted that appropriate use of the GFM is inherently limited by scale and content. The grid spacing used in the GFM (61 meters or 200 feet), discussed in Section 6.3.2.1 of the *Geologic Framework Model (GFM3.1) Analysis Model Report* (CRWMS M&O 1999a), limits the size of features that can be resolved by the model. Users of the GFM must also consider the data reduction discussed in Section 6.1.1 and the selection of faults discussed in Section 6.1.2 of the *Geologic Framework Model (GFM3.1) Analysis Model Report* (CRWMS M&O 1999a) to determine whether the GFM is appropriate for specific applications.

3.2.6 Alternative Interpretations

One of the principal areas of uncertainty, the interpretation of the Tertiary-Paleozoic unconformity, has led to several alternative interpretations (see CRWMS M&O 1999a, Section 6.4.1.10). Other interpretations of this unconformity have been suggested, including interpretations of gravity data (Majer et al. 1998) and seismic data (Brocher et al. 1998, Figures 7, 8, and 14; Feighner et al., Figure 7b). These interpretations of the unconformity were not used in the GFM because they cannot be reconciled with the geologic map data (Day et al. 1997). These map data indicate a minimum of 335 meters (1,100 feet) of combined vertical displacement in the vicinity of borehole p#1 on the Paintbrush Canyon fault and the fault on the west side of the hill south of borehole p#1. This issue is discussed in detail in the *Geologic Framework Model (GFM3.1) Analysis Model Report* (CRWMS M&O 1999a).

It is recognized that by the inclusion of offsite boreholes (VH-1, VH-2, J#12, and JF#3) and regional data, the methodology can generate viable alternative interpretations that differ from the interpretations presented by GFM3.1. This is especially true in the less constrained areas of the model. Additionally, selection of different modeling techniques (i.e., computer triangulation, hand contouring, or geostatistical methods) or consideration of different data sets could result in viable alternative interpretations. It is also recognized that different methods of extrapolating to offsite boreholes (VH-1, VH-2, J#12, and JF#3) and regional data can result in different model results. The GFM was constructed to allow extrapolations from the model boundaries to the offsite data that are consistent with the trends indicated by the data within the model boundaries and the conceptual model.

The thickness of the Topopah Spring Tuff (Tpt) shown in Figure 3-11 could be alternatively interpreted as thickening into the structural low in Crater Flat. Using this conceptual model, the formation thickness could be shown to increase toward the southwest instead of decreasing as shown in the figure. The thickness of the Topopah Spring Tuff lower vitrophyre (Ttpv3) shown in Figure 3-12 could also be shown to thicken toward the southwest using the same conceptual model, or by using a different interpolation scheme to the data from offsite borehole VH-2, which is 6.4 kilometers (3.9 miles) from the edge of the model and indicates a thick vitrophyre as

discussed in Section 6.4.1.4 of the *Geologic Framework Model (GFM3.1) Analysis Model Report* (CRWMS M&O 1999a). The GFM was constructed to be consistent with the trends shown by borehole and geologic map data within the model boundaries, which suggest thinning toward the west.

In addition, the thickness of both the Tram Tuff (Tct) and the Prow Pass Tuff (Tcp) could be interpreted differently, particularly in the northeast corner of the model. Regional trends could be interpreted to suggest that these tuffs have a more pronounced and abrupt thinning to the northeast beneath the overlying Calico Hills Formation (Ta) than assumed in the GFM. The GFM was constructed to be consistent with the trends shown by borehole data within the model boundaries.

At the time this report was prepared, no other known alternative interpretations to the GFM methodologies or results have been documented.

3.2.7 Model Validation

The GFM was validated by predicting the subsurface geology for two boreholes and one tunnel, and comparing the predictions to the borehole data. The purpose of the validation was to assess whether the GFM provides an adequate representation of the geology of the Yucca Mountain site.

3.2.7.1 Validation Criteria

To assess whether the GFM provides an adequate representation of the geology of the site (CRWMS M&O 1999a), the validation criteria were formulated as follows:

- The model was considered valid if the majority of actual results were within the expected window of uncertainty (as described in Section 3.2.5 of this report and in Section 6.6.1 of the *Geologic Framework Model (GFM3.1) Analysis Model Report* (CRWMS M&O 1999a)).
- For results not within the expected window of uncertainty, the results were analyzed to find a cause. In some cases, anomalous geologic complexities may result in a modeled prediction outside the window but which does not affect the overall model integrity. In such cases, the results did not affect the model validation.
- The model would be considered invalid if the majority of the predictions were not within the expected window of uncertainty and a reasonable geologic cause (i.e., an unpredictable geologic feature) could not be determined.
- Because the GFM was constructed by mapping (predicting) rock layer thicknesses, thickness predictions were given the greatest importance in the validation.

Some anomalous rock layer contacts or structures were expected, given the geologically complex setting of Yucca Mountain on the flank of a major caldera complex, but the model was expected to provide an adequate representation of the total stratigraphic package.

Uncertainty is discussed above in Section 3.2.5 and in Section 6.5 of the *Geologic Framework Model (GFM3.1) Analysis Model Report (CRWMS M&O 1999a)*.

3.2.7.2 Predictions for Boreholes SD-6 and WT-24 and the ECRB Cross-Block Drift

Predictions were made using GFM3.0, which was completed before boreholes SD-6, WT-24, and the ECRB cross-block drift were constructed. The model was then updated to incorporate the new data in GFM3.1 (the current version). The predictions for SD-6 and the ECRB cross-block drift illustrate the predictive capability of the model, and the uncertainty in an area constrained by borehole data, while the predictions for WT-24 are illustrative of a less constrained area.

3.2.7.2.1 Predictions for Borehole SD-6

The predicted depth of stratigraphic contacts for borehole SD-6 and the actual results were compared (Figure 3-21). Of the 26 predicted contact elevations, 22 (85 percent) were within the expected window of uncertainty. In borehole SD-6, the contact elevations not predicted within the expected window of uncertainty were Tpb1, Ta, Tcp, and Tcb. The source of the elevation mismatches was thickness mismatches in two units. As described in the *Geologic Framework Model (GFM3.1) Analysis Model Report (CRWMS M&O 1999a, Section 6.6.2.1)*, model unit Ttpv1 was 7 meters (22 feet) thinner than predicted and unit Ta was 8 meters (24 feet) thinner than predicted. These two thickness errors caused the subsequent elevation prediction errors. In terms of the model validation criteria, the source of the thickness prediction errors for Ttpv1 and Ta must be examined. Like all of the subunits within the Topopah Spring Tuff, unit Ttpv1 formed in response to multiple depositional and post depositional processes. In view of the steep thickness gradient in this area, the prediction error for Ttpv1 in SD-6 is considered to be reasonable.

The Calico Hills Formation (Ta) was 7 meters (24 feet) thinner than expected, which, in view of the model-isochore map (Figure 3-14), is within an acceptable uncertainty range because of the thickness gradient that passes through the area surrounding SD-6.

The cumulative elevation error caused by the thickness differences of Ttpv1 and Ta also affected the elevation prediction at the top of the Prow Pass Tuff, which was 24 meters (80 feet) higher than predicted. The Prow Pass Tuff was only 3 meters (9 feet) thicker than expected, suggesting that the tuff may be on a structural high that formed after deposition of the Prow Pass Tuff but before deposition of the Calico Hills Formation; the Prow Pass Tuff thickness map is given in Figure 3-15. The model shows no effect of a possible pre-Calico structure on the potential RHH (Figure 3-13).

It is important to note that the total Topopah Spring Tuff thickness prediction was within 4 percent of actual, suggesting that the observed thickness variations of the subunits are largely a function of depositional and postdepositional processes operating within the formation. The actual thickness was 315 meters (1,035 feet), and the predicted thickness was 330 meters (1,083 feet).

In summary, the model meets each validation criterion for the SD-6 predictions. Where contact elevations and thicknesses were not predicted within the expected window of uncertainty, the causes can be ascribed to unpredictable geologic features. Because it is relatively well

constrained by surrounding boreholes, borehole SD-6 illustrates the model's predictive capabilities and the effects of geologic variability on model predictions in a constrained area.

3.2.7.2.2 Predictions for Borehole WT-24

Borehole WT-24 was located outside the area constrained by boreholes when it was drilled, and, thus, provides an assessment of uncertainty for the GFM in a less constrained area. In addition, WT-24 is located in an area that is more stratigraphically and structurally complex than borehole SD-6, so the predictions at WT-24 are expected to be less accurate (that is, the window of uncertainty is greater due to geologic complexity and lack of subsurface data). The nearest borehole to WT-24 is approximately 975 meters (3,200 feet) away (borehole G-2; Figure 2-1) and no others are within 1,524 meters (5,000 feet). However, because the subsurface geology in the area surrounding WT-24 and G-2 is stratigraphically complex, WT-24 is more appropriately considered as being in a less constrained area. For evaluation purposes, however, the predictions were compared to the maximum uncertainty windows for constrained areas discussed in Section 3.2.5.

Figure 3-22 shows the predicted stratigraphic depths for borehole WT-24 and the actual results. Only 12 of 24 elevation predictions (50 percent) were within the expected window of uncertainty. However, as discussed in the *Geologic Framework Model (GFM3.1) Analysis Model Report* (CRWMS M&O 1999a, Section 6.6.2.2), the mismatch for the other 12 units is, in part, the result of cumulative errors. The errors in the predicted thickness of 5 model units (Tpp, Tptpul, RHHtop, Tptpmn, and Tptpln) caused elevation errors in all 12 units. The causes of error in each of the five unit thickness predictions are discussed below.

As illustrated in Figure 3-9, the Pah Canyon Tuff (model unit Tpp) thickens toward the north in the area of WT-24. Without the constraint of WT-24, few data are available to constrain the thickness of Tpp in this area, and the thickness is not predictable with a high degree of precision. In this context, the thickness prediction error is reasonable.

The model shows that the way in which the Topopah Spring Tuff units Tptpul, RHHtop, Tptpmn, and Tptpln were formed resulted in variable thicknesses that also are not predictable to a high degree of accuracy. This feature of the geology is believed to be the source of additional cumulative deviation errors. The model-isochores map for the potential RHH (Figure 3-13), which includes units RHHtop, Tptpmn, and Tptpln (and also Tptpll), shows that the thickness changes rapidly in this interval through the area of WT-24. In view of the steep thickness gradient and the variable nature of the units, the thickness prediction errors for these units are reasonable.

It is important to note that the prediction for the Topopah Spring Tuff was thicker than expected. Most of this discrepancy was contributed by the anomalous Tptpln, which was predicted to be absent in the borehole. Without this anomalous unit, the predicted formational thickness would closely match the actual formational thickness minus the thickness of the Tptpln. This small difference suggests that the areal modeling approach is appropriate for the geology of the modeled areas. Observed differences are most likely caused by singular geologic variabilities related to the depositional and postdepositional processes that affected individual rock layers.

The bottom of the Calico Hills Formation was not penetrated in borehole WT-24, even though drilling progressed to more than 91 meters (300 feet) below the predicted depth of the top of the unit. There is no subsurface control for Calico Hills thickness east of borehole G-2; the bottom of Calico Hills is not exposed anywhere to the northeast, so its maximum thickness is unknown. The poor subsurface constraints in the northern part of the modeled area do not permit definition of the maximum expected uncertainty regarding the thickness of the Calico Hills Formation in this area.

In summary, the model meets each validation criterion for the WT-24 predictions. Where contact elevations and thicknesses were not predicted within the expected window of uncertainty, the causes can be ascribed to the unpredictable geologic features. Because it is not well constrained by surrounding boreholes, borehole WT-24 illustrates the geologic variability expected to be found in less constrained areas.

3.2.7.2.3 Predictions for ECRB Cross-Block Drift

Table 3-1 shows the predicted and actual locations of stratigraphy contacts for the ECRB cross-block drift. The vertical difference between predicted and actual stratigraphic contacts was calculated by the transformation of tunnel stations into elevations, correction for stratal tilt, and subtraction of one from the other. Two of the three contacts were encountered within the expected window of uncertainty for these horizons at this location (± 12 meters (40 feet)). In the west end of the tunnel, faults with vertical displacements of 3 meters to greater than 5 meters (10 feet to greater than 16 feet) appear to have caused most of the difference between predicted and actual elevations for the Tptpln contact. Although the faults in the west end of the tunnel were not mapped at the surface, they were not wholly unanticipated because it was known beforehand that structural deformation increases in proximity to the Solitario Canyon fault, and that small faults are present in the mountain. In the ECRB cross-block drift, the Tptpln contact is within 198 meters (650 feet) horizontally of the Solitario Canyon fault. As a result, the prediction error for the Tptpln contact, while outside the expected window of uncertainty, can be explained in terms of geologic variability without affecting validation of the model (the faults are too small to have been included in the model). Had they been known beforehand, the small faults could have been accounted for by adjusting stratigraphic elevations without modeling the faults.

The predictions for the cross-block drift suggest that the GFM will provide predictions of subsurface stratigraphy for future repository tunneling within the expected window of uncertainty. Predictions may be affected on the far western edge near the Solitario Canyon fault and elsewhere if small, unmapped faults like those in the cross-block drift are encountered at other locations.

Table 3-1. Predicted and Actual Stratigraphy for the ECRB Cross-Block Drift

Contact	Predicted Station	Actual Station	Vertical Difference
Tptpmn (top)	10+78	10+15	7 meters (23 feet)
Tptpll (top)	15+21	14+44	8 meters (26 feet)
Tptpln (top)	24+10	23+26	23 meters (75.5 feet)

NOTE: ECRB = Enhanced Characterization of the Repository Block

3.2.7.2.4 Validation Results

The predictions of subsurface geology made using GFM3.0 for boreholes SD-6 and WT-24 and the ECRB cross-block drift were used to validate the GFM. The results show that the preponderance of subsurface stratigraphy was predicted within the expected window of uncertainty, and the model satisfied all validation criteria. Predictions that lay outside the window of uncertainty can be explained in terms of geologic variability and were not the result of deficiencies in the model. Because a certain amount of geologic variability was known to be an inherent part of Yucca Mountain and some anomalies were anticipated, the results of the predictions are considered to demonstrate that the GFM provides an adequate representation of the geology of Yucca Mountain.

3.3 ROCK PROPERTIES MODEL

This section provides a summary description of the Rock Properties Model Version 3.1 (RPM3.1). A more detailed discussion can be found in the *Rock Properties Model (RPM3.1) Analysis Model Report* (CRWMS M&O 1999b).

3.3.1 Introduction

The RPM is a description of the distributions of rock material properties, including matrix porosity, whole-rock bulk density, matrix-saturated hydraulic conductivity, lithophysal porosity, and whole-rock thermal conductivity for many of the stratigraphic units described in the GFM. The manner in which these properties are modeled, and a summary of the results, are described in the following subsections. The software QA documentation, planning documents, modeling implementation procedures, and scientific notebooks for the RPM are described in the *Rock Properties Model (RPM3.1) Analysis Model Report* (CRWMS M&O 1999b, Sections 2 and 3).

3.3.2 Summary of Data Inputs and Model Software

This section summarizes the inputs and software used to construct the RPM. Additional details can be found in the *Rock Properties Model (RPM3.1) Analysis Model Report* (CRWMS M&O 1999b, Section 4.1).

3.3.2.1 Inputs

This section provides a brief summary of the input data from the *Rock Properties Model (RPM3.1) Analysis Model Report* (CRWMS M&O 1999b, Section 4.1).

Seven different classes of data were used as input to the RPM. The first four categories are based on actual measurements of rock material properties in the laboratory or on geophysical measurements obtained in the field. The fifth group is also derived from in situ geophysical measurements. However, because it is sufficiently different from the four previous groups, and is used for a different purpose, it is discussed separately. The remaining two classes of input data are self-explanatory:

- Laboratory core porosity data
- Computed petrophysical porosity data

- Laboratory-measured secondary property data
- X-ray diffraction (XRD) indicators of mineral alteration
- Petrophysical indicators of hydrous-phase mineral alteration
- Observed (measured) lithostratigraphic contacts
- Modeled lithostratigraphic contacts.

3.3.2.2 Assumptions

In the context of this PMR, assumptions are those assertions that influence data or input parameters. For the RPM, an assumption was made that there is a correlation between porosity and other rock properties, and that this correlation could be used to derive other input data using porosity as a surrogate. This assumption is discussed in Section 5 of the *Rock Properties Model (RPM3.1) Analysis Model Report (CRWMS M&O 1999b)*.

In addition to assumptions, the RPM uses certain methodological premises upon which the model construction is founded. These are the use of stratigraphic coordinates and conditional Monte Carlo simulation. Details of the application of these assumptions and methodologies are provided in Section 3.3.3.

3.3.2.3 Software

The RPM was constructed using selected GSLIB (geostatistical subroutine library) modules and software routines to produce the geostatistical models. During the construction of the model, the software was used as intended by its developers. Additional information about the software and its qualification can be found in the *Rock Properties Model (RPM3.1) Analysis Model Report (CRWMS M&O 1999b, Section 3)*.

3.3.3 Construction of the Model

This section presents a conceptual description of the approach used in the geostatistical modeling and a brief discussion of how this stochastic material property models fit into the overall performance modeling of the Yucca Mountain site. The methodology is described in greater detail in the *Rock Properties Model (RPM3.1) Analysis Model Report (CRWMS M&O 1999b, Section 6)*.

3.3.3.1 Conceptual Model

3.3.3.1.1 Causes of Heterogeneity

The conceptual model applied to the RPM uses the fact that the lithologic units at Yucca Mountain were produced by relatively widespread, but temporally variable, geologic processes. In particular, the volcanic activity responsible for the formation of Yucca Mountain was episodic with thick, widespread ash deposits produced by nearly instantaneous (in terms of geologic time) eruptions separated by thin inter-eruption deposits that probably represent much longer intervals of time. If the time represented by a progressively accumulating geologic deposit is considered to be preserved in the vertical dimension, then the resulting conceptual model is one of

successive subhorizontal layers that may be broken and tilted or folded and otherwise moved about at some later time.

As described in Section 3.2.3, the GFM component of the ISM provides such a layered representation of Yucca Mountain. However, further refinements are necessary to account for heterogeneity. Geologic studies of the volcanogenic rocks at Yucca Mountain, and of similar deposits elsewhere in the world, indicate that the geologic processes responsible for deposition of these materials vary temporally and areally. For example, variations in cooling rates caused by local conditions affect the material properties in the resultant rocks. This spatial variation of process has produced spatial heterogeneity of material properties in all three dimensions. However, the spatial distribution of material properties within geologic layers is not simply random. Knowledge of property values at one location imposes limits on the values of those properties likely to exist at nearby locations.

3.3.3.1.2 Geostatistical Methods

Geostatistical simulation comprises a large class of modeling techniques that can produce very complex and, therefore, presumably highly realistic numerical representations of spatially variable properties. Simulation may be thought of as expanding the actual information available in a stochastic manner that also is compatible with additional information derived from the data ensemble and the spatial context of those data. The process builds on the geologic assumptions that unsampled locations near a known value will tend to resemble that value, whereas unsampled locations at increasing distances from a known value tend progressively to resemble that value less and less. This intuition is observed statistically across a suite of several equiprobable simulations.

The philosophical framework of simulation is simple. Using concepts of random variables, a model of the probability density function (*pdf*) can be developed for a material property of interest at all locations in space. By transforming the measured data to their respective positions on the probability density function and using simple kriging (Deutsch and Journel 1992, pp. 62 and 137), the desired *pdfs* can be made conditional to a set of measured values. Alternative realizations are simply generated by sampling from these *pdfs*. The variance of individual, location-specific *pdfs* will vary with the amount of geologic uncertainty. Near conditioning data (Figure 3-23c), the *pdf* associated with an unsampled location will be relatively narrow. Where less information is known, such as away from data or in the vicinity of conflicting measurements, the *pdf* will be relatively broad (Figure 3-23a, b), leading to generation of a wide range of likely values across a suite of realizations. Because the underlying kriging algorithm used to derive the *pdfs* is an exact interpolator, the *pdf* degenerates to a spike with probability = 1 at a measured location (Figure 3-23(d)).

The current approach to modeling rock properties (as part of the ISM) strikes a balance between a simple hollow-shell geologic framework model and the near-infinite complexity of the real world. Geostatistical methods, in general, are one of a variety of methods for distributing isolated measurements of different attributes in space and, thus, for modeling spatial heterogeneity. Selected major lithostratigraphic horizons are used as the constraining (framework) boundaries for a statistically based description of the measured rock material

properties that were sampled within those boundaries. Geostatistical methods were used to create the material property descriptions constituting the RPM.

Geostatistical simulation places principal emphasis on reproducing the input data values and the overall statistical character (including the spatial correlation characteristics) exhibited by the data ensemble (i.e., the total collection of input values). Models produced by geostatistical simulation typically do not grade smoothly between measured data values; rather, they are highly variable yet they represent the broad heterogeneity structure of the measurements. These techniques are conceptually equivalent to the Monte Carlo simulation process frequently used in engineering analyses. In common with other Monte Carlo simulation approaches, the emphasis is less on the specific predicted values (which are in effect simply the products of a random number generator with certain desirable properties) than on evaluation of the uncertainty associated with performance measures computed to represent the behavior of the modeled system. A schematic diagram, Figure 3-24, illustrates the geostatistical process for combining the statistical description of the geology with the Monte Carlo generation of multiple replicate models.

3.3.3.2 Modeling Techniques

This section summarizes the geostatistical modeling techniques used to produce the rock properties models, including reference to the various computer codes and software routines that generated the models. Sequential Gaussian simulation is used to generate the primary porosity models, whereas linear coregionalization is used to generate the derivative models of secondary properties. This is accomplished by using porosity values as a surrogate for the additional rock properties (i.e., they are derived from porosity). The concept of porosity as a surrogate is based on empirically observed correlations of porosity with the relevant secondary properties. This method was applied to estimate material properties that typically are of greater interest in performance modeling than porosity itself. These other material properties were generally undersampled at Yucca Mountain. The process of indicator kriging is used to produce the model of hydrous-phase mineral alteration that constrains the distribution of the derivative models of saturated hydraulic conductivity in two of the model units. Indicator kriging is a variant of ordinary kriging, in which the variable of interest is estimated as a weighted linear combination (average) of the available observed values within some local neighborhood of influence. In common with ordinary kriging, the weights applied to the observed values are calculated in accordance with the spatial continuity model developed from the combined indicator dataset.

Each major lithologic interval selected for modeling has been modeled in a stratigraphic coordinate system that reflects the original, pre-faulting depositional continuity of these deposits (Figure 3-25). Stratigraphic coordinates use the same east-west and north-south coordinates (Nevada State Plane coordinate system, defined in feet) as the borehole from which the relevant data were obtained. However, the vertical coordinate of a sample is represented as the relative fractional position of that sample within the thickness of the entire unit at that horizontal location. The stratigraphic coordinate concept effectively removes the effects of depositional thinning away from the source volcanic vent(s) and of postdepositional tilting and deformation and, therefore, it positions samples from equivalent portions of the overall unit at the same nominal internal position within a rectangular volume.

The RPM was constructed on grids with a 200- by 200-meter (656- by 656-foot) horizontal node spacing and variable vertical node spacing. Additional details on grid construction are provided in the *Rock Properties Model (RPM3.1) Analysis Model Report* (CRWMS M&O 1999b, Section 6.4.6).

The form of simulation applied by the RPM is conditional simulation. Conditional simulations are numerically anchored to a specific set of real-world data, and they exhibit three properties that add to their usefulness in evaluating the effects of geologic uncertainty on physical process models. The beneficial properties of the conditional simulations are that they:

- Reproduce known data values at the same locations within the model as those represented by real-world samples
- Reproduce the full range of measurement variability represented by the univariate descriptive statistics of the known data values
- Reproduce the bivariate statistics (i.e., two-point spatial correlation structure, of the input data).

The RPM generated 50 replicate models of porosity at all unsampled locations for each of the four model units, conditioned to the observed porosity data from the input boreholes. The sequential modeling process for these 50 porosity models was implemented as follows:

1. All data values were converted to positions on a univariate standard-normal ($\mu = 0$, $\sigma^2 = 1$) distribution using a graphical normal-score transform as illustrated in Figure 3-26. This transformation does nothing to the spatial correlation structure because the relative positions of all values with respect to each other are preserved (i.e., the transform is quantile-preserving).
2. The spatial correlation structure was identified using the normal-score transformed values and modeled using standard variography.
3. The transformed measured data were mapped into the model volume; samples located (only fortuitously) at a node in the stratigraphic coordinate grid were assigned to that node and the node was not simulated.
4. A sequential random path, which will visit each unsampled node once and only once was defined.
5. At each node along this path, a search was conducted for nearby data and any previously simulated grid nodes. The search parameters (anisotropic radii; number of data to use) are user specified.
6. The closest data were identified and weighted by their geological distance (in contrast to their Euclidean distance), as defined in the stratigraphic coordinate system according to the mathematical formulation of the spatial continuity model (variogram). Because the normal-score transformed values are relative positions on a cumulative distribution

function, the resultant value is also a relative position on the same cumulative distribution function.

7. A value (in normal-score space) was drawn at random from the conditional probability distribution defined in step 6, and this value is assigned to represent the porosity at that point. The simulation process then moves to the next unsampled location along the random path defined in step 4, and the process was repeated beginning with step 5.
8. After all originally unsampled grid nodes were simulated using the logic of steps 5 through 7, the resulting spatial array of normal-score values were back-transformed to the original porosity space using the inverse of the normal score transform of step 1. At this point, the simulation process is complete.

Because porosity values are drawn at random for each unsampled grid node, the values obtained in different simulation runs will be different. Indeed, the weighting scheme used to develop the conditional expectation in each independent simulation will be different, as well, because the same path through the 3-D grid is not used in successive simulations. Additionally, because the data search process considers previously simulated grid nodes as well as measured data (nonvarying), the nearby values used to estimate the conditional expectation also will vary among simulation runs. At grid locations that are well constrained by consistent measured data, the variability of the simulated values across a suite of simulations will be small, as described by the spatial continuity model. However, at grid locations far from any conditioning measured data, or at grid nodes that are in the vicinity of conflicting measurements, the spread of porosity values that will be generated by the simulation algorithm across different computer runs will be broad, approaching the univariate variance of the data when considered without regard for spatial position. Uncertainty, measured by variability across the suite of simulations, is small where much is known about the rock mass, and it becomes progressively greater at longer distances from actual sampled values.

3.3.3.3 Modeling of Hydrous-Phase Mineral Alteration

Volcanic glass within the lower two modeling units (CHn and Tcp) was variably altered to (dominantly) zeolite minerals throughout a major portion of the model area. These altered rocks exhibit markedly reduced saturated hydraulic conductivity in comparison with unaltered materials of approximately the same porosity. The rock properties modeling effort attempted to include XRD mineralogic data, which provide virtually 100 percent certain identification of hydrous-phase mineral alteration, and the less accurate but more abundant and widely distributed petrophysical indicators of such alteration.

3.3.3.3.1 Calibrating Soft Indicators of Hydrous-Phase Mineral Alteration

Because the available petrophysical data provide a less-than-100 percent certain identification of the hydrous-phase alteration, it was necessary to calibrate these values to account for the added uncertainty. The calibration effort involved samples from the CHn and Tcp model units for which depth-matched pairs of both XRD mineral analyses and petrophysical bound-water contents could be obtained. Core bound-water content was computed as the difference between the oven-dried and relative humidity porosity values, and is initially identical to the

delta-porosity value described in the *Rock Properties Model (RPM3.1) Analysis Model Report* (CRWMS M&O 1999b, Section 6.4.5.1). Petrophysical bound-water content was computed as the difference between the total porosity and effective porosity log traces (the petrophysical derived porosity values corresponding to oven dried and relative humidity, respectively). Comparison of depth-matched core and petrophysical bound-water data indicates that the laboratory core measurement process gave a bound-water content of approximately twice that indicated by the down-hole petrophysical measurements (Figure 3-27). Although a precise explanation for the discrepant measurements is uncertain, the empirical relationship can be used to adjust the core measurements to provide a common basis with the petrophysical values. Adjusted values for core bound-water content have been used in the calibration work that follows.

Figure 3-28 presents a scatterplot of total hydrous-phase mineral content versus adjusted bound-water content. In general, an increase in adjusted bound-water content corresponds directly to an increase in total hydrous minerals. The calibration consists of cross-tabulating the number of pairs in each of the categories:

- Hydrous-phase mineral content:
 - Greater than 5 percent
 - Less than or equal to 5 percent.
- Adjusted bound-water content:
 - Less than or equal to 0.03
 - Greater than 0.03 to less than 0.04
 - Greater than 0.04 to less than 0.05
 - Greater than 0.05.

The cross-tabulated counts of soft-value pairs were converted to a decimal proportion, and these values were taken as the prior probability of obtaining the specified total hydrous-phase mineral content given a specified adjusted bound-water content. The derivation of these soft, prior-probability values is discussed in the *Rock Properties Model (RPM3.1) Analysis Model Report* (CRWMS M&O 1999b, Section 6.4.7). In contrast, XRD hydrous-phase mineral contents were coded as hard probability values of zero or one.

3.3.3.3.2 Indicator Kriging of Hydrous-Phase Mineral Alteration

Both hard and soft indicators of hydrous-phase mineral alteration were combined and supplied as input for indicator kriging. As before, indicator kriging is a variant of ordinary kriging, in which the variable of interest is estimated as a weighted linear combination (average) of the available observed values within some local neighborhood of influence. In common with ordinary kriging, the weights applied to the observed values are calculated in accordance with the spatial continuity model developed from the combined indicator dataset. Necessarily, alteration in the CHn and T_{cp} model units was modeled separately, even though the two units were combined for purposes of estimating the prior probability values discussed above.

CHn Model Unit—The variogram model for hydrous-phase mineral alteration in the CHn model unit is presented in Figure 3-29, and the parameters of the fitted variogram model are given in Table 3-2.

Tcp Model Unit—The variogram model for hydrous-phase mineral alteration in the Tcp model unit is presented in Figure 3-30. The parameters of the fitted variogram model are given in Table 3-2.

3.3.3.4 Postprocessing of Simulated Models

3.3.3.4.1 Incorporation of Specific Attributes Into Simulated Models

The actual rocks at Yucca Mountain are the composite result of numerous geologic processes that overlap in space and time. Consequently, rock properties modeling involves more than the simple generation of a set of porosity values. This is particularly true for the models of derivative material properties that have been generated by coregionalization with porosity. This section presents the techniques used to incorporate two specific types of secondary geologic attributes into the raw simulated property models.

Vitrophyres—The widely variable hydraulic conductivity values associated with the densely welded vitrophyric core samples of the Topopah Spring Tuff (lithostratigraphic units Tptrv1 and Tptpv3) have been described by Flint (1998, p. 38) as resulting from microfractures present within these glassy, brittle rocks. Additional consideration of these samples (Flint 1998, Figure 12) suggests that vitrophyric samples may independently be identified by their uniformly very low porosity (less than approximately 0.05; CRWMS M&O 1999b, Section 6.4.5.1, Figure 21). Accordingly, the simulated models of saturated hydraulic conductivity for the TSw model unit were postprocessed so that if the corresponding porosity value was less than 0.05, the coregionalized hydraulic conductivity value was discarded. Under the assumption that such low-porosity grid nodes represent vitrophyre or other essentially nonporous brittle materials, a saturated hydraulic conductivity value (K_s) was generated by random sampling from a uniform population with a range of 10^{-14} to 10^{-6} m/sec. A conceptual representation of the logic underlying the modeling of vitrophyric rock units is presented in Figure 3-31.

Hydrous-Phase Mineral Alteration—Hydrous-phase mineral alteration is inferred to represent a secondary alteration process that affected vitric tuffaceous materials at some time after formation of the original rock mass, although generally before tectonic faulting and tilting. Consequently, there appears to be little or no direct correlation of saturated hydraulic conductivity with matrix porosity for altered (zeolitized) samples (CRWMS M&O 1999b, Section 6.4.5.1, Figure 20). The histogram of altered hydraulic conductivity values appears virtually indistinguishable from a Gaussian population.

Table 3-2. Variogram Parameters for Spatial Continuity Model, Alteration in the CHn and Tcp Model Units

Nest No.	Model Type	Range (feet)			Sill	Rotation Angle (degrees)			Anisotropy Ratio	
		Maximum (horizontal)	Intermediate	Minimum (vertical)		1	2	3	1	2
CHn Model Unit										
—	Nugget	—	—	—	0.005	—	—	—	—	—
1	Spherical	4,000	1,500	30	0.010	0	0	0	0.3750	0.0075
2	Spherical	7,000	4,000	500	0.035	0	0	0	0.5714	0.0714
Tcp Model Unit										
—	Nugget	—	—	—	0.010	—	—	—	—	—
1	Spherical	2,500	2,500	150	0.025	0	0	0	1	0.060
2	Spherical	15,000	15,000	150	0.058	0	0	0	1	0.010

This modeling philosophy has been implemented for the RPM by postprocessing the initial coregionalized hydraulic conductivity models (for both the CHn and Tcp model units) grid node by grid node, together with a corresponding indicator kriging model (Section 3.3.3.2) indicating the probability of significant hydrous-phase mineral alteration. If the grid node under consideration was considered unaltered (probability of alteration less than 0.5), the coregionalized K_s value was retained, and the processing moved to the next grid node. If the node was considered altered (probability of alteration greater than 0.5), then the coregionalized K_s value was discarded in favor of a normally distributed random value sampled from a population with the appropriate mean and variance. A schematic diagram of this postprocessing procedure is presented in Figure 3-32.

3.3.3.4.2 Uncertainty Modeling

As part of the current modeling exercise, 50 replicate, statistically indistinguishable models of porosity for each model unit (one set each for matrix and lithophysal porosity in the TSw model unit; see Section 3.3.3.2) and 50 replicate models for each one of the derivative properties (bulk density, matrix-saturated hydraulic conductivity, and thermal conductivity for the TSw model unit, were generated. Each of the replicate simulations honors the measured porosity data at the sample locations (subject to the discretization limits), and exhibits the full range of variability captured by the histogram of the relevant property, the appropriate range of spatial correlation, and (for the derivative properties) the appropriate correlation coefficient with porosity. In effect, there is nothing objective about any single simulated (or coregionalized) model to prefer it over any other model of that suite. The only meaningful distinguishing feature within a suite of replicate models is the arbitrarily selected random number seed that was used to initiate the simulation process.

Because there are few, if any, objective differences to distinguish the members of each suite of simulated property models, thus, it follows logically that the variability among members of a

suite represents an empirical estimate of the geologic uncertainty associated with each material property. Geologic uncertainty, in this context, is defined as the uncertainty that results from less-than-exhaustive sampling or other measurement. The difficulty arises, however, as how best to represent this uncertainty in a simple and concise manner.

An uncertainty model has been generated for each material property-modeling unit combination by computing the node-by-node standard deviations for each set of 50 replicate models. This process produces uncertainty models that are themselves spatially heterogeneous. By theory and in practice, variability among simulations—and uncertainty, as defined by the standard deviation—is small in close proximity to measured sample values. Variability among simulations and uncertainty are high at great distances from measured data, or in the vicinity of conflicting measured values. Values such as the total range of the modeled property or the interquartile range could also be computed during this postprocessing step.

With respect to alternative uncertainty models, it is also important to remember that the best measure of geologic uncertainty for the potential nuclear waste repository at Yucca Mountain is the impact of that uncertainty on some relevant measure of repository system performance. Potential examples of such global performance measures might be particle or radionuclide transport rates. Development of these types of comprehensive uncertainty assessments is beyond the scope of the rock properties modeling effort.

3.3.3.4.3 "Expected-Value" Modeling

A set of summary expected-value models, referred to as E-type estimates, has been generated for each suite of simulated models by computing the arithmetic mean of the 50 replicate simulated values generated at each grid node. Because of the logistical difficulty of presenting the full simulated results for 50 models times 19 unique material property-model unit combinations, the results of this geostatistical modeling exercise (described in Section 3.3.4 below) are presented in terms of an E-type estimate. The first characteristic, that involving reproduction of the measured (porosity) values at the actual measurement locations, is maintained. However, the ensemble of modeled E-type values no longer represents the full range of univariate variability of the measurement ensemble (the second characteristic). Additionally, the two-point spatial correlation character (variogram) of the E-type model no longer reproduces that of the underlying measurements (the third characteristic). Specifically, because of averaging across the replicate simulations, the E-type model typically grades relatively smoothly and continuously from one (exactly reproduced) measured value to the next (in three dimensions) as opposed to individual simulations. Thus, the apparent spatial continuity of the E-type model typically is much greater than that observed for the data. This is the smoothing effect that is typical of virtually all interpolation (in contrast to simulation) algorithms, including kriging, nearest-neighbor estimation, and inverse-distance-to-a-power weighting.

3.3.4 Model Results

This section presents illustrative examples of the results and discusses generalized heterogeneity features as revealed by the summary E-type models. An additional discussion of the results can be found in the *Rock Properties Model (RPM3.1) Analysis Model Report* (CRWMS M&O 1999b, Section 6.5). Each model unit and each modeled material property within that

model unit is discussed. A general discussion of each realization of the simulated model is provided in the model validation section (Section 3.3.7).

Cross sections through each of the summary E-type models indicate substantial vertical and lateral heterogeneity within each of the four model units. The E-type models show material properties that are broadly compatible with the conceptual model (Section 3.3.3.1) of layered volcanic stratigraphy at Yucca Mountain.

3.3.4.1 Paintbrush Tuff Nonwelded Unit (PTn)

Heterogeneity of the matrix porosity within the PTn model unit is shown in Figure 3-33 in both stratigraphic and Nevada State Plane coordinates. As indicated by the projection arrows connecting the two halves of the figure, the vertically exaggerated rectangular volume in stratigraphic coordinates is back-transformed to Nevada State Plane coordinates. Thus, the material property values assume their correct relative positions within the tilted and faulted strata of Yucca Mountain. Cross-sectional views of porosity heterogeneity are presented in Figure 3-34.

Porosity values within the PTn model unit generally are high, varying from about 30 percent to more than 60 percent. A region of low porosity (approximately 10 percent), present in the southwestern portion of the model area, is associated with borehole H-6. Porosity values appear to be relatively continuous over distances of about 1,524 to 3,048 meters (5,000 to 10,000 feet), as expected from the input range of the spatial continuity. Porosity trends are primarily anisotropic from northwest to southeast, also as expected from the variogram model (top surface of the block diagram of Figure 3-33).

Generally, bulk density (Figure 3-35) varies spatially as an inverse of porosity, as expected from the strong negative correlation coefficient of -0.912. Bulk density values vary from less than 1.0 g/cm³ to nearly 2.0 g/cm³, though densities are generally low across the modeled area. Prominent regions of higher density are associated with borehole H-6, shown on the southernmost east-west cross section, and particularly with borehole G-2 near the northern boundary of the modeled region at the intersection of the north-south and northernmost east-west cross sections. At borehole G-2, the density exceeds 1.9 g/cm³ at two horizons, presumably corresponding to the Pah Canyon and Yucca Mountain Tuffs, which are moderately welded in this part of the model area.

Heterogeneity in matrix-saturated hydraulic conductivity values is shown in Figure 3-36. Hydraulic conductivity values generally are between 10⁻⁵ and 10⁻⁷ m/sec. Note that in this figure and in the similar figures following, hydraulic conductivity values are shown in log₁₀ units; e.g., 10⁻⁷ m/sec = -7.0. Lower conductivities, on the order of 10⁻⁸ m/sec, are modeled in the vicinities of boreholes H-6 and G-2. These values are coincident with the lower matrix porosities in these regions from which the hydraulic conductivity values are coregionalized.

3.3.4.2 Welded Topopah Spring Tuff Unit (TSw)

The heterogeneity of material properties within the TSw model unit is presented in Figures 3-37 through 3-43. Note that matrix porosity, as indicated in Figures 3-37 and 3-38, is very low, mostly less than 10 to 15 percent, and relatively constant in magnitude across the entire modeled

region. This minimal variability is consistent with the definition of this unit as densely welded tuff. However, the front face of the block diagram, shown in stratigraphic coordinates in Figure 3-37, and the cross-section views of Figure 3-38, indicate that increased matrix porosity is associated with the major lithophysae-bearing intervals within the unit, most particularly with what, in the GFM, would be the vapor-phase-corroded crystal-rich nonlithophysal interval near the top of the unit.

The heterogeneity in lithophysal porosity is shown in stratigraphic (Figure 3-39) and in Nevada State Plane (Figure 3-40) views. Lithophysal porosity generally is low in this welded unit compared to the porosity of a nonwelded tuff such as the PTn model unit. However, maximum porosity values within the lithophysal intervals still locally exceed 30 to 35 percent. Figure 3-40 clearly indicates two such intervals of high porosity, corresponding approximately to the upper and lower lithostratigraphic units (Ttpul and Ttpll). These are separated by an interval of low-porosity (on the order of 10 percent) equivalent to the middle nonlithophysal lithostratigraphic unit (Ttpmn). Note, however, that there is a fairly large amount of lateral heterogeneity within each of the elevated porosity intervals. This is caused by the measured porosity data as propagated away from borehole locations by the spatial continuity model and produces both the apparent layering and the variations within those layers. There are no detailed lithostratigraphic (or other) subunits explicitly modeled within the TSw model unit. All property heterogeneity in the RPM is a function strictly of the measured material properties.

Bulk density heterogeneity, illustrated in Figure 3-41, is coregionalized from lithophysal porosity. Density values typically are above 2.0 g/cm^3 throughout most of the relatively lithophysae-free region. Bulk density is particularly high (approaching 2.5 g/cm^3) in the lower parts of the TSw model unit, as indicated by the red colors. A prominent, high-density interval is associated with the lower vitrophyre in the central part of the modeled region (approximately corresponding to lithostratigraphic unit Ttpv3). However, bulk-rock density values associated with the upper lithophysal horizon, in particular, may be as low as 1.5 to 1.8 g/cm^3 . The alteration of lithophysal and nonlithophysal intervals is clearly represented through the bulk density model.

Thermal conductivity also is coregionalized from lithophysal porosity in an effort to predict the thermal conductivity of volumes of rock influenced by the presence of lithophysal cavities 0.1 meter or larger in diameter. Figure 3-42 presents the E-type model of spatial heterogeneity in thermal conductivity. High values of thermal conductivity (greater than approximately 1.3 to 1.4 W/m-K and shown in yellow and orange tones) are associated with the lower portion of the TSw model unit and with the presumed low-lithophysae "middle nonlithophysal" lithostratigraphic unit (Ttpmn). Particularly high thermal conductivity values, approaching 1.5 W/m-K , are present at the base of the TSw unit, presumably associated with the densely welded vitric lithostratigraphic unit. In contrast, the portions with the highest lithophysal content, containing lithophysal cavities up to a meter in diameter, appear to be characterized by bulk-rock thermal conductivities less than 1.0 W/m-K (blue and blue-green colors in Figure 3-42).

Heterogeneity in matrix-saturated hydraulic conductivity is presented in Figure 3-43, and is coregionalized from the matrix porosity model shown in Figures 3-37 and 3-38. Matrix conductivities are less than 10^{-11} m/sec through much of the lower part of the model unit. As

expected from the higher matrix porosity values associated with the lithophysae-bearing portions of the TSw model unit, matrix hydraulic conductivity values are markedly higher, 10^{-9} to 10^{-10} m/sec (yellow to green tones), in these vapor-phase-altered portions of the unit. Some of these higher conductivity values may also be associated with vapor-phase corrosion of the welded tuff within the crystal-rich nonlithophysal unit. Note, however, that matrix hydraulic conductivity does not include conductivity that is attributable to flow through lithophysal cavities.

3.3.4.3 Calico Hills Nonwelded Unit (CHn)

Variations in the matrix porosity of the CHn model unit are presented in Figures 3-44 and 3-45. Porosity values generally are high (20 to 40 percent) throughout the unit, particularly in contrast to the low porosity values typical of the overlying TSw model unit (10 to 15 percent). An expansion of the porosity color scale indicates that a mass of particularly high porosity occupies the central portion of the modeled volume. Porosity values locally approach 50 percent within this region.

Variations in bulk density in the CHn model unit are presented in Figure 3-46. Density values vary from less than 1.3 g/cm^3 to more than 2.0 g/cm^3 , depending on location, although the majority of this nonwelded unit exhibits limited variation in bulk density at 1.5 to 1.75 g/cm^3 . Generally speaking, bulk density varies inversely with porosity, as anticipated from the coregionalization relationship.

Heterogeneity in the matrix-saturated hydraulic conductivity for the CHn model unit is shown in Figure 3-47. Although hydraulic conductivity is derived by coregionalization with matrix porosity, the relationship between the two material properties is not precisely straightforward because of the presence of hydrous-phase mineral alteration (predominantly zeolitic) within the unit. Matrix conductivities typically are 10^{-6} to 10^{-7} m/sec (greens to reds) within the unaltered portion of the CHn, and typically less than 10^{-11} m/sec elsewhere (blue). The block diagram in the upper part of Figure 3-47 indicates that vitric (to devitrified) materials are limited to the upper portion of the model unit, and more particularly to the southwestern portion of the modeled volume. The overall impression is of a wedge of vitric (unaltered) material tapering to a feather edge toward the northeast. Zeolitic (altered) rocks are shown in tones of blue underlying and replacing the green- through red-colored volume to the north. Recall that the saturated hydraulic conductivity of altered samples is essentially uncorrelated with matrix porosity. The lower portion of Figure 3-47 presents cross-sectional views of the hydraulic conductivity field within the model unit and illustrates some of the complex interfingering relationships of altered and unaltered rock types.

3.3.4.4 Prow Pass Tuff (Tcp)

Figures 3-48 and 3-49 present the spatial heterogeneity of matrix porosity within the Tcp model unit. Because the Prow Pass Tuff is mostly nonwelded, the porosity values typically are high, varying from 20 to nearly 40 percent across large volumes of the model. Lower porosity values, typically less than 15 percent, are evident along the northern boundary of the modeled volume. Lower porosity values also occur as a poorly defined lobate mass generally low within the

central-eastern part of the region. This may correspond to the "moderately welded" portion of this unit.

Variations in bulk density, shown in Figure 3-50, substantiate the variations in porosity described in the preceding paragraph. Densities well in excess of 2.1 g/cm^3 are prominently displayed along the northern boundary of the model in the vicinity of borehole G-2. High densities on the order of 2.0 g/cm^3 are also visible in the east-central portion of the block, corresponding to the low-porosity lobe. Elsewhere across the modeled volume, bulk densities are between 1.75 and 2.0 g/cm^3 (shown in green colors).

Heterogeneity in matrix-saturated hydraulic conductivity is presented in Figure 3-51. In a manner similar to the overlying CHn model unit, a bimodal distribution of conductivity values that corresponds to altered and unaltered rock types is quite prominent. Lower hydraulic conductivity values, typically less than 10^{-10} m/sec , are associated with regions affected by hydrous-phase mineral alteration. Markedly higher values of hydraulic conductivity, varying from 10^{-10} to 10^{-7} m/sec , are associated with the vitric-to-devitrified continuum of matrix porosity values in regions unaffected by alteration. The block diagram in the upper portion of Figure 3-51 indicates that the upper and lower margins of the Prow Pass Tuff essentially are completely altered. Reference to the cross-sectional views in the lower half of Figure 3-51 indicates that the unaltered portions of the unit correspond to the devitrified interior core of the ash flow.

3.3.5 Model Uncertainties and Limitations

This section presents the uncertainties and limitations associated with the RPM. First, a number of limitations of both methodology and data that restrict the accuracy of the models generated by this analysis are described. Next, the results of a stochastic uncertainty analysis are presented in an attempt to quantify the geologic uncertainty that results from the limited site characterization.

3.3.5.1 Limitations

There are a number of factors that may best be described as limitations of the data or of the modeling process itself. These limitations, discussed below, include:

- Errors and biases in the sample data used in the analysis
- The use of porosity as a surrogate for other material properties
- The combination of numerous lithostratigraphic units into four major modeling units
- The effect of geologic departures from the assumptions inherent in the use of the stratigraphic coordinate system.

3.3.5.1.1 Errors and Biases in Sample Data

Stochastic simulation is a statistical-probabilistic methodology and reproduction of various target statistical measures is an important part. As such, errors (uncertainties) incorporated into the statistical description of the rock mass will be propagated through the simulation process into the

output models. These errors are of two principal types: measurement sensitivity limits and preferential sampling bias. Each of these forms of error, as they affect the RPM, is discussed in the subsections below.

Measurement Sensitivity Limits—Measurement of the matrix-saturated hydraulic conductivity values for core samples appears to have had a lower detection limit of roughly 10^{-12} to 10^{-11} m/sec. Samples with hydraulic conductivity below this lower limit are reported in the data set as *no flow*. Omitting these samples entirely would lead to an unrealistically high set of modeled hydraulic conductivity values. On the other hand, substituting the no-flow samples with an arbitrary low value prior to the simulation process would tend to skew the results toward that arbitrary low conductivity. Therefore, the effect of these no-flow samples has been simulated explicitly during postprocessing by setting an appropriate fraction of values equal to the arbitrary value of 10^{-14} m/sec at randomly selected grid nodes within each model unit. This adjustment to approximate the non-negligible number of nonflowing laboratory samples assumes that there is no particular spatial correlation among these samples.

Preferential Sampling Bias—The laboratory measurements of thermal conductivity are systematically biased by preferential sampling of core specimens that are more coherent, with generally lower porosity. This bias was identified by differences in the histograms of porosity for those laboratory thermal-test specimens (CRWMS M&O 1999b, Figure 28) versus the overall histogram of porosity for the Topopah Spring welded unit. An additional influence with respect to thermal conductivity is the effect of larger-than-core-size lithophysal cavities on the thermal conductivity of the rock mass as a whole. An attempt was made to reduce the impact of this identified sampling bias for thermal conductivity by constructing an unbiased reference distribution of thermal conductivity values for the simulation. This was done using a porosity-weighted distribution of estimated thermal conductivities (CRWMS M&O 1999b, Section 6.4.5.3), where the porosity values were obtained by systematic sampling of the entire TSw model unit.

Similar sampling bias also affects the matrix hydraulic conductivity determinations because laboratory testing is skewed slightly toward measurements of the more conductive samples (low-permeability samples take longer to run) in certain boreholes. This bias was not addressed explicitly in this modeling work because the total number of hydraulic conductivity data analyses done in the laboratory is quite large (greater than 400) compared to the number of thermal conductivity determinations (approximately 50 total; 35 for the TSw model unit), and several boreholes (notably UZ#16, SD-9) were sampled on a systematic basis for the hydraulic property.

3.3.5.1.2 Porosity as a Surrogate

A fundamental limitation of the rock properties modeling effort is the use of porosity as a surrogate for the derivative properties of more general interest to the design and performance assessment analysts. These derivative properties, such as matrix-saturated hydraulic conductivity, are related to the principal modeled property only through a correlation coefficient, generally indicated as r . To the extent that the absolute value of r is less than one, using surrogate values increases the uncertainty in the secondary properties. Nevertheless, use of a non-zero correlation coefficient combined with the incorporation of spatial correlation in the modeling of those properties works to decrease the uncertainty in those properties. This is in

contrast to modeling methodologies that discount either or both of these observable statistical characteristics. Knowing that a particular region exhibits high porosity values most likely translates to higher-than-average matrix permeability in the same region. However, actual measured values of derivative properties are not reproduced within the simulated (coregionalized) models in the same manner that measured porosity values located at a grid node are reproduced by construction. Again, the issue is whether the modeled uncertainty in material properties translates to unacceptable uncertainty in an objective performance measure when evaluated over a number of statistically indistinguishable simulated models.

Another limitation associated with the porosity-as-a-surrogate mechanism involves the hydraulic conductivity values that are not correlated with porosity. Other work (Flint 1998, Figures 12(a) and (b)) describes a group of low-porosity samples that exhibit apparently random permeabilities with respect to their uniformly low porosity values. These samples are interpreted as exhibiting behavior consistent with the existence of microfractures, largely in vitrophyric rocks (lithostratigraphic units (Tptrv1) and (Tptpv3)). The implication is that the permeability that was measured is not truly a matrix property, even though microfracture-related flow is measurable at the core scale. These erratic permeability values have been modeled as a random overprint imposed only on extremely low-porosity (less than 0.05) grid nodes (interpreted as representing vitrophyre). Because there are only 12 microfractured "vitrophyre-like" samples, it is impossible to determine whether these values are spatially correlated in their own right. However, to the extent that the measured data truly represent vitrophyre as a rock type (geologically restricted to the upper (Tptrv1) and lower (Tptpv3) margins of the TSw unit), it is possible to generate microfractured permeability values at inappropriate spatial locations within the TSw model unit. This limitation is presumed to be relatively minor; the restriction of generating these values to extremely low-porosity grid nodes (typically between 5 and 7 percent of the TSw grid) suggests that such rocks might be susceptible to microfracturing even though they would not belong to the vitrophyre-type small-scale lithostratigraphic units (see also Flint 1998, Figures 12(a) and (b)). Additionally, conditioning of the interior of the TSw model unit to porosity values substantially in excess of 0.05 produces models that are very unlikely to exhibit extremely low porosity values except near the margins, where measured porosities of this magnitude are observed.

A somewhat similar limitation affects the modeling of altered hydraulic conductivity values within the CHn and T_{cp} model units. Although the hydrous-mineral-phase alteration responsible for these reduced matrix permeability values is correlated spatially (Sections 3.3.4.4 and 3.3.4.3), it is unclear whether the permeability values within those altered regions are correlated. Adequate, spatially distributed measured *K*_s data do not exist to provide an estimate of the spatial correlation structure of these materials. In any event, because there is no reliable relationship between porosity and matrix permeability for these altered specimens, it is unclear what would serve as a surrogate for modeling the spatial continuity for these materials. Accordingly, the spatial distribution of altered permeability has been treated as random within the spatial envelope of altered rocks and has been assigned values sampled from a normal population with the appropriate mean and variance. To the extent that altered permeabilities are, in fact, spatially correlated, this modeling approach increases the uncertainty. Across the full suite of simulated models, however, the variability of rock properties (and, presumably, of process modeling results as well) is likely to be greater than had the properties been spatially correlated, thus allowing a quantitative evaluation of the consequences of that uncertainty.

3.3.5.1.3 Underestimation of Porosity and Hydraulic Conductivity in the TSw Model Unit

Another limitation related to the use of porosity as a surrogate for hydraulic conductivity affects the modeling of parts of the TSw model unit. For non-cored boreholes in this model unit, the available petrophysical data provide only an estimate of lithophysal porosity because the density logging tool is sensitive to the total amount of void space in the rock mass, including the influence of large lithophysal cavities. To overcome this limitation, a "surrogate for porosity-as-a-surrogate" was adopted whereby the water-filled porosity data from the computed volumetric water content (VWC) were inserted into the matrix porosity data files for the named lithophysal zones only. However, because matrix saturations, particularly in the crystal-rich lithophysal zone (Tptrl) and crystal-poor upper lithophysal zone (Tptpul), are less than one where these units are present above the static water level, substitution of the VWC data for matrix porosity underestimates the true matrix porosity (such as would be obtained from core) of the rock (CRWMS M&O 1999b, Figure 12). Coregionalization of the matrix-saturated hydraulic conductivity from porosity models conditioned to the lowered matrix porosity data produces models of K_s that are systematically low in localized regions.

The effect of underestimating porosity is limited almost exclusively to the upper lithophysal intervals (Tptrl and Tptpul). Matrix saturations within the crystal-poor lower lithophysal zone (Tptpll) are typically sufficiently high and there is little mismatch between measured core porosity values and the VWC measurements. Second, the effect becomes an issue only for areas populated by non-cored boreholes. The greatest density of cored boreholes is in the area of the potential repository. Near the cored boreholes, the porosity (and hydraulic conductivity) models are strongly conditioned by the laboratory-measured matrix porosity data. Furthermore, Figure 5 of the *Rock Properties Model (RPM3.1) Analysis Model Report* (CRWMS M&O 1999b) indicates that the principal holes lacking cores, the WT-series, are located primarily in regions near the periphery or surrounding the volume modeled by the RPM. Third, the additional uncertainty caused by the substitution of VWC data for measured matrix porosity values has already been incorporated into the simulated models. For regions within the vicinity of the potential repository where non-cored boreholes (such as borehole USW- 5 (H-5)) compete with cored holes (e.g., SD-9), any discordance between the laboratory measurements and the VWC substitute will result in the simulation algorithm generating a wider range of simulated values (in the appropriate stratigraphic interval) than would be the case in the absence of that discordance. Thus, uncertainty, as measured across the suite of simulations (Figure 3-24), has been increased, which is a realistic reflection of the state of the knowledge associated with the limitations imposed by the use of non-core drilling techniques: i.e., the matrix porosity is unknown.

3.3.5.1.4 Use of Major Stratigraphic Units as Modeling Units

A quite different, but potentially important, limitation of the approach used in development of the RPM is the use of composite major stratigraphic intervals and an internal stratigraphic coordinate system as the geometric basis for modeling. There are only four such model units while there are many different lithostratigraphic units (tabulated in Table 1-1). To the extent that the stratigraphic coordinate transformation for each of these major modeling units does not reposition equivalent parts of the model unit at the same stratigraphic position, continuity modeling is conducted between rocks formed at significantly different pressure-temperature conditions. The result is increased uncertainty across the suite of replicate simulations as the

simulation algorithm tries to resolve inconsistencies in the measured material properties between borehole locations.

This limitation is probably of minimal effect within the major ash-flow units at Yucca Mountain, particularly for the Topopah Spring welded unit, which effectively is an instantaneous deposit of massive proportions. Although the rock unit thins southward away from its source, the same physical and chemical conditions responsible for the ultimate physical properties of the rock almost certainly varied with relative vertical position within the cooling rock mass. The same logical argument applies, to a large extent, to the Prow Pass Tuff modeling unit and to the multiple-cooling-unit Calico Hills nonwelded interval.

The justification for treating the PTn modeling interval as a single rock-properties unit is somewhat weaker. This modeling unit contains two distinctly different pyroclastic-flow deposits (the Pah Canyon and Yucca Mountain Tuffs) separated by intervals of unrelated and reworked volcanic materials. The decision to model a single PTn entity was based on two factors: (1) In general, the properties of the rocks within the PTn unit are similar (almost all are nonwelded tuffaceous materials, particularly within the potential repository footprint), especially in comparison with overlying and underlying materials. (2) The individual pyroclastic flows are typically very thin, leading not only to a vastly increased bookkeeping task for selecting and tracking sample data but—more importantly—to a greatly reduced statistical mass relevant to any one unit. Ultimately the decision to represent the PTn model unit as a whole was a pragmatic one.

3.3.5.1.5 Faulting, Erosion, and the Stratigraphic Coordinate System

Another limitation related to the use of a stratigraphic coordinate system is that the presence of erosional unconformities or within-unit faulting will work to confound the petrologic and material-property equivalence of rocks assigned the same stratigraphic (vertical) coordinate. Faults are known to affect several boreholes at Yucca Mountain (USW WT-1 (WT-1), USW WT-11 (WT-11), UE-25 ONC#1 (ONC#1), and USW UZ-7a (UZ-7a)). Borehole p#1 is affected by erosion, and Moyer and Geslin (1995, pp. 8–31) report progressive lateral truncation of inferred depositional units within the Calico Hills Formation and Prow Pass Tuff across the model area. The effects of vertical fault displacement have been included in the computation of the stratigraphic coordinates, based on the best available information. In all cases, this compensation involves the same separations and uncertainties as the GFM. The locations and extent of erosional complexities are probably less well constrained than the effects of faulting. However, in all cases, there should be no discontinuities between the adjustments to stratigraphic coordinates applied to the RPM effort and the representation of the GFM.

A factor working to offset uncertainties related to the stratigraphic coordinate transformation is that all of the properties modeling activities were conducted within that conceptual and mathematical framework. Specifically, the quantitative description of spatial correlation behavior (variograms) was conducted after the conversion to stratigraphic coordinates. If undetected faulting or erosion worked to juxtapose samples of differing rock properties, the observed range of spatial correlation should be reduced, and this higher lateral variability would be reflected in the simulated property models. For a given set of conditioning data, a lesser

degree of spatial correlation also will translate into more variability across the suite of realizations and, thus, more uncertainty is reflected (accurately) in the suite of simulated models.

3.3.5.2 Stochastic Uncertainty Assessment

Uncertainty in rock material properties should be evaluated rigorously in terms of the consequences of that variability on a particular computed performance measure. However, the postprocessing step that produces the E-type models is easily adapted to generate models of spatially distributed variability across the suite of simulations. Such a spatially varying representation may be thought of as a first-order uncertainty model.

This type of summary model has been generated for this modeling activity as the node-by-node standard deviations of the 50 individual simulated rock property models. There is no particular reason to prefer the standard deviation approach other than general user familiarity. It also would be possible to represent the variability of individual stochastic simulations in one summary model through use of the inter-quartile range or the 10th-to-90th-percentile difference. In almost any such uncertainty model, the magnitude of the spatially varying uncertainty will decrease effectively to zero at sample locations and increase to some maximum value at great distances from conditioning samples or in close proximity to samples exhibiting conflicting values. In all cases, it is important to conceptually separate the difference between spatial heterogeneity and uncertainty.

PTn Model Unit—A block view of the PTn model unit in stratigraphic coordinates, presented in Figure 3-52, shows the uncertainty model of porosity for this unit. Uncertainty is generally low (shown in blue colors) in the immediate vicinity of boreholes containing conditioning measurements and increases to higher values away from these locations. Uncertainty is spatially heterogeneous within the model as well. However, because most boreholes penetrate most of each unit, the general pattern of heterogeneity in uncertainty will be that exhibited on the top surface of the model unit.

TSw Model Unit—Block models presenting the uncertainty models of matrix and lithophysal porosity in the TSw model unit are presented in Figures 3-53 and 3-54, respectively. Uncertainty in the figures is calculated as the node-by-node standard deviation of the replicate simulated material property models. As anticipated, uncertainty is lowest in the vicinity of boreholes containing conditioning measurements, and uncertainty increases away from those borehole locations. Note that there are slight differences in the uncertainty models for matrix and lithophysal porosity, even though the borehole coverage at this stratigraphic level is essentially identical.

CHn Model Unit—The uncertainty model for matrix porosity in the CHn model unit is presented in Figure 3-55, also as the node-by-node standard deviation of the 50 replicate simulated models of this property. Low values of uncertainty are indicated by shades of blue, and these regions are associated with the boreholes containing conditioning data that penetrate this model unit. Spatial heterogeneity of uncertainty can be seen on the front face of the block model (Figure 3-55). However, the dominant pattern of uncertainty will be vertically downward and associated with the vertical boreholes.

Tcp Model Unit—A block view of uncertainty in matrix porosity for the Tcp model unit, computed as the standard deviation of the replicate simulated models, is presented in Figure 3-56. Uncertainty is lowest in the immediate vicinity of the boreholes penetrating this unit, and increases away from these locations of conditioning data. It is interesting to note the marked increase in uncertainty within the Tcp model unit compared to the uncertainty model for the CHn model unit presented in Figure 3-55. This increase is most noticeable in the northeast corner of the modeled volume (also note the increase in the maximum value of the standard deviation in these two figures, colored red on the color scale). The cause of this marked change in uncertainty is the loss of borehole UE-25 WT#16 (WT-16) data from the Tcp data set. Additional increases in modeled uncertainty in the Tcp model unit, particularly in the eastern portion of the area, result from the loss of data from boreholes UE-25 WT#14 (WT#14) and UE-25 WT#15 (WT#15) (outside the modeled volume) and borehole ONC#1 (within the modeled volume).

3.3.6 Alternative Interpretations

At the time this report was prepared, no known alternative interpretations to the RPM methodologies or results have been documented.

3.3.7 Model Validation

A fundamental premise of the Monte Carlo simulation approach is that each individual realization is a plausible model of the unknown real world, and that variation among the different stochastic realizations represents a probabilistic distribution of outcomes consistent with all that is known. Presumably, the only meaningful difference between individual realizations is that a different random number seed was used to initiate the simulation process (definition of a random path). Because conditional simulations theoretically possess the attributes of data reproduction described in Section 3.3.3.1.2 (including reproduction of the ensemble statistical character), it should be possible to test the validity of the individual simulated models in terms of statistical similarity to the data, by examining the three relevant criteria for simulated models specified in Section 3.3.3.2:

- Reproduction of the known data values at the same locations within the model as represented by the real-world samples
- Reproduction of the full range of measurement variability represented by the univariate descriptive statistics of the known data values (the histogram)
- Reproduction of the bivariate statistics (i.e., or two-point spatial correlation structure) of the input data (the variogram).

Because of the large number of suites of simulated models generated for the RPM, it is impractical to present validation statistics for every material property-model unit combination. Instead, illustrative examples validating selected simulated suites are presented in the *Rock Properties Model (RPM3.1) Analysis Model Report (CRWMS M&O 1999b, Section 6.7)*.

Based on the information presented in the *Rock Properties Model (RPM3.1) Analysis Model Report* (CRWMS M&O 1999b, Sections 6.7.1 through 6.7.4), it appears reasonable to conclude that the individual simulated rock properties models (including the coregionalized models of derivative properties) meet the stated criteria with respect to model validation, and that the models as complete entities closely resemble the input data used to construct these descriptive models. Specifically, the primary porosity models reproduce the input measurements used to condition the simulations within the limits imposed by the discretization of the models. Additionally, both the primary simulated models and the derivative coregionalized models exhibit the full range of material property variability exhibited by the conditioning data ensemble. Furthermore, the simulated models reproduce the bivariate spatial correlation structure (variogram) observed in the data ensemble; the coregionalized models will reproduce this structure by construction. For the coregionalized models, the correlation coefficient between the derivative property and the underlying porosity simulation is reproduced within reasonable limits, given the fact that the target correlations typically are based on global correlations (without regard for model unit).

The summary E-type models also reproduce the input conditioning measurements, but the statistical character of the models as a whole departs from the ensemble statistics of the underlying data. Univariate variability (histograms) is reduced, with the extreme tails of the distribution of values are reduced, and the form of the distribution is more normalized. The spatial correlation structure (variograms) of the E-type models is similarly distorted. Continuity is observed to be somewhat greater in the summarized models, approaching a one-to-one correlation in some instances. Additionally, cross-variable correlations appear to be strengthened by the averaging process implicit in the E-type models. All of these characteristics are expected from the mechanics of the summary process.

3.4 MINERALOGIC MODEL

This section provides a summary description of the Mineralogic Model Version 3.0 (MM3.0). A more detailed discussion can be found in the *Mineralogic Model (MM3.0) Analysis Model Report* (CRWMS M&O 1999c).

3.4.1 Introduction

The MM is a 3-D weighted, inverse distance model developed for Yucca Mountain to support the analyses of hydrologic properties, radionuclide transport, mineral health hazards, repository performance, and repository design. It was developed specifically for incorporation into the ISM and enables the prediction of calculated mineral abundances at any position, within any region or within any stratigraphic unit in the ISM area. The manner in which the MM was constructed, and a summary of the results, is provided in the following subsections. The software QA documentation, planning documents, modeling implementation procedures, and scientific notebooks for the MM are described in the *Mineralogic Model (MM3.0) Analysis Model Report* (CRWMS M&O 1999c, Sections 2 and 3).

3.4.2 Summary of Data Inputs and Model Software

This section summarizes the inputs and software used to construct the MM. Additional details can be found in the *Mineralogic Model (MM3.0) Analysis Model Report* (CRWMS M&O 1999c).

3.4.2.1 Inputs

The inputs for the MM consist of stratigraphic surfaces from GFM3.1, quantitative XRD analyses of mineral abundances, and the potentiometric surface. Data inputs, and their respective DTNs, are provided in the *Mineralogic Model (MM3.0) Analysis Model Report* (CRWMS M&O 1999c, Section 4.1) and a brief discussion of the input data is given in the following subsections. The borehole locations used in the MM are shown in Figure 3-57.

3.4.2.2 Assumptions

In the context of this PMR, assumptions are those assertions that influence data or input parameters. For the MM, the assumption was made that sample-collection methods for drill-cuttings did not severely affect the mineral-abundance data or the MM predictions based on those data. Therefore, drill-cuttings mineral-abundance data were used as input for the MM. Another data assumption is mineralogy within a model unit is spatially correlated. The assumptions are discussed in Section 5 of the *Mineralogic Model (MM3.0) Analysis Model Report* (CRWMS M&O 1999c).

In addition to assumptions, the MM uses certain methodological premises (stratigraphic coordinates and inverse distance weighting simulation) upon which the model construction is founded. Details of the application of these assumptions and methodologies are provided in Section 3.4.3.

3.4.2.3 Software

The MM was constructed with the commercially available software STRATAMODEL Version 4.1.1 (Landmark Graphics Corporation, Houston, Texas), which is a program designed for 3-D mineralogic modeling. During model construction, the software was used as intended by its developers. Additional information on the software and its qualification can be found in the *Mineralogic Model (MM3.0) Analysis Model Report* (CRWMS M&O 1999c, Section 3).

3.4.3 Construction of the Model

STRATAMODEL performs distance-weighted interpolations of borehole data within the stratigraphic units specified by the framework to produce a volumetric distribution of the mineralogic properties associated with each stratigraphic horizon.

The modeling process elaborated below consists of four sequential steps:

1. Modification of ASCII-format export files from GFM3.1: Missing values in the vicinity of faults were supplied by interpolation.

2. Creation of the stratigraphic framework: Stratigraphic surfaces from GFM3.1 were joined in three dimensions to create a stratigraphic framework.
3. Incorporation of mineralogic data from boreholes: Quantitative XRD analyses of mineral abundance as a function of geographic position (borehole location) and sample elevation were placed within the 3-D stratigraphic framework.
4. Calculation of mineralogic distribution data for the entire 3-D model with the use of a deterministic, inverse-distance-weighting function: Measured mineralogic data at each borehole were used to predict mineral abundances at all locations in the model.

3.4.3.1 Modification of GFM3.1 Files

The GFM3.1 ASCII-format export files that were used to create the stratigraphic framework for the MM lack elevation values at some grid nodes and along fault traces. These omissions occur only in the ASCII-format export files, not in GFM3.1. However, to create the stratigraphic framework, STRATAMODEL requires values for all grid nodes. Therefore, the GFM3.1 ASCII-format files were modified to fill in values in the vicinity of major faults before the creation of the stratigraphic framework (see Section 6.2.1 of the *Mineralogic Model (MM3.0) Analysis Model Report* (CRWMS M&O 1999c)). To provide these missing values in a controlled and reasonable manner, elevations for the undefined grid nodes were interpolated from adjacent grid points using the Stratamap function in STRATAMODEL. For example, if the values adjacent to an undefined grid node were 600 and 700 meters (183 and 213 feet), the interpolated value would be 650 meters (198 feet).

3.4.3.2 Creation of Stratigraphic Framework

The stratigraphic framework for the MM was created from 22 stratigraphic surfaces obtained from GFM3.1. An example—the surface of the Tiva Canyon Tuff vitric zone nonwelded subzone (Tpcpv1)—is illustrated in Figure 3-58. The surface is notable for the fine resolution of the topography, including faults such as the Solitario Canyon fault to the west. The 22 stratigraphic surfaces were linked via STRATAMODEL into a stratigraphic framework to define 22 volumetric sequences, as listed in Table 1-1 and illustrated in Figures 3-59 and 3-60. Many of the sequences in MM3.0 incorporate several stratigraphic units where each sequence is labeled with the units forming its upper and lower surfaces (Table 1-1, Figure 3-61). Some sequences were further subdivided into layers (Table 1-1, footnotes “f” and “g”) to reflect observed mineralogic variations.

The 22 sequences were defined to keep the MM as simple as possible and, at the same time, to accurately define the zeolitic, vitric, and repository host units at Yucca Mountain (Table 1-1). The individual sequences are described below, and a more detailed description of their mineralogic characteristics is given in Attachment II of the *Mineralogic Model (MM3.0) Analysis Model Report* (CRWMS M&O 1999c).

Sequence 22, the uppermost sequence, includes all stratigraphic units above the vitric zone of the crystal-poor member of the Tiva Canyon Tuff (Tpcpv) because these units share a common devitrification mineralogy dominated by feldspar plus silica minerals. The next sequence (Sequence 21) consists of the upper two subzones (Tpcpv3 and Tpcpv2) of the Tiva Canyon

vitrophyre (Tpcpv). These subzones are combined in the MM because they share a similar abundance of welded glass.

The hydrogeologic Paintbrush nonwelded unit (PTn) is represented by Sequence 20, which extends from the nonwelded subzone of the lower vitric zone of the Tiva Canyon Tuff (Tpcpv1) to the upper vitric zone of the Topopah Spring Tuff (Tpcpv2). This sequence includes six stratigraphic units that have differing proportions of glass and smectite that cannot be captured within the larger scale of the MM.

The remaining Topopah Spring Tuff below Sequence 20 is represented as eight sequences in the MM: the upper vitrophyre (Tptrv1, Sequence 19), the upper quartz-latitude to rhyolite transition (Tptrn-Tptrf, Sequence 18), the four lithophysal and nonlithophysal units (Sequences 17 through 14—Tptpul, Tptpmn, Tptpll, and Tptpln, respectively), and units of welded and nonwelded vitrophyre at the base. The uppermost of these two vitrophyres includes Tptpv3 and Tptpv2 and is represented as Sequence 13, which is subdivided into two equal-thickness layers. As described in the *Mineralogic Model (MM3.0) Analysis Model Report* (CRWMS M&O 1999c, Section 6.2.2), the uppermost layer represents the "altered zone," or region of intense smectite and zeolite alteration that occurs in many boreholes at the contact of Tptpln and Tptpv3. The nonwelded vitrophyre (Tptpv1) and the underlying bedded tuff (Tpbt1) were combined into Sequence 12 in the MM because of their similar character in many boreholes and because Tpbt1 is generally thin and not well represented in the mineralogic data.

The Calico Hills Formation and the underlying bedded tuff are represented as Sequences 11 and 10, respectively, and were further subdivided into four layers. The layers have distinct mineralogic abundances in the MM and were created to allow modeling of variable zeolitization with depth in the Calico Hills Formation.

In GFM3.1, the Prow Pass Tuff, Bullfrog Tuff, and Tram Tuff are each represented by six stratigraphic units (a total of 18). In the MM, these 18 units were combined into a total of four zeolitic (or vitric) sequences (9, 7, 5, and 3) and three devitrified nonzeolitic sequences (8, 6, and 4). These sequences are shown in Table 1-1 and in Figure 3-61). These sequences reflect the characteristic alterations between units at this depth that can be readily zeolitized and those that have devitrified to feldspar plus silica minerals where zeolitization does not occur.

The uppermost zeolitic Sequence 9 (Tcupv) is defined by the upper vitric subunit of the Prow Pass Tuff (Tcupv). (Note that the word "vitric" and the symbol "v" are used in GFM3.1 to describe original vitric units, even through these units may now be zeolitic.)

The upper zeolitic (or vitric) sequence in the Prow Pass Tuff is underlain by nonzeolitic Sequence 8 (Tcupc-Tcuplc) representing the devitrified center of the Prow Pass Tuff (Tcupc-Tcuplc). Sequence 8 includes the upper crystalline, middle densely welded, and lower crystalline subunits. Zeolitic Sequence 7 includes the lower vitric portion of the Prow Pass Tuff (Tcuplv), the bedded tuff of the Prow Pass Tuff (Tcupbt), and the upper vitric subunit of the Bullfrog Tuff (Tcupbv). Nonzeolitic Sequence 6 (Tcupbc-Tcupblc) consists of the devitrified Bullfrog Tuff and combines three subunits (Tcupbc, Tcupbmd, and Tcupblc). Zeolitic Sequence 5 (Tcupblv-Tcupbtv), includes the lower vitric and bedded tuff of the Bullfrog Tuff (Tcupblv-Tcupbvt) in addition to the upper vitric unit of the Tram Tuff (Tcupbtv). Nonzeolitic Sequence 4 (Tcupbc-Tcupblc)

includes the devitrified center of the Tram Tuff (Tctuc, Tctmd, and Tctlc). Zeolitic Sequence 3 (Tctlv-Tctbt) is the base of the Tram Tuff (Tctlv and Tctbt).

Units older than the Tram Tuff have differing zeolitic characteristics, but they are undifferentiated and are combined as Sequence 2 (Tund). The lowermost sequence in the MM, Sequence 1, is the Paleozoic sequence.

The MM consists of 22 sequences and a total of 26 layers. The layers include the subdivision of Tptpv3-Tptpv2 into two layers and the subdivision of the Calico Hills Formation into four layers. With 26 layers and a total of 45,756 (186 by 246) grid nodes per layer, there are a total of 1,189,656 cells in the model. Each cell contains 16 values, including percentage abundance for the 10 mineral groups (listed in Section 3.4.3.3), cell volume, cell location (x, y), elevation (z), sequence number, and layer number. Any cell in the model can be queried to obtain these values. North-south (Figure 3-59) and east-west cross sections (Figure 3-60) show the distributions and thicknesses of the stratigraphic units used as the framework of the MM (Table 1-1).

3.4.3.3 Incorporation of Mineralogic Data From Boreholes

Mineralogic data (discussed in *Mineralogic Model (MM3.0) Analysis Model Report* (CRWMS M&O 1999c, Section 4.1)) are available for 24 boreholes (see Figure 3-57) in the form of data files that provide the mineralogy as a function of sample depth (i.e., elevation). Because of their close proximity, the data from boreholes UZ-N31 and UZ-N32 were combined in the MM. Ten mineral groups or classes were incorporated in MM3.0:

- Sorptive zeolites (the sum of clinoptilolite, heulandite, mordenite, chabazite, erionite, and stellerite)
- Nonsorptive zeolite (analcime)
- Smectite and illite
- Volcanic glass
- Tridymite
- Cristobalite and opal-CT
- Quartz
- Feldspars
- Mica
- Calcite.

The borehole data files were imported into STRATAMODEL in a process that involved mapping the elevations of the mineralogic samples onto the stratigraphic elevations obtained from

GFM3.1. At each borehole and for each sequence, an arithmetic mean was calculated from the mineralogic data, and these means were used to construct the MM.

A stratigraphic coordinate system approach, similar to that described in the Section 3.3.3.2, was used in the construction of MM3.0. The advantages of the stratigraphic coordinate system are that all mineralogic data are correctly associated with a sequence and that the stratigraphic relationship of data from differing boreholes is preserved. Therefore, mineralogic data were assigned to the correct sequence by small making adjustments to apparent elevations where needed (described in CRWMS M&O 1999c, Attachment II).

3.4.3.4 Calculation of Mineral Distributions

The final stage of the MM construction in STRATAMODEL is the distribution of the mineralogic data in three dimensions. In MM3.0, a distance-weighting method was used to estimate mineral distributions. The 3-D mineral distributions were calculated using an inverse-distance-weighting function that operates solely within sequences. That is, mineral abundances in a given sequence were calculated solely from mineralogic data within that sequence. The distance weighting function is defined in the *Mineralogic Model (MM3.0) Analysis Model Report* (CRWMS M&O 1999c, Section 6.2.4).

3.4.4 Model Results

In the following sections, the results of the modeling efforts for MM3.0 are discussed, and the model outputs are illustrated using cross sections and map views of individual surfaces. The location and extent of the north-south and east-west cross sections are shown in relation to the ESF in Figure 3-62.

3.4.4.1 Model Limits and Illustration of Results

Figures 3-57 and 3-62 show the distribution of boreholes on which the MM is based. (Colors in the background of Figure 3-62 are keyed to the abundance of volcanic glass in Sequence 20, the PTn unit.) The boreholes, which are the source of the mineralogic data, are confined to the central portion of the model area; thus, the MM results are poorly constrained outside of the subregion indicated by the outlined box in Figure 3-62. This is a small central area in which mineralogic data are abundant, relative to the total model area. This limitation should be kept in mind when considering the visualizations generated from the MM. Another model limitation, shown in Figure 3-62, is illustrated as regions in which Sequence 20 is absent. These regions occur in linear zones in the vicinity of faults where the MM resolution of fault geometry is poor. Therefore, accurate mineralogic predictions (results) should not be expected adjacent to faults. Sequence 20 also is absent in broad areas where it has been removed by erosion.

3.4.4.2 Sorptive Zeolite Distribution

Zeolite abundance is shown in Figure 3-63 as a range of colors from purple (0 percent) to orange (85 percent or greater). Sorptive zeolites at Yucca Mountain play an important role in models of radionuclide retardation and thermohydrology, and in repository design. Sorptive zeolites occur in varying amounts below the potential RHH in four distinct stratigraphic groups that are separated by nonzeolitic intervals. The potential RHH, as shown in Table 1-1, includes the lower

part of Sequence 17 of the MM and all of Sequences 16 through 14. Zeolite distributions with respect to the potential RHH are displayed in Figures 3-64 and 3-65. The distribution of sorptive zeolites is closely related to the internal stratigraphy of the tuffs. As described in Section 3.4.3.2, sorptive zeolites occur within the upper vitric, basal vitric, and basal bedded tuff units of each formation of the Crater Flat Group (Tram Tuff, Bullfrog Tuff, and Prow Pass Tuff). The devitrified centers of the Crater Flat Group tuffs lack zeolites. The net result is an alternating sequence of zeolitic and nonzeolitic rocks. However, the extent of zeolitization in the uppermost zeolitic group differs geographically from the others. In the south and west, the first occurrence of abundant zeolites below the RHH is in the lower vitric unit of the Prow Pass Tuff (Sequence 7; Tcplv-Tcbuv). Toward the north and east, the first occurrence of abundant zeolites extends into the bedded tuff below the Calico Hills Formation (Sequence 10; Tacbt), into the Calico Hills Formation (Sequence 11; Tac), and, ultimately, to the vitric units of the Topopah Spring Tuff (Sequence 12 (Tptpv1-Tpbt1) and Sequence 13 (Tptpv3-Tptpv2)).

The position of the water table relative to zeolitized rocks and the potential repository is shown in Figures 3-64 and 3-65. In the north-south cross section (Figure 3-64), zeolite-rich rocks separate the potential RHH from the water table throughout the section shown. The east-west cross section (Figure 3-65) also shows zeolites occurring between the potential RHH and the water table. Further east of this cross section (and east of the potential repository vicinity), faulting displaces the units downward so that Sequence 12 is below the water table and devitrified, nonzeolitic rock from the Topopah Spring Tuff at the water table.

The progressive development of zeolitization from northeast to southwest is illustrated in a series of map views through the Calico Hills Formation (Tac; Sequence 11) and into the upper vitric Prow Pass Tuff (Tcpuv; Sequence 9); see Figures 3-66 through 3-71. The transition zone between regions of high (greater than 5 percent) and low (0 to 5 percent) zeolite abundance is an important feature to model accurately because it occurs in highly porous rocks below the potential repository (Loeven 1993, pp. 37-39). The reason is that a decrease in zeolite abundance is associated with decreased radionuclide sorptive capacity and increased permeability (Loeven 1993, Table 6). Because a higher permeability allows greater interaction between zeolites and water, it is possible that the transition zone may be a zone of enhanced radionuclide sorption in which fluids have better access to sorptive minerals.

There is a striking reduction in zeolite abundance from east to west in the upper half of the Calico Hills Formation. The reduction occurs across a north-south boundary and is well defined in the region of boreholes WT-2 and UZ#16 (Figures 3-66 and 3-67). The location and abruptness of this transition are very poorly constrained to the north and west of H-5, and moderately constrained to the south between WT-1 and G-3. In the lower half of the Calico Hills Formation, extensive zeolitization occurs in borehole SD-7, and moderate zeolitization occurs in SD-12 and H-6 (Figures 3-68 and 3-69). This leads to a complex transition zone in which a high-zeolite deposit extends westward from SD-7. The detailed sampling of SD-7 and SD-12 suggests a transition zone that may be vertically and horizontally heterogeneous. In SD-7, sills of more than 25 percent zeolite alternate with largely vitric samples in the lower half of the Calico Hills Formation, suggesting an interfingered transition zone. In contrast, SD-12 shows a rather uniform development of increasing zeolitization with depth. These data indicate that the general reduction in zeolitization to the southwest may be strongly overprinted by patchy intervals of the highly zeolitized Calico Hills Formation.

The bedded tuff below the Calico Hills Formation (Tactb; Sequence 10) is zeolitized in boreholes SD-7, WT-2, SD-12, and H-5 (Figure 3-70). The transition zone to low zeolite abundance is confined to the west and southwest, around boreholes SD-6, H-3, and G-3, however, SD-6 contains about 15 percent smectite and perhaps should be viewed as a part of the zone of abundant sorptive mineralogy. There are no data for this sequence at H-6.

The upper vitric Prow Pass Tuff (Tcupv; Sequence 9) has a zeolite distribution similar to that of Tactb, except that there are data at H-6 indicating abundant zeolites (Figure 3-71). In addition, SD-6 lacks both smectite and zeolites, and H-4 has a low abundance of zeolites (10 percent) in this sequence. Zeolitization is complete throughout the MM in Sequence 7 (Tcplv-Tcbuv), which includes the lower vitric and bedded tuffs of the Prow Pass Tuff and the upper vitric unit of the Bullfrog Tuff.

In general, the MM represents the transition zone between zeolitized and non-zeolitized areas as a rather sharp boundary modified by the local effects at particular boreholes. The southwest portion of the area modeled as a whole, is characterized by low zeolite abundances (less than 10 percent). Values near 0 percent in the Calico Hills Formation (Tac; Sequence 11) are restricted to regions adjacent to nonzeolite-bearing boreholes such as G-3, H-3, and H-5. There is little control on the extrapolation of zeolite data in the northeast, northwest, and southeast regions of the MM. The predicted values of extensive zeolitization in the north are strongly influenced by boreholes such as USW G-1 (G-1) and G-2. It is possible that any or all of these regions may be characterized by more moderate values of zeolitization.

The most abundant zeolites at Yucca Mountain are clinoptilolite and mordenite (Bish and Chipera 1989, p. 13). Heulandite is fairly common at Yucca Mountain but is combined with clinoptilolite in the XRD analyses because the two minerals have the same crystal structure. The nonsorptive zeolite analcime occurs as a higher temperature alteration product at greater depths, and its occurrence deepens stratigraphically from the Prow Pass Tuff in G-2 to the Tram Tuff in G-1, and older lavas in G-3.

Chabazite is generally a rare zeolite at Yucca Mountain, but samples from the Calico Hills Formation (Tac; Sequence 11) in SD-7 contained significant amounts (up to 9 percent) in an approximately 14-meter (46-foot)-thick zeolitized interval consisting of clinoptilolite and chabazite overlying a clinoptilolite and mordenite zone (*Mineralogic Model (MM3.0) Analysis Model Report* (CRWMS M&O 1999c, Section 6.3.2)). This occurrence indicates that the sorptive zeolite assemblages may be more complex at the southern end of the exploratory block than previously predicted.

Localized occurrences of a few other zeolites also were found at Yucca Mountain. Stellerite is common in fractures of the Topopah Spring Tuff and is particularly common in both the fractures and matrix of the Topopah Spring Tuff (Ttptln, Sequence 14; and Ttptll, Sequence 15) in borehole UZ#16. Phillipsite is a rare zeolite at Yucca Mountain and was found only in the altered zone above the water table at the top of the basal vitrophyre of the Topopah Spring Tuff (Carlos et al. 1995, pp. 39, 47). Laumontite occurs in very small amounts (less than 4 percent) in deep, altered tuffs in borehole p#1 and perhaps in G-1 (Bish and Chipera 1989).

Erionite is another rare zeolite at Yucca Mountain and was first observed in the altered zone at the top of the Topopah Spring Tuff basal vitrophyre. However, it has since been found in significant quantities (up to 34 percent) in the drill core from a 3-meter (10-foot)-thick sequence in the bulk rock underlying the Topopah Spring Tuff basal vitrophyre in borehole UZ-14. It was also recorded in trace amounts (1 percent) in a breccia zone in the south ramp of the ESF. Although the occurrence of erionite is sporadic, and where found, its abundance typically is low, it is an important health concern due to its known carcinogenicity.

3.4.4.3 Smectite and Illite Distribution

Smectite is a swelling clay with a high cation-exchange capacity. Where present in significant amounts, it can act as a relatively impermeable barrier to fluid flow. It effectively sorbs many cationic species, such as Pu(V) in bicarbonate water and, therefore, can be an important factor in calculations of radionuclide retardation (Vaniman et al. 1996). Illites are clays with a higher layer charge than smectites, which reduces their effective cation-exchange capacity and eliminates their impermeable character. At greater depths, illite develops as a prograde product of smectite alteration, particularly in the northern and central portions of the MM where a fossil geothermal system occurs (Bish and Aronson 1993, pp. 151–155).

Smectite and illite are present in low abundance throughout Yucca Mountain except in some thin horizons and at depth in the region of boreholes G-1 and G-2. The distribution of these minerals with respect to north-south and east-west cross sections constructed through the potential repository is shown in Figures 3-72 and 3-73, respectively. The XRD analyses indicate the presence of smectite in virtually all analyzed samples, although typically in amounts of less than 5 percent. The volumes of smectite and illite increase at depth, particularly in the fossil geothermal system. Above the water table, there are two zones of up to 75 percent smectite in the Paintbrush Group. One is within the vitric nonwelded section above the Topopah Spring Tuff (PTn, Sequence 20), and the other is at the top of the basal vitrophyre of the Topopah Spring Tuff (upper layer of Sequence 13 (Ttpv3–Ttpv2)). These smectites typically have nonexpandable illite contents of 10 to 20 percent (Bish and Aronson 1993, pp. 151–152). Beneath the water table (depths greater than 1,006 meters (3,300 feet) below ground surface), the ancient (approximately 10.7 million years ago) geothermal system generated abundant smectite and illite, but with a much higher illite content of up to about 80 to 90 percent (Bish and Aronson 1993, Figures 3 and 4, pp. 152–153). However, the illitic clays occur at such great depths that they are of little importance for transport modeling at Yucca Mountain.

3.4.4.4 Volcanic Glass Distribution

Volcanic glass is a highly reactive, metastable material that is readily altered in the presence of water to form assemblages including zeolites and clays. The distribution of volcanic glass relative to the potential repository location is an important factor in evaluating possible repository-induced mineral reactions and assessing their impact on repository performance. Volcanic glass is almost entirely restricted to regions above the water table at Yucca Mountain (Figures 3-62, 3-74, and 3-75). The location of the water table is displayed in Figures 3-64 and 3-65. The largest deposits of volcanic glass are in the PTn unit (Sequence 20), the lower vitrophyre of the Topopah Spring Tuff (top of Sequence 13 (Ttpv3–Ttpv2)), and in vitric, zeolite-poor regions of the Calico Hills Formation (Sequence 11; Tac) in the southwestern and

western regions of the MM. The distribution of volcanic glass in the Calico Hills Formation is inversely correlated with zeolite abundance. Volcanic glass and zeolite occur together in the transition zone between high- and low-abundance zeolite.

3.4.4.5 Silica Polymorph Distribution

The common silica polymorphs at Yucca Mountain include quartz, cristobalite, opal-CT, and tridymite. These minerals could potentially affect repository performance because of their chemical reactivity, mechanical response to temperature, and potential impact on human health during mining operations. Repository-induced heating may accelerate the chemical reactions of cristobalite, opal-CT, and tridymite to quartz, which is the stable silica polymorph. In addition, all of the silica minerals are susceptible to dissolution and precipitation. Therefore, the potential exists for a substantial redistribution of silica with changes in the permeability and porosity of the matrix and fractures in the repository environment as a result. The results of the MM, showing ambient conditions, can be used to model the effects of thermal and geochemical reactions of metastable silica polymorphs on repository performance in 3-D. Tridymite and cristobalite undergo phase transitions between 100 and 275°C, which may have an impact on the mechanical integrity of the repository (Thompson and Wennemer 1979, pp. 1018–1025). The α to β transformation in cristobalite is of particular concern in thermal-load designs because of effects on porosity, permeability, and mechanical strength. Importantly, the crystalline silica polymorphs (quartz, cristobalite, and tridymite) are all regulated health hazards.

Cristobalite and tridymite occur in the potential RHH. Opal-CT is usually found in association with sorptive zeolites. Tridymite occurs above the water table and primarily above the potential RHH, particularly in those parts of the Topopah Spring and Tiva Canyon Tuffs where vapor-phase crystallization is common (Figures 3-76 and 3-77). Pseudomorphs of quartz that replace tridymite in deep fractures and cavities are evidence of the instability of tridymite under low-temperature aqueous conditions. Tridymite occurrences were interpreted as a possible limit on past maximum rises in the water table at Yucca Mountain (Levy 1991, pp. 483–484). Volumes of exceptionally high tridymite content are restricted to the upper strata within the Tiva Canyon and Topopah Spring Tuffs, but these rarely exceed 20 percent.

Cristobalite is typically a devitrification product that is found in virtually every sample above the water table. Opal-CT, which is a typical byproduct of zeolitization, is found below the water table before disappearing at depths at or below the Tram Tuff. Cristobalite and opal-CT are combined in the MM, partly because the extra analytical procedures necessary to distinguish them were not commonly applied to the borehole data, but also because the two minerals dissolve to similar aqueous silica concentrations. As is evident in Figures 3-78 and 3-79, cristobalite and opal-CT are abundant in the devitrified tuffs of the Paintbrush Group. Occurrences below the Paintbrush Group units are primarily opal-CT in tuffs containing abundant sorptive zeolites. Cristobalite and opal-CT disappear at depth and are replaced by quartz-bearing assemblages.

Quartz is common in the lower Topopah Spring Tuff and is abundant at depth in the Crater Flat Group (Figures 3-80 and 3-81).

3.4.5 Model Uncertainties and Limitations

Several uncertainties are associated with the MM in regions distant from the boreholes. In particular, there are striking geographic differences in mineral abundances that relate to past geologic processes. These are most obvious in the stratigraphic depth of zeolitization that increases to the southwest (from the Calico Hills Formation in the northwest to the Prow Pass Tuff in the southwest), across the MM (Figures 3-66 through 3-71). The location of the transition from vitric to zeolitic in the Calico Hills Formation is uncertain, given the currently available data. There is considerable uncertainty associated with the trend of the transition to the north and west of borehole UZ-14 because of significant differences in data from UZ-14, G-2, and WT-24. There also is uncertainty related to the nature of the transition. It is unclear whether the depth to zeolitization decreases rapidly and smoothly along a well-defined front, or whether the zeolitized zones are interfingered with vitric zones along a highly irregular front.

The most important limitation of the modeling results is the scarce mineralogic data in the region beyond the western border of the potential repository. The uncertainty in the boundary regions of the MM also is elevated because of the limited number of sampling locations (see Figures 3-57 and 3-62).

Quantitative mineralogic data from several boreholes were obtained primarily from cuttings rather than cores (all of WT-1 and USW WT-2 (WT-2), most of H-4, and smaller but important portions of H-3, H-5, and p#1). Drill cuttings have a tendency to average mineral abundance over a finite depth range, and the more consolidated rock fragments may be over-represented with respect to the softer, more friable rock fragments. It is difficult to predict the magnitude of the potential error without obtaining additional mineralogic data. However, the modeling process of the MM uses all of the available data, and this tends to reduce the impact of any single data point.

3.4.6 Alternative Interpretations

At the time this report was prepared, no known alternative interpretations to the MM methodologies or results have been documented.

3.4.7 Model Validation

The model validation was based on two criteria. First, the model was required to reproduce the input data, including the adjustments described in the *Mineralogic Model (MM3.0) Analysis Model Report* (CRWMS M&O 1999c, Attachment II). In this validation step, model-generated mineral abundance predictions (output) were compared against the input values at borehole locations where these data were available.

The second criterion checks that the model predictions are reasonable, given the input mineralogy from the surrounding or adjacent borehole sources. In practice, this means that at a given location, the predicted mineral-abundance values for each of the 10 mineral groups or classes in the model (listed in Section 3.4.3.3) are similar to the mineral-abundance values measured in the adjacent boreholes. To be acceptably similar, the predictions for the given test case should be within the range of the minimum and maximum measured values in adjacent

boreholes, and should be within one standard deviation or within 1 weight percent of the average measured values for adjacent boreholes.

The model was tested for the second criterion using two basic cases. In the first case, the mineralogic predictions for a unit with relatively uniform mineralogy were compared to the average values of all borehole data for that unit. In the second case, the predictions for a unit with distinctly varying mineralogy were compared to average values of adjacent holes only.

3.4.7.1 Case 1. Middle nonlithophysal zone of the Topopah Spring Tuff: Tptpmn

This unit is a devitrified tuff with a relatively constant feldspar content, but also with highly variable ratios of tridymite:crystalite:quartz. All of the borehole data were used to construct the average, standard deviation, minimum, and maximum of the input data. Values were predicted at a location near the center of the potential repository, west of boreholes UZ-N31 and UZ-N32. As shown in Table 3-3, the predicted values are bounded by the minimum and maximum, and are within one standard deviation of the average input values. The predicted value for feldspar is similar to the average, and it is consistent with the uniform feldspar content of the unit. The values for the silica polymorphs are within the one-standard-deviation limits, and they are consistent with the variability observed in the input values.

Table 3-3. Mineralogy of the Topopah Spring Tuff and Upper Calico Hills Formation

Case 1: Middle Nonlithophysal Topopah Spring Tuff (Ttpmn)												
Prediction Location	Borehole	SMEC	ZEO	TRID	CR/CT	QRTZ	FELD	GLAS	ANAL	MICA	CALC	
Easting: 170657.9 m Northing: 233202.1 m Elevation: 1140.8674 m	a#1	1	0	0	12	21	66	0	0	0.1	0	0
	a#1	3	0	2	13	18	60	0	0	0.1	0	0
	a#1	2	0.1	0.1	16	13	67	0	0	0.1	0	0
	G-1	2	0	0.1	22	3	72	0	0	0.1	0	0
	G-1	1	0	6	27	4	67	0	0	0.1	0	0
	G-3	1	0	0	17	6	70	0	0	1	0	0
	G-3	1	0	6	22	1	65	0	0	1	0	0
	G-4	3	0	4	23	4	66	0	0	0	0	0
	G-4	3	0	17	13	4	62	0	0	0	0	0
	G-4	1	0	0	28	3	68	0	0	0	0	0
	H-3	1	0	0	26	4	68	0	0	1	0	0
	H-3	2	0	0.1	27	2	69	0	0	1	0	0
	H-4	3	0	12	14	1	68	0	0	1	0	0
	H-4	1	0	0	20	11	67	0	0	0	0	0
	H-4	1	0	0	21	7	71	0	0	0	0	0
	H-5	3	0	3	28	1	59	0	0	0.1	0	0
	H-5	0.1	0	0	40	2	55	0	0	1	0	0
	NRG-6	2	0	4	31	4	54	0	0	0	0	0
	NRG-6	3	0	1	29	10	54	0	0	0.1	0	0
	NRG-6	2	0	5	17	17	55	0	0	0.1	0	0
	NRG-6	3	0	2	33	3	57	0	0	0	0	0
	NRG-6	3	0	3	27	10	55	0	0	0.1	0	0
	NRG-6	2	0	3	32	4	54	0	0	0	0	0
	NRG-7	3	0	6	16	20	57	0	0	0.1	0	0
	NRG-7	3	0	3	21	16	55	0	0	0.1	0	0
	NRG-7	3	0	1	22	18	52	0	0	0.1	0	0
	NRG-7	4	0	2	26	13	57	0	0	0.1	0	0
	NRG-7	3	0	5	9	29	56	0	0	0.1	0	0
	NRG-7	3	0	0.1	24	17	53	0	0	0.1	0	0
	p#1	2	0	0.1	3	30	67	0	0	0.1	0	0
	SD-7	4	0	2	25	15	53	0	0	0.1	0	0
	SD-7	3	0	2	35	4	53	0	0	0.1	0	0
	SD-7	5	0	4	31	5	52	0	0	0.1	0	0
	SD-7	3	0	4	35	2	52	0	0	0.1	0	0
	SD-7	5	0	3	34	3	52	0	0	0.1	0	0
	SD-7	3	0	2	35	3	54	0	0	0.1	0	0
	SD-9	3	0	2	28	11	54	0	0	0.1	0	0
	SD-9	3	0	3	28	8	55	0	0	0.1	0	0
	SD-9	2	0	8	11	21	55	0	0	0.1	0	0
	SD-9	3	0	4	26	9	53	0	0	0.1	0	0
	SD-12	4	0	2	30	8	53	0	0	0.1	0	0
	SD-12	5	0	4	26	11	52	0	0	0.1	0	0
	SD-12	5	0	3	34	5	54	0	0	0.1	1	0
	SD-12	4	0	4	28	9	54	0	0	0.1	0	0
	SD-12	3	0	4	34	3	54	0	0	0.1	0	0
UZ-14	3	0	5	32	4	52	0	0	0	0	0	
UZ-14	3	0	3	29	9	53	0	0	0.1	0	0	
UZ-14	5	0	4	31	5	55	0	0	0.1	0	0	
UZ-14	3	0	4	20	16	55	0	0	0	0	0	
UZ-14	4	0	4	33	7	54	0	0	0.1	0	0	
UZ-14	5	0	5	32	5	50	0	0	0.1	0	0	
UZ-16	3	0	0.1	16	21	57	0	0	0.1	0	0	
UZ-16	3	0	1	13	23	57	0	0	0.1	0	0	

Table 3-3. Mineralogy of the Topopah Spring Tuff and Upper Calico Hills Formation (Continued)

Case 1: Middle Nonlithophysal Topopah Spring Tuff (Ttpmnn) (Continued)											
Prediction Location	Borehole	SMEC	ZEO	TRID	CR/CT	QRTZ	FELD	GLAS	ANAL	MICA	CALC
	UZ#16	3	0	3	27	12	57	0	0	0.1	0
	UZ#16	3	0.1	1	26	10	56	0	0	0.1	0
	UZ#16	4	1	4	27	6	54	0	0	0.1	0
	WT-1	1	0	3	9	25	61	0	0	1	1
	WT-1	1	0	6	16	20	56	0	0	1	0
	WT-2	2	0	10	22	6	58	0	0	1	0
	WT-2	1	0	10	19	8	61	0	0	1	0
	average	2.7	0.0	3.3	24.2	9.8	58.0	0.0	0.0	0.2	0.0
	stdev	1.2	0.1	3.2	8.0	7.4	6.0	0.0	0.0	0.3	0.2
	max	5	1	17	40	30	72	0	0	1	1
	min	0.1	0	0	3	1	50	0	0	0	0
	prediction	1.8	0.0	2.2	31.8	3.0	57.4	0.0	0.0	0.4	0.0
Case 2: Upper Calico Hills Formation (Tac)											
Zeolitic Region											
Prediction Location	Borehole	SMEC	ZEO	TRID	CR/CT	QRTZ	FELD	GLAS	ANAL	MICA	CALC
Easting: 171206.6 m Northing: 234543.2 m Elevation: 838.8435 m	G-1	0.1	74.0	0.0	19.0	3.0	5.0	0.0	0.0	0.0	0.0
	NRG-7	1.0	80.0	0.0	13.0	2.0	8.0	0.0	0.0	0.0	0.0
	NRG-7	0.1	84.0	0.0	7.0	4.0	7.0	0.0	0.0	0.1	0.0
	SD-9	0.1	74.0	0.0	20.0	3.0	6.0	0.0	0.0	0.1	0.0
	SD-9	4.0	70.0	0.0	14.0	6.0	9.0	0.0	0.0	0.1	0.0
	SD-9	0.1	71.0	0.0	16.0	4.0	10.0	0.0	0.0	0.1	0.0
	SD-9	8.0	71.0	0.0	19.0	2.0	5.0	0.0	0.0	0.0	0.0
	SD-9	0.1	73.0	0.0	18.0	5.0	9.0	0.0	0.0	0.1	0.0
	average	1.7	74.6	0.0	15.8	3.6	7.4	0.0	0.0	0.1	0.0
	stdev	2.9	4.9	0.0	4.3	1.4	1.9	0.0	0.0	0.1	0.0
	max	8.0	84.0	0.0	20.0	6.0	10.0	0.0	0.0	0.1	0.0
	min	0.1	70.0	0.0	7.0	2.0	5.0	0.0	0.0	0.0	0.0
	prediction	0.7	75.4	0.0	16.1	3.2	6.4	0.3	0.0	0.0	0.0
Nonzeolitic Region											
Prediction Location	Borehole	SMEC	ZEO	TRID	CR/CT	QRTZ	FELD	GLAS	ANAL	MICA	CALC
Easting: 170901.8 m Northing: 231921.9 m Elevation: 933.9188 m	H-3	0.4	0.8	0.0	6.0	7.8	29.2	58.3	0.0	0.8	0.0
	SD-6	0.1	16.0	0.0	5.0	31.0	47.0	0.0	0.0	0.0	0.0
	SD-7	0.1	0.0	0.0	2.0	1.0	6.0	91.0	0.0	0.0	0.0
	SD-7	0.1	0.0	0.0	2.0	2.0	6.0	90.0	0.0	0.0	0.0
	SD-12	0.0	1.0	0.0	2.0	2.0	6.0	89.0	0.0	0.1	0.0
	SD-12	1.0	4.0	0.0	7.0	2.0	8.0	78.0	0.0	0.1	0.0
	SD-12	1.0	2.0	0.0	1.0	2.0	6.0	88.0	0.0	0.1	0.0
	SD-12	0.1	6.0	0.0	2.0	2.0	5.0	85.0	0.0	0.1	0.0
	SD-12	1.0	4.0	0.0	3.0	2.0	8.0	82.0	0.0	0.1	0.0
	SD-12	1.0	6.0	0.0	3.0	3.0	6.0	81.0	0.0	0.1	0.0
	SD-12	1.0	7.0	0.0	3.0	2.0	5.0	82.0	0.0	0.1	0.0
	WT-2	1.0	1.0	0.0	8.0	11.0	40.0	40.0	0.0	1.0	0.0
	average	0.6	4.0	0.0	3.7	5.7	14.4	72.0	0.0	0.2	0.0
	stdev	0.5	4.5	0.0	2.3	8.5	15.2	27.2	0.0	0.3	0.0
	max	1.0	16.0	0.0	8.0	31.0	47.0	91.0	0.0	1.0	0.0
	min	0.0	0.0	0.0	1.0	1.0	5.0	0.0	0.0	0.0	0.0
	prediction	0.8	2.9	0.0	5.8	7.3	25.3	58.5	0.0	0.6	0.0

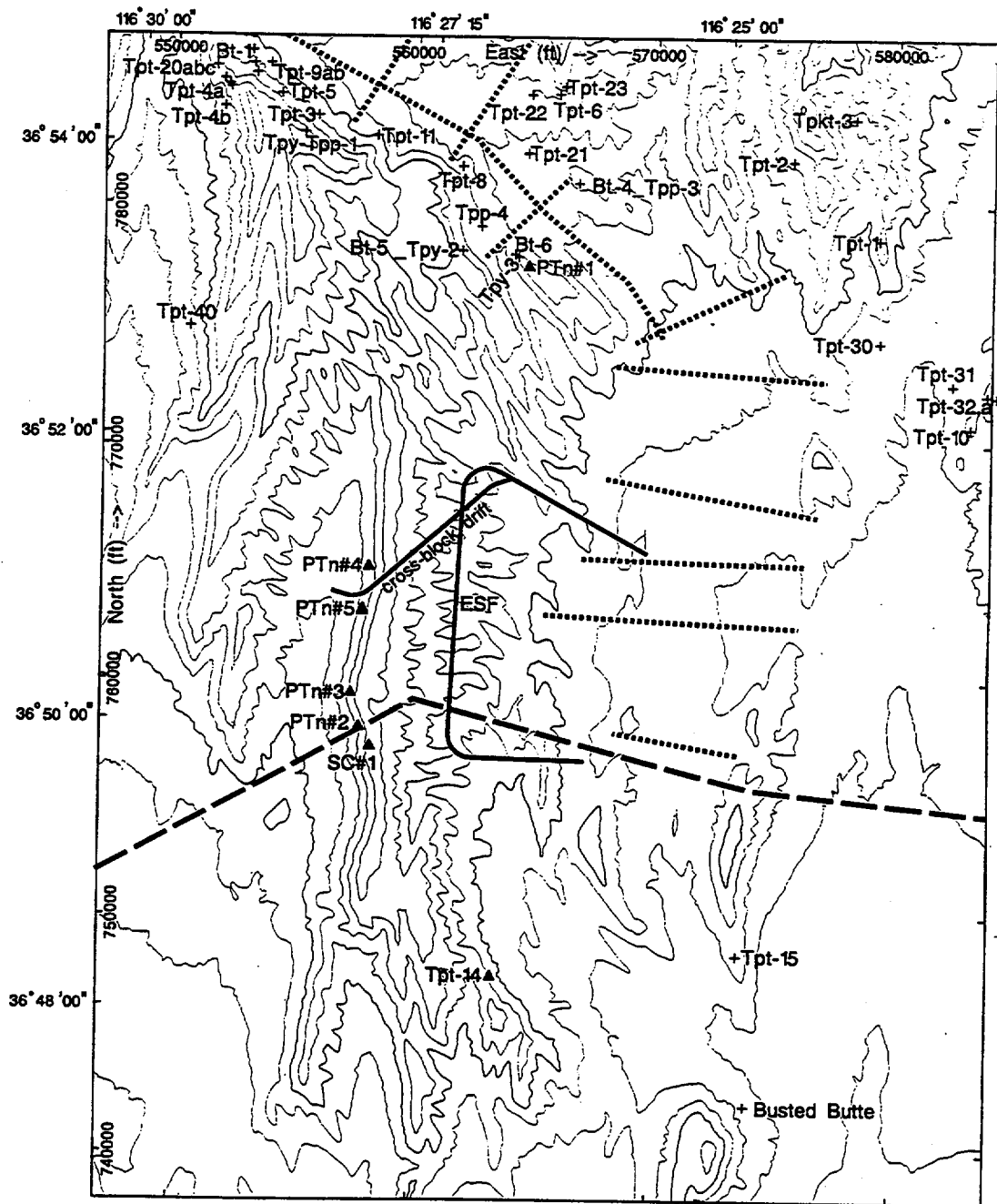
NOTE: Values shown are mineral abundances in weight percent.

3.4.7.2 Case 2. The upper part (25 percent) of the Calico Hills Formation: Tac

This unit shows a highly variable zeolite and volcanic glass content from the northeast to the southwest. Consequently, the model validation for this unit takes the geographic variation into account by testing at two locations within regions of different zeolite abundance. In this case, the criterion is that the predicted values at the test location should be similar to the input values for the set of nearest boreholes. As for Case 1, acceptable similarity is defined as a predicted value within one standard deviation of the average.

Location 1 (zeolitic region) is within the potential repository footprint and lies within a triangle defined by boreholes G-1, SD-9, and NRG-7. The predicted mineralogy of the test location should be similar to the values for the surrounding boreholes. The predicted values meet the test criterion (Table 3-3).

Location 2 (nonzeolitic region) is within the potential repository footprint and lies within a region defined by boreholes H-3, SD-6, SD-12, SD-7, and WT-2. The predicted values should be similar to the average mineralogy of the surrounding confining boreholes. This criterion is satisfied also (Table 3-3).



- ESF - Exploratory Studies Facility
- ▲ Measured Section
- + Corroborative Measured Section
- Regional Seismic Profile
- Gravity Profile

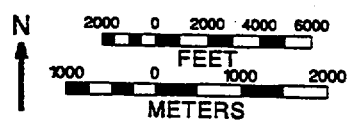
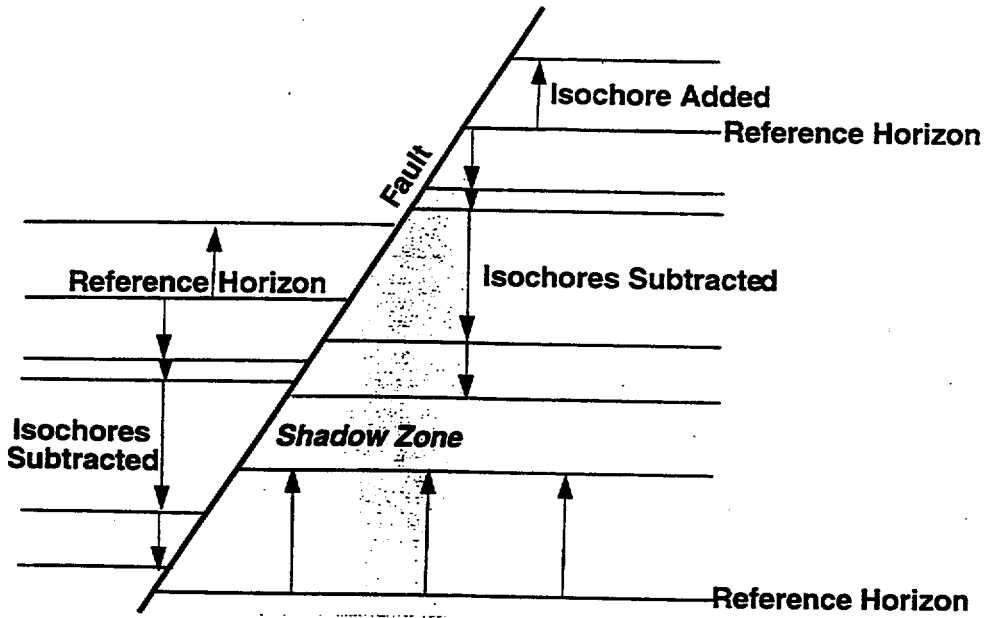


Figure 3-1. Locations of Measured Sections, Gravity Profiles, and Seismic Profiles (CRWMS M&O 1999a, Figure 5)



NOTE: Isochores are added or subtracted from reference horizons to assemble the rock units in the model. Because the process does not cross faults, a shadowzone develops beneath dipping faults.

Figure 3-2. Isochore Method
(CRWMS M&O 1999a, Figure 10)

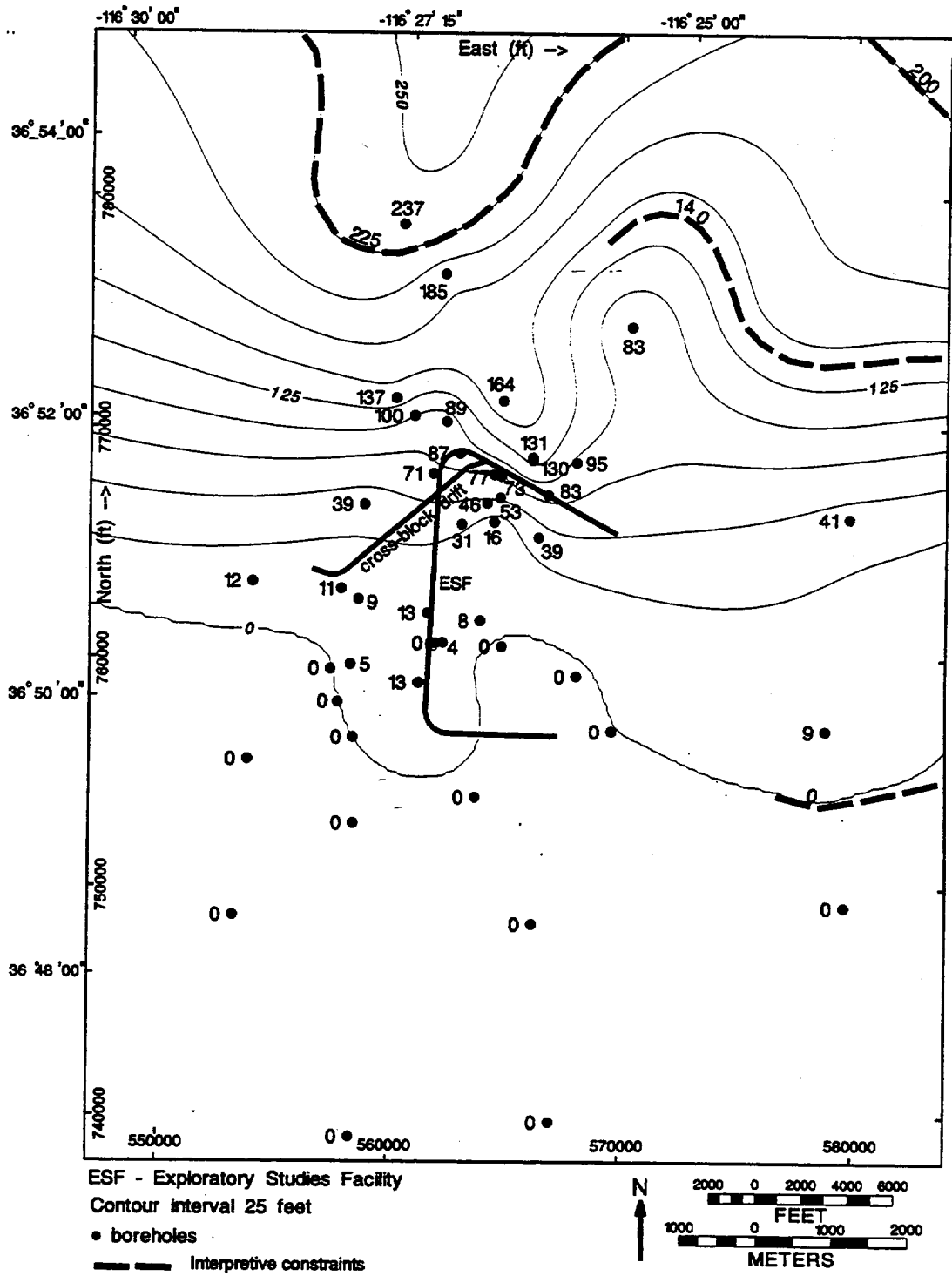
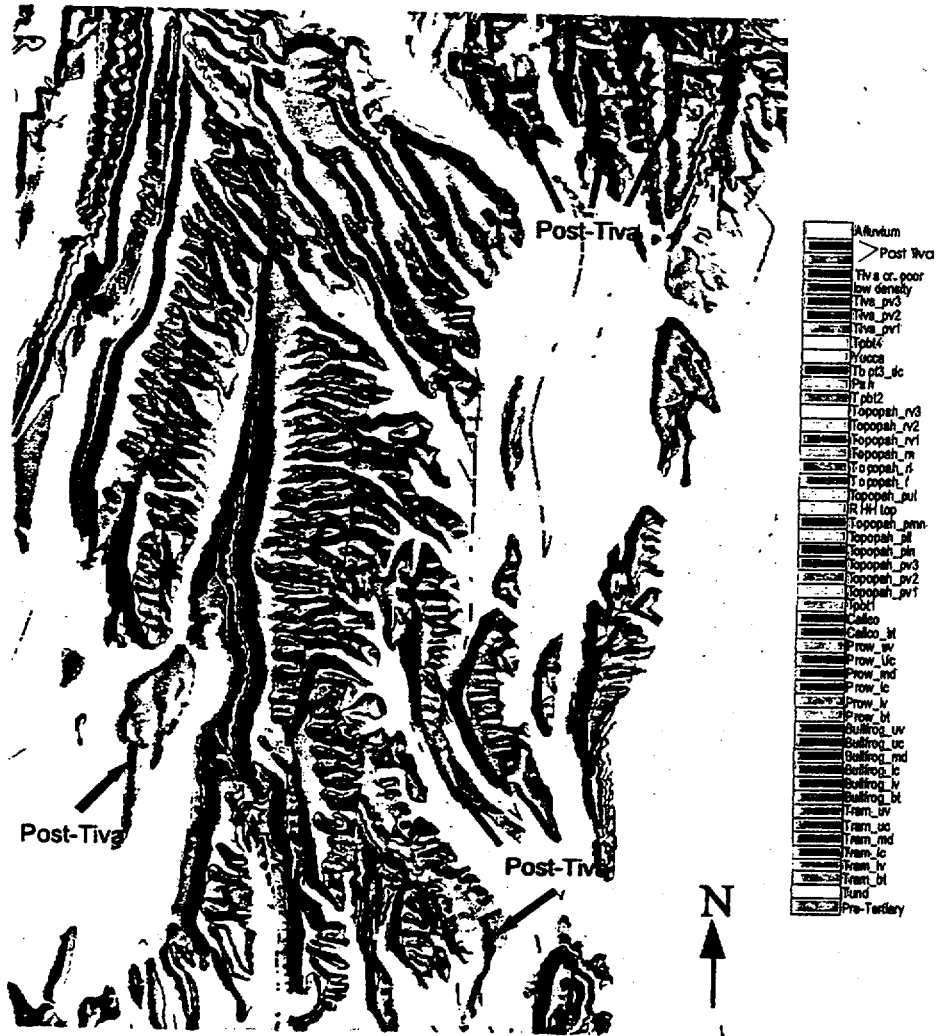


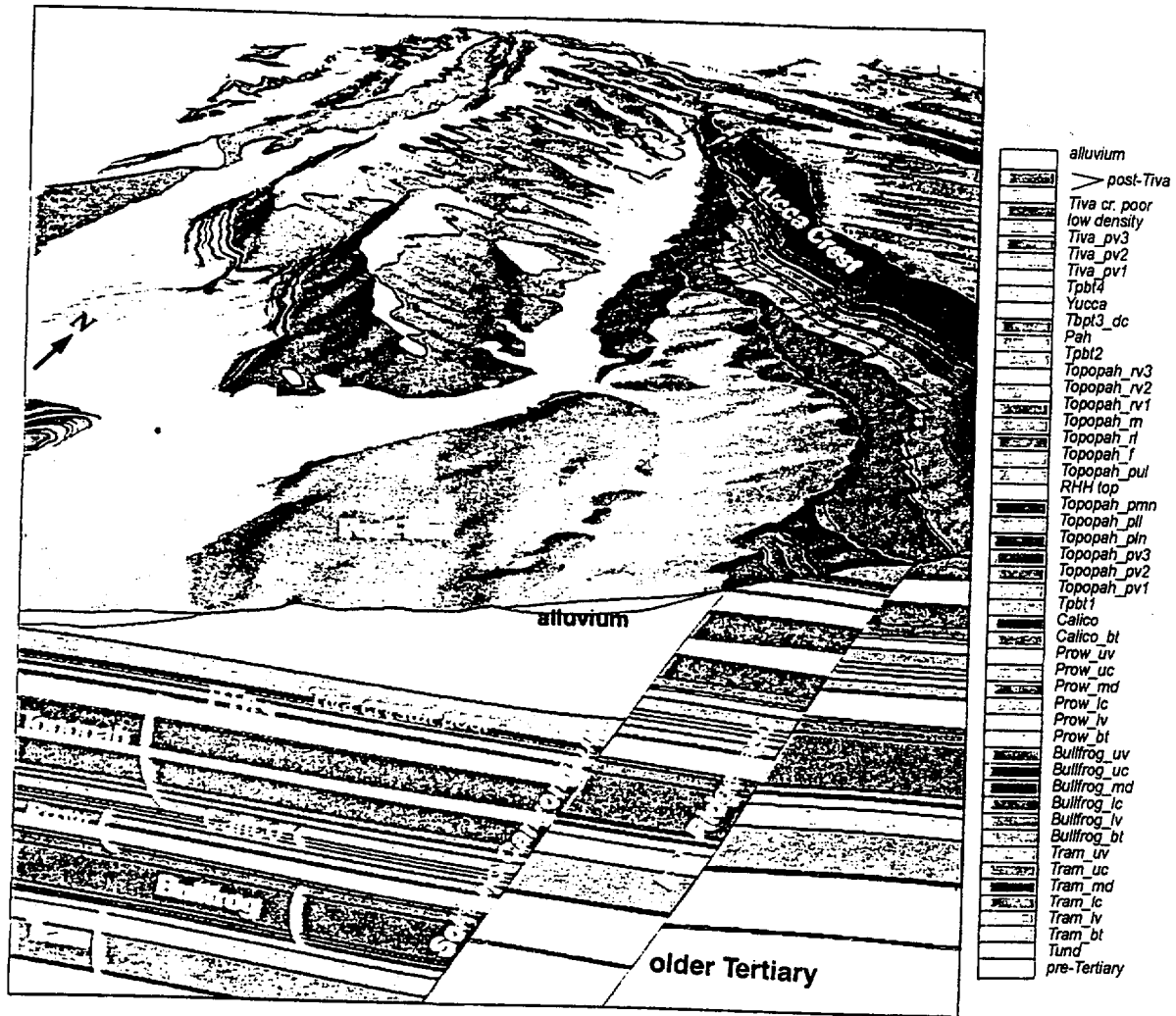
Figure 3-3. Interpretive Constraints
(CRWMS M&O 1999a, Figure 9)



NOTES: Formation names are spelled out in the color key for clarity. Refer to Table 5 for stratigraphic nomenclature.

This figure is a perspective view and not to scale. The area displayed is equivalent to the GFM model boundaries.

Figure 3-4. Location of Post-Tiva Rock Units (Vertical View of GFM Model Area. Defined in Figure 1-3) (CRWMS M&O 1999a, Figure 13)



NOTES: Formation names are spelled out in the color key for clarity. Refer to Table 1-1 for stratigraphic nomenclature.

Figure 3-5. Wedge of Post-Tiva Rocks in Solitario Canyon (View to North of Slice Through GFM) (CRWMS M&O 1999a, Figure 14)

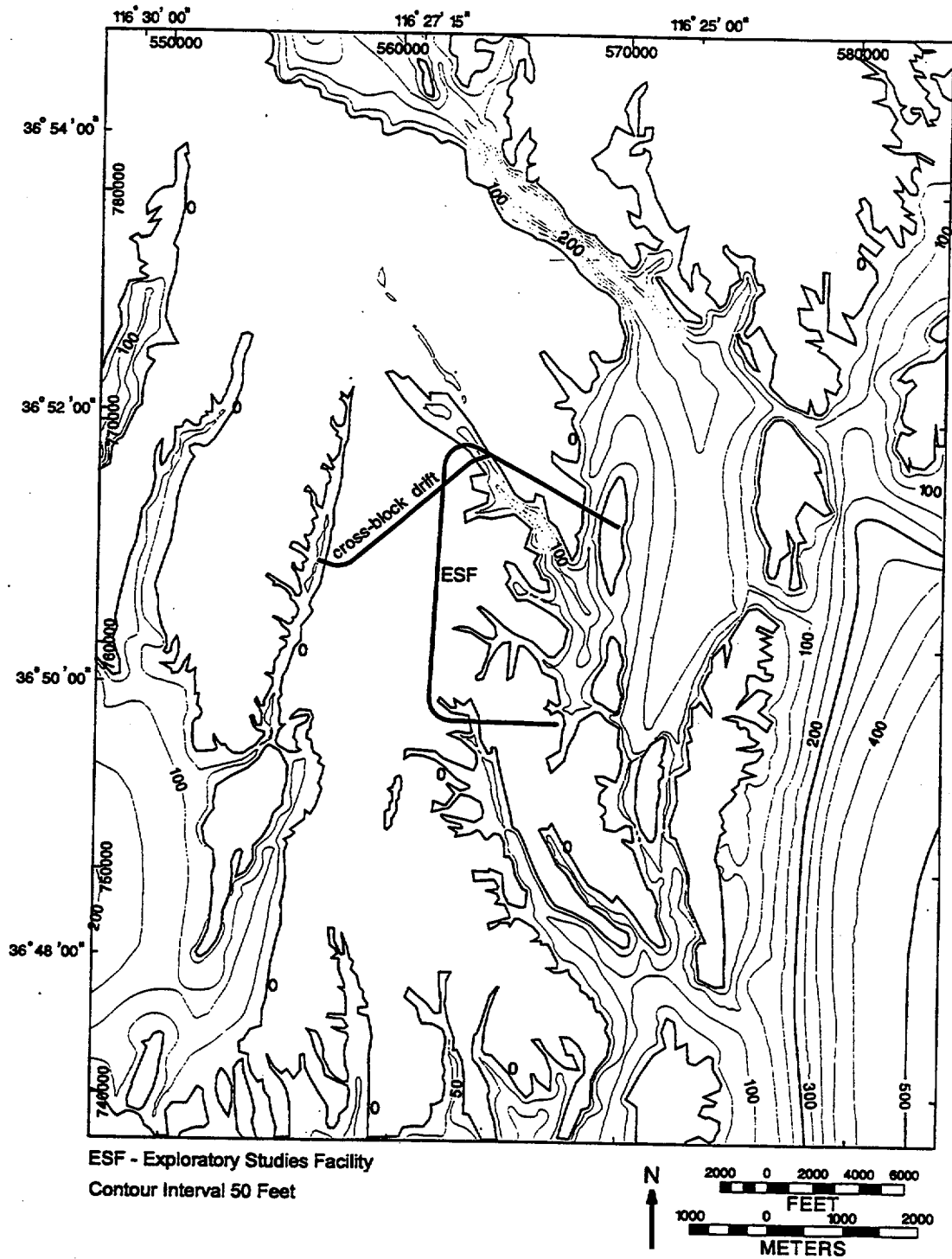


Figure 3-6. Model-Isochore Map of Alluvium (CRWMS M&O 1999a, Figure 15)

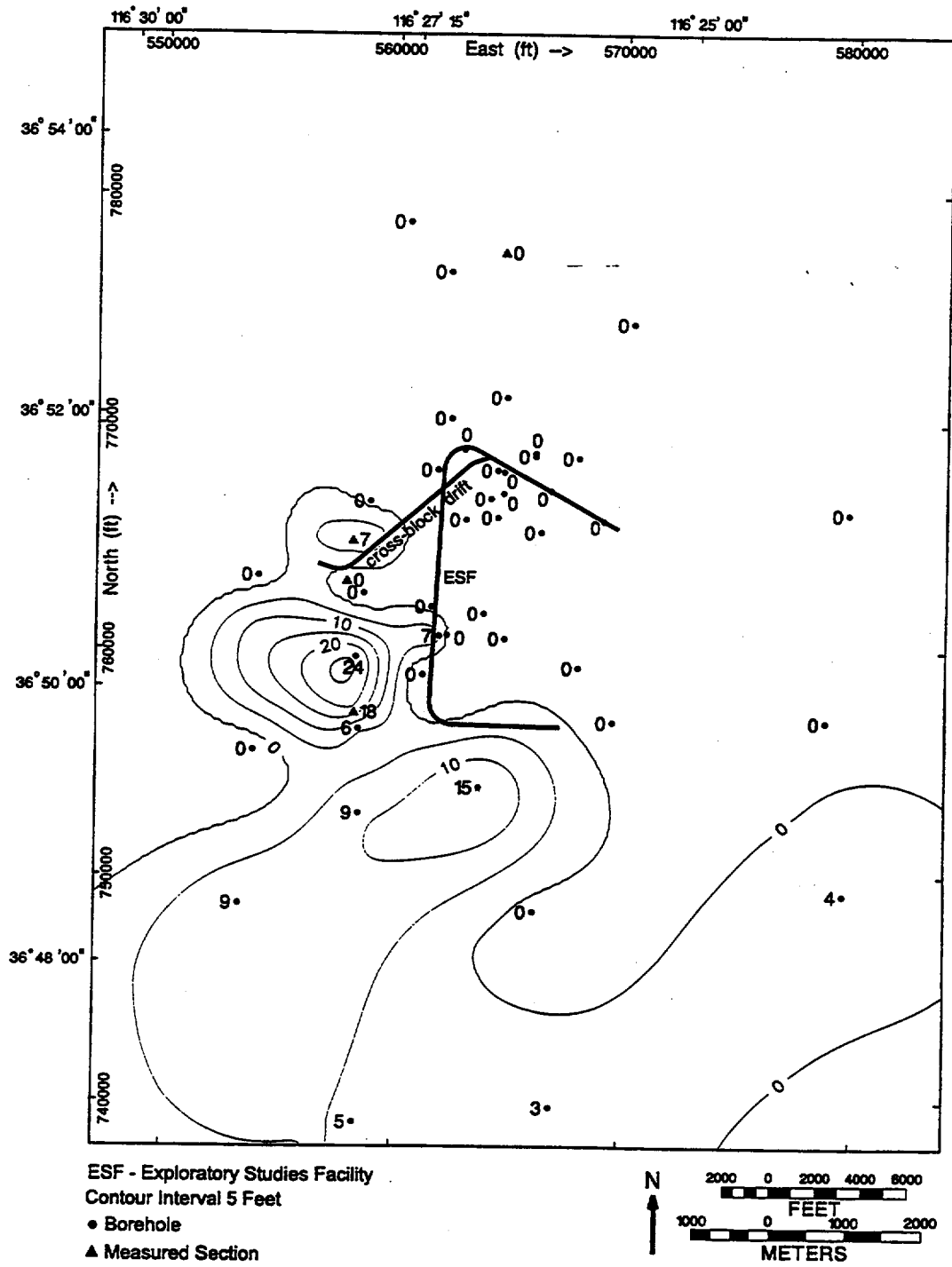
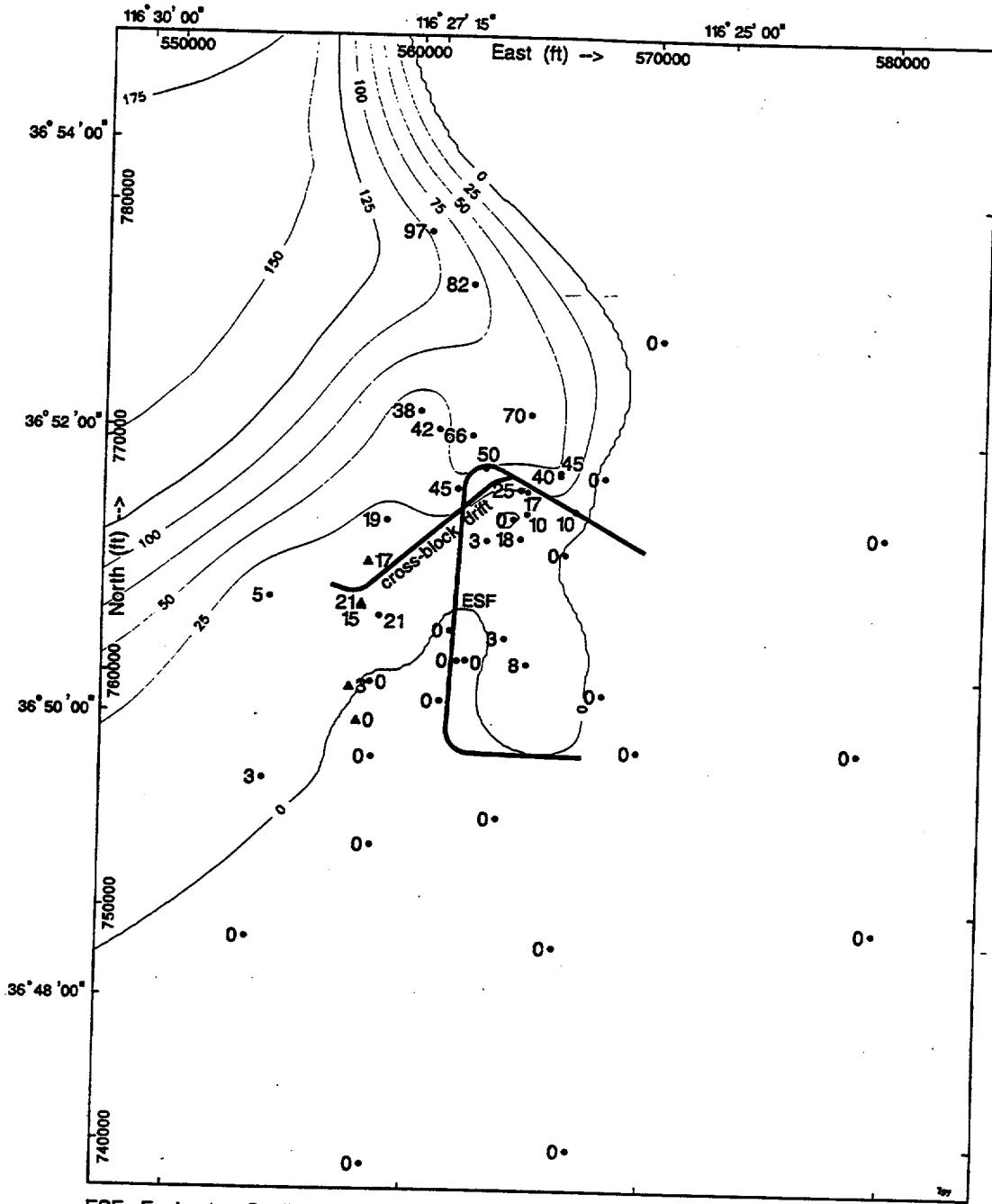


Figure 3-7. Model-Isochore Map of Tiva Canyon Tuff Crystal-Poor Member Vitric Zone Densely Welded Subzone (Tpcpv3)
 (CRWMS M&O 1999a, Figure 16)



ESF - Exploratory Studies Facility

Contour Interval 25 Feet

● Borehole

▲ Measured Section

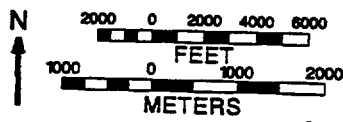
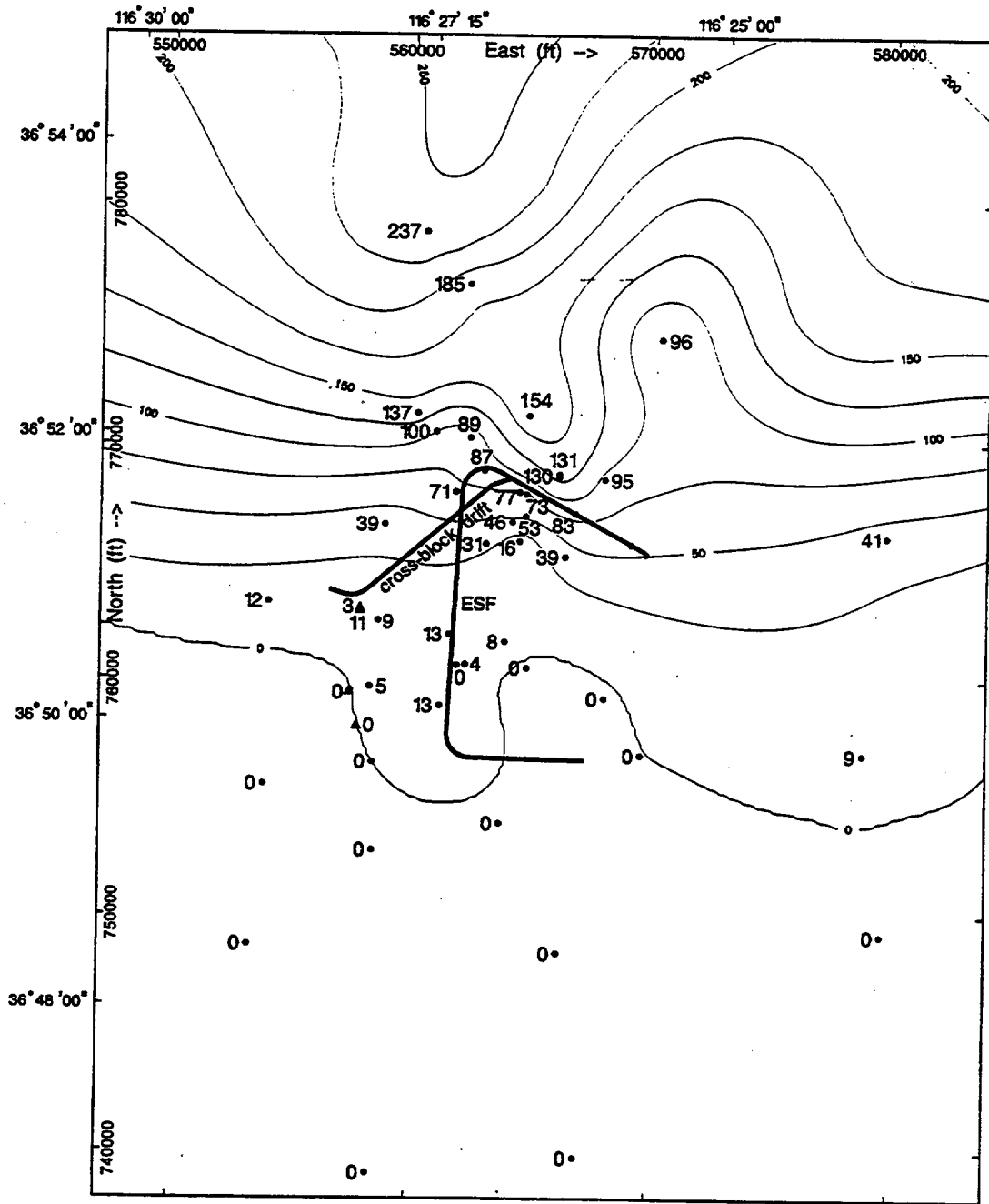


Figure 3-8. Model-isochores Map of Yucca Mountain Tuff (Tpy)
(CRWS M&O 1999a, Figure 17)



ESF - Exploratory Studies Facility

Contour Interval 25 Feet

● Borehole

▲ Measured Section

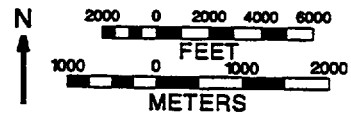
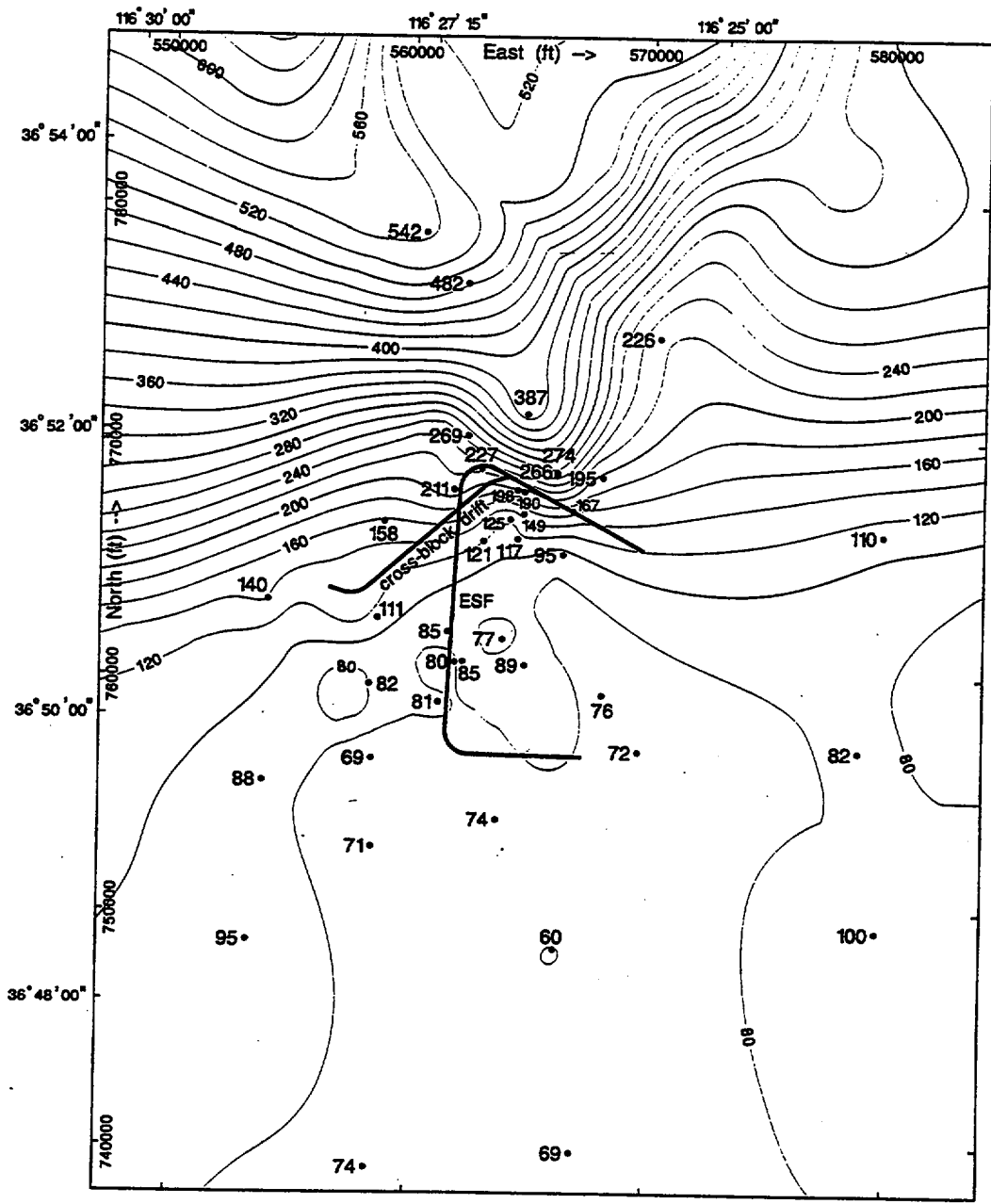


Figure 3-9. Model-Isochore Map of Pah Canyon Tuff (Tpp)
(CRWMS M&O 1999a, Figure 18)



ESF - Exploratory Studies Facility
 Contour Interval 20 Feet
 • Borehole

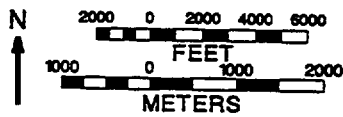
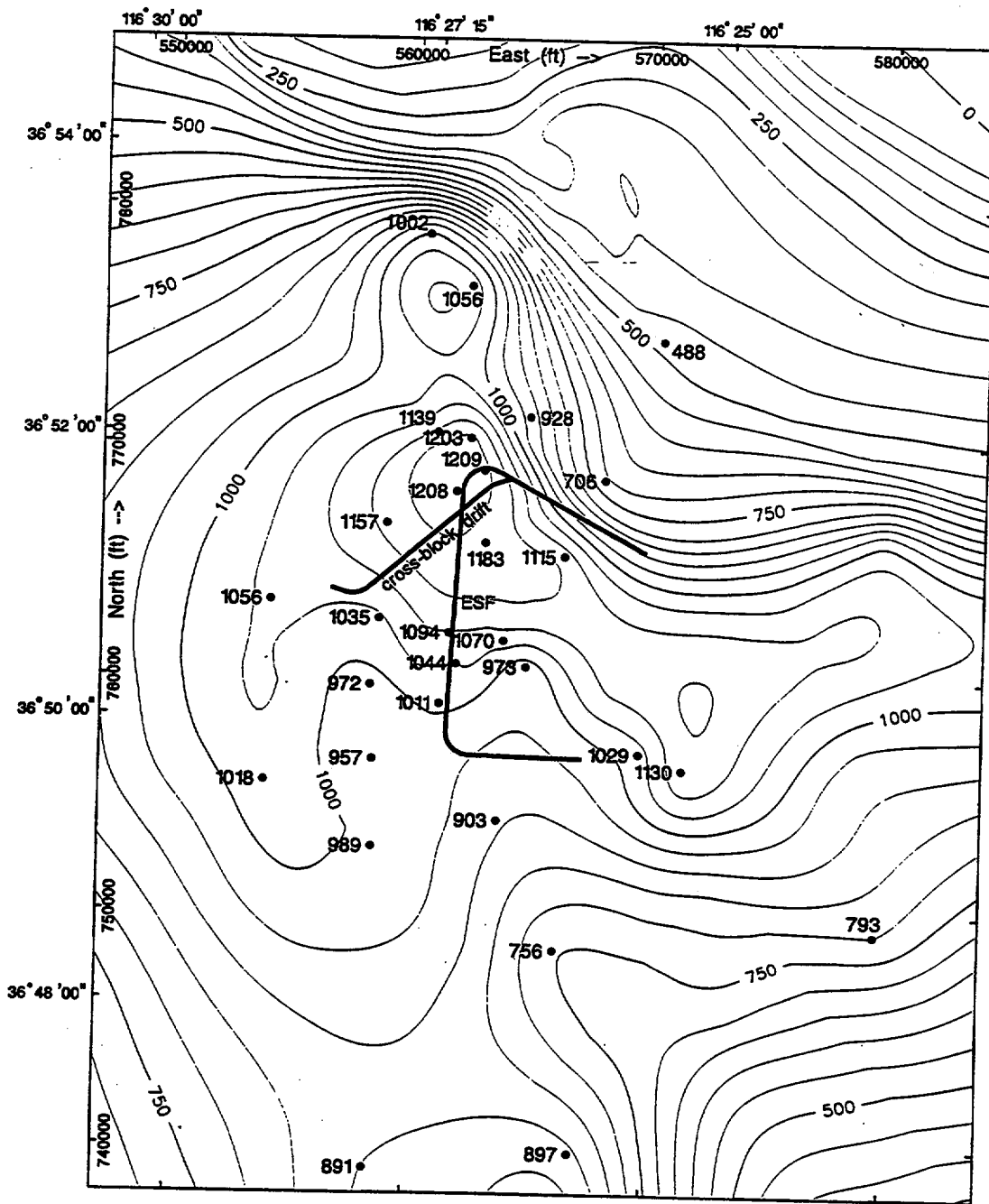


Figure 3-10. Model-Isochore Map of Paintbrush Tuff Nonwelded Unit (PTn)
 (CRWMS M&O 1999a, Figure 19)



ESF - Exploratory Studies Facility
 Contour Interval 50 Feet
 • Borehole

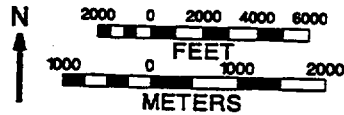


Figure 3-11. Model-Isochore Map of Topopah Spring Tuff (Tpt)
 (CRWMS M&O 1999a, Figure 20)

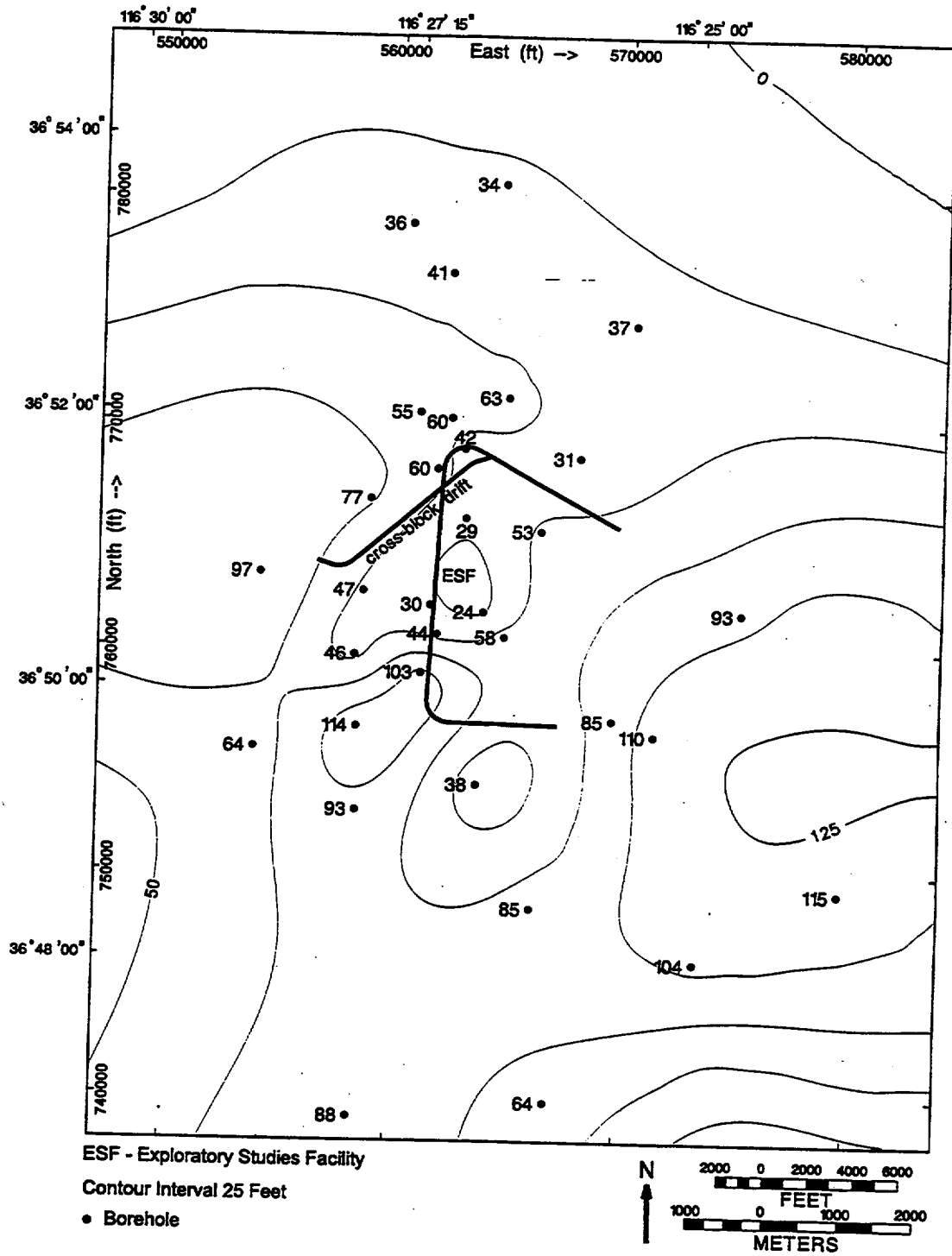
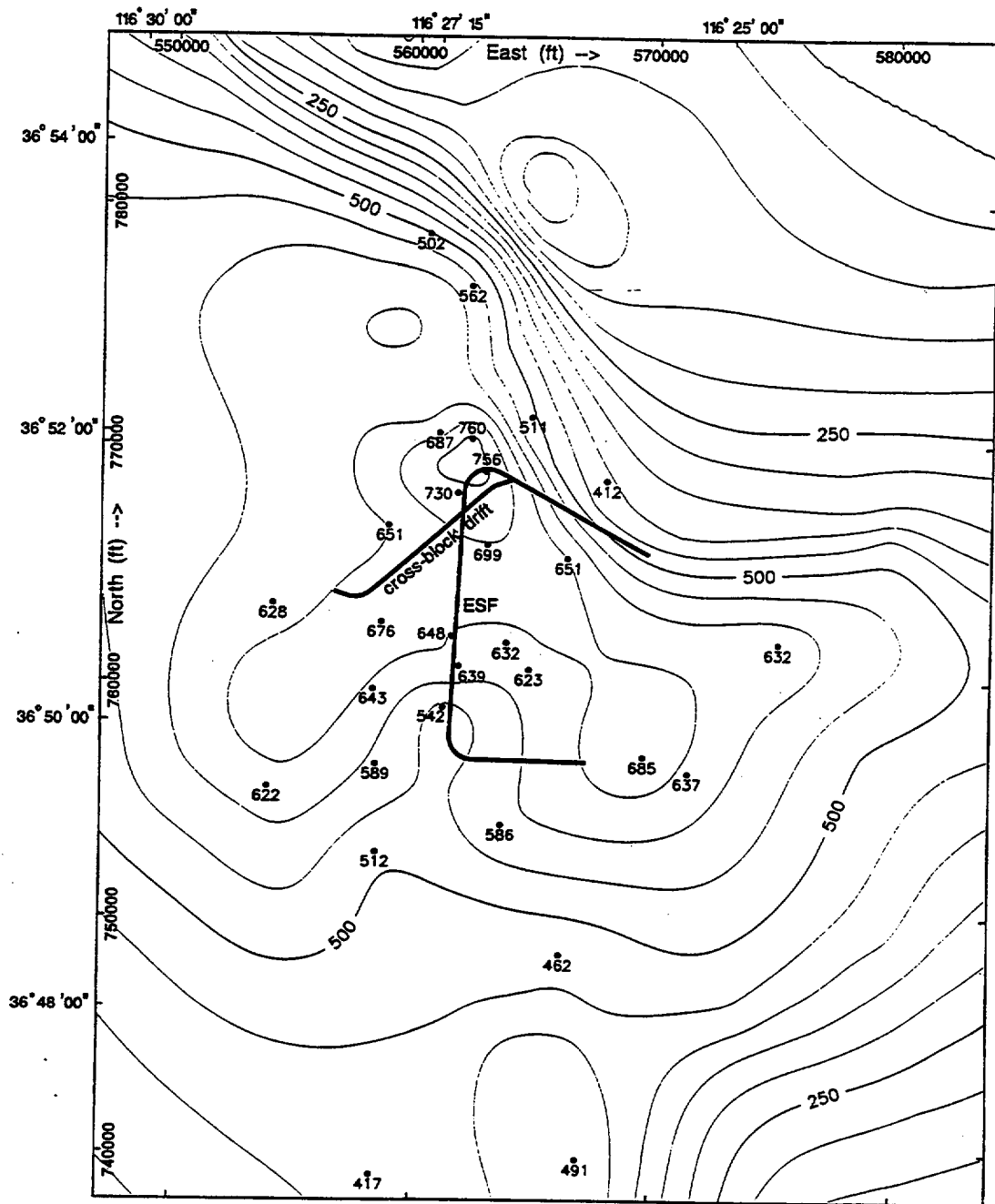


Figure 3-12. Model Isochore Map of Topopah Spring Tuff Crystal-Poor Member Vitric Zone Densely Welded Subzone (Tptpv3) (CRWMS M&O 1999a, Figure 21)



ESF - Exploratory Studies Facility

Contour Interval 50 Feet

● Borehole

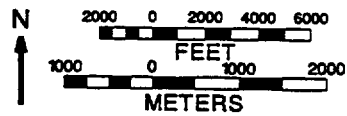


Figure 3-13. Model-isochores Map of Repository Host Horizon (RHH)
(CRWMS M&O 1999a, Figure 23)

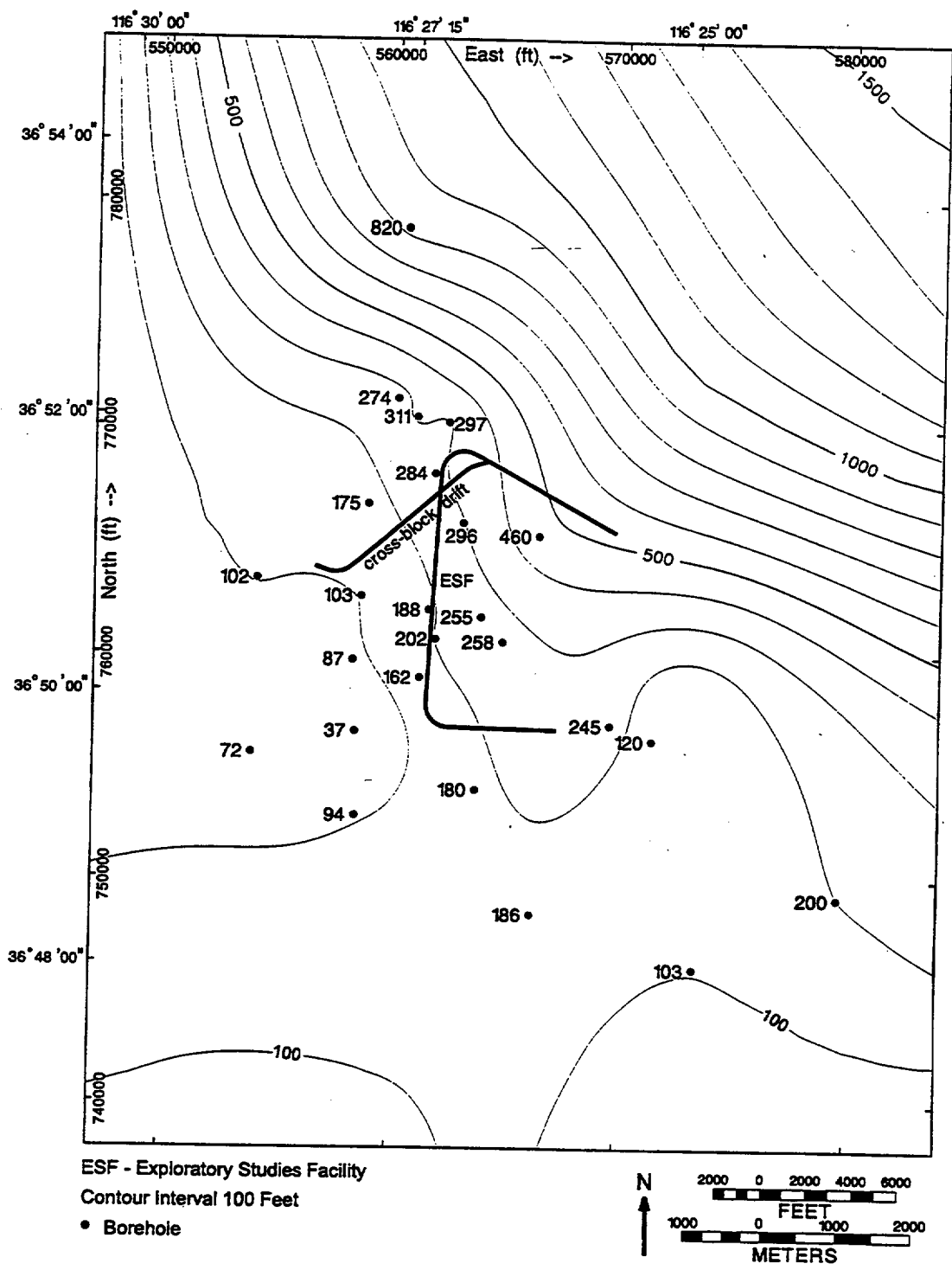
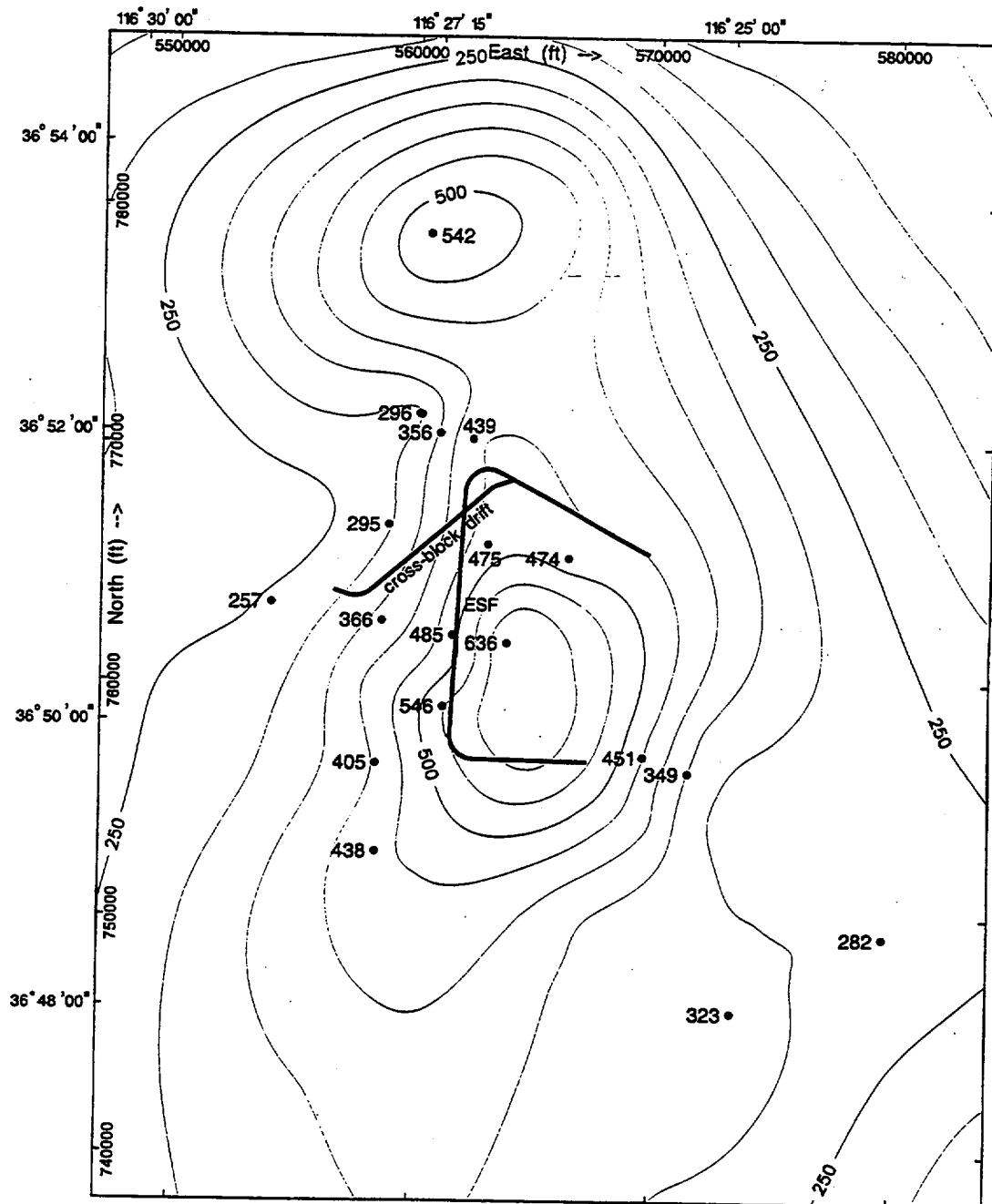


Figure 3-14. Model-Isochore Map of Calico Hills Formation (Ta)
(CRWMS M&O 1999a, Figure 24)



ESF - Exploratory Studies Facility
 Contour Interval 50 Feet
 • Borehole

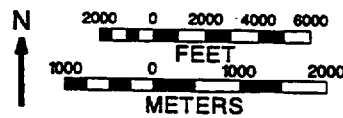


Figure 3-15. Model-Isochore Map of Prow Pass Tuff (T_{cp})
 (CRWMS M&O 1999a, Figure 25)

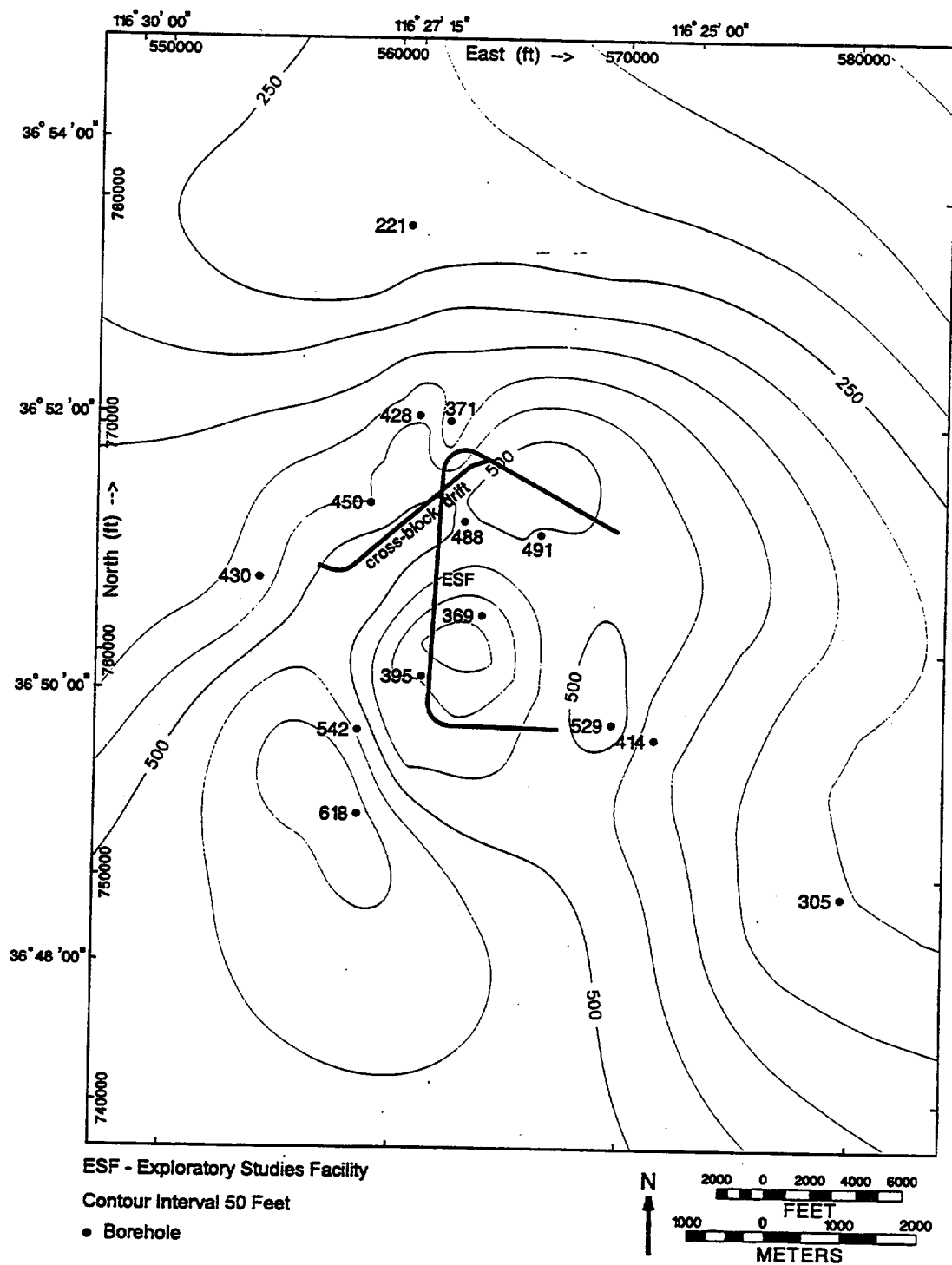
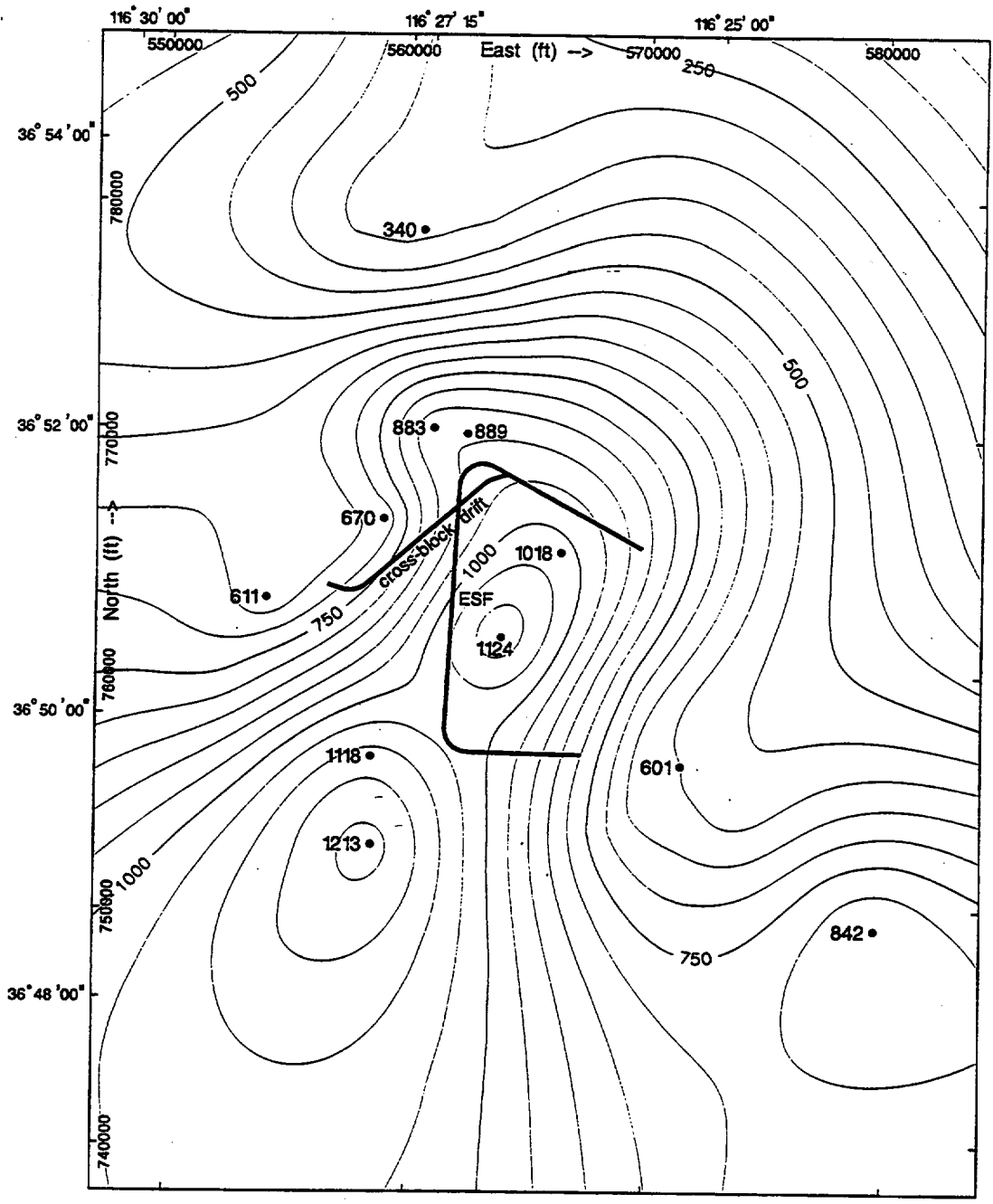


Figure 3-16. Model-Isochore Map of Bullfrog Tuff (Tcb)
 (CRWMS M&O 1999a, figure 26)



ESF - Exploratory Studies Facility
 Contour Interval 50 Feet
 ● Borehole

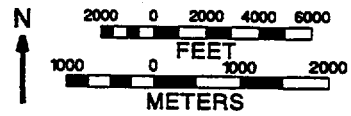
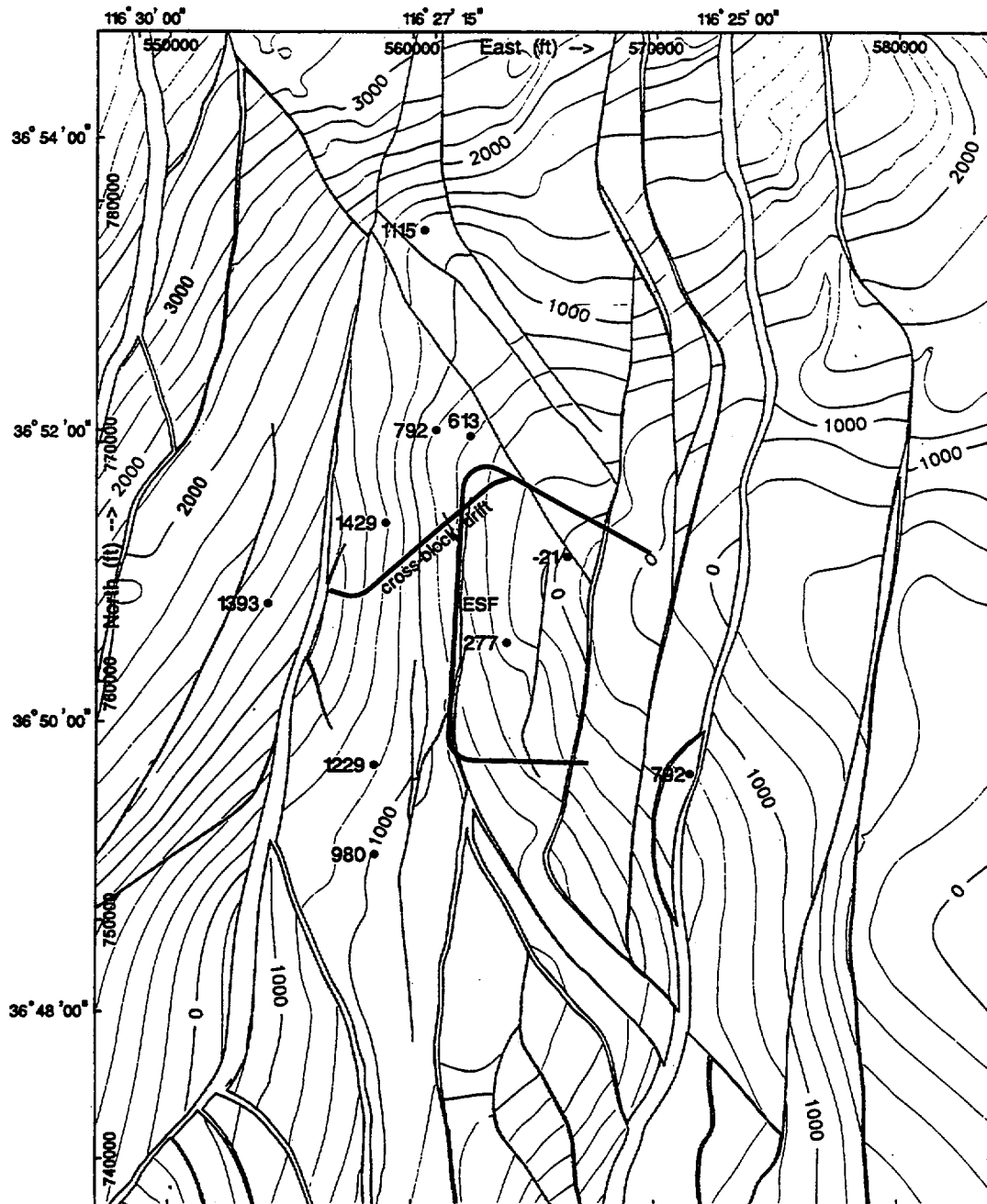


Figure 3-17. Model-Isochore Map of Tram Tuff (Tct)
 (CRWMS M&O 1999a, Figure 27)

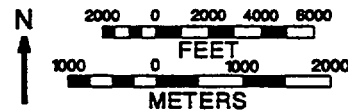


ESF - Exploratory Studies Facility

Contour Interval 200 Feet

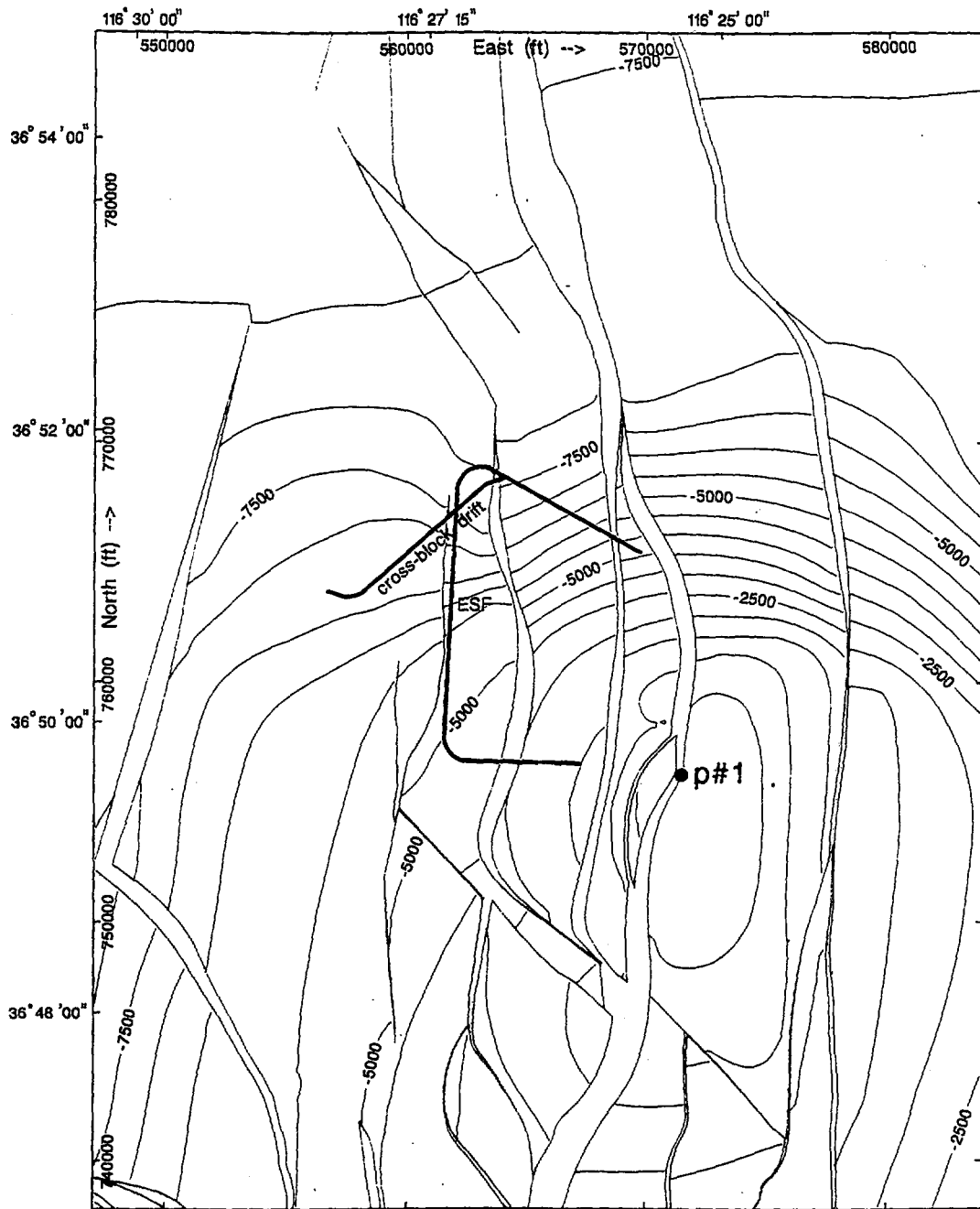
• Borehole

— Fault

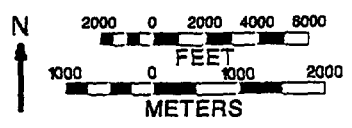


NOTE: Traces of major faults that displace the older Tertiary units are shown in red. Blank areas indicate fault displacements.

Figure 3-18. Elevation Map of Top of Older Tertiary Units (Tund)
(CRWMS M&O 1999a, Figure 28)

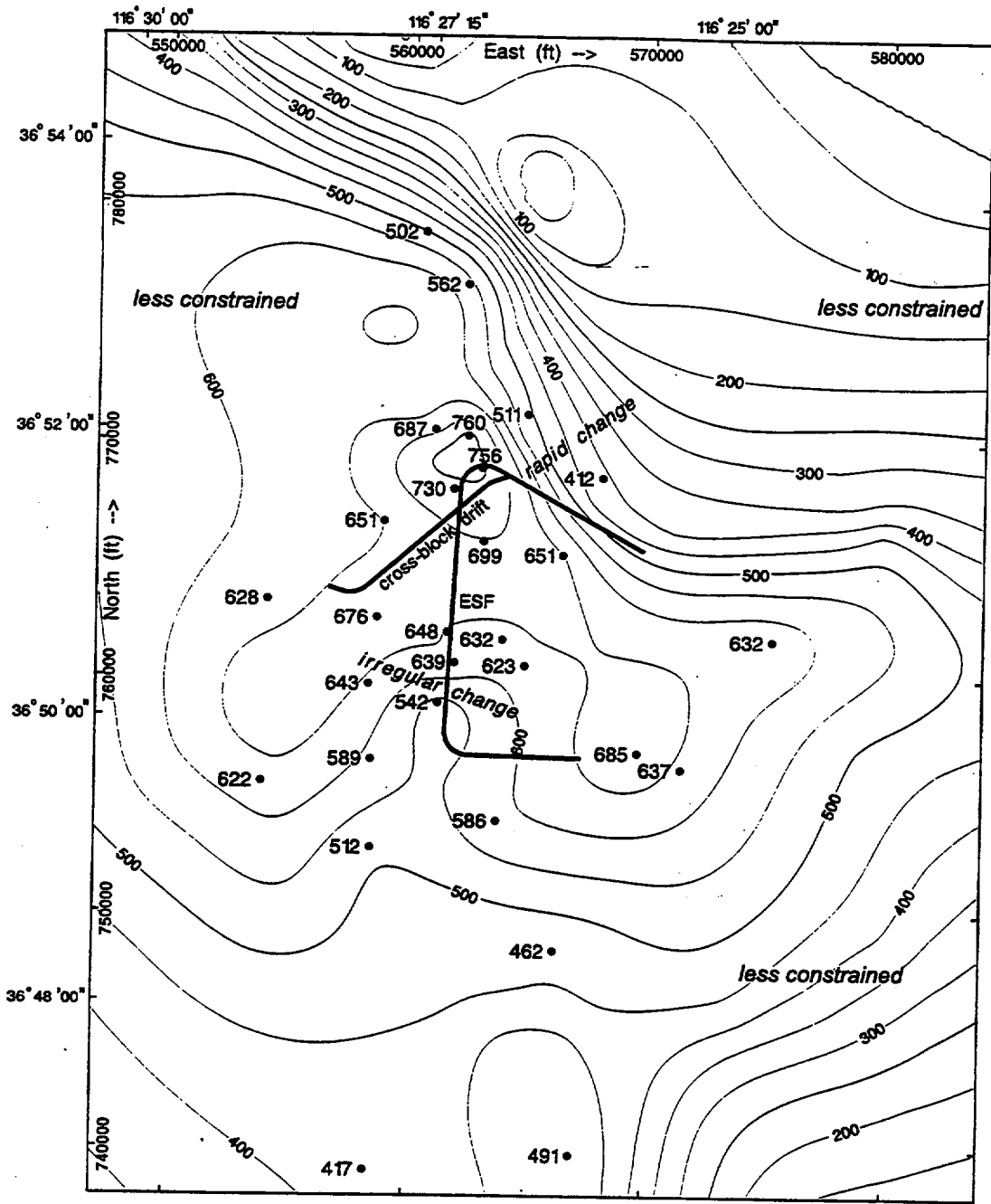


ESF - Exploratory Studies Facility
 Contour Interval 500 Feet
 ● Borehole
 / Fault



NOTE: Traces of major faults that displace the older Tertiary units are shown in red. Blank areas indicate fault displacements.

Figure 3-19. Elevation Map of Tertiary-Paleozoic Unconformity (CRWMS M&O 1999a, Figure 29)



ESF - Exploratory Studies Facility
 Contour Interval 50 Feet
 • Borehole

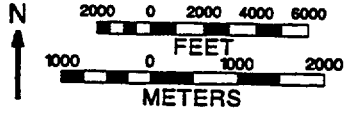


Figure 3-20. Model-Isochore Map of Repository Host Horizon Showing Less Constrained Areas (CRWMS M&O 1999a, Figure 33)

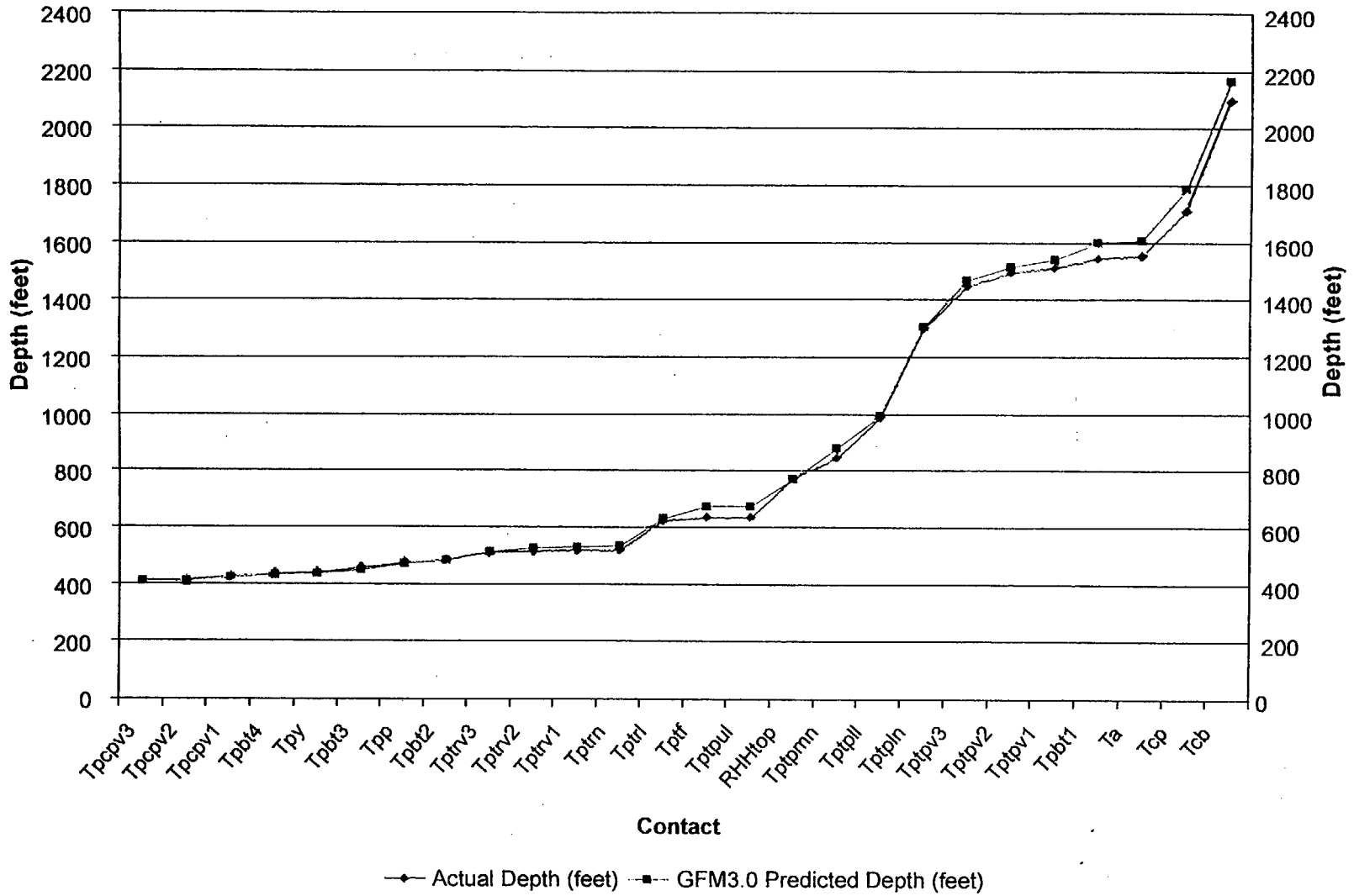


Figure 3-21. SD-6 Comparison of Predicted Versus Actual Contact Depths (Measured at Unit Tops)
 (CRWMS M&O 1999a, Figure 34)

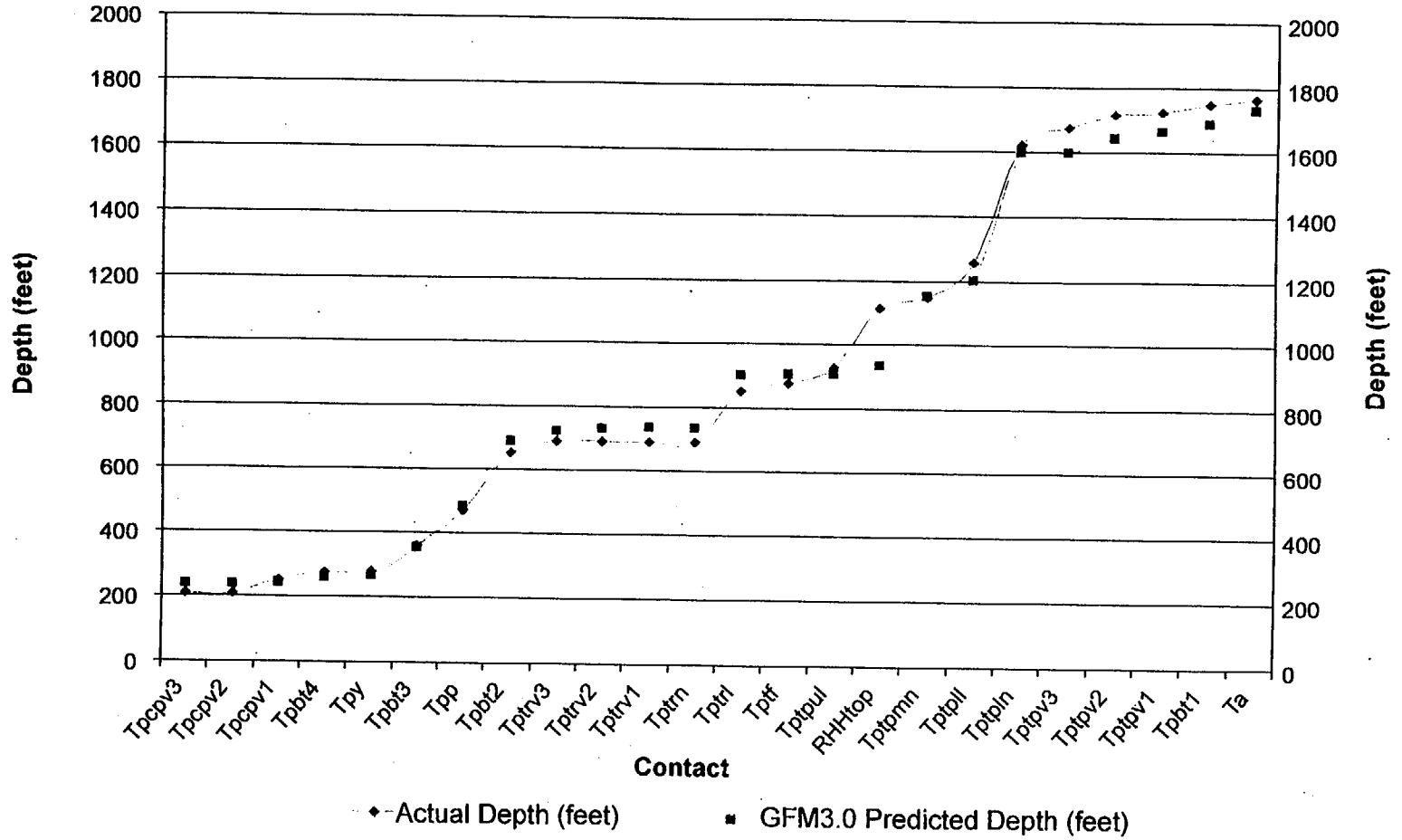


Figure 3-22. WT-24 Comparison of Predicted Versus Actual Contact Depths (Measured at Unit Tops)
 (CRWMS M&O 1999a, Figure 35)

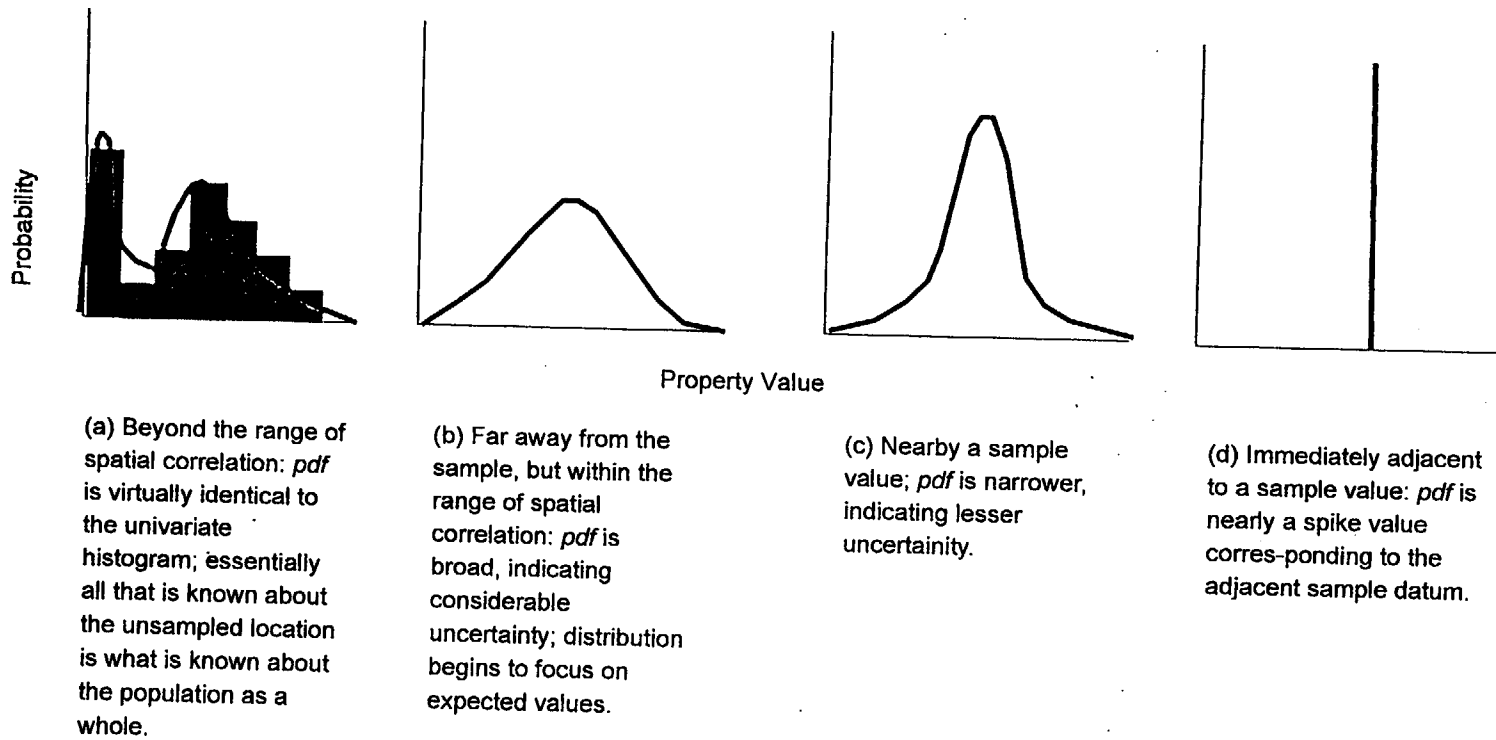


Figure 3-23. Conceptual Probability Density Functions Representing the Uncertainty Associated With Various Unsampled Locations

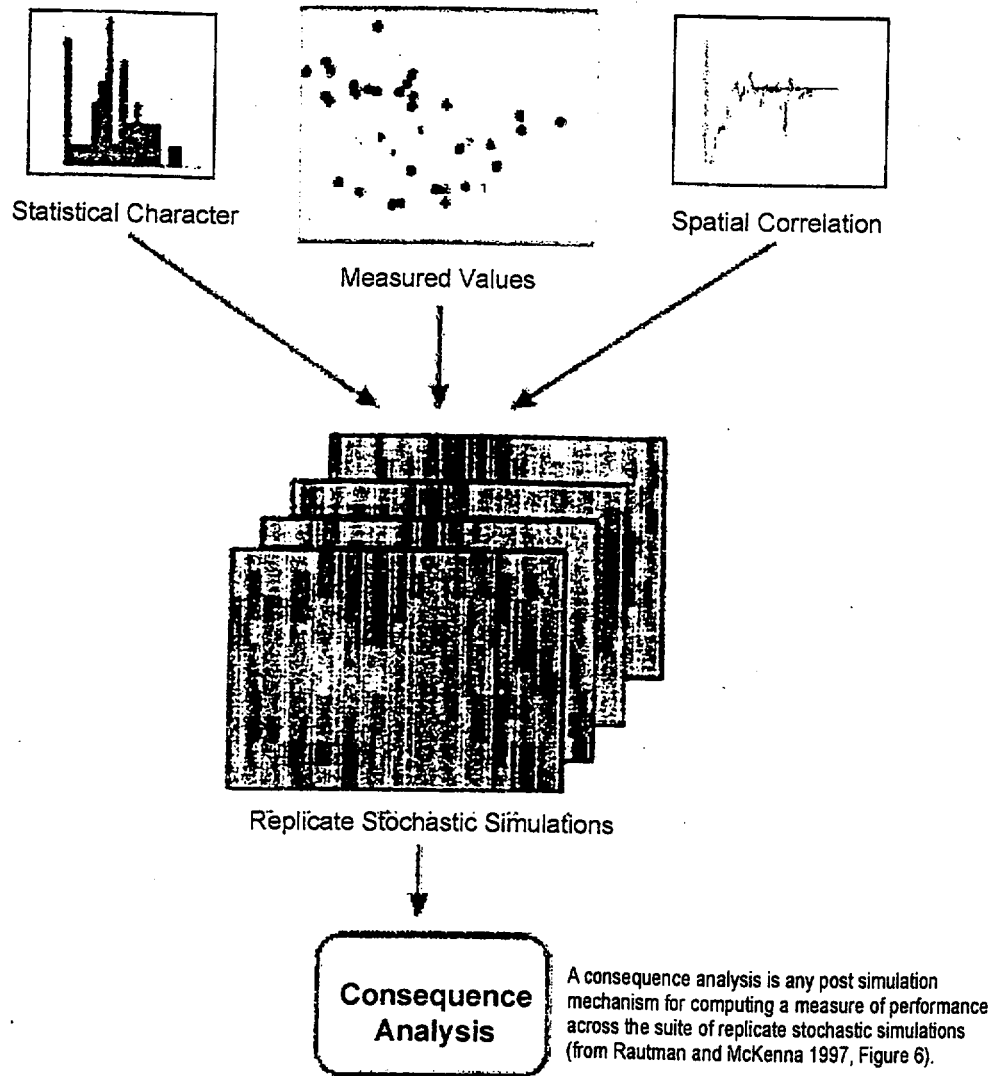


Figure 3-24. Conceptual Representation of a Monte Carlo Process Incorporating Geostatistical Simulation Techniques (CRWMS M&O 1999b, Figure 3)

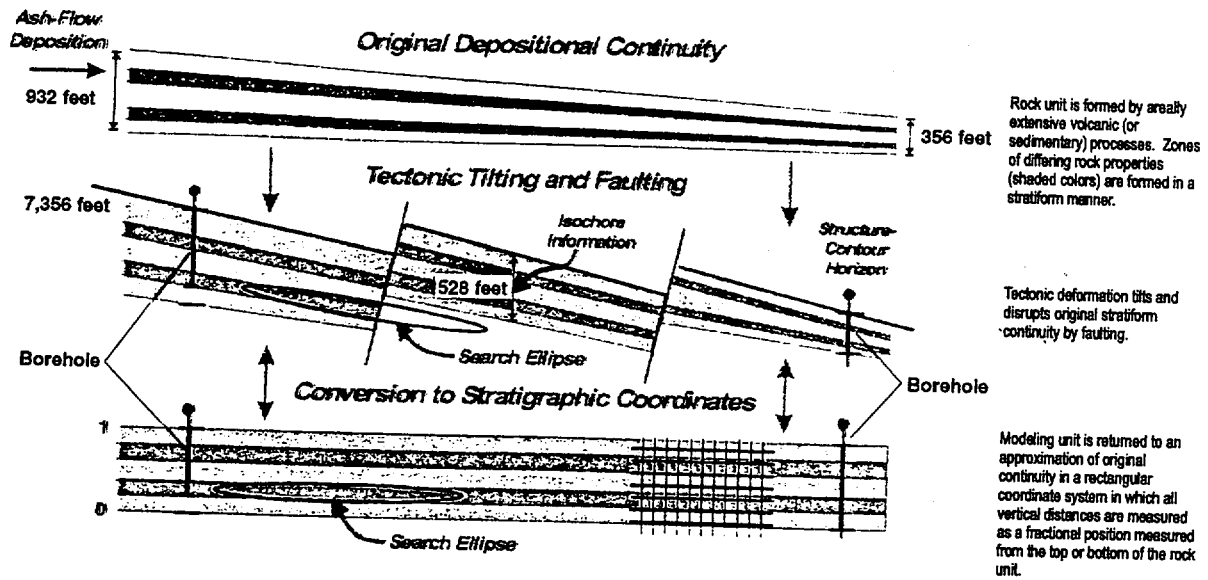
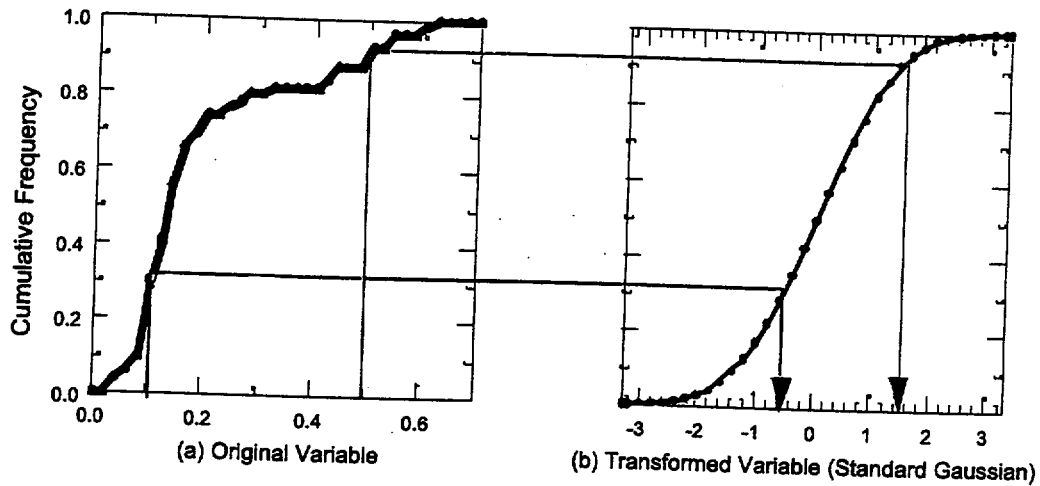
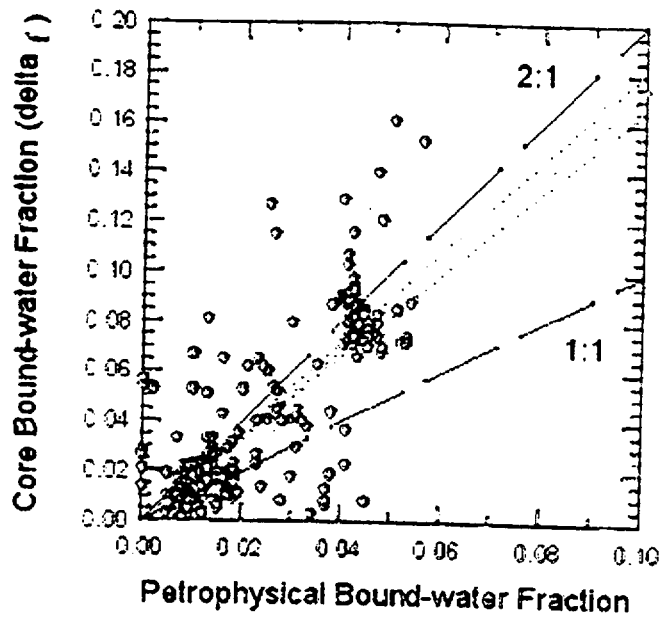


Figure 3-25. Conceptual Illustration of the Construction and Use of Stratigraphic Coordinates



NOTE: A population with virtually any univariate distribution (a) can be transformed to any other univariate distribution (b) in a manner represented by the arrows such that the quantile relationships among the data are preserved. The reverse transformation is also possible in the same manner.

Figure 3-26. Graphical Representation of the Quantile-Preserving Normal-Score Transform Process Using Cumulative Distribution Functions (CRWMS M&O 1999b, Figure 31)



NOTE: The regression line (solid with 95% upper and lower confidence limits (red dotted)) has been forced through the origin and has a slope of 1.74; unconstrained regression has $r^2 = 0.67$. (R-squared for a constrained line is not meaningful.)

Figure 3-27. Scatterplot of Core Versus Petrophysically Derived Bound-Water Content for 354 Depth-Matched Pairs of Samples (CRWMS M&O 1999b, Figure 32)

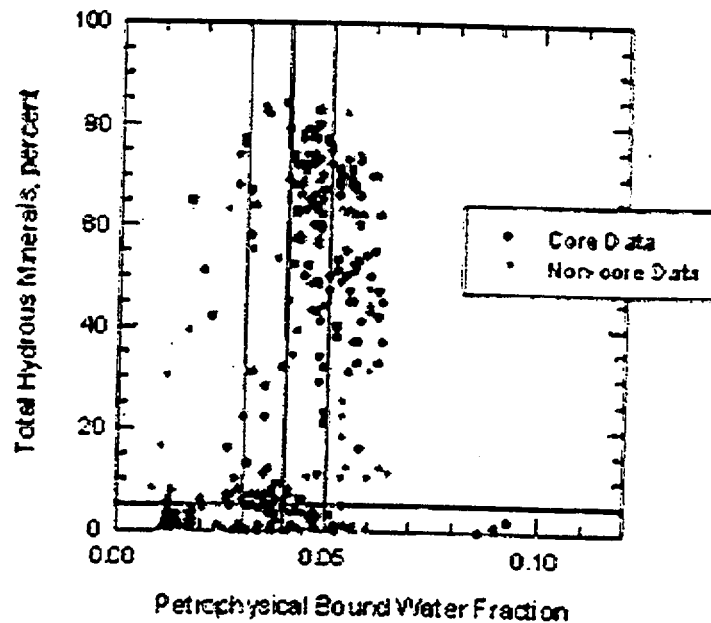
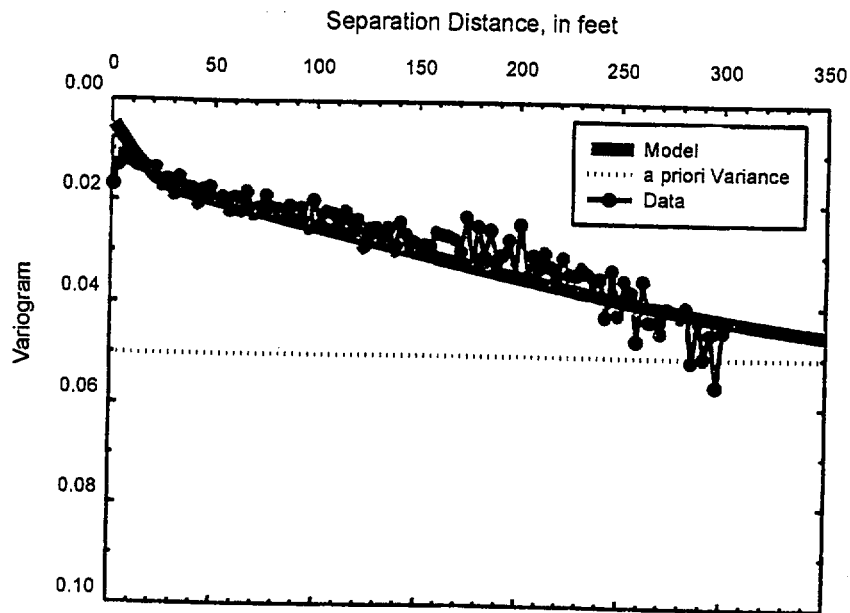
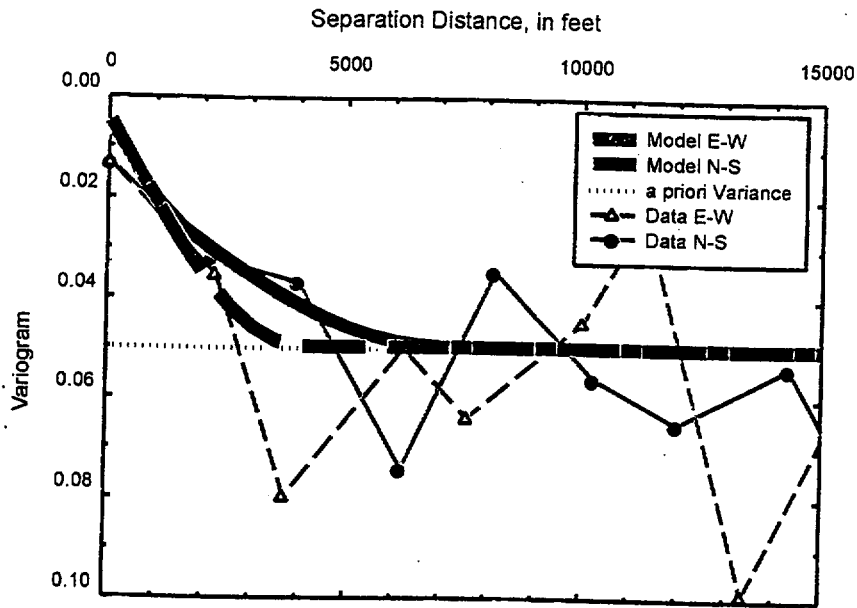


Figure 3-28. Scatterplot of Total Hydrous-Phase Mineral Content Versus Adjusted Bound-Water Content for 334 Depth-Matched Pairs of Samples (CRWMS M&O 1999b, Figure 33)

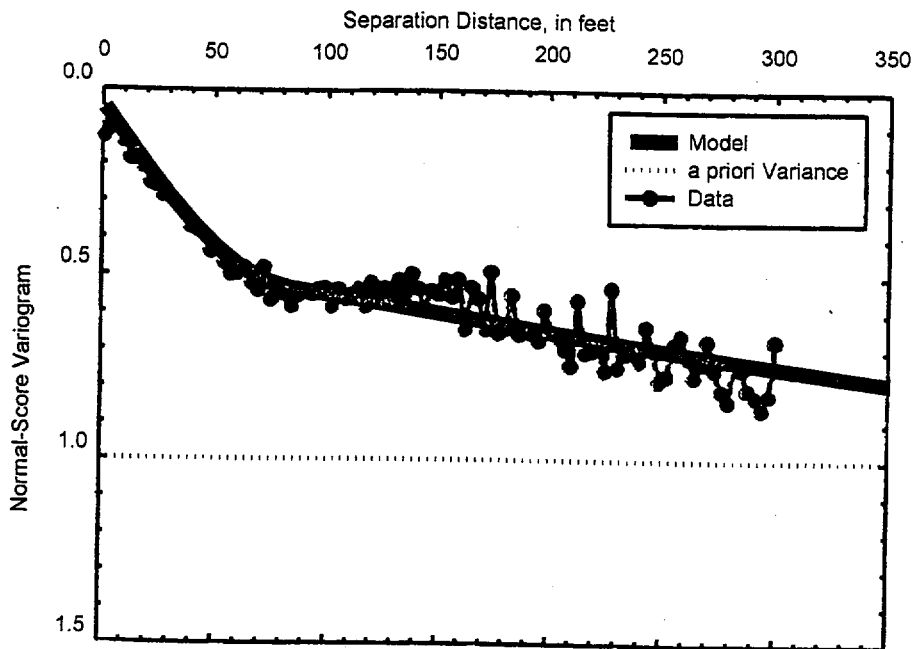


(a) Stratigraphically Vertical

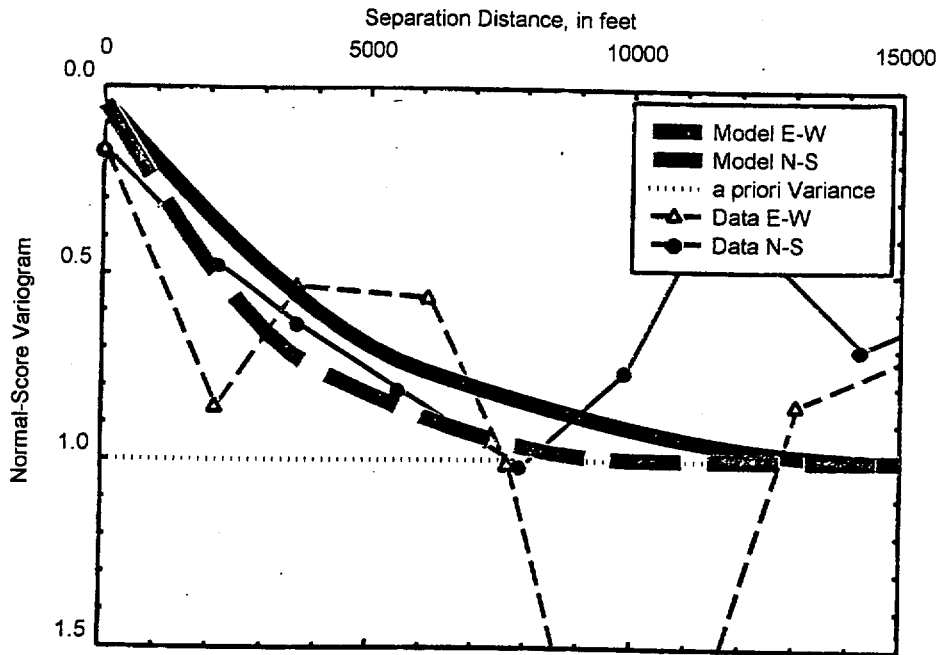


(b) Stratigraphically Horizontal

Figure 3-29. Indicator Variogram and Fitted Model Computed for Hydrous-Phase Mineral Alteration in the CHn Model Unit
(Modified after CRWMS M&O 1999b, Figure 34)



(a) Stratigraphically Vertical



(b) Stratigraphically Horizontal

Figure 3-30. Indicator Variogram and Fitted Model Computed for Alteration in the Tcp Model Unit (Modified after CRWMS M&O 1999b, Figure 35)

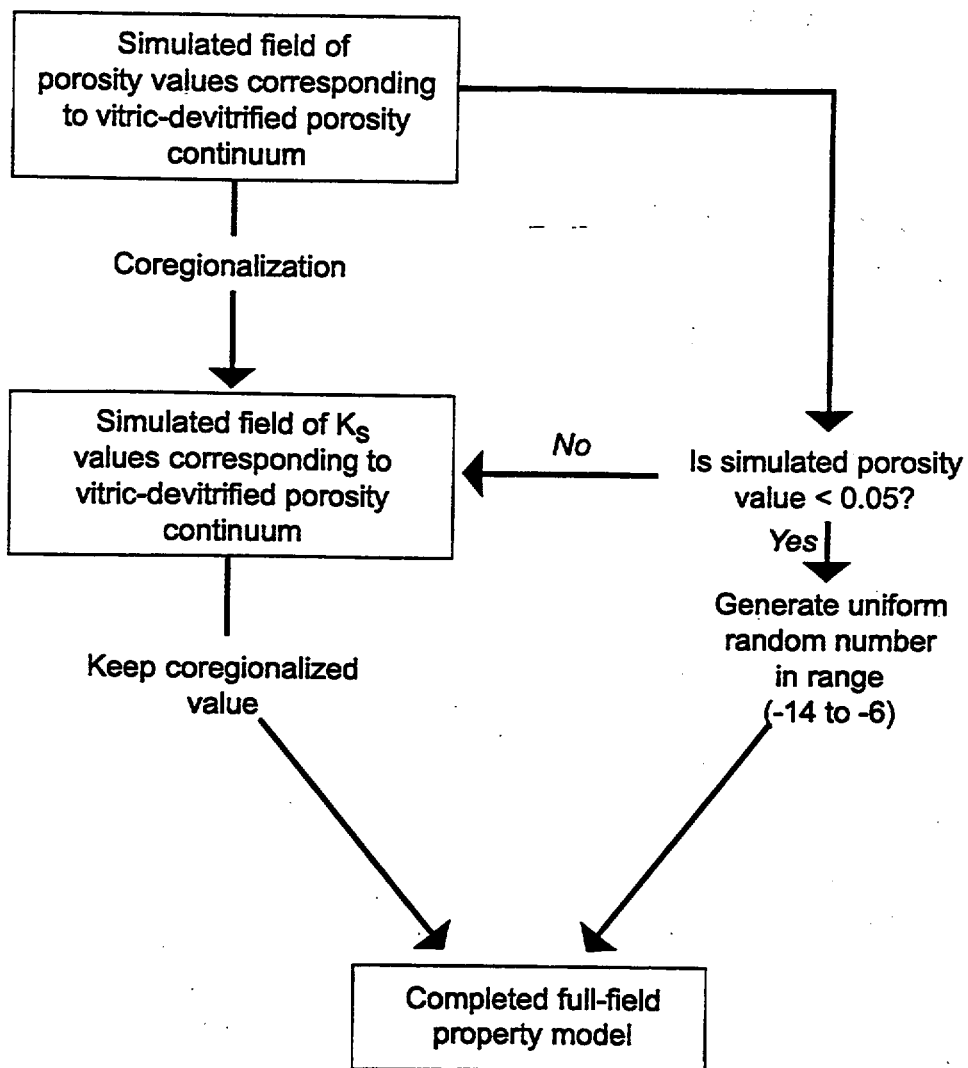


Figure 3-31. Logic Diagram for Postprocessing Porosity and Hydraulic Conductivity Simulations To Recognize Vitrophyre Rock Type (CRWMS M&O 1999b, Figure 36)

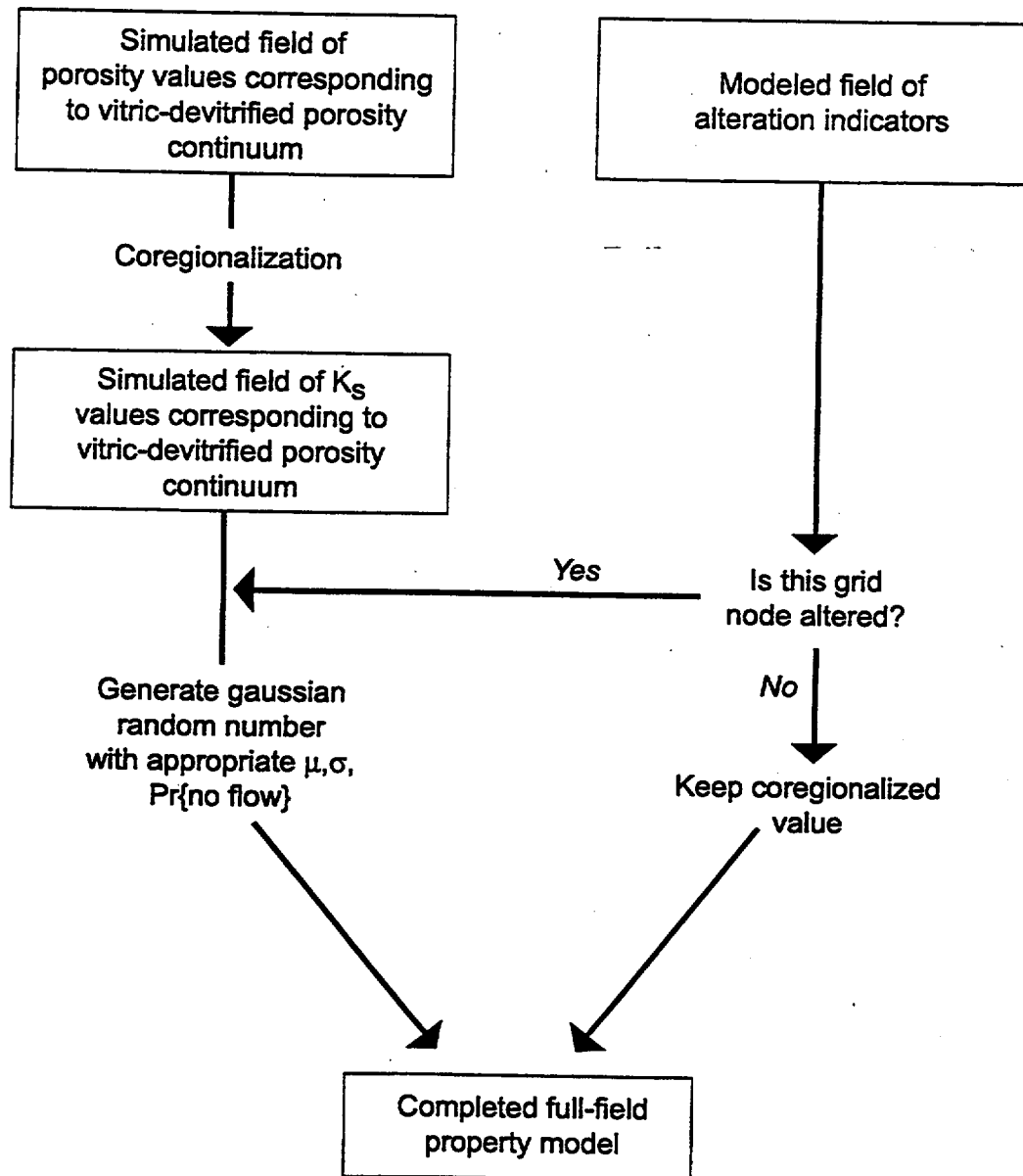


Figure 3-32. Logic Diagram for Postprocessing Porosity and Alteration Indicator Simulations To Recognize Hydraulic Conductivity Dependence on Alteration State (CRWMS M&O 1999b, Figure 37)

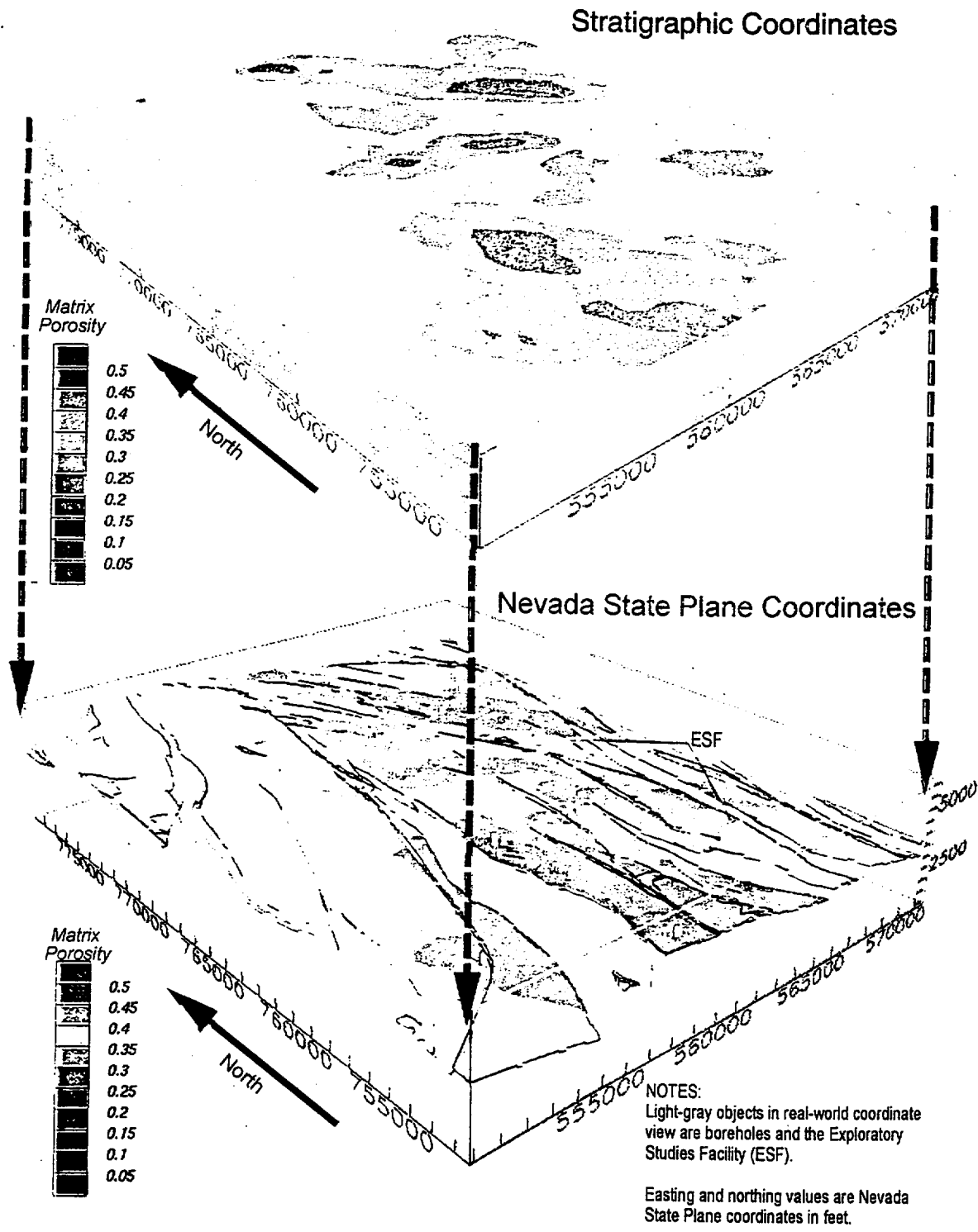


Figure 3-33. Perspective Diagrams Showing E-Type Model Matrix Porosity in the PTn Model Unit in Both Stratigraphic and Real-World Coordinates (CRWMS M&O 1999b, Figure 38)

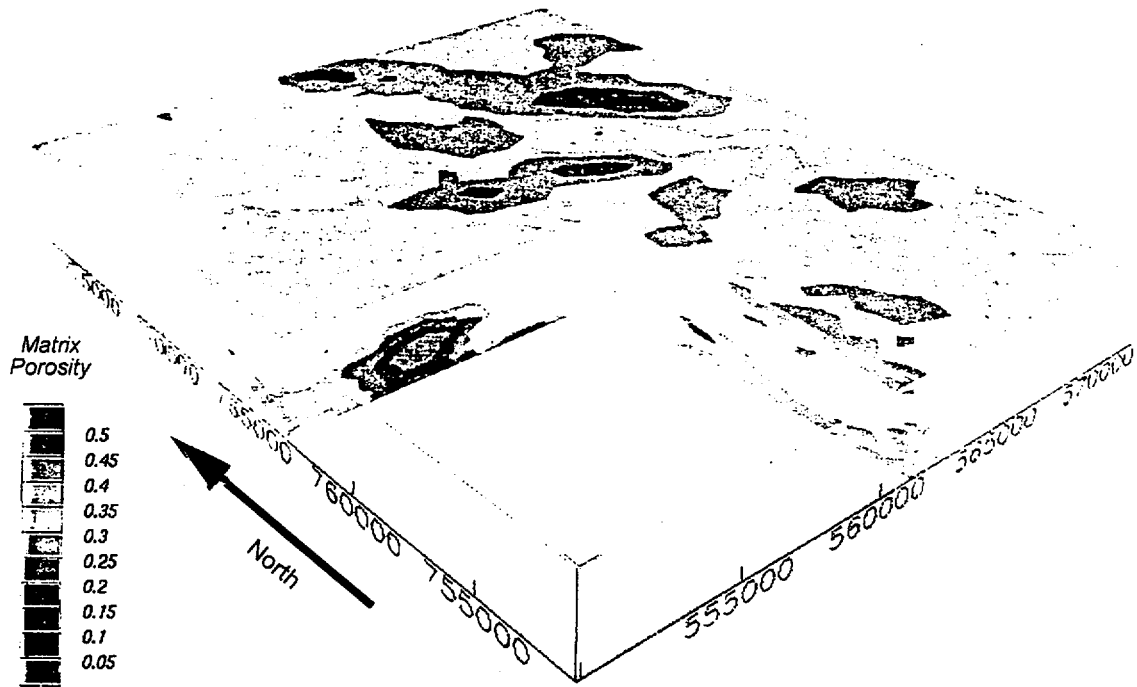


Figure 3-34. Cross-Sectional Views Showing E-Type Heterogeneity of Matrix Porosity in the PTn Model Unit in Stratigraphic Coordinates

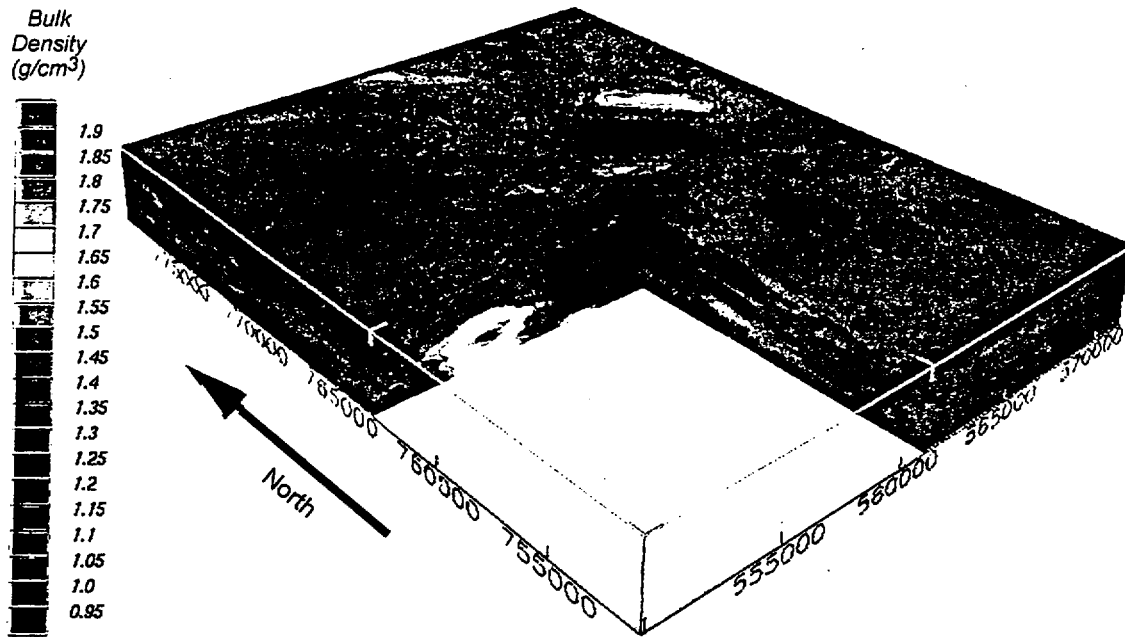


Figure 3-35. Cross-Sectional Views Showing E-Type Heterogeneity of Bulk Density in the PTn Model Unit in Stratigraphic Coordinates

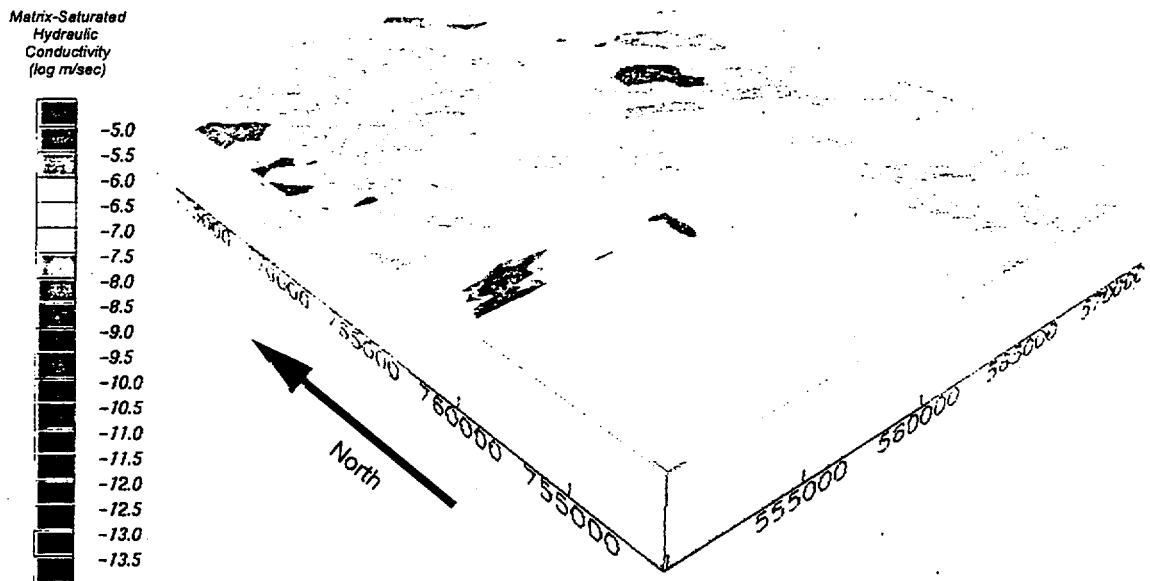


Figure 3-36. Cross-Sectional Views Showing E-Type Heterogeneity of Matrix-Saturated Hydraulic Conductivity in the PTn Model Unit in Stratigraphic Coordinates

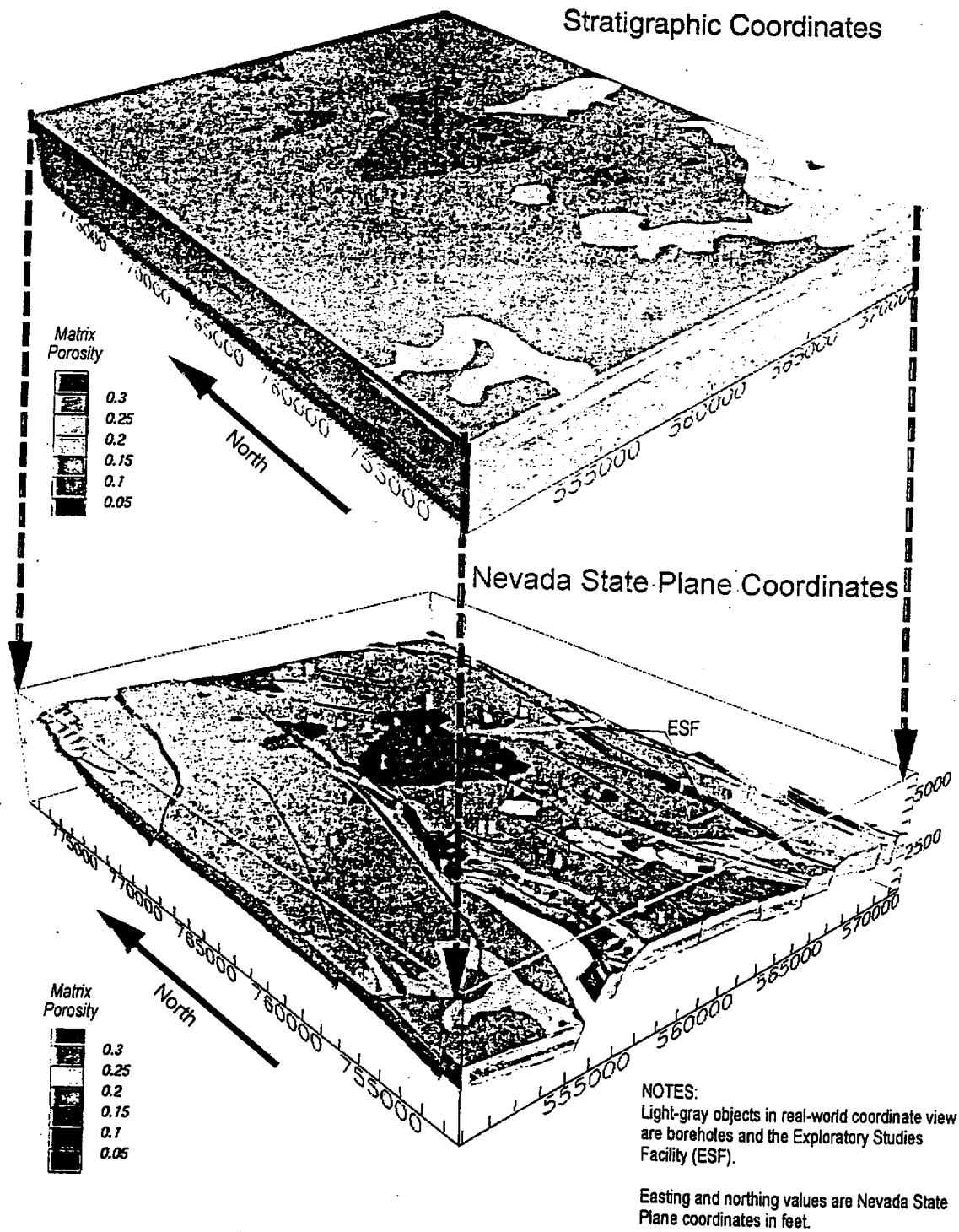


Figure 3-37. Perspective Diagrams Showing E-Type Matrix Porosity in the TSw Model Unit in Both Stratigraphic and Real-World Coordinates (CRWMS M&O 1999b, Figure 42)

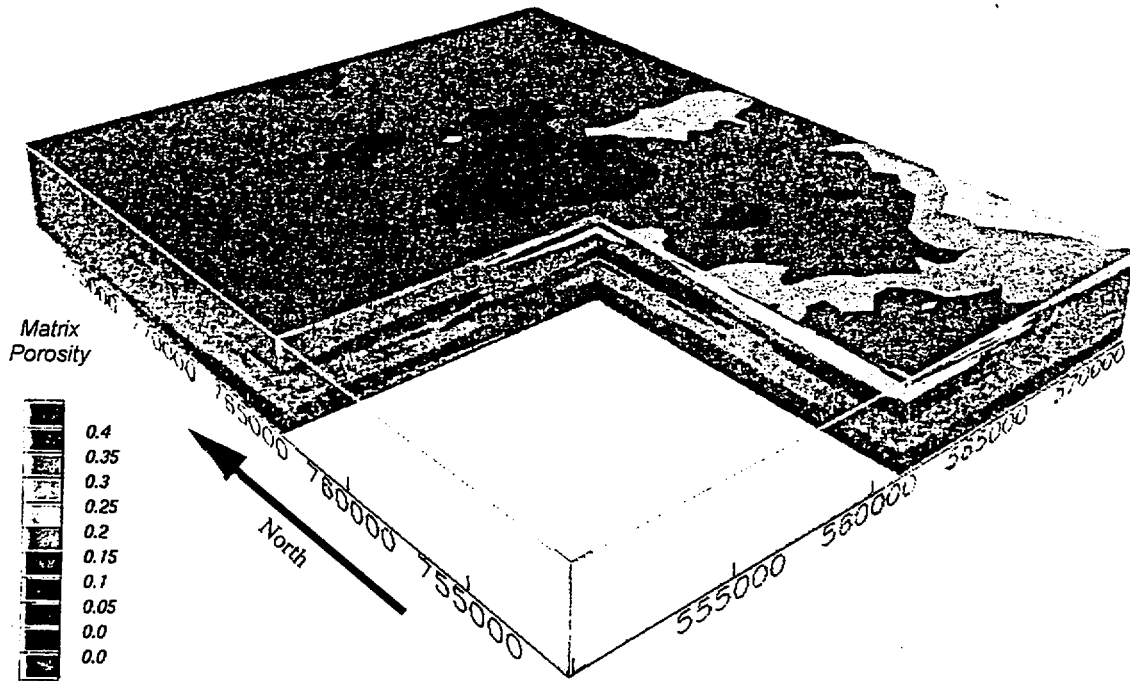


Figure 3-38. Cross-Sectional Views Showing E-Type Heterogeneity of Matrix Porosity in the TSw Model Unit in Stratigraphic Coordinates

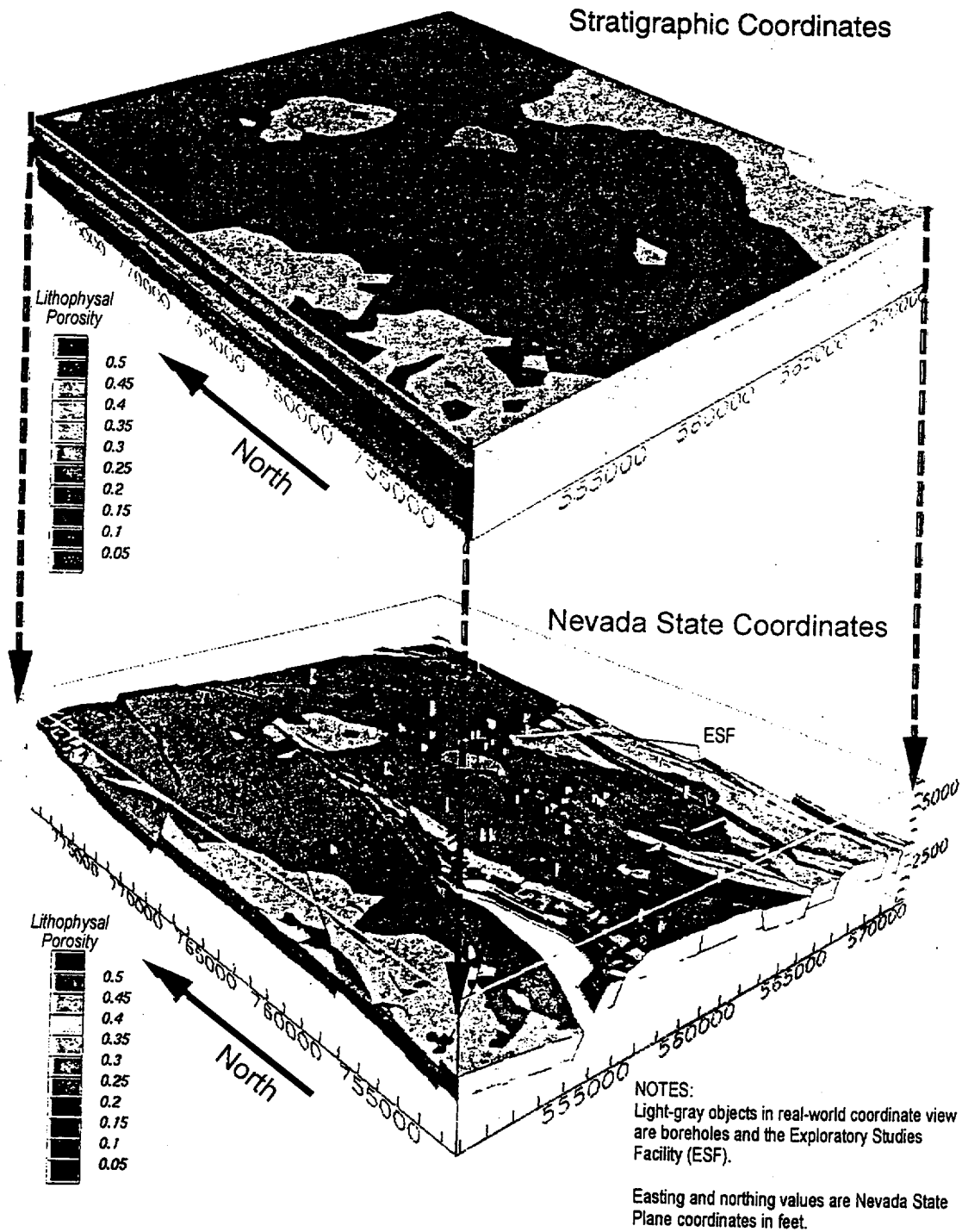


Figure 3-39. Perspective Diagrams Showing E-Type Lithophysal Porosity in the TSw Model Unit in Both Stratigraphic and Real-World Coordinates (CRWMS M&O 1999b Figure 44)

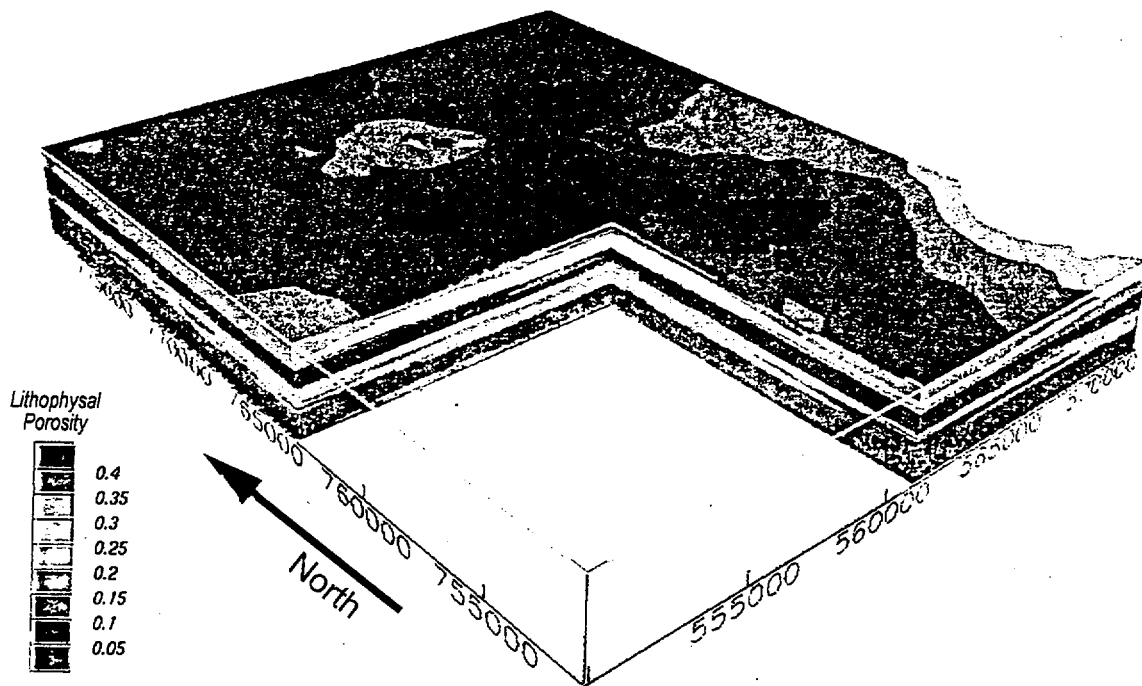


Figure 3-40. Cross-Sectional Views Showing E-Type Heterogeneity of Lithophysal Porosity in the TSw Model Unit in Stratigraphic Coordinates

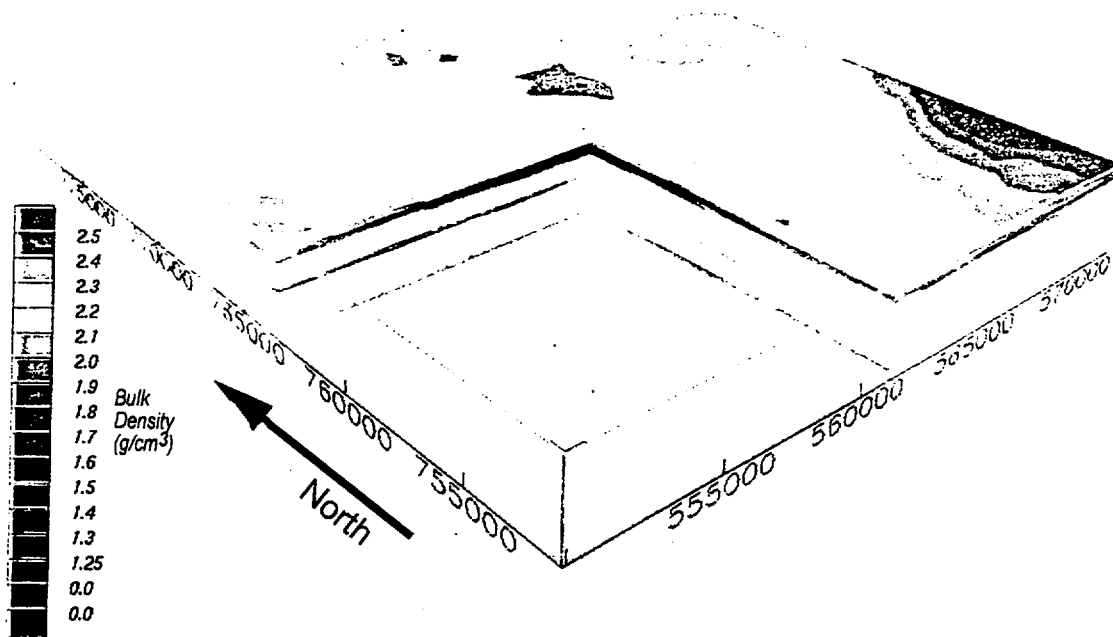


Figure 3-41. Cross-Sectional Views Showing E-Type Heterogeneity of Bulk Density in the TSw Model Unit in Stratigraphic Coordinates

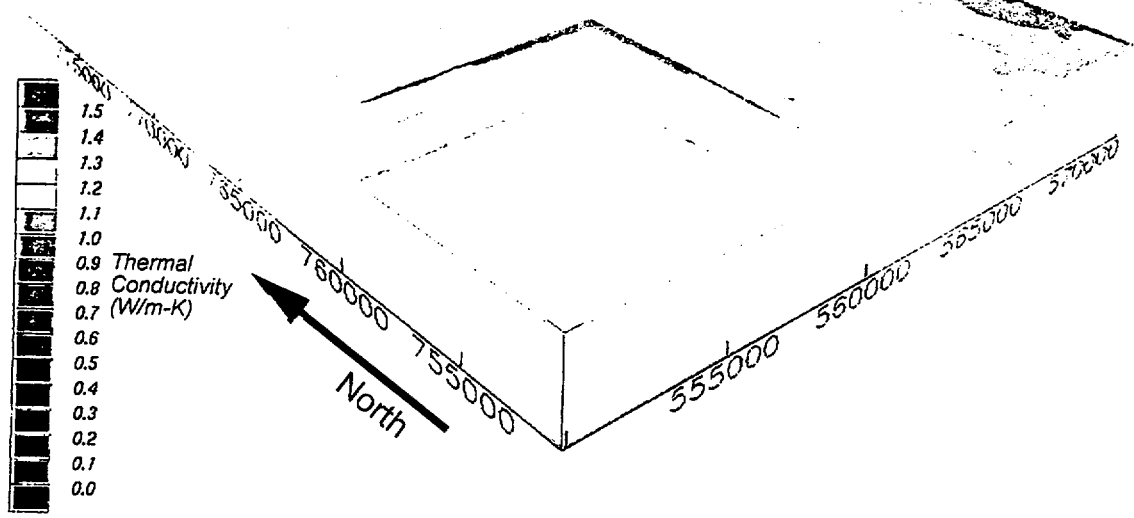


Figure 3-42. Cross-Sectional Views Showing E-Type Heterogeneity of Thermal Conductivity in the TSw Model Unit in Stratigraphic Coordinates

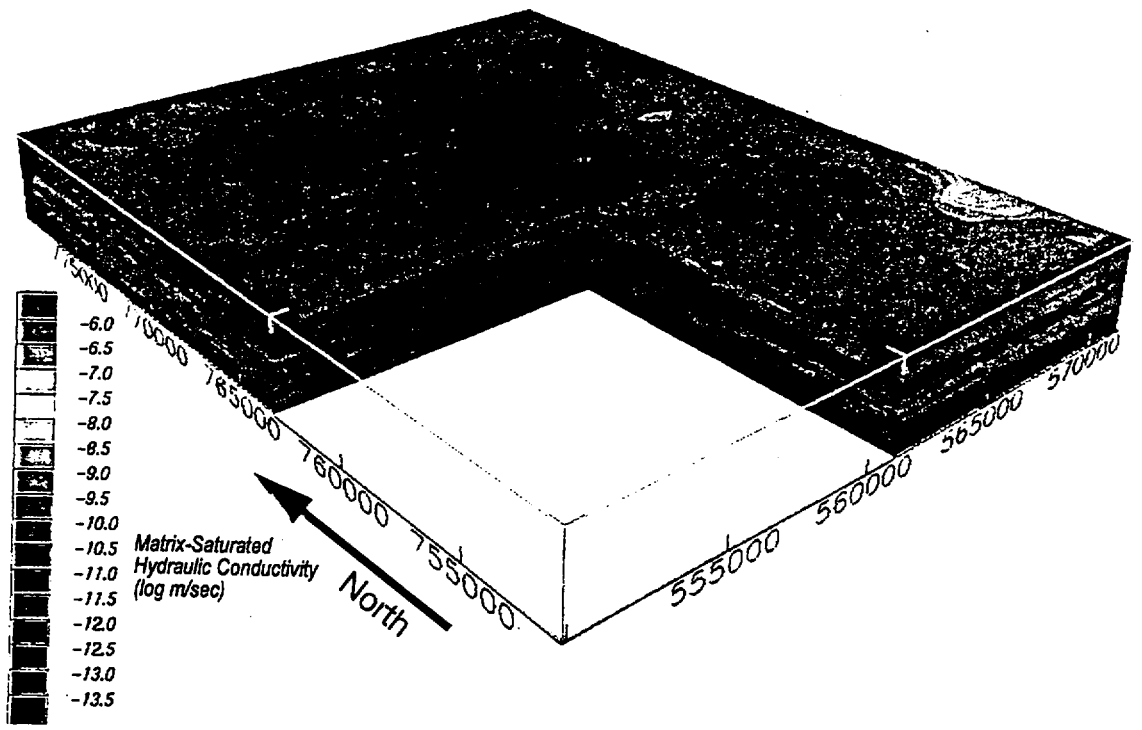


Figure 3-43. Cross-Sectional Views Showing E-Type Heterogeneity of Matrix-Saturated Hydraulic Conductivity in the TSw Model Unit in Stratigraphic Coordinates

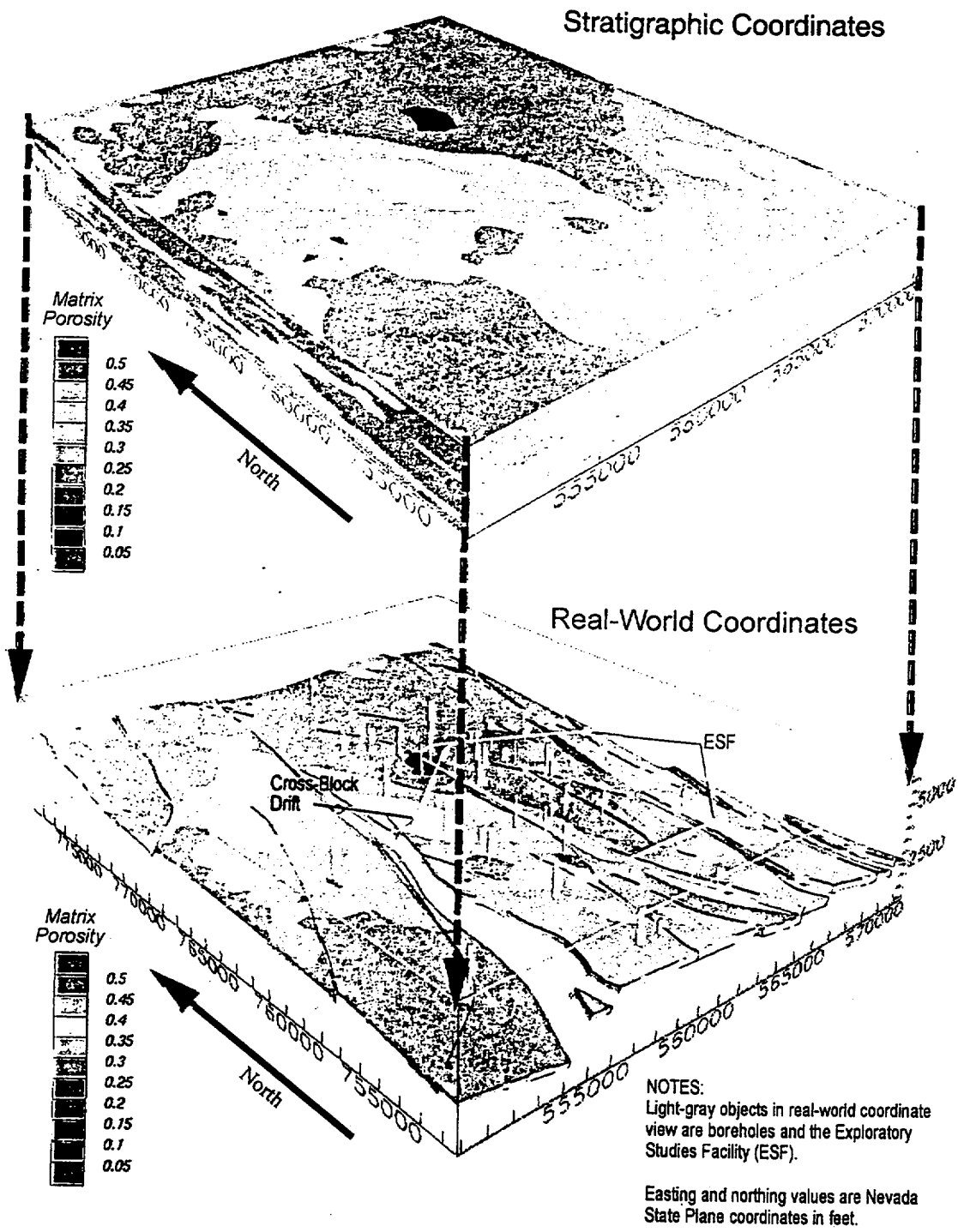


Figure 3-44. Perspective Diagrams Showing E-Type Matrix Porosity in the CHn Model Unit in Both Stratigraphic and Real-World Coordinates (CRWMS 1999b, Figure 49)

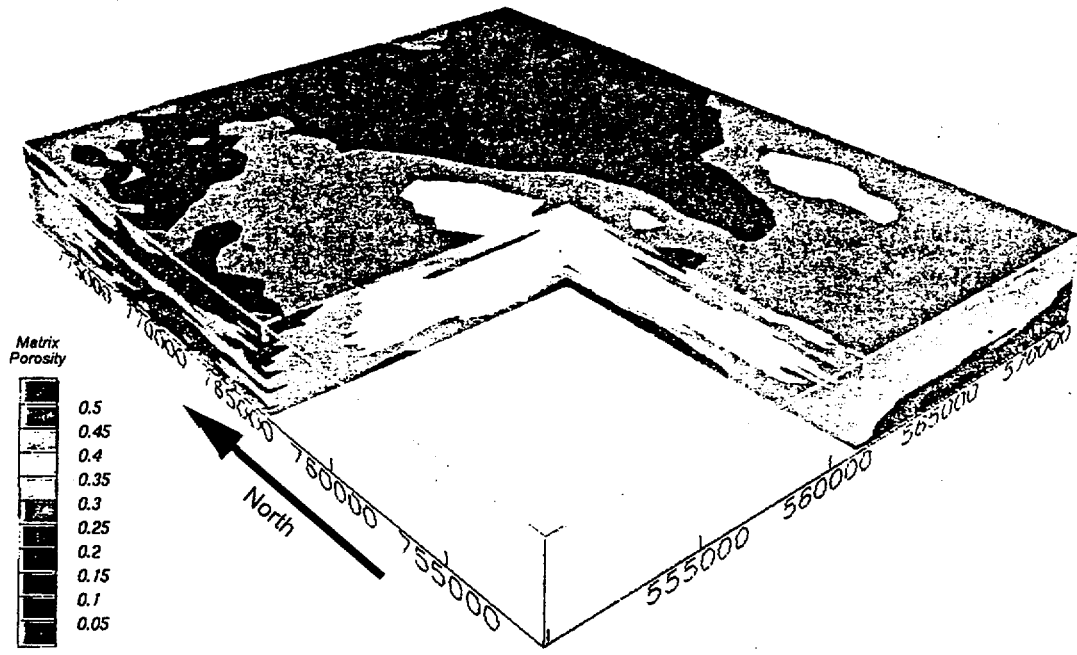


Figure 3-45. Cross-Sectional Views Showing E-Type Heterogeneity of Matrix Porosity in the CHn Model Unit in Stratigraphic Coordinates

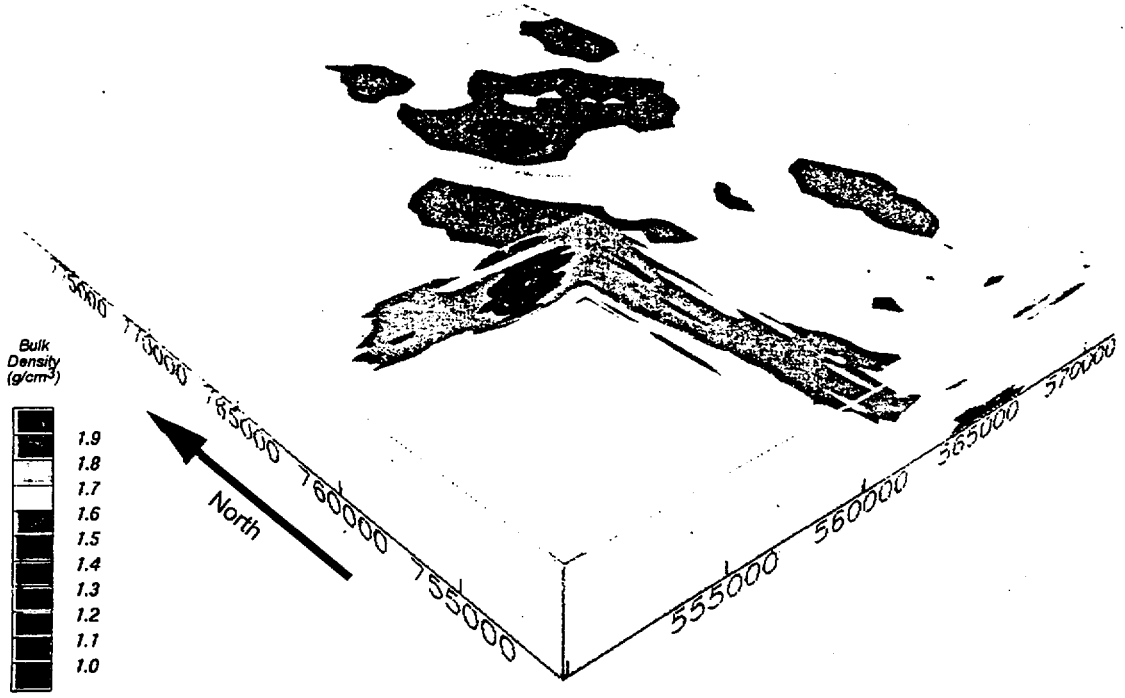


Figure 3-46. Cross-Sectional Views Showing E-Type Heterogeneity of Bulk Density in the CHn Model Unit in Stratigraphic Coordinates

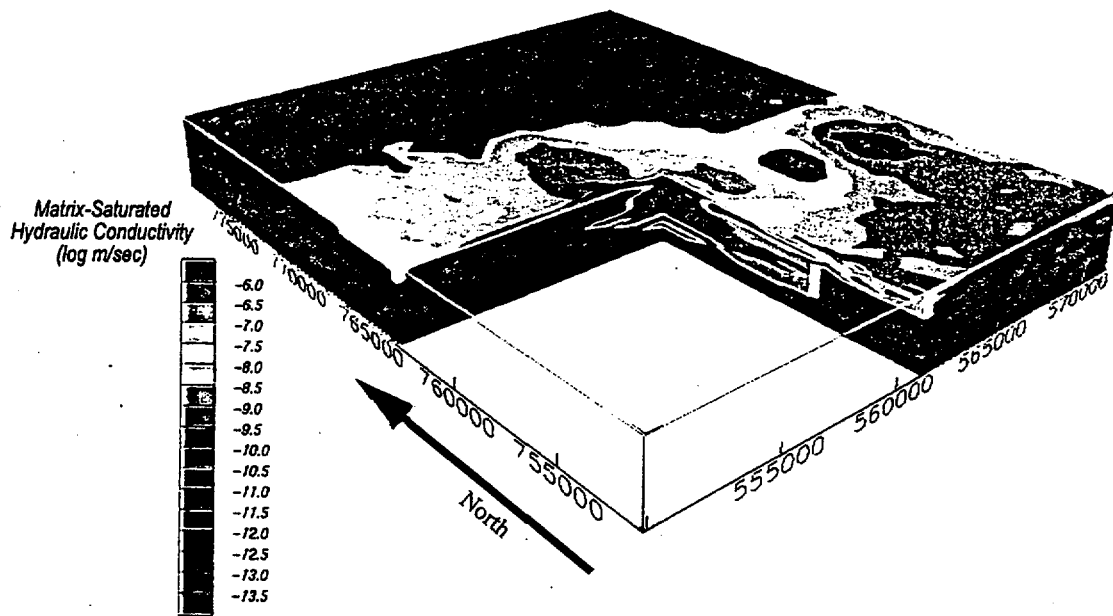
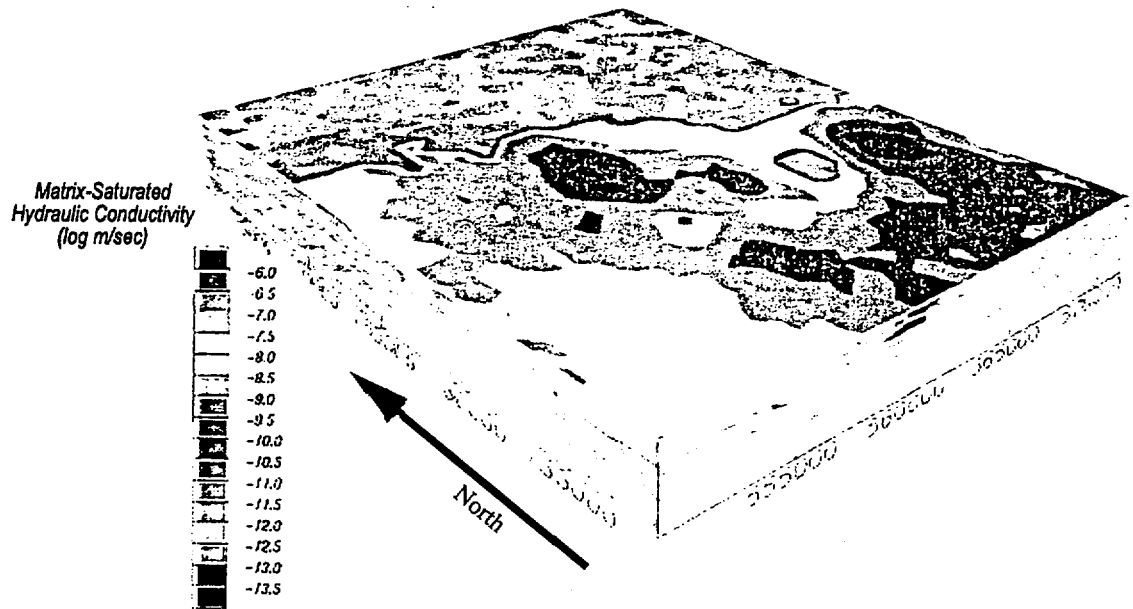


Figure 3-47. Block Diagram and Cross-Sectional Views Showing E-Type Heterogeneity of Matrix-Saturated Hydraulic Conductivity in the CHn Model Unit in Stratigraphic Coordinates

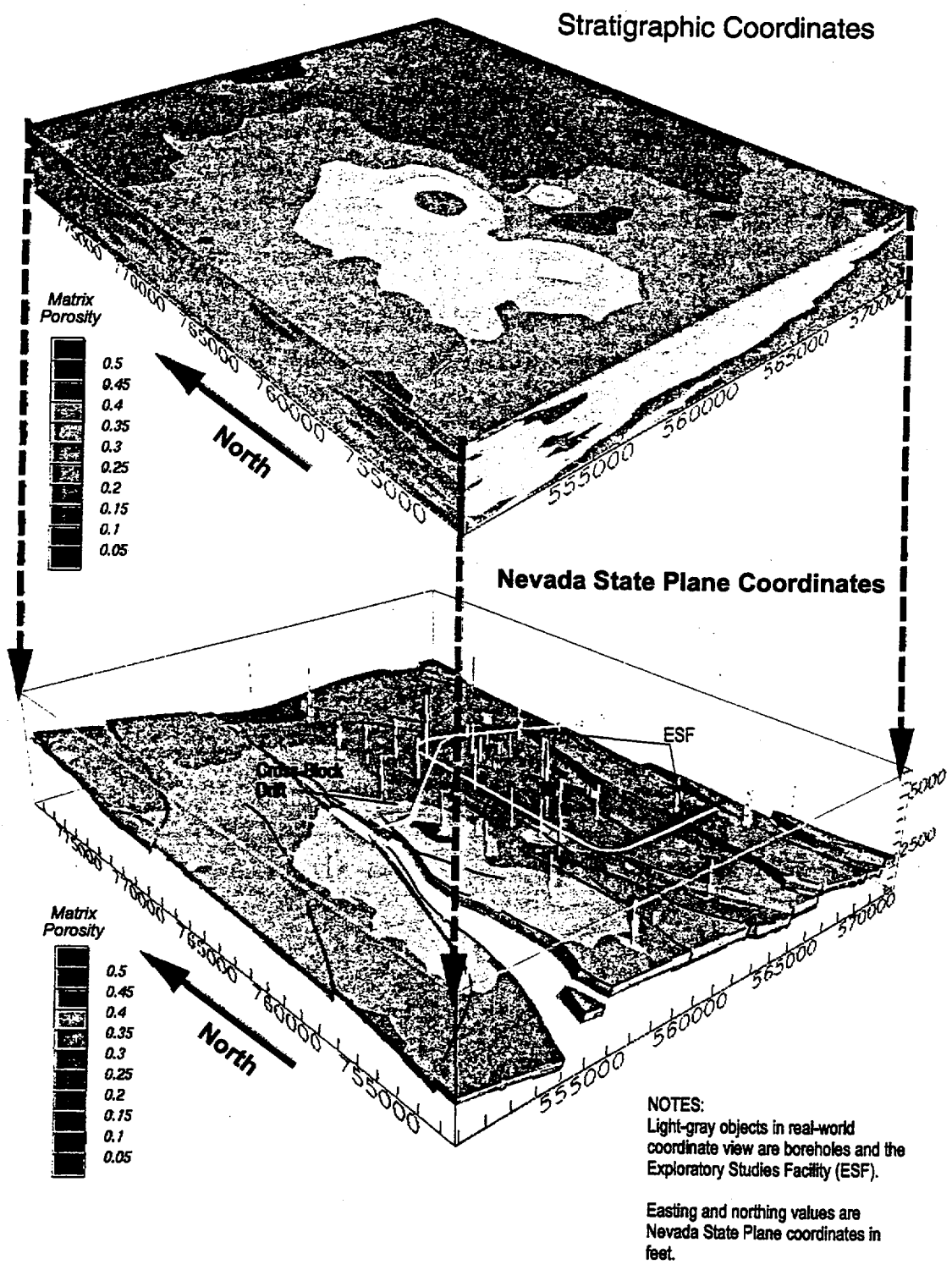


Figure 3-48. Perspective Diagrams Showing E-Type Model Matrix Porosity in the Tcp Model Unit in Both Stratigraphic and Real-World Coordinates (CRWMS M&O 1999b, Figure 53)

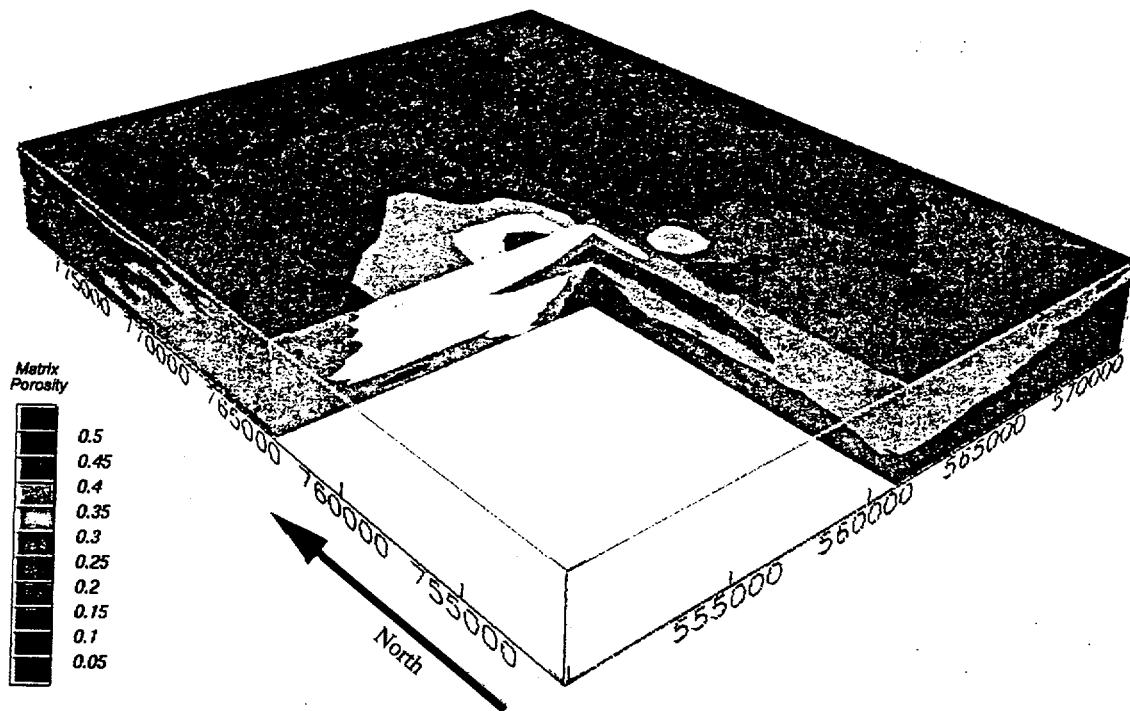


Figure 3-49. Cross-Sectional Views Showing E-Type Heterogeneity of Matrix Porosity in the Tcp Model Unit in Stratigraphic Coordinates

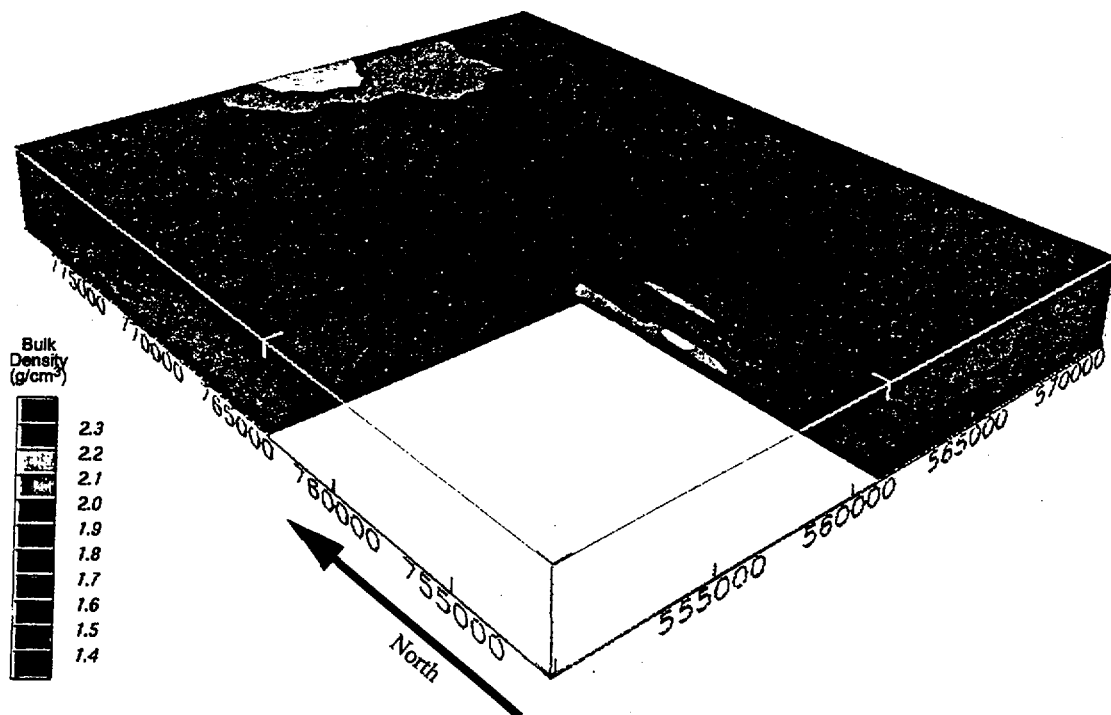


Figure 3-50. Cross-Sectional Views Showing E-Type Heterogeneity of Bulk Density in the Tcp Model Unit in Stratigraphic Coordinates

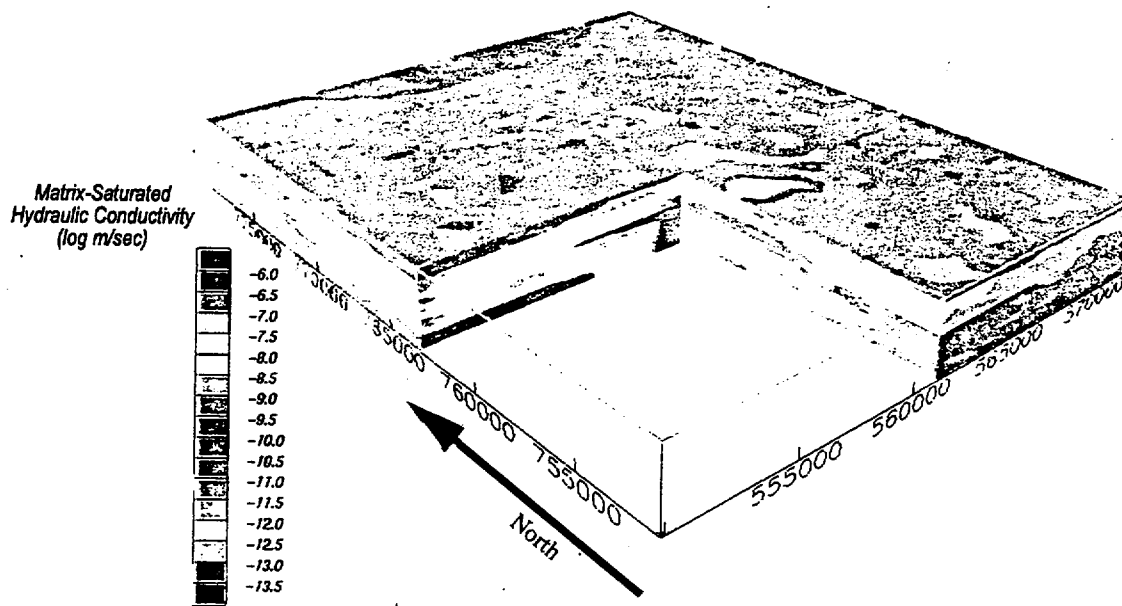
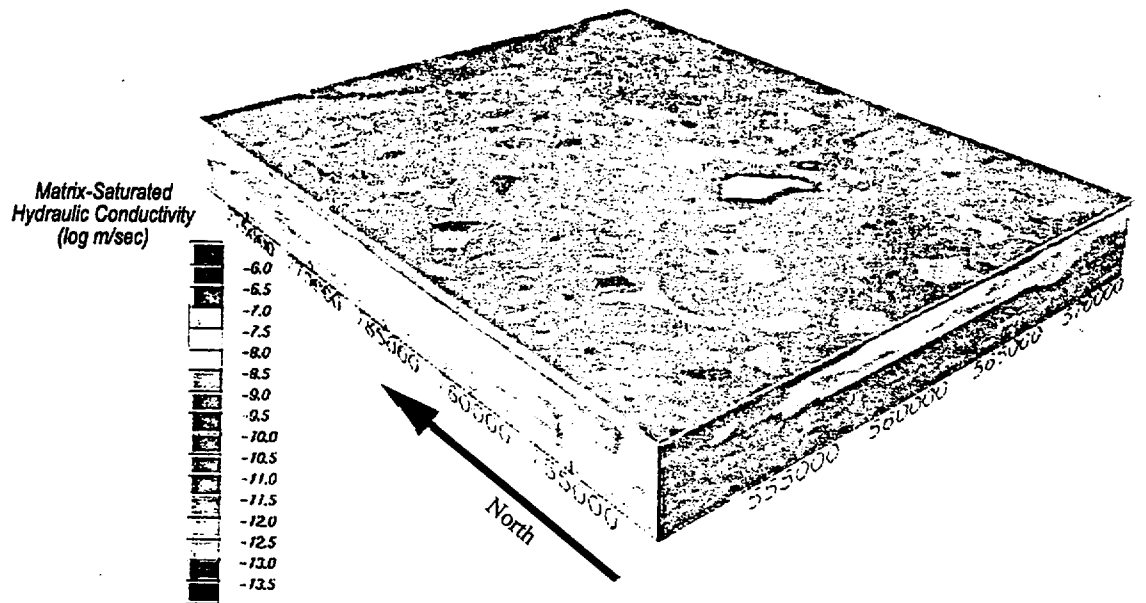


Figure 3-51. Block Diagram and Cross-Sectional Views Showing E-Type Heterogeneity of Matrix-Saturated Hydraulic Conductivity in the TcP Model Unit in Stratigraphic Coordinates

Legibility of the coordinates can be deduced from Figure 51 on page 3F-44 of this document.

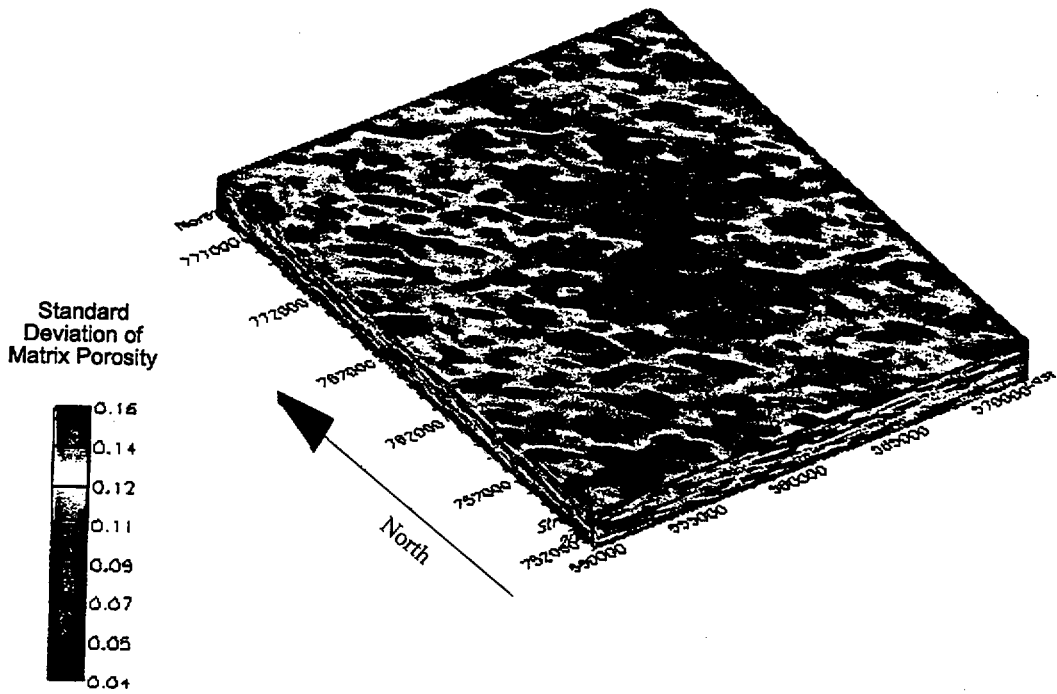


Figure 3-52. Uncertainty Model Showing E-Type Standard Deviation of Matrix Porosity in the PTn Model Unit (CRWMS M&O 1999b, Figure 57)

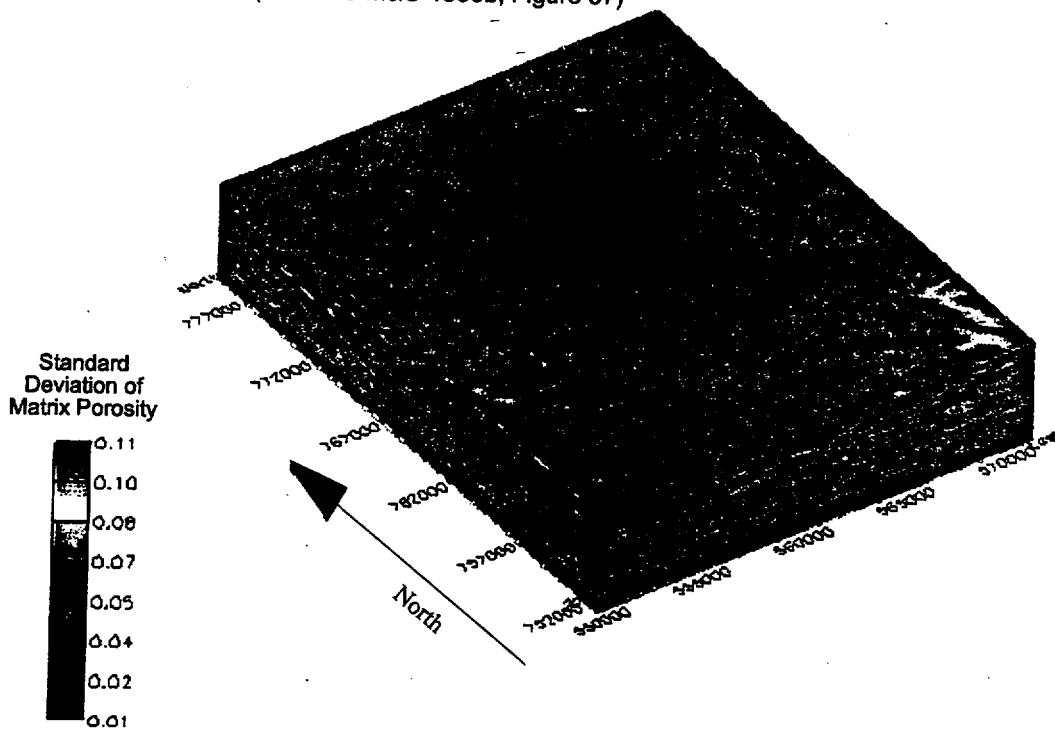


Figure 3-53. Uncertainty Model Showing E-Type Standard Deviation of Matrix Porosity in the TSw Model Unit (CRWMS M&O 1999b, Figure 58)

Legibility of the coordinates can be deduced from Figure 51 on page 3F-44 of this document.

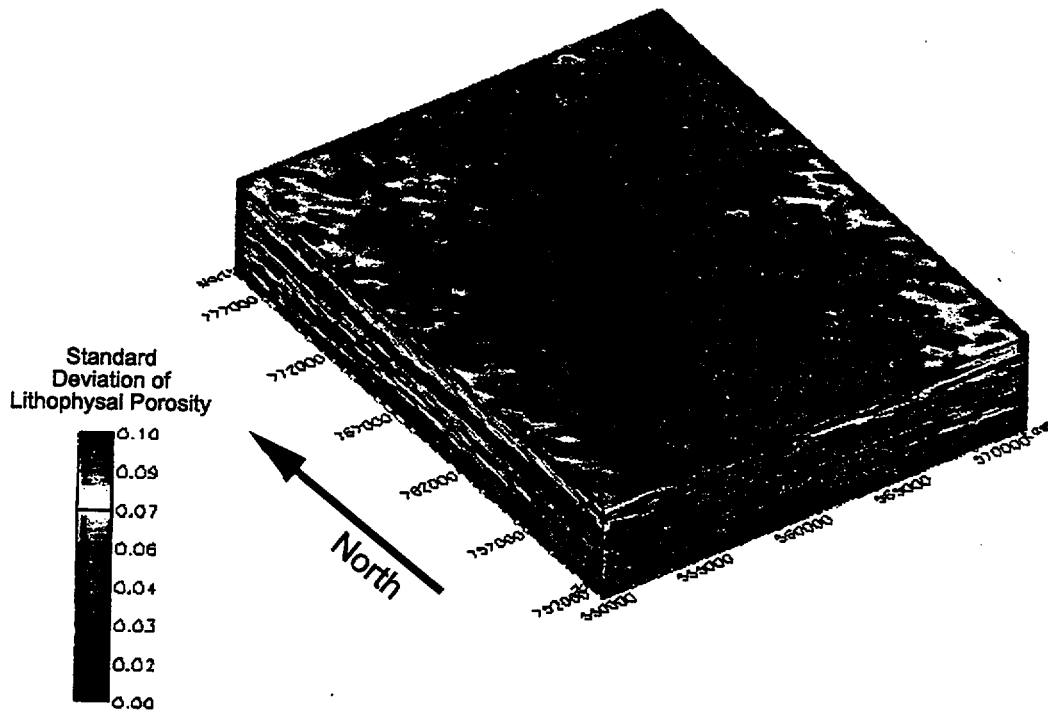


Figure 3-54. Uncertainty Model Showing E-Type Standard Deviation of Lithophysal Porosity in the TSW Model Unit (CRWMS M&O 1999b, Figure 59)

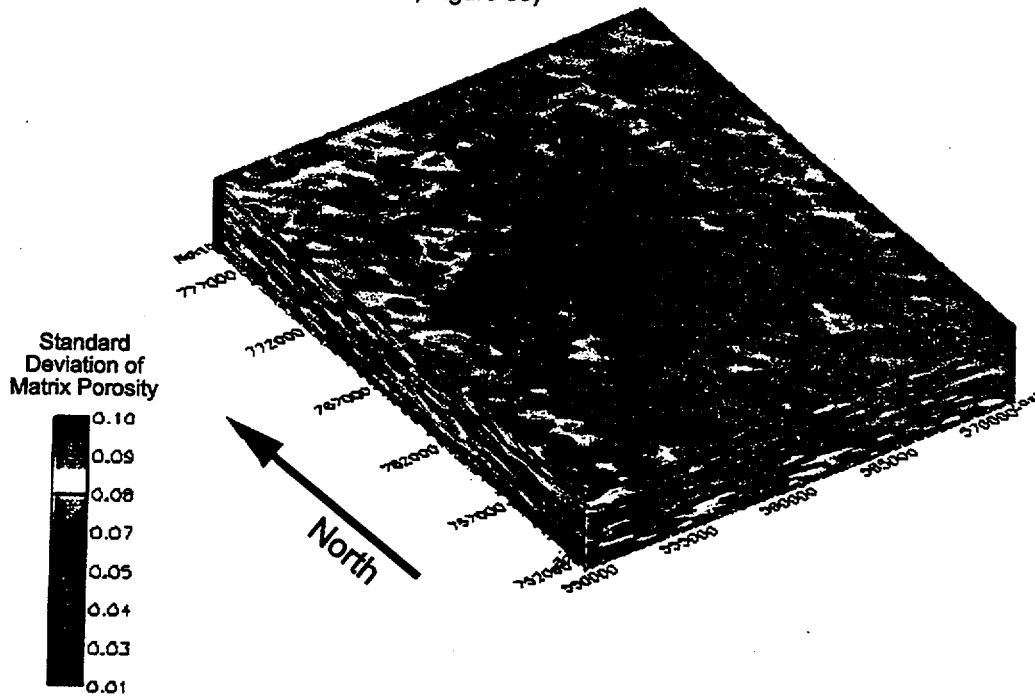


Figure 3-55. Uncertainty Model Showing E-Type Standard Deviation of Matrix Porosity in the CHn Model Unit (CRWMS M&O 1999b, Figure 60)

Legibility of the coordinates can be deduced from Figure 51 on page 3F-44 of this document.

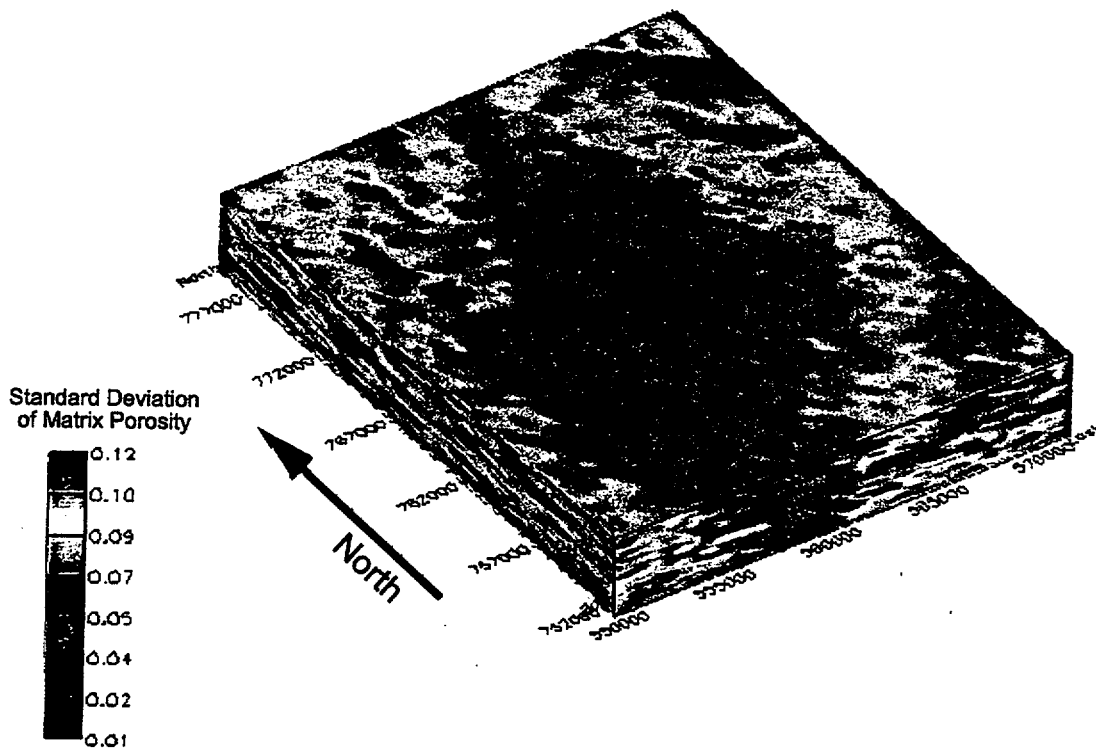


Figure 3-56. Uncertainty Model Showing E-Type Standard Deviation of Matrix Porosity in the Top Model Unit (CRWMS M&O 1999b, Figure 61)

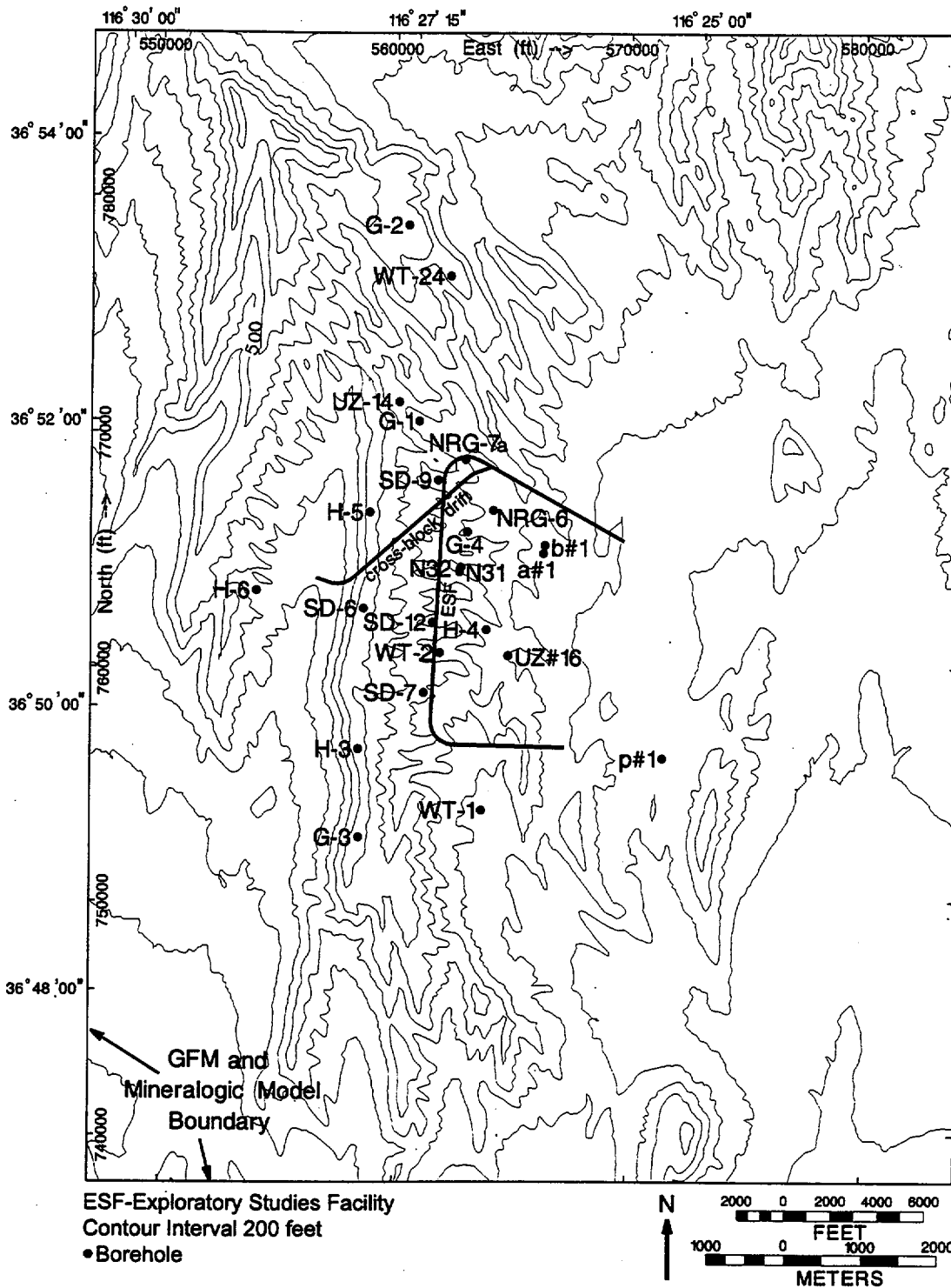


Figure 3-57. Locations of Boreholes Used in MM3.0 (CRWMS M&O 1999c, Figure 3)

Legibility of the coordinates can be deduced from Figure 51 on page 3F-44 of this document.

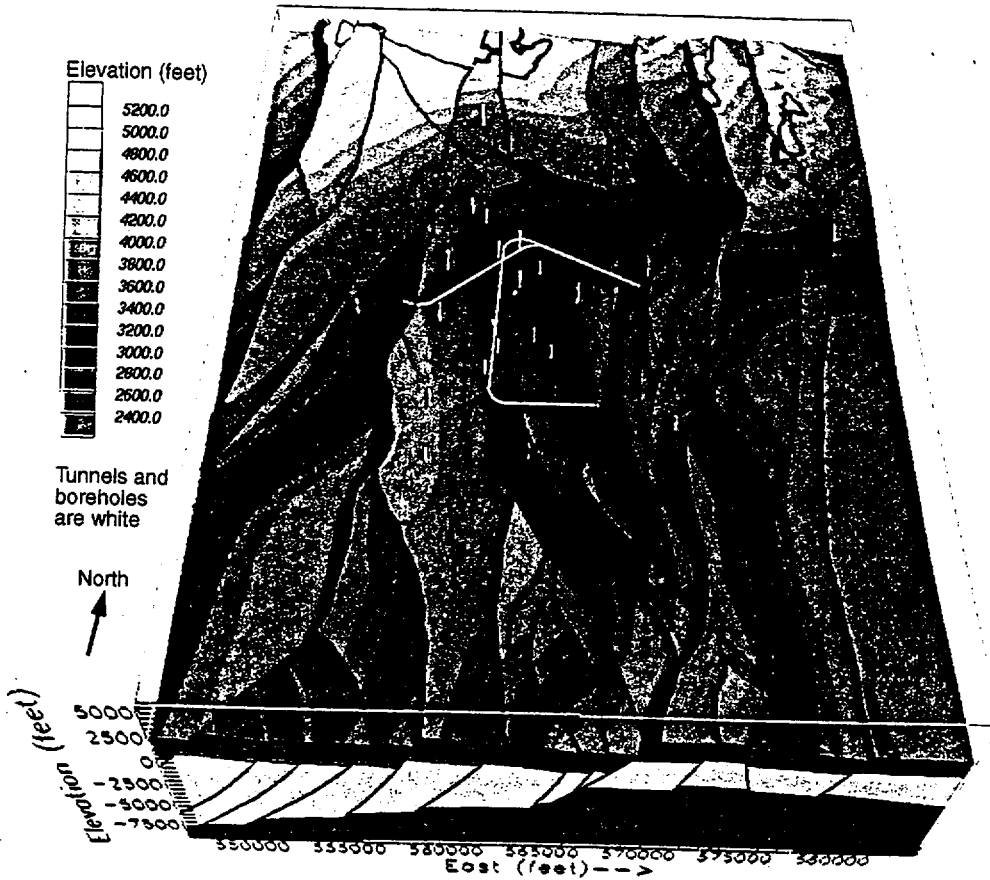


Figure 3-58. Shaded Relief View of Tpcpv1, Nonwelded Subzone of Vitric Zone of Tiva Canyon Tuff

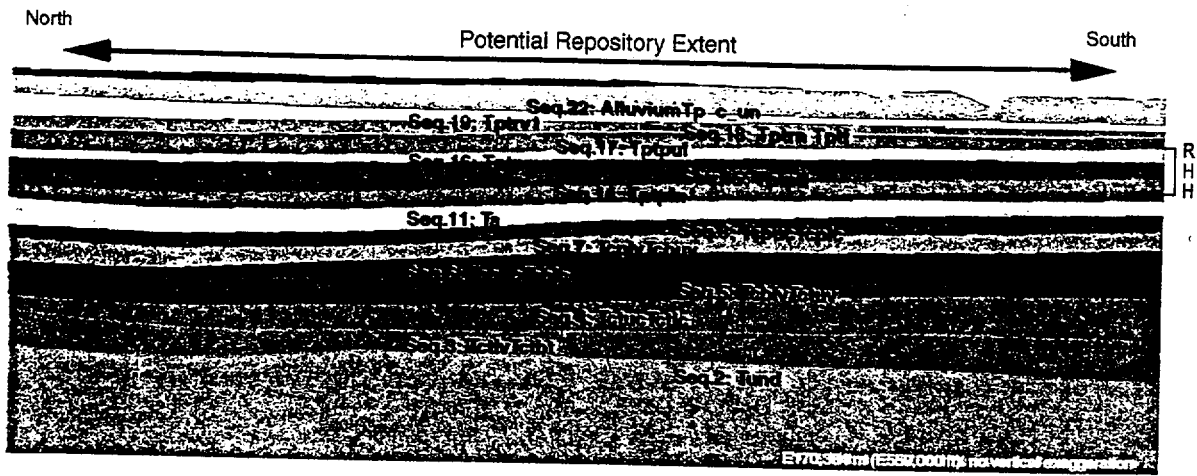


Figure 3-59. North-South Cross Section Illustrating Sequences Used in MM3.0

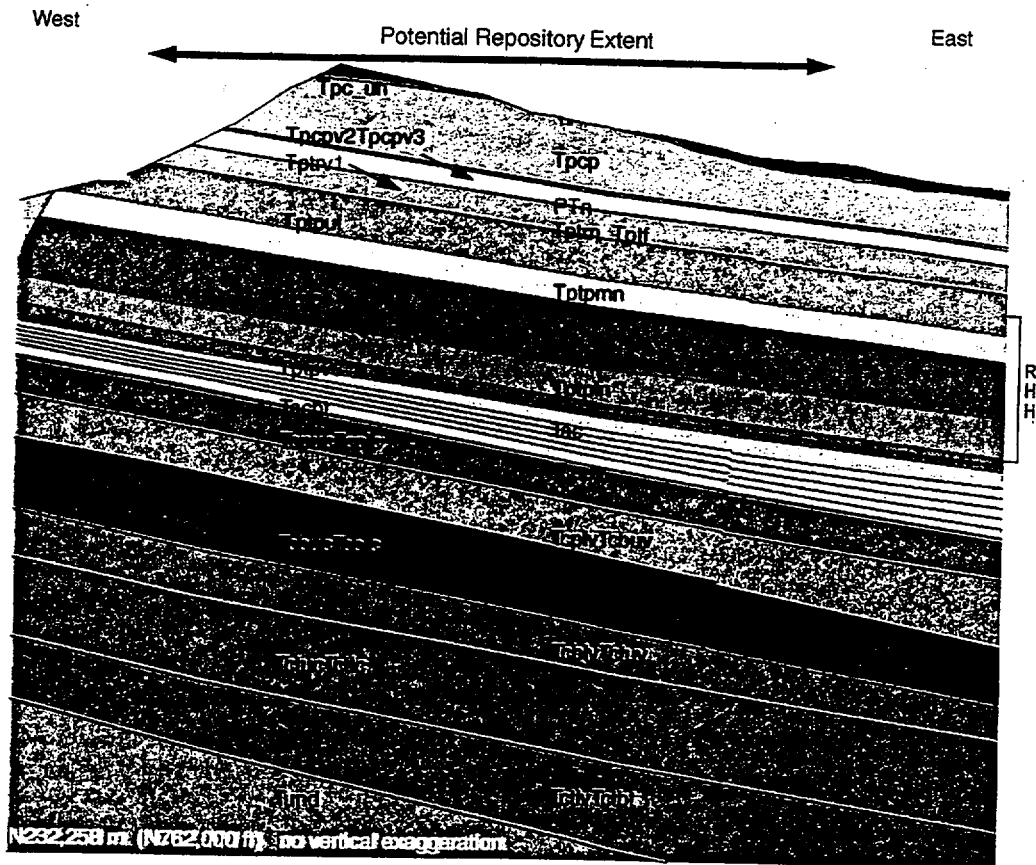


Figure 3-60. East-West Cross Section Illustrating Sequences Used in MM3.0

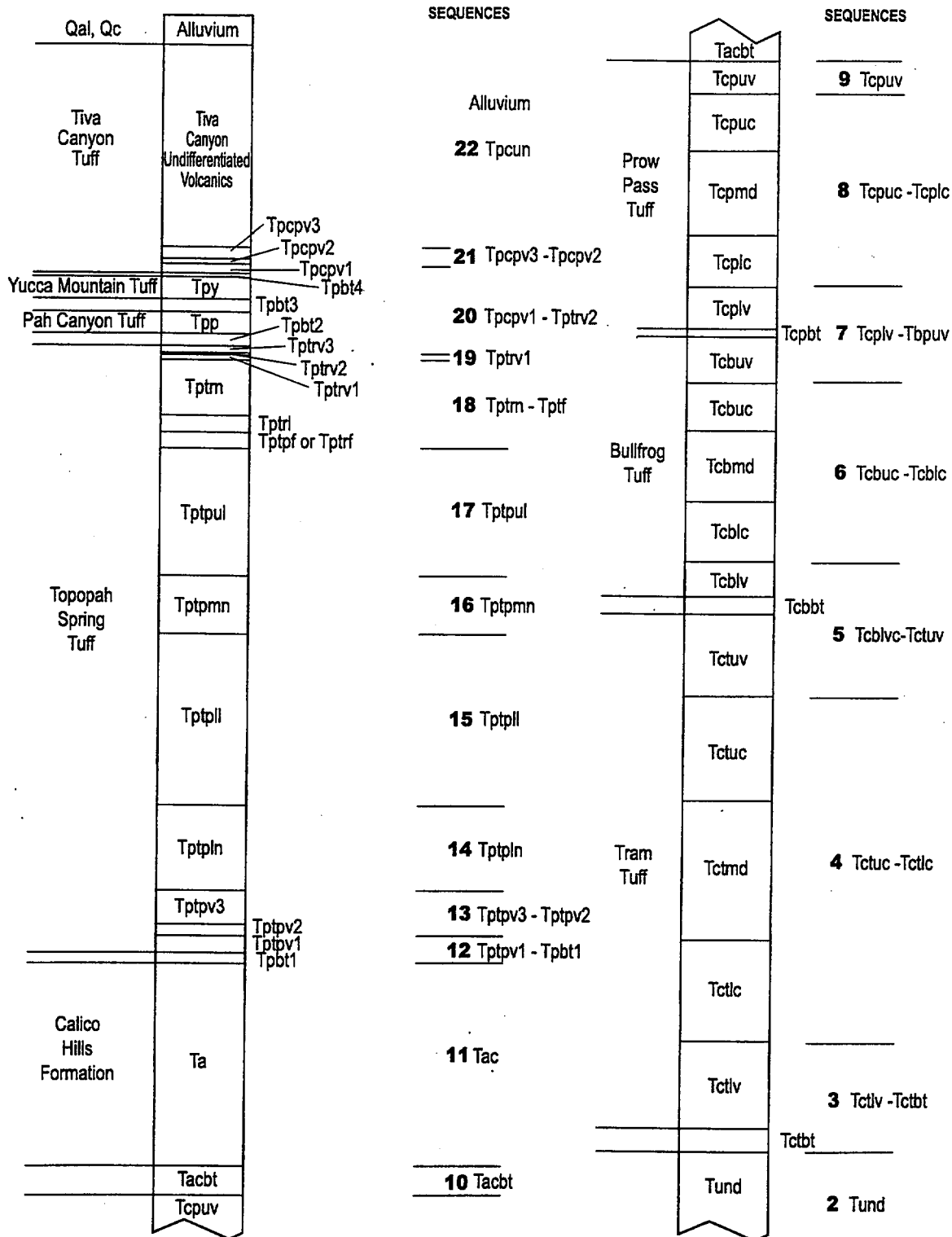
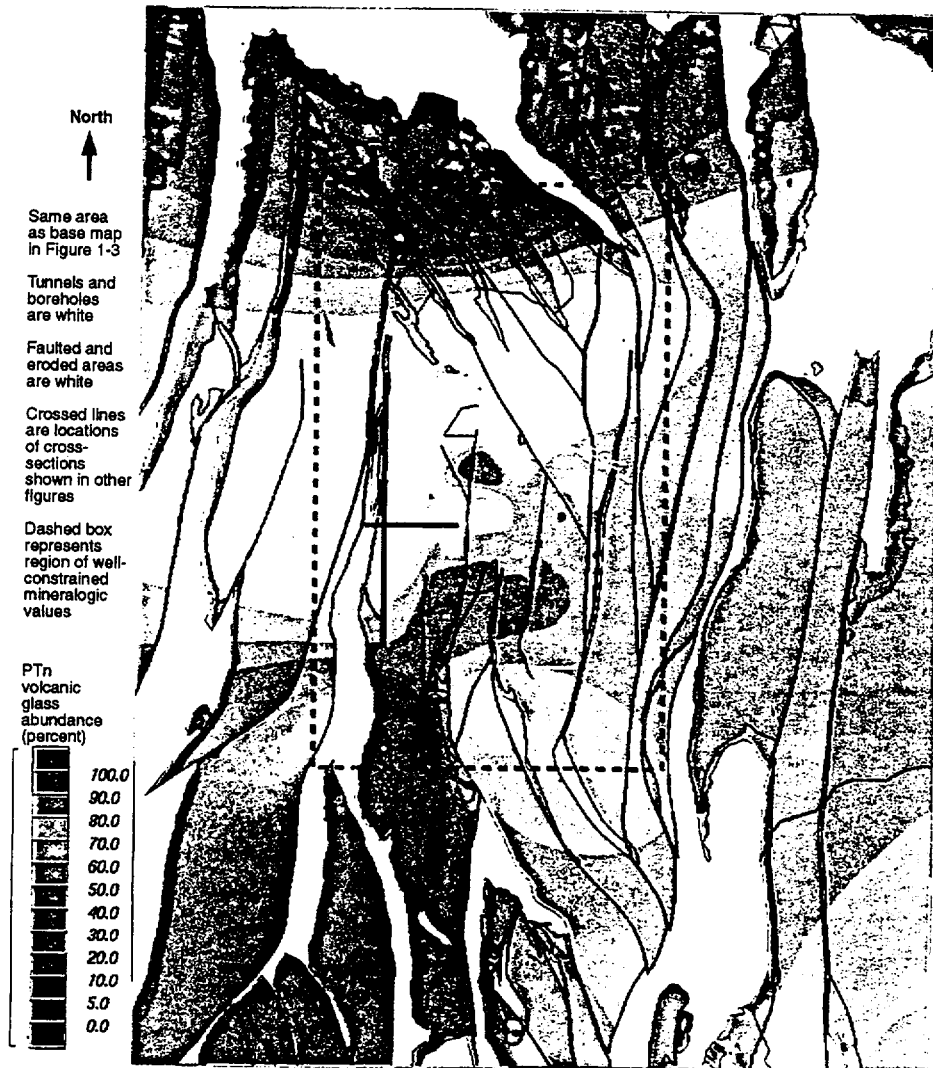


Figure 3-61. Schematic Stratigraphic Column Showing Approximate Thicknesses of Units Listed in Table 1-1 (CRWMS M&O 1999c, Figure 7)



NOTE: Only that portion of the ESF that cuts through Sequence 20 is displayed.

Figure 3-62. Map View of Volcanic Glass Distribution in the PTn Unit, Tpcpv1-Tptrv2 (Sequence 20) for Entire MM3.0

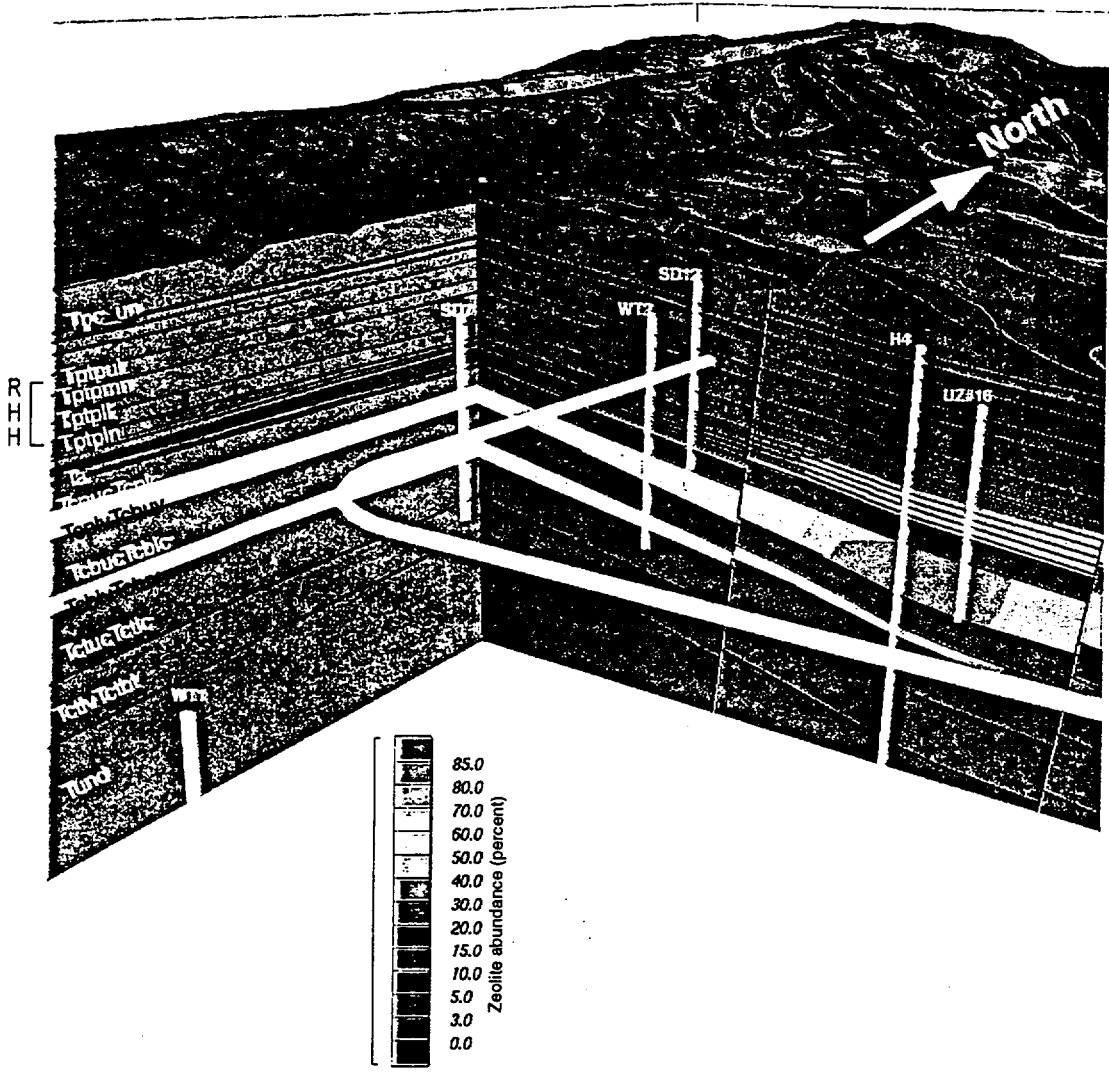


Figure 3-63. Zeolite Distribution in North-South and East-West Cross-Sections Through Center of Potential Repository Block

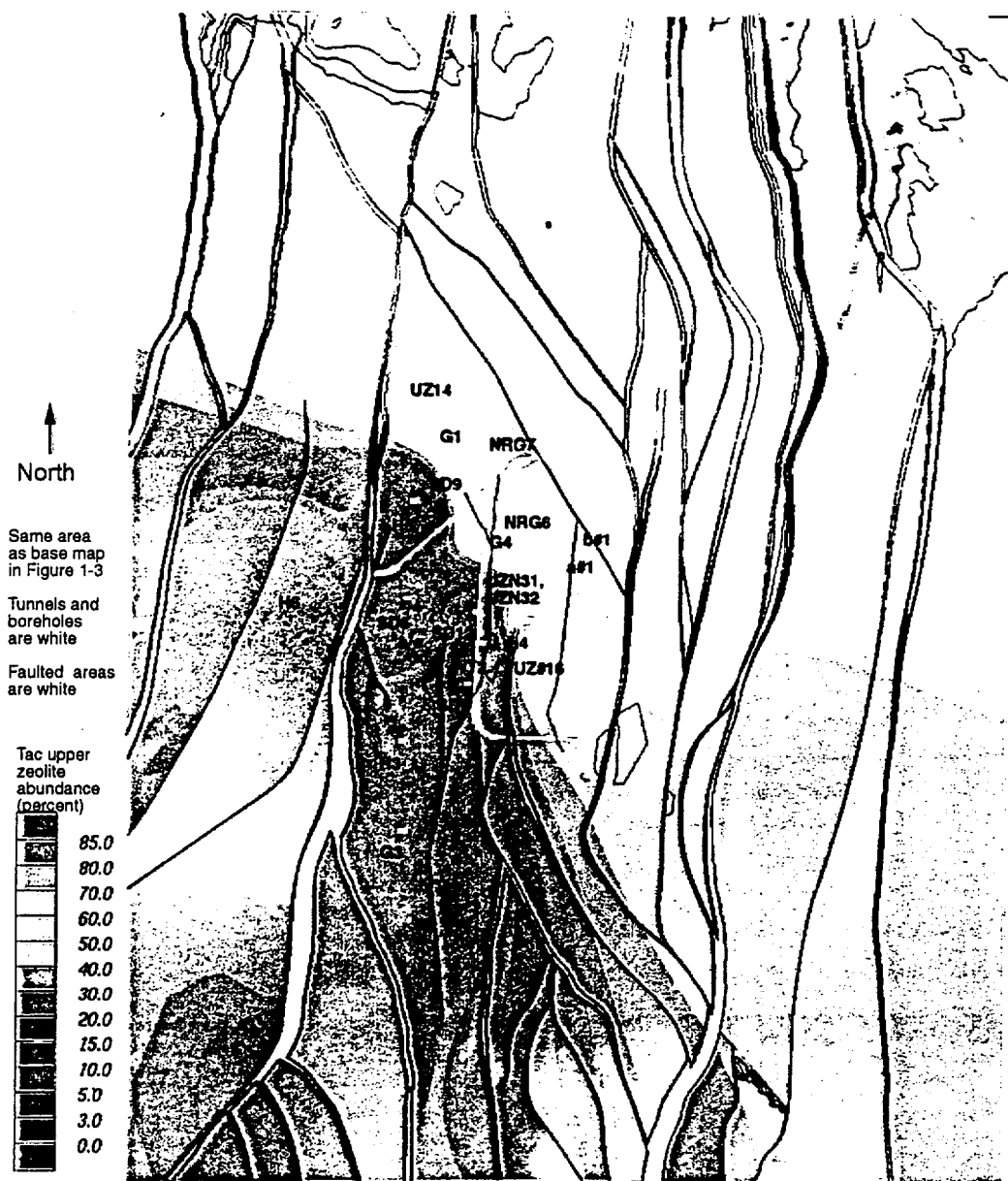


Figure 3-66. Zeolite Distribution in Map View of Upper Layer (Layer 14) of Calico Hills Formation (Tac, Sequence 11)

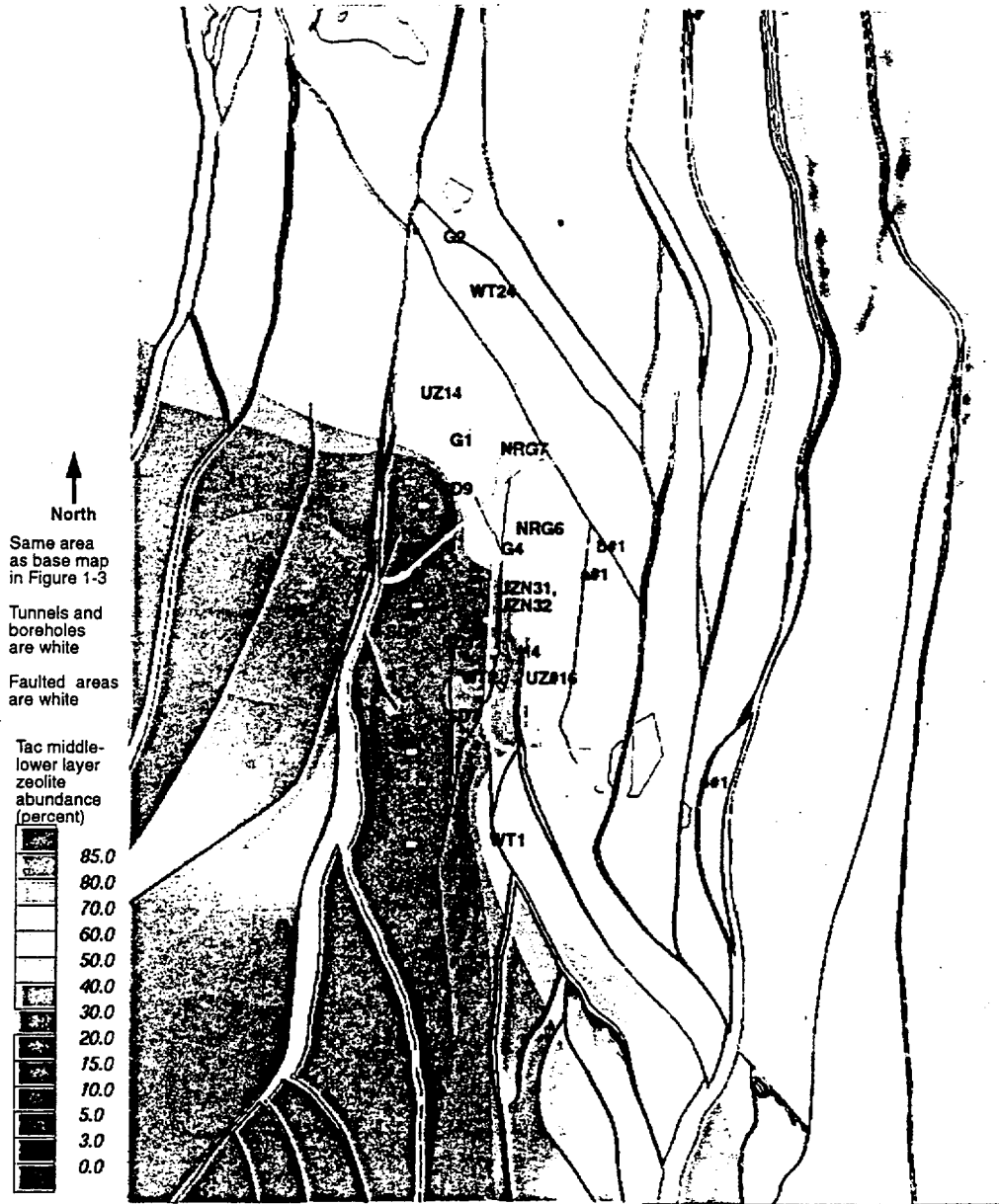


Figure 3-68. Zeolite Distribution in Map View of Middle-Lower Layer (Layer 12) of Calico Hills Formation (Tac, Sequence 11)

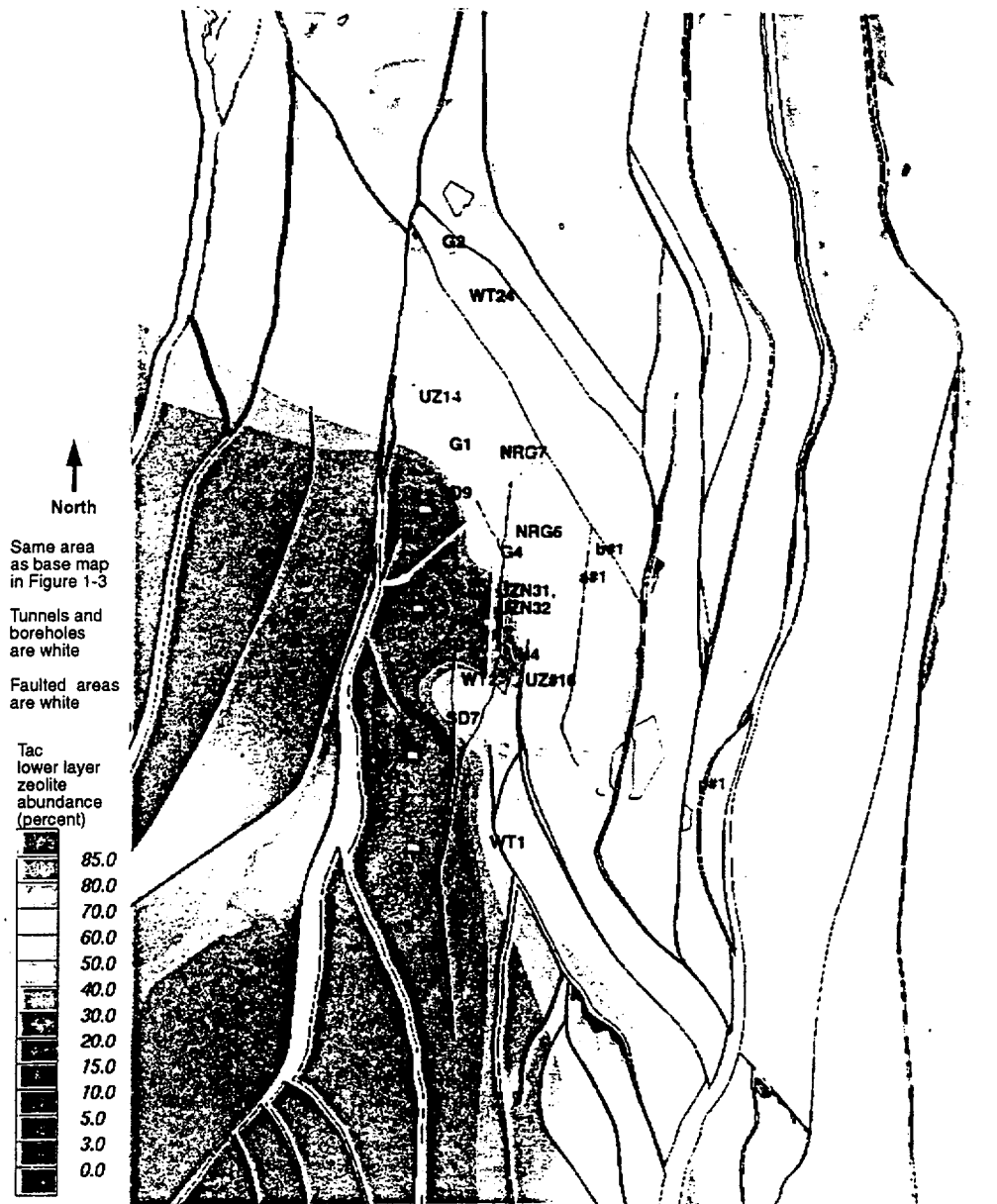


Figure 3-69. Zeolite Distribution in Map View of Lower Layer (Layer 11) of Calico Hills Formation (Tac, Sequence 11)

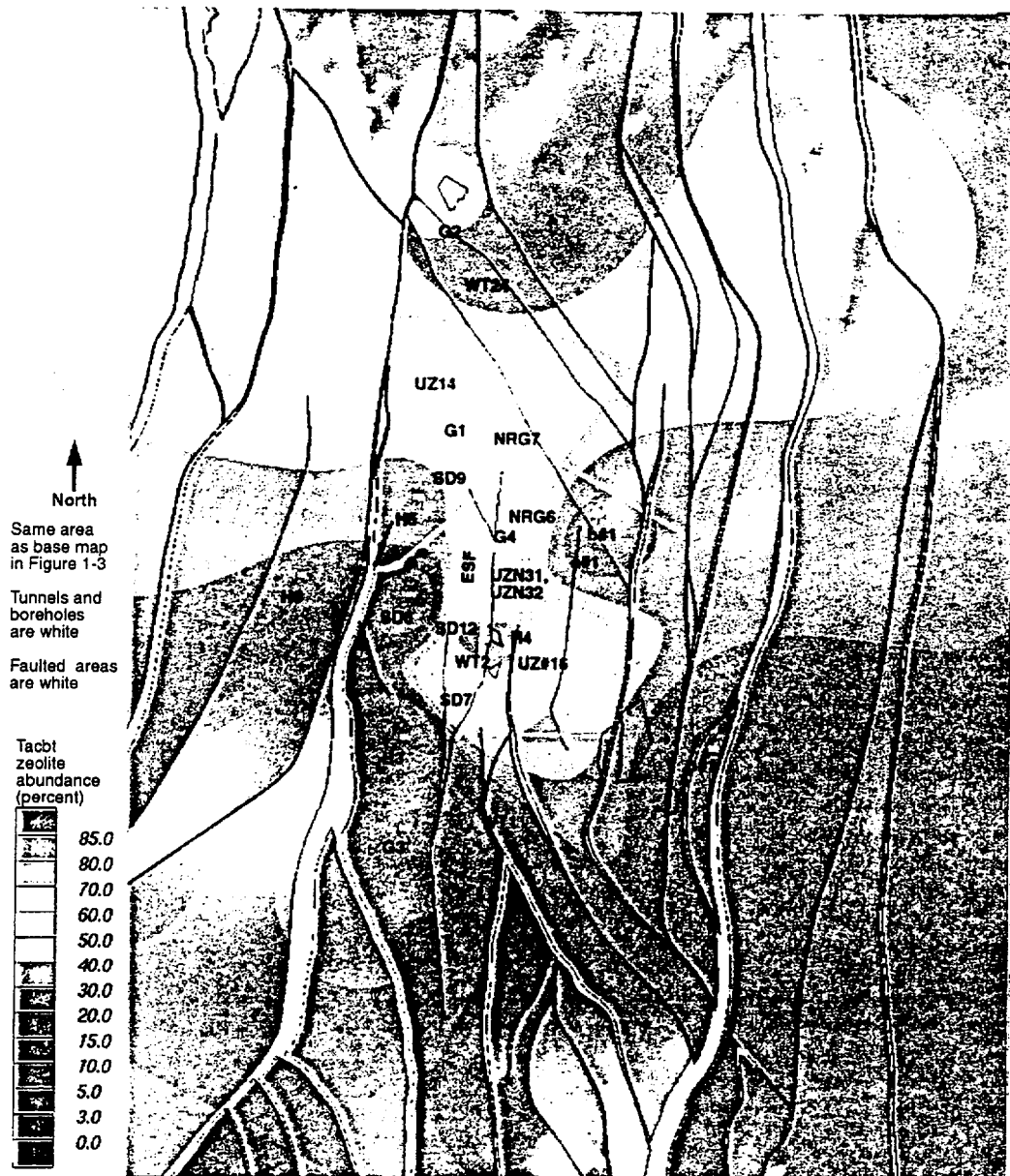


Figure 3-70. Zeolite Distribution in Map View of Bedded Tuff Below Calico Hills Formation (Tacbt, Sequence 10)

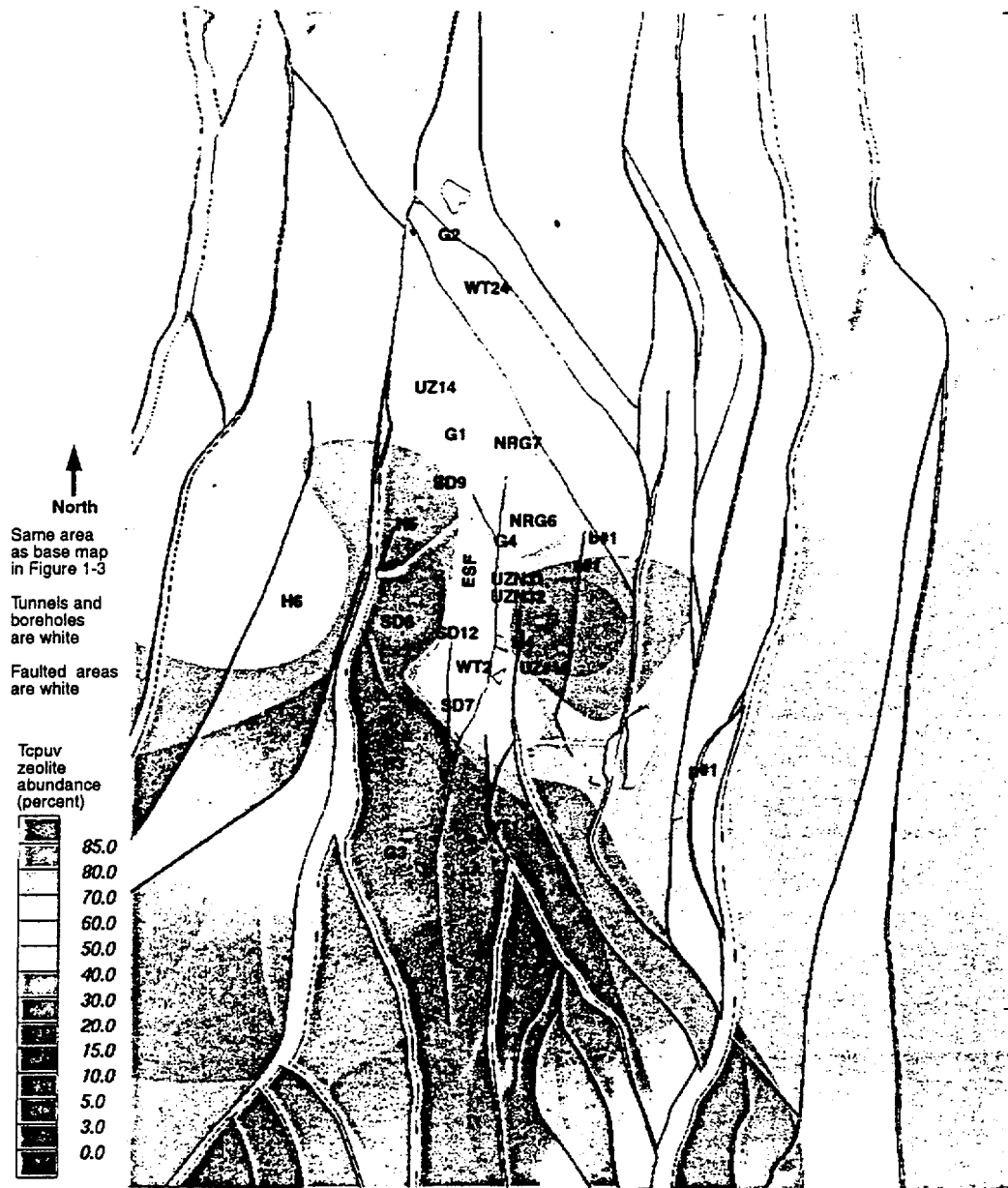


Figure 3-71. Zeolite Distribution in Map View of Upper Vitric Zone of Prow Pass Tuff (Tcpuv, Sequence 9)

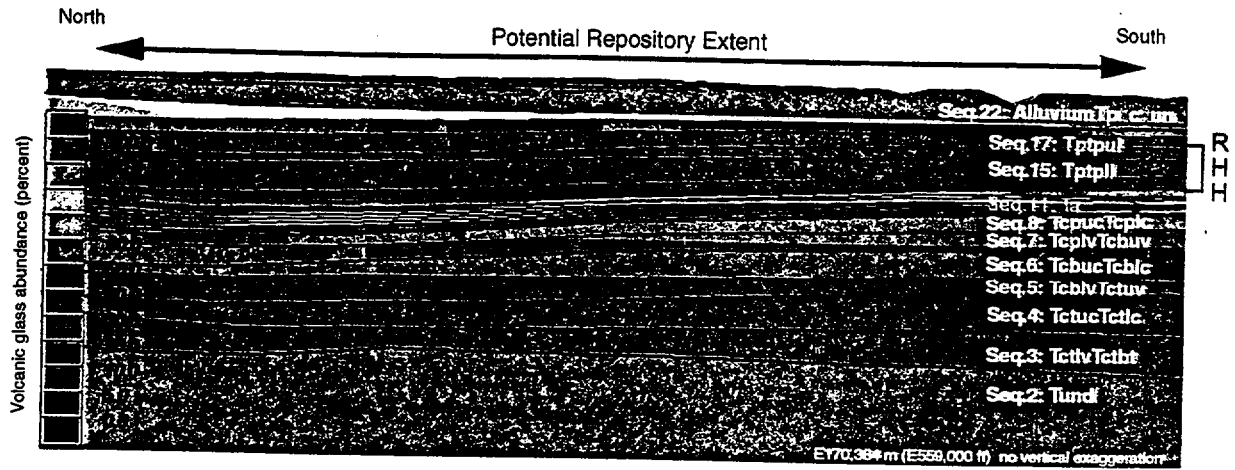


Figure 3-74. Volcanic Glass Distribution in North-South Cross-Section Through Potential Repository Block

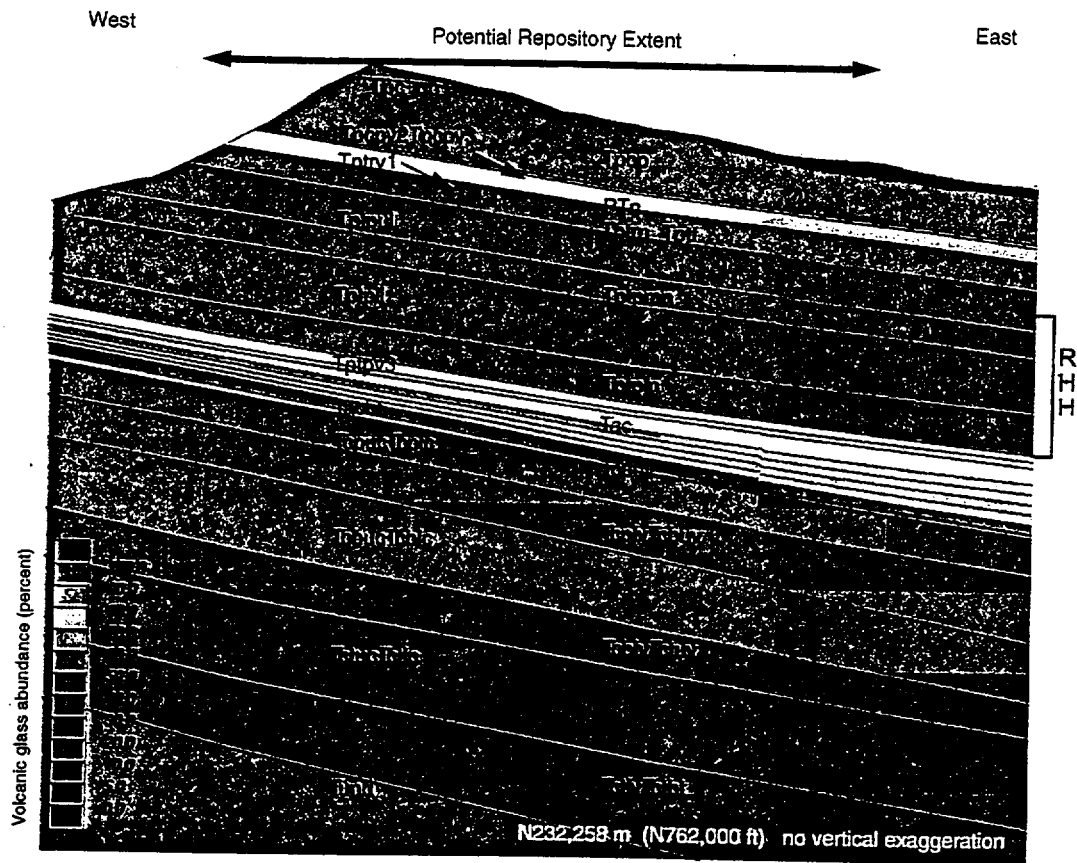


Figure 3-75. Volcanic Glass Distribution in East-West Cross-Section Through Potential Repository Block

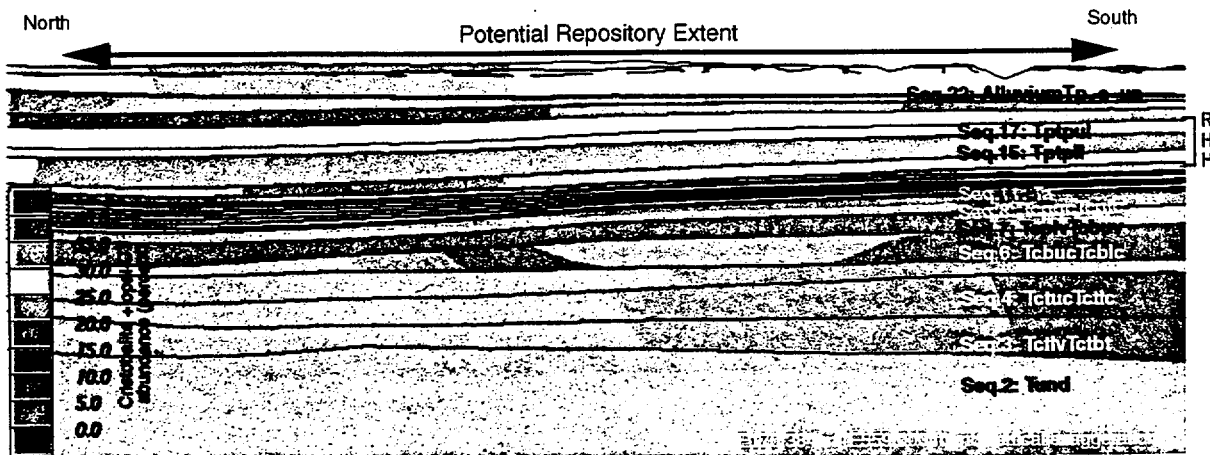


Figure 3-78. Cristobalite + Opal-CT Distribution in North-South Cross-Section Through Potential Repository Block

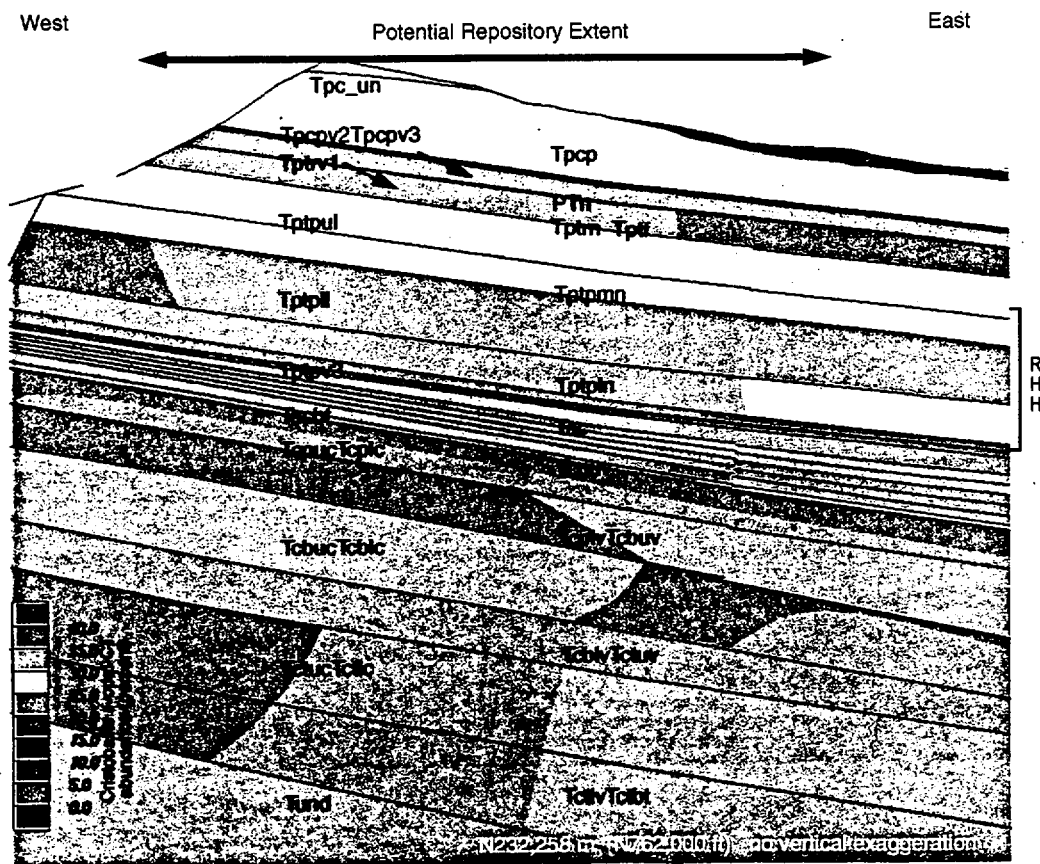


Figure 3-79. Cristobalite + Opal-CT Distribution in East-West Cross-Section Through Potential Repository Block

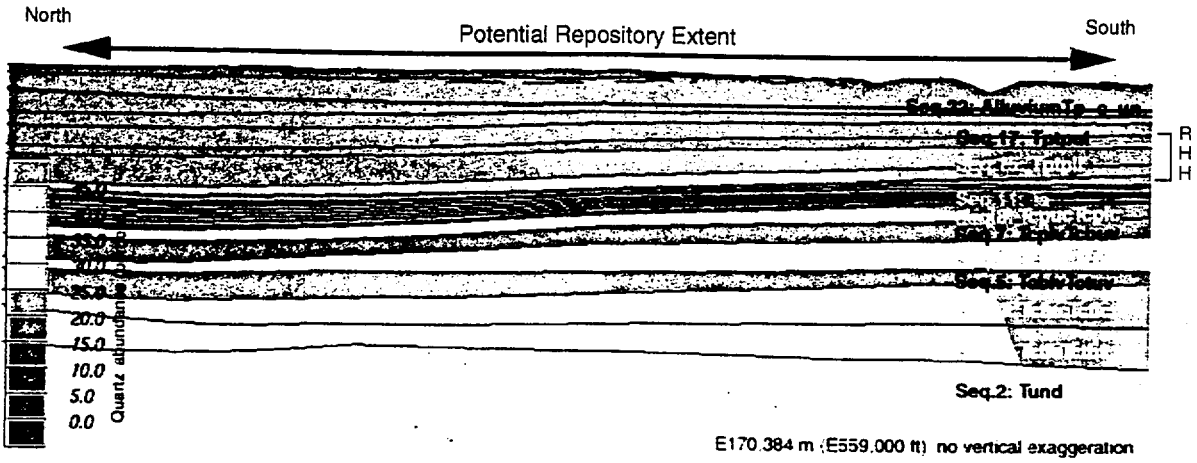


Figure 3-80. Quartz Distribution in North-South Cross-Section Through Potential Repository Block

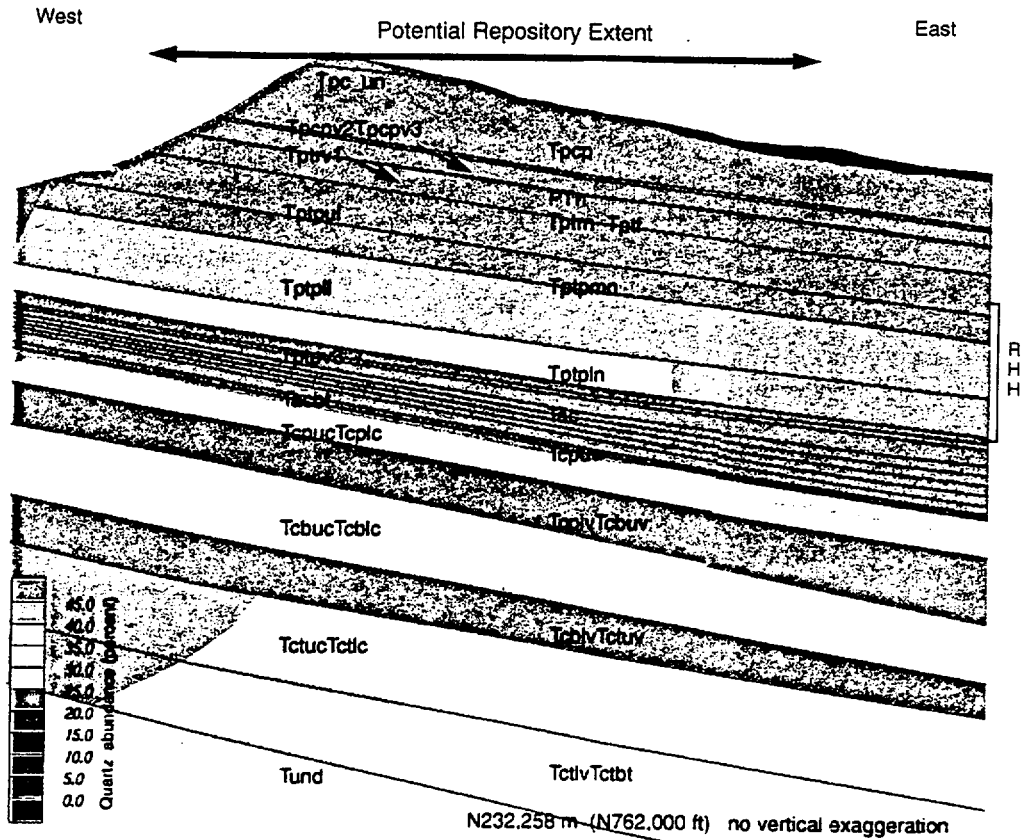


Figure 3-81. Quartz Distribution in East-West Cross-Section Through Potential Repository Block

INTENTIONALLY LEFT BLANK

4. RELATIONSHIP WITH THE NUCLEAR REGULATORY COMMISSION ISSUE RESOLUTION STATUS REPORTS

The Nuclear Regulatory Commission (NRC) has identified ten Key Technical Issues (KTIs). Nine of these issues are technical questions that the NRC views as major uncertainties; the tenth KTI is a nontechnical issue related to development of the U.S. Environmental Protection Agency Standard. The KTIs must be addressed in the Safety Analysis Report, which will accompany the application for construction authorization if the site is recommended for repository development. The NRC staff have indicated that they plan to structure their review of the PMRs within the framework of the KTIs as described in the corresponding Issue Resolution Status Reports.

The ISM provides a conceptual picture of the geologic structure and stratigraphy, along with the basic rock properties and mineralogy of the Yucca Mountain site. This information is used in other PMRs, most notably the Unsaturated Zone Flow and Transport and the Saturated Zone Flow and Transport PMRs, and in design analyses. As part of Revision 1 to the Issue Resolution Report on Structural Deformation and Seismicity, the NRC staff documented their review of the GFM (NRC 1998, p. 48, pp. 57–58, and Appendix F). For their review, the NRC staff conducted evaluations of the GFM to address the following questions:

- Are the input data necessary and sufficient to define faults and stratigraphy in the model?
- Do modeled fault traces and surfaces and stratigraphic boundary surfaces match the field data?
- Were the essential databases provided by DOE with the model?
- Are alternative representations—or interpretations—of stratigraphy and faults warranted?
- Is it possible to reasonably incorporate alternative interpretations of subsurface fault geometry into GFM3.0? [*The current version of the model is GFM3.1.*]
- What observations or limitations relative to representations of faults and stratigraphic horizons in GFM3.1 might require further explanation?

The NRC staff consider the GFM adequate to depict faults, fault blocks, stratigraphic horizons, and topography, and to provide a geologic framework for displaying and evaluating parameter distributions for other site characteristics. As a result of their review, the NRC staff have adopted the GFM for their independent evaluations and analyses of the Yucca Mountain site. The NRC staff have not identified any technical issues with respect to the GFM.

INTENTIONALLY LEFT BLANK

5. REFERENCES

5.1 DOCUMENTS CITED

- Bish, D.L. and Aronson, J.L. 1993. "Paleogeothermal and Paleohydrologic Conditions in Silicic Tuff from Yucca Mountain, Nevada." *Clays and Clay Minerals*, 41 (2), 148-161. Long Island City, New York: Pergamon Press. TIC: 224613.
- Bish, D.L. and Chipera, S.J. 1989. *Revised Mineralogic Summary of Yucca Mountain, Nevada*. LA-11497-MS. Los Alamos, New Mexico: Los Alamos National Laboratory. ACC: NNA.19891019.0029.
- Brocher, T.M.; Hunter, W.C.; and Langenheim, V.E. 1998. "Implications of Seismic Reflection and Potential Field Geophysical Data on the Structural Framework of the Yucca Mountain-Crater Flat Region, Nevada." *Geological Society of America Bulletin*, 110 (8), 947-971. Boulder, Colorado: Geological Society of America. TIC: 238643.
- Buesch, D.C.; Spengler, R.W.; Moyer, T.C.; and Geslin, J.K. 1996. *Proposed Stratigraphic Nomenclature and Macroscopic Identification of Lithostratigraphic Units of the Paintbrush Group Exposed at Yucca Mountain, Nevada*. Open-File Report 94-469. Denver, Colorado: U.S. Geological Survey. ACC: MOL.19970205.0061.
- Buesch, D.C. and Spengler, R.W. 1999. "Correlations of Lithostratigraphic Features with Hydrogeologic Properties, a Facies-Based Approach to Model Development in Volcanic Rocks at Yucca Mountain, Nevada." *Proceedings of Conference on Status of Geologic Research and Mapping in Death Valley National Park, Las Vegas, Nevada, April 9-11, 1999*. Open File Report 99-153, 62-64. Denver, Colorado: U.S. Geological Survey. TIC: 245245.
- Byers, F.M., Jr.; Carr, W.J.; Christiansen, R.L.; Lipman, P.W.; Orkild, P.P.; and Quinlivan, W.D. 1976. *Geologic Map of the Timber Mountain Caldera Area, Nye County, Nevada*. Miscellaneous Investigations Series Map I-891. Denver, Colorado: U.S. Geological Survey. TIC: 204573.
- Carlos, B.A.; Chipera, S.J.; and Bish, D.L. 1995. *Distribution and Chemistry of Fracture-Lining Minerals at Yucca Mountain, Nevada*. LA-12977-MS. Los Alamos, New Mexico: Los Alamos National Laboratory. ACC: MOL.19960306.0564.
- Carr, M.D.; Waddell, S.J.; Vick, G.S.; Stock, J.M.; Monsen, S.A.; Harris, A.G.; Cork, B.W.; and Byers, F.M., Jr. 1986. *Geology of Drill Hole UE25p#1: A Test Hole Into Pre-Tertiary Rocks Near Yucca Mountain, Southern Nevada*. Open-File Report 86-175. Menlo Park, California: U.S. Geological Survey. ACC: HQS.19880517.2633.
- CRWMS M&O 1997. *Determination of Available Volume for Repository Siting*. BCA000000-01717-0200-00007 REV 00. Las Vegas, Nevada: CRWMS M&O. ACC: MOL.19971009.0699.

CRWMS M&O 1998. *Yucca Mountain Site Description*. B00000000-01717-5700-00019 REV 00. Las Vegas, Nevada: CRWMS M&O. ACC: MOL.19981202.0492.

CRWMS M&O 1999a. *Geologic Framework Model (GFM3.1) Analysis Model Report*. MDL-NBS-GS-000002 REV 00. Las Vegas, Nevada: CRWMS M&O. ACC: MOL.19991027.0206.

CRWMS M&O 1999b. *Rock Properties Model (RPM3.1) Analysis Model Report*. MDL-NBS-GS-000004 REV 00. Las Vegas, Nevada: CRWMS M&O. ACC: MOL.19991027.0207.

CRWMS M&O 1999c. *Mineralogical Model (MM3.0) Analysis Model Report*. MDL-NBS-GS-000003 REV 00. Las Vegas, Nevada: CRWMS M&O. ACC: MOL.19991027.0208.

CRWMS M&O 1999d. *M&O Site Investigations*. Activity Evaluation, January 23, 1999. Las Vegas, Nevada: CRWMS M&O. ACC: MOL.19990317.0330.

CRWMS M&O 1999e. *M&O Site Investigations*. Activity Evaluation, September 28, 1999. Las Vegas, Nevada: CRWMS M&O. ACC: MOL.19990928.0224.

Day, W.C.; Dickerson, R.P.; Potter, C.J.; Sweetkind, D.S.; San Juan, C.A.; Drake, R.M., II; and Fridrich, C.J. 1997. *Bedrock Geologic Map of the Yucca Mountain Area, Nye County, Nevada*. Administrative Report. Denver, Colorado: U.S. Geological Survey. ACC: MOL.19980310.0122.

Day, W.C.; Dickerson, R.P.; Potter, C.J.; Sweetkind, D.S.; San Juan, C.A.; Drake, R.M., II; and Fridrich, C.J. 1998. *Bedrock Geologic Map of the Yucca Mountain Area, Nye County, Nevada*. Geologic Investigations Series I-2627. Denver, Colorado: U.S. Geological Survey. ACC: MOL.19981014.0301.

Deutsch, C.V. and Journel, A.G. 1992. *GSLIB Geostatistical Software Library and User's Guide*. New York, New York: Oxford University Press. TIC: 224174.

DOE (U.S. Department of Energy) 1998a. *Quality Assurance Requirements and Description*. DOE/RW-0333P, Rev. 8. Washington, D.C.: U.S. Department of Energy, Office of Civilian Radioactive Waste Management. ACC: MOL.19980601.0022.

DOE 1998b. *Introduction and Site Characteristics*. Volume 1 of *Viability Assessment of a Repository at Yucca Mountain*. DOE/RW-0508. Washington, D.C.: U.S. Department of Energy, Office of Civilian Radioactive Waste Management. ACC: MOL.19981007.0028.

Feighner, M.A.; Daley, T.M.; Gritto, R.; and Majer, E.L. 1998. *Report: Results of VSP Analysis in P # 1*. Milestone SP3B6AM4. Berkeley, California: Lawrence Berkeley National Laboratory. ACC: MOL.19980507.0948.

Flint, L.E. 1998. *Characterization of Hydrogeologic Units Using Matrix Properties, Yucca Mountain, Nevada*. Water-Resources Investigations Report 97-4243. Denver, Colorado: U.S. Geological Survey. ACC: MOL.19980429.0512.

Levy, S.S. 1991. "Mineralogic Alteration History and Paleohydrology at Yucca Mountain, Nevada." *High Level Radioactive Waste Management-- Proceedings of the Second Annual International Conference, Las Vegas, Nevada, April 28-May 3, 1991, 1*, 477-485. La Grange Park, Illinois: American Nuclear Society. TIC: 204272.

Loeven, C. 1993. *A Summary and Discussion of Hydrologic Data from the Calico Hills Nonwelded Hydrogeologic Unit at Yucca Mountain, Nevada*. LA-12376-MS. Los Alamos, New Mexico: Los Alamos National Laboratory. ACC: NNA.19921116.0001.

Majer, E.L.; Johnson, L.R.; Vasco, D.W.; and Parker, P. 1998. *Results of Gravity Modeling of the Paleozoic Basement*. Milestone SP3B6DM4. Berkeley, California: Lawrence Berkeley National Laboratory. ACC: MOL.19980507.0940.

Moyer, T.C. and Geslin, J.K. 1995. *Lithostratigraphy of the Calico Hills Formation and Prow Pass Tuff (Crater Flat Group) at Yucca Mountain, Nevada*. Open-File Report 94-460. Denver, Colorado: U.S. Geological Survey. ACC: MOL.19941208.0003.

NRC (U.S. Nuclear Regulatory Commission) 1998. *Issue Resolution Status Report Key Technical Issue: Structural Deformation and Seismicity*. Rev. 1. Washington, D.C.: U.S. Nuclear Regulatory Commission. ACC: MOL.19981202.0550.

Ponce, D.A. and Langenheim, V.E. 1994. *Preliminary Gravity and Magnetic Models Across Midway Valley and Yucca Wash, Yucca Mountain, Nevada*. Open-File Report 94-572. Menlo Park, California: U.S. Geological Survey. ACC: MOL.19990406.0399.

Rautman, C.A. and McKenna, S.A. 1997. *Three-Dimensional Hydrological and Thermal Property Models of Yucca Mountain, Nevada*. SAND97-1730. Albuquerque, New Mexico: Sandia National Laboratories. ACC: MOL.19980311.0317.

Thompson, A.B. and Wennemer, M. 1979. "Heat Capacities and Inversions in Tridymite, Cristobalite, and Tridymite-Cristobalite Mixed Phases." *American Mineralogist*, 64, 1018-1026. Washington, D.C.: Mineralogical Society of America. TIC: 239133.

Vaniman, D.; Furlano, A.; Chipera, S.; Thompson, J. and Triay, I. 1996. "Microautoradiography in Studies of Pu(V) Sorption by Trace and Fracture Minerals in Tuff." *Scientific Basis for Nuclear Waste Management XIX, Symposium held November 27-December 1, 1995, Boston, Massachusetts*, 412, 639-646. Pittsburgh, Pennsylvania: Materials Research Society. TIC: 233877.

5.2 CODES, STANDARDS, REGULATIONS, AND PROCEDURES

AP-2.14Q, Rev. 0, ICN 0. *Review of Technical Products*. Washington, D.C.: U.S. Department of Energy, Office of Civilian Radioactive Waste Management. ACC: MOL.19990701.0616.

AP-3.10Q, Rev. 1, ICN 0. *Analyses and Models*. Washington, D.C.: U.S. Department of Energy, Office of Civilian Radioactive Waste Management. ACC: MOL.19990702.0314.

AP-3.11Q, Rev. 0, ICN 0. *Technical Reports*. Washington, D.C.: U.S. Department of Energy, Office of Civilian Radioactive Waste Management. ACC: MOL.19990701.0620.

AP-SIII.1Q, Rev. 0, ICN 0. *Scientific Notebooks*. Washington, D.C.: U.S. Department of Energy, Office of Civilian Radioactive Waste Management. ACC: MOL.19990702.0311.

QAP-2-0, Rev. 5. *Conduct of Activities*. Las Vegas, Nevada: CRWMS M&O. ACC: MOL.19980826.0209.

QAP-SIII-1, Rev. 3. *Scientific Investigation Control*. Las Vegas, Nevada: CRWMS M&O. ACC: MOL.19980929.0029.

QAP-SIII-2, Rev. 1. *Review of Scientific Documents and Data*. Las Vegas, Nevada: CRWMS M&O. ACC: MOL.19980219.0733.

QAP-SIII-3, Rev. 2. *Scientific Notebooks*. Las Vegas, Nevada: CRWMS M&O. ACC: MOL.19971105.0040.

Enclosure 1
Integrated Site Model Process Model Report, Rev. 00

**OFFICE OF CIVILIAN RADIOACTIVE WASTE MANAGEMENT
DOCUMENT INPUT REFERENCE SHEET**

1. Document Identifier No./Rev.:		Change:	Title:						
TDR-NBS-GS-000002 REV 00		N/A	Integrated Site Model Process Model Report						
Input Document		3. Section	4. Input Status	5. Section Used In	6. Input Description	7. TBV/TBD Priority	8. TBV Due To		
2. Technical Product Input Source Title and Identifier(s) with Version							Unqual.	From Uncontrolled Source	Un-confirmed
2a									
1	DTN: MO9510RIB00002.004. RIB Item: Stratigraphic Characteristics: Geologic/Lithologic Stratigraphy. Submittal date: 06/26/1996.	Table 2-5	N/A	Section 3.2.3, Table 1-1	Yucca Mountain Stratigraphic Nomenclature	N/A	N/A	N/A	N/A
2	DTN: LADV831321AQ97.001. Mineralogic Variation in Drill Holes. Submittal date: 05/28/1997.	S97466-001-6, 8,11-13, and 15	TBV # 868	Section 3.4.4.2	Mineralogy, borehole SD-7: Smectite, Tridymite, Cristoballite, Quartz, Feldspar, Glass, Mica Group, Clinoptilolite, Mordenite, Opal-Ct, and Chabazite	1	N/A	N/A	X
3	64 FR 8640. Disposal of High-Level Radioactive Wastes in a Proposed Geologic Repository at Yucca Mountain, Nevada Proposed Rule 10 CFR 63. TIC: 245670.	10 CFR 63.115(4) (b)	N/A	Section 1.5	Proposed rule as published in Federal Register.	N/A	N/A	N/A	N/A
4	Bish, D.L. and Aronson, J.L. 1993. "Paleogeothermal and Paleohydrologic Conditions in Silicic Tuff from Yucca Mountain, Nevada." <i>Clays and Clay Minerals</i> , 41 (2), 148-161. Long Island City, New York: Pergamon Press. TIC: 224613.	pp. 151-155 and 152-153, Figures 3 & 4	N/A	Section 3.4.4.3	General Reference to Smectite and Illite Distribution	N/A	N/A	N/A	N/A
5	Bish, D.L. and Chipera, S.J. 1989. <i>Revised Mineralogic Summary of Yucca Mountain, Nevada</i> . LA-11497-MS. Los Alamos, New Mexico: Los Alamos National Laboratory. ACC: NNA.19891019.0029.	p. 13	N/A	Section 3.4.4.2	General Reference to Zeolite abundance at Yucca Mountain	N/A	N/A	N/A	N/A
6	Brocher, T.M.; Hunter, W.C.; and Langenheim, V.E. 1998. "Implications of Seismic Reflection and Potential Field Geophysical Data on the Structural Framework of the Yucca Mountain-Crater Flat Region, Nevada." <i>Geological Society of America Bulletin</i> , 110 (8), 947-971. Boulder, Colorado: Geological Society of America. TIC: 238643.	pp. 947-971, Figures 7, 8, and 14	N/A	Sections 3.2.2 1 and 3.2.6	Figures 7, 8, and 14	N/A	N/A	N/A	N/A
7	Buesch, D.C. and Spengler, R.W. 1999. "Correlations of Lithostratigraphic Features with Hydrogeologic Properties, a Facies-Based Approach to Model Development in Volcanic Rocks at Yucca Mountain, Nevada." <i>Proceedings of Conference on Status of Geologic Research and Mapping in Death Valley National Park, Las Vegas, Nevada, April 9-11, 1999, Open File Report 99-153</i> , 62-64. Denver, Colorado: U.S. Geological Survey. TIC: 245245.	pp. 62-64	N/A	Table 1-1	For the purposes of GFM3.1, each formation in the Crater Flat Group was subdivided into six zones based on the requirements of the users of the Geologic Framework Model. The subdivisions are upper vitric (uv), upper crystalline (uc), moderately to densely welded (md), lower crystalline (lc), lower vitric (lv), and bedded tuff (bt)	N/A	N/A	N/A	N/A

**OFFICE OF CIVILIAN RADIOACTIVE WASTE MANAGEMENT
DOCUMENT INPUT REFERENCE SHEET**

1. Document Identifier No./Rev.:		Change:	Title:						
TDR-NBS-GS-000002 REV 00		N/A	Integrated Site Model Process Model Report						
Input Document			4. Input Status	5. Section Used In	6. Input Description	7. TBV/TBD Priority	8. TBV Due To		
2. Technical Product Input Source Title and Identifier(s) with Version		3. Section					Unqual.	From Uncontrolled Source	Un-confirmed
2a									
8	Buesch, D.C.; Spengler, R.W.; Moyer, T.C.; and Geslin, J.K. 1996. <i>Proposed Stratigraphic Nomenclature and Macroscopic Identification of Lithostratigraphic Units of the Paintbrush Group Exposed at Yucca Mountain, Nevada</i> . Open-File Report 94-469. Denver, Colorado: U.S. Geological Survey. ACC: MOL.19970205.0061.		Table 2	N/A	Table 1-1	Nomenclature	N/A	N/A	N/A
9	Byers, F.M., Jr.; Carr, W.J.; Christiansen, R.L.; Lipman, P.W.; Orkild, P.P.; and Quinlivan, W.D. 1976. <i>Geologic Map of the Timber Mountain Caldera Area, Nye County, Nevada</i> . Miscellaneous Investigations Series Map I-891. Denver, Colorado: U.S. Geological Survey. TIC: 204573.		Map	N/A	Sections 3.2.4.1.6, 3.2.4.1.7, and 3.2.4.1.8	Geologic Map Data	N/A	N/A	N/A
10	Carlos, B.A.; Chipera, S.J.; and Bish, D.L. 1995. <i>Distribution and Chemistry of Fracture-Lining Minerals at Yucca Mountain, Nevada</i> . LA-12977-MS. Los Alamos, New Mexico: Los Alamos National Laboratory. ACC: MOL.19960306.0564.		pp. 39 & 47	N/A	Section 3.4.4.2	General Reference to occurrence of phillipsite at Yucca Mountain	N/A	N/A	N/A
11	Carr, M.D.; Waddell, S.J.; Vick, G.S.; Stock, J.M.; Monsen, S.A.; Harris, A.G.; Cork, B.W.; and Byers, F.M., Jr. 1986. <i>Geology of Drill Hole UE25p#1: A Test Hole Into Pre-Tertiary Rocks Near Yucca Mountain, Southern Nevada</i> . Open-File Report 86-175. Menlo Park, California: U.S. Geological Survey. ACC: HQS.19880517.2633.		p. 6, Figures 15, 14, and 11	N/A	Sections 3.2.4.1.10, 3.2.4.1.6, 3.2.4.1.7, and 3.2.4.1.8	Tertiary Paleozoic unconformity interpretation	N/A	N/A	N/A
12	CRWMS M&O 1997. <i>Determination of Available Volume for Repository Siting</i> . BCA000000-01717-0200-00007 REV 00. Las Vegas, Nevada: CRWMS M&O. ACC: MOL.19971009.0699.		pp. 43-50	N/A	Section 3.2.3, Table 1-1	RHHtop definition	N/A	N/A	N/A

**OFFICE OF CIVILIAN RADIOACTIVE WASTE MANAGEMENT
DOCUMENT INPUT REFERENCE SHEET**

1. Document Identifier No./Rev.:		Change:	Title:						
TDR-NBS-GS-000002 REV 00		N/A	Integrated Site Model Process Model Report						
Input Document		3. Section	4. Input Status	5. Section Used In	6. Input Description	7. TBV/TBD Priority	8. TBV Due To		
2. Technical Product Input Source Title and Identifier(s) with Version							Unquat.	From Uncontrolled Source	Un-confirmed
2a									
13	CRWMS M&O 1999a. <i>Geologic Framework Model (GFM3.1) Analysis Model Report</i> . MDL-NBS-GS-000002 REV 00B. Las Vegas, Nevada. ACC: MOL.19991027.0206.	Entire	TBV # 3734	Sections 1, 2.2.1, 3, 3.2, 3.2.1, 3.2.2, 3.2.2.1, 3.2.2.2., 3.2.3, 3.2.4, 3.2.4.2, 3.2.4.2.3, 3.2.5, 3.2.6, 3.2.7.1, 3.2.7.2.1, and 3.2.7.2.2.,	Described as one of components of ISM.	1	x	N/A	N/A
14	CRWMS M&O 1999b. <i>Rock Properties Model (RPM3.1) Analysis Model Report</i> . MDL-NBS-GS-000004 REV 00B. Las Vegas, Nevada. ACC: MOL.19991027.0207.	Entire	TBV # 3735	Sections 2.2.2, 3, 3.3.1, 3.3.2.1, 3.3.2.2, 3.3.3, 3.3.3.2, 3.3.3.3.1, 3.3.3.4.1, 3.3.4, 3.3.5.1, and 3.3.7	In Section 1.2, described as one of components of ISM. Section 2.2.2 describes changes to RPM between ISM 2.0 and ISM 3.1.	1	x	N/A	N/A
15	CRWMS M&O 1999c. <i>Mineralogical Model (MM3.0) Analysis Model Report</i> . MDL-NBS-GS-000003 REV 00B. Las Vegas, Nevada. ACC: MOL.19991027.0208.	Entire	TBV # 3736	Sections 1, 1.4, 2.2.3, 3, 3.4, 3.4.1, 3.4.2, 3.4.2.1, 3.4.2.2, 3.4.2.3, 3.4.3.1, 3.4.3.2, 3.4.3.3, 3.4.3.4, and 3.4.7	Described as one of components of ISM.	1	N/A	N/A	N/A

**OFFICE OF CIVILIAN RADIOACTIVE WASTE MANAGEMENT
DOCUMENT INPUT REFERENCE SHEET**

1. Document Identifier No./Rev.:		Change:	Title:						
TDR-NBS-GS-000002 REV 00		N/A	Integrated Site Model Process Model Report						
Input Document		3. Section	4. Input Status	5. Section Used In	6. Input Description	7. TBV/TBD Priority	8. TBV Due To		
2. Technical Product Input Source Title and Identifier(s) with Version							Unqual.	From Uncontrolled Source	Un-confirmed
2a									
16	CRWMS M&O 1999d. <i>M&O Site Investigations. Activity Evaluation, January 23, 1999. Las Vegas, Nevada: CRWMS M&O. ACC: MOL.19990317.0330.</i>	Entire	N/A	1.3	General Reference	N/A	N/A	N/A	N/A
17	CRWMS M&O 1999e. <i>M&O Site Investigations. Activity Evaluation, September 28, 1999. Las Vegas, Nevada: CRWMS M&O. ACC: MOL.19990928.0224.</i>	Entire	N/A	1.3	General Reference	N/A	N/A	N/A	N/A
18	CRWMS M&O 1998. <i>Yucca Mountain Site Description. B00000000-01717-5700-00019 REV 00. Las Vegas, Nevada: CRWMS M&O. ACC: MOL.19981202.0492.</i>	p. 3.3-3	N/A	Section 3.2.4.2.4	Stratigraphic and structural concepts and background.	N/A	N/A	N/A	N/A
19	Day, W.C.; Dickerson, R.P.; Potter, C.J.; Sweetkind, D.S.; San Juan, C.A.; Drake, R.M., II; and Fridrich, C.J. 1997. <i>Bedrock Geologic Map of the Yucca Mountain Area, Nye County, Nevada. Administrative Report. Denver, Colorado: U.S. Geological Survey. ACC: MOL.19980310.0122.</i>	Entire Map	TBV # 3579	Sections 2.2.1, 3.2.2.1, 3.2.3.3, 3.2.4.1.4, 3.2.4.2.2, 3.2.4.2.4, 3.2.5, and 3.2.6, Table 1-1	Geological Map	1	X	N/A	N/A
20	Day, W.C.; Dickerson, R.P.; Potter, C.J.; Sweetkind, D.S.; San Juan, C.A.; Drake, R.M., II; and Fridrich, C.J. 1998. <i>Bedrock Geologic Map of the Yucca Mountain Area, Nye County, Nevada. Geologic Investigations Series I-2627. Denver, Colorado: U.S. Geological Survey. ACC: MOL.19981014.0301.</i>	Entire Map	N/A	3.2.2.1	Geologic Map	N/A	N/A	N/A	N/A
21	Deutsch, C.V. and Journel, A.G. 1992. <i>GSLIB Geostatistical Software Library and User's Guide. New York, New York: Oxford University Press. TIC: 224174.</i>	pp. 62 & 137	N/A	Section 3.3.3.1.2	General Reference	N/A	N/A	N/A	N/A
22	DOE (U.S. Department of Energy) 1998a. <i>Quality Assurance Requirements and Description. DOE/RW-0333P, Rev. 8. Washington, D.C.: U.S. Department of Energy, Office of Civilian Radioactive Waste Management. ACC: MOL.19980601.0022.</i>	pp. 2-19 and 2-20	N/A	Sections 1.3	Required Reference	N/A	N/A	N/A	N/A

**OFFICE OF CIVILIAN RADIOACTIVE WASTE MANAGEMENT
DOCUMENT INPUT REFERENCE SHEET**

1. Document Identifier No./Rev.:		Change:	Title:						
TDR-NBS-GS-000002 REV 00		N/A	Integrated Site Model Process Model Report						
Input Document		3. Section	4. Input Status	5. Section Used In	6. Input Description	7. TBV/TBD Priority	8. TBV Due To		
2. Technical Product Input Source Title and Identifier(s) with Version							Unqual.	From Uncontrolled Source	Un-confirmed
2a									
23	DOE 1998b. <i>Introduction and Site Characteristics. Volume 1 of Viability Assessment of a Repository at Yucca Mountain.</i> DOE/RW-0508. Washington, D.C.: U.S. Department of Energy, Office of Civilian Radioactive Waste Management. ACC: MOL.19981007.0028.	pp. 2-38, 2-19, and 2-20	N/A	Sections 3.2.4.1.4, 3.2.4.1.5, 3.2.4.1.6, 3.2.4.1.7, and 3.2.4.1.8	General Reference	N/A	N/A	N/A	N/A
24	Feighner, M.A.; Daley, T.M.; Gritto, R.; and Majer, E.L. 1998. <i>Report: Results of VSP Analysis in P # 1. Milestone SP3B6AM4.</i> Berkeley, California: Lawrence Berkeley National Laboratory. ACC: MOL.19980507.0948.	Figure 7b	N/A	Section 3.2.6	Offset of Pz at p#1	N/A	N/A	N/A	N/A
25	Flint, L.E. 1998. <i>Characterization of Hydrogeologic Units Using Matrix Properties, Yucca Mountain, Nevada.</i> Water-Resources Investigations Report 97-4243. Denver, Colorado: U.S. Geological Survey. ACC: MOL.19980429.0512.	p. 38 and Figures 12, 12(a), & 12(b)	N/A	Sections 3.3.3.4.1 and 3.3.5.1	Used as a general reference to describe the laboratory techniques used to measure properties of core samples used and as a relatively specific reference to provide proper attribution of numerous concepts.	N/A	N/A	N/A	N/A
26	Levy, S.S. 1991. "Mineralogic Alteration History and Paleohydrology at Yucca Mountain, Nevada." <i>High Level Radioactive Waste Management: Proceedings of the Second Annual International Conference, Las Vegas, Nevada, April 28-May 3, 1991, 1, 477-485.</i> La Grange Park, Illinois: American Nuclear Society. TIC: 204272.	pp. 483-484	N/A	Section 3.4.4.5	General reference to Tridymite occurrences interpreted as possible limit on rise of the maximum water table at Yucca Mountain.	N/A	N/A	N/A	N/A
27	Loeven, C. 1993. <i>A Summary and Discussion of Hydrologic Data from the Calico Hills Nonwelded Hydrogeologic Unit at Yucca Mountain, Nevada.</i> LA-12376-MS. Los Alamos, New Mexico: Los Alamos National Laboratory. ACC: NNA.19921116.0001.	pp. 37-39 and Table 6	N/A	Section 3.4.4.2	General reference to Zeolitic alteration affect on the hydraulic conductivities of vitric nonwelded and zeolitized tuffs.	N/A	N/A	N/A	N/A
28	Majer, E.L.; Johnson, L.R.; Vasco, D.W.; and Parker, P. 1998. <i>Results of Gravity Modeling of the Paleozoic Basement.</i> Milestone SP3B6DM4. Berkeley, California: Lawrence Berkeley National Laboratory. ACC: MOL.19980507.0940.	Figure 3b	N/A	Sections 3.2.2.4, 3.2.4.1.10, and 3.2.6	General Reference; description of activity and results	N/A	N/A	N/A	N/A

**OFFICE OF CIVILIAN RADIOACTIVE WASTE MANAGEMENT
DOCUMENT INPUT REFERENCE SHEET**

1. Document Identifier No./Rev.:		Change:	Title:						
TDR-NBS-GS-000002 REV 00		N/A	Integrated Site Model Process Model Report						
Input Document			4. Input Status	5. Section Used In	6. Input Description	7. TBV/TBD Priority	8. TBV Due To		
2. Technical Product Input Source Title and Identifier(s) with Version		3. Section					Unqual.	From Uncontrolled Source	Un-confirmed
2a	Moyer, T.C. and Geslin, J.K. 1995. <i>Lithostratigraphy of the Calico Hills Formation and Prow Pass Tuff (Crater Flat Group) at Yucca Mountain, Nevada</i> . Open-File Report 94-460. Denver, Colorado: U.S. Geological Survey. ACC: MOL.19941208.0003.	pp. 8-31	N/A	Section 3.3.5.1.5	Reference used to indicate that certain known complicating geologic conditions exist at Yucca Mountain	N/A	N/A	N/A	N/A
29									
30	Ponce, D.A. and Langenheim, V.E. 1994. <i>Preliminary Gravity and Magnetic Models Across Midway Valley and Yucca Wash, Yucca Mountain, Nevada</i> . Open-File Report 94-572. Menlo Park, California: U.S. Geological Survey. ACC: MOL.19990406.0399.	p. 6	N/A	Sections 3.2.2.1 and 3.2.3.3	General reference to geologic interpretation	N/A	N/A	N/A	N/A
31	NRC (U.S. Nuclear Regulatory Commission) 1998. <i>Issue Resolution Status Report Key Technical Issue: Structural Deformation and Seismicity</i> . Rev. 1. Washington, D.C.: U.S. Nuclear Regulatory Commission. ACC: MOL.19981202.0550.	pp. 3, 19, and 48, pp. 57-58, and Appendix F	N/A	Section 4	Section 4.2 describes subissues identified in IRSR. Section 4.2.3 identifies the viable fracture models subissue and notes that it is not addressed by the ISM. Section 4.2.4 identifies the tectonics and crustal conditions subissue not discussed.	N/A	N/A	N/A	N/A
32	Rautman, C.A. and McKenna, S.A. 1997. <i>Three-Dimensional Hydrological and Thermal Property Models of Yucca Mountain, Nevada</i> . SAND97-1730. Albuquerque, New Mexico: Sandia National Laboratories. ACC: MOL.19980311.0317.	p. 142	N/A	Figure 3-23	Description of a rock layer	N/A	N/A	N/A	N/A
33	Thompson, A.B. and Wennemer, M. 1979. "Heat Capacities and Inversions in Tridymite, Cristobalite, and Tridymite-Cristobalite Mixed Phases." <i>American Mineralogist</i> , 64, 1018-1026. Washington, D.C.: Mineralogical Society of America. TIC: 239133.	pp. 1018-1025	N/A	Section 3.4.4.5	General reference to Tridymite	N/A	N/A	N/A	N/A
34	Vaniman, D.; Furlano, A.; Chipera, S.; Thompson, J. and Triay, I. 1996. "Microautoradiography in Studies of Pu(V) Sorption by Trace and Fracture Minerals in Tuff." <i>Scientific Basis for Nuclear Waste Management XIX, Symposium held November 27-December 1, 1995, Boston, Massachusetts</i> , 412, 639-646. Pittsburgh, Pennsylvania: Materials Research Society. TIC: 233877.	pp. 639-646	N/A	Section 3.4.4.3	General reference to Plutonium Sorption.	N/A	N/A	N/A	N/A

Enclosure 2
YMP Deliverable Acceptance Review Form

YMP-244-R3
05/20/1999

YUCCA MOUNTAIN SITE CHARACTERIZATION PROJECT
DELIVERABLE ACCEPTANCE REVIEW (YDAR)

QA: Q


Page 1 of 1

YDAR No. _____

Date DC YDAR No. _____
Assigned: _____

Signatures on this document represent signers' acknowledgment that the applicable procedure has been read, understood, and complied with.

SECTION I - DELIVERABLE ACCEPTANCE REVIEW REQUEST

1. DELIVERABLE TITLE/DESCRIPTION: Integrated Site Model Process Model Report, Rev. 00		2. CURRENT DOCUMENT NO.: TDR-NBS-GS-000002 <input type="checkbox"/> N/A	3. REV/ICN/Draft: (current) REV 00 <input type="checkbox"/> N/A
4. DELIVERABLE ID NO.: SLP58CM3	5. DELIVERABLE DUE DATE: 10/29/99		
6. WBS NO.: 1.2.21.3.I	7. QA DESIGNATION: <input checked="" type="checkbox"/> QA: Q <input type="checkbox"/> QA: L <input type="checkbox"/> QA: N/A		
8. RESPONSIBLE ASSISTANT MANAGER/DIRECTOR: S. P. Mellington		ORG: Off. of Project Execution	
9. YAP 30.12 REVIEW REQUIRED: <input checked="" type="checkbox"/> Yes <input type="checkbox"/> No <input type="checkbox"/> N/A	12. REQUESTED BY: Mike Lugo Print Name		
10. YMP-REQUIRED REVIEWS REQUIRED: <input checked="" type="checkbox"/> Yes <input type="checkbox"/> No <input type="checkbox"/> N/A	Regulatory and Licensing (702)295-4761 Organization Phone No.		
11. COMPLETED TDIF FORM (copy) <input type="checkbox"/> or TRANSMITTAL LETTER TO DATABASE ADMINISTRATOR (copy) <input type="checkbox"/> ATTACHED DTN No. _____ <input checked="" type="checkbox"/> N/A <input type="checkbox"/> Additional Material Attached	Signature:  Date: October 29, 1999		

SECTION II - DELIVERABLE REVIEW RESULTS

13. ACCEPTED WITH CONDITIONS, DELIVERABLE (Provide reason/instructions in this block) N/A

13a. REV/ICN/Draft (current):
RESPONSIBLE CONTRACTING OFFICER'S REPRESENTATIVE/
TECHNICAL MONITOR: _____
Signature Date

13b. DC: copy of YDAR to OPC-PP&C, and Requestor: _____
Date

14. ACCEPTED REJECTED (Provide reason/instructions in Block 16) 15. Technical Impacts: Yes No

14a. REV/ICN/Draft (current):
15a. TECHNICAL IMPACT STATEMENT:

16. COMMENTS:

17. RESPONSIBLE CONTRACTING OFFICER'S REPRESENTATIVE/TECHNICAL MONITOR:

Signature Date

SECTION III - DELIVERABLE REVIEW COMPLETION

18. YDAR copy to Contracting Officer's Representative/Technical Monitor: _____
Date

19. YDAR copy to Requestor/M&O PP&C/YMSCO OPC: _____
Date

20. DOCUMENT CONTROL (YDAR Completion)

Signature Date

Enclosure 3
DTN and Q-status Listing

ISM DATA VERIFICATION/QUALIFICATION STATUS as of 11/17/99

DIRS DTNs	DATA			
	Need To Be Verified	Verified	Need To Be Qualified	Qualified
GS940708314211.035	X	X	X	X
GS950108314211.001	X	X	X	X
GS950108314211.002	X	X	X	X
GS950108314211.003	X	X	X	X
GS950108314211.004	X	X	X	X
GS950108314211.005	X	X	X	X
GS960908314224.020	X		X	
GS970808314221.002	X		X	
GS970808314224.016	X		X	
GS980708312242.010	X		X	
GS980808312242.014	X		X	
GS981108314224.005	X	X	X	X
LA000000000086.002	X	X	X	X
LA9908JC831321.001			X	
LA9910DB831321.001			X	
LA9910JC831321.001			X	
LADB831321AN98.002			X	
LADV831321AQ97.001	X		X	
LADV831321AQ97.007	X		X	
LADV831321AQ99.001	X	X	X	X
LAJC831321AQ98.005	X	X	X	X
LASC831321AQ96.002	X	X	X	X
LASC831321AQ98.001	X		X	
LASC831321AQ98.003	X	X	X	X
LASL831322AQ97.001	X	X	X	X
LB980130123112.003	X		X	
MO9510RIB00002.004	X		X	
MO9609RIB00038.000			X	
MO9804MWDGFM03.001			X	
MO9807COV98003.000			X	
MO9811MWDGFM03.000			X	
MO9901MWDGFM31.000			X	
MO9906GPS98410.000	X	X	X	X
MO9910POROCALC.000			X	
MO9911INPUTRPM.000			X	
SNF40060198001.001	X	X	X	X
SNF40060298001.001	X	X	X	X
SNL01A05059301.005	X	X	X	X
SNL01A05059301.007	X	X	X	X
TOTAL = 39	28	18	39	18
% of Data Verified & Qualified		18/28=64%	18/39=46%	

ISM CODES/ROUTINES/MODELS STATUS as of 11/17/99

CODES/ROUTINES		MODELS	
Code/Routine ID	Qualified	MODEL ID	Validated
BUD	X	Rock Properties 3.1	X
COORDS	X	Minerologic 3.0	X
COREGPC	X	GFM 3.1	X
Earthvision 4.0	X		
ETYPE	X	TOTAL = 3	3
EVS 3.75	X		
GAM3 1.2	X	% Models V'ed	3/3=100%
GSLIB 1.4 BACKTR 1.2	X		
GSLIB 1.4 BICALB 2.0	X		
GSLIB 1.4 NSCORE V	X		
GSLIB 1.4 SGSIM 1.4	X		
GSLIB 1.4 TRANS 1.3	X		
GSLIB 2.0 IK3D 2.0	X		
HISTPLT 1.2	X		
MATCH	X		
MATCHUP	X		
MS EXCEL95	X		
MS EXCEL97	X		
SIGMA PLOT 2.0	X		
SIGMA PLOT 5.0	X		
STRATAMODEL 4.1.1			
STRATC4	X		
TWOFOOT	X		
VARIO 1.16	X		
VARIO 1.20	X		
VARIOFIT 1.2	X		
VITROPHYRE	X		
ZEOLITE5	X		
TOTAL = 28	27		
% Codes/Routines Q'ed	27/28=96%		

Criteria for Determining Compliance with PMR Goals
On Verification/Qualification/Validation of
Data, Software, and Models for the
Integrated Site Model PMR

The formulas used in determining compliance with the PMR deliverable evaluation criteria are explained below.

For the data verification and data qualification criteria, these percentages were measured at the data level that is reflected on the Document Input Reference Sheets (DIRS) for the three supporting Analysis and Model Reports (AMRs). These are the Data Tracking Numbers (DTNs) that were used as direct input to the AMRs, and does not include those DTNs that are on the DIRS forms only as references.

Data Verification

$$\% \text{ Complete} = \frac{\text{Number of data inputs that have been verified}}{\text{Number of data inputs originally labeled Q-TBV}} \times 100$$

From the total set of data inputs used in the three AMRs, this criterion focuses on removing the TBVs from those data inputs that had been labeled Q-TBV as a result of the CARs that were issued last year.

Data Qualification

$$\% \text{ Complete} = \frac{\text{Number of data inputs that are Q}}{\text{Number of data inputs that need to be Q}} \times 100$$

From the total set of data inputs used in the three AMRs, this criterion focuses on those data inputs that are being directly relied upon to support our technical conclusions for the safety case, and therefore need to be Q.

Software Qualification

$$\% \text{ Complete} = \frac{\text{Number of software codes/routines that have been qualified}}{\text{Number of software codes/routines used in the PMR/AMRs}} \times 100$$

Model Validation

$$\% \text{ Complete} = \frac{\text{Number of models that have been validated}}{\text{Number of models in the PMR/AMRs}} \times 100$$

Enclosure 4
WBS Planning Sheet

WBS Planning Sheet			
Date:			
Revision:			
Element	1.2.21.3.1	Title:	Integrated Site Process Model Report
SubProduct	1.2.21.3	Title:	Suitability Criteria Compliance Evaluation
Product	1.2.21	Title:	Site Recommendation (SR)
Element Team Leader (DOE)	TYNAN M	Element Manager	LUGO M
SubProduct Team Leader (DOE)	SULLIVAN T	SubProduct Manager	HANSON G
Product Manager (DOE)	BROCOUM S	Product Manager	KING J

Fiscal Year Cost Estimates (1000s)					
EOC	FY 2000	FY 2001	FY 2002	FY 2003	Total
Labor	2,951	1,087	0	0	4,038
Non-Labor	647	265	0	0	912
Total	3,598	1,352	0	0	4,950

Description/Work Scope

The three-dimensional Integrated Site Model (ISM) of Yucca Mountain, Nevada, version ISM3.1, will be an updated geometric representation of selected rock units and structures (a geologic framework model) plus a set of rock properties and mineralogy models and data sets. The ISM3.1 PMR will provide a summary and synthesis of the following component models: Geologic Framework Model3.1; Rock-Properties Model3.1; and the Mineralogic- Model 3.0. The summaries will include discussions of the following: descriptions of the models, supporting codes, components, and/or analyses; the input data and its qualification status; data, code, and model validation; model construction; model results and feeds to users (e.g., UZ or SZ flow and transport); model uncertainties; and credible alternative interpretations. The ISM3.1 PMR and the component models will be produced according to the appropriate procedure(s).

Revision 00 of this PMR is due November 1, 1999 for DOE acceptance review in accordance with the criteria stated below. The due date is based on the CR-99-008, but subject to change after baselining IPS.

Deliverables		
ID	Title/Description/Acceptance Criteria	Due Date
SLP59CM3	Submit ISM PMR Rev 01	01-DEC-2000
	<p>Description</p> <p>This Process Model Report will address the following aspects related to the model:</p> <ul style="list-style-type: none"> Description of the model and submodels Abstraction of the model into TSPA Relevant data and data uncertainties Assumptions and bases Model results (outputs) Information on code verification/model validation Opposing views Information necessary to support regulatory evaluations <p>This Process Model Report will be a revision to the synthesis report provided in Rev 00. Any new information not available at the time Rev 00 was issued, including comments from the external organizations, should be addressed. This report will primarily reference supporting analyses and modeling documentation, documents developed outside the Project, and other key documents (e.g., Topical Reports and other Process Model Reports). Each of the analyses and models that are related to the Process Model Report will be documented in accordance with AP-3.10Q Analyses and Models. This documentation will be summarized in the Process Model Report, but will not be physically part of the report. The Process Model Report itself will be developed using procedure AP-3.11Q, Technical Reports.</p> <p>In developing this Process Model Report, and the supporting analyses and models, the subject matter experts will be cognizant of existing documentation (internal and external) that is related to the process model to ensure that the depth and breadth of the available technical information has been adequately considered.</p>	
	<p>Evaluation Criteria</p> <p>1) The technical content of the PMR meets the requirements identified in the scope of work definition and is complete, clearly written, defensible, and traceable to the supporting AMRs so that independent</p>	

Date:		WBS Planning Sheet	
Revision:			
Element	1.2.21.3.1	Title:	Integrated Site Process Model Report
SubProduct	1.2.21.3	Title:	Suitability Criteria Compliance Evaluation
Product	1.2.21	Title:	Site Recommendation (SR)
Element Team Leader (DOE)	TYNAN M	Element Manager	LUGO M
SubProduct Team Leader (DOE)	SULLIVAN T	SubProduct Manager	HANSON G
Product Manager (DOE)	BROCOUM S	Product Manager	KING J

Deliverables (continued)		
ID	Title/Description/Acceptance Criteria	Due Date
SLP59CM3	Submit ISM PMR Rev 01	01-DEC-2000

Evaluation Criteria (continued)

reviewers can understand and verify how data sets were used in AMRs, PMRs and the abstractions that support TSPA-SR.

2) The qualification status of at least 90% of those data used as input to the PMR and its supporting AMRs will be verified (i.e., their Q status will have been determined). These data inputs will be identified in the Document Input Reference Sheets (DIRS) for the PMR and AMRs. At least 80% of those data needed to be qualified and used as input to the PMR and its supporting AMRs will be qualified. The PMR will be reviewed and evaluated to verify that, for the technical data (as defined in AP SIII.3Q) in the deliverable:

a) For data that have completed the verification process, the data cited in the PMR and supporting AMRs are labeled or referenced as qualified, accepted, or unqualified in accordance with the AP-SIII.3Q, AP-3.15Q, and AP-SIII.2Q. Unqualified data supporting the postclosure safety case requiring qualification will be identified or referenced.

b) Priority in the verification/qualification process has been give to data that support the safety case, as identified in the Repository Safety Strategy Rev. 3. It is anticipated that some data sets will be determined to be unqualified and the PMR may identify results of analyses supporting the postclosure safety case that utilize, in whole or in part, unqualified data.

c) Within the PMR or a cover letter provide a complete list of DTNs and Q-status for data, analyses, model input and output, and software used directly in the PMR and in the supporting AMRs or other supporting analyses.

Using an approach that was documented in qualification plans per AP-SIII.2Q, developed inputs and selected acquired data are being prepared for the ISM PMR. This will establish the basis for this model to provide qualified inputs to other process models.

3) At least 80% of software code used in development and/or control of resulting models or manipulation of data presented in the PMR, supporting AMRs, and other supporting analyses will be qualified and maintained in accordance with AP-SI.1Q controlled by the M&O. For software that is not qualified, the qualification status is identified or referenced. A listing of the location of software and status for the PMR and supporting AMRs and other supporting analyses will be provided in the PMR or as a cover letter. All PMRs will be reviewed and evaluated to verify that:

a) The software codes used in development of models that are documented in the deliverable have been assigned a unique identifier and are maintained in accordance with AP-SI.1Q.

b) The software codes used to develop or manipulate the data presented in the deliverable have been assigned a unique identifier and are maintained in accordance with AP-SI.1Q.

c) The software code is retrievable and usable, and the results reported in the deliverable are reproducible.

4) At least 80% of the models used in the development of the PMR and supporting AMRs will be verified and maintained in accordance with AP-3.10Q and AP-3.15Q. For models that are not verified, the verification status is identified or referenced.

5) Documentation of the following is provided:

a) the user-defined input parameters (parameter values) that are used to run the codes/software that are used to support TSPA-SR

b) the actual numerical value/distribution used for each parameter and the rationale for its selection

c) the source(s) for each parameter value and any intermediate calculations/data manipulations used to

WBS Planning Sheet			
Date:			
Revision:			
Element	1.2.21.3.1	Title:	Integrated Site Process Model Report
SubProduct	1.2.21.3	Title:	Suitability Criteria Compliance Evaluation
Product	1.2.21	Title:	Site Recommendation (SR)
Element Team Leader (DOE)	TYNAN M	Element Manager	LUGO M
SubProduct Team Leader (DOE)	SULLIVAN T	SubProduct Manager	HANSON G
Product Manager (DOE)	BROCOUM S	Product Manager	KING J

Deliverables (continued)

ID	Title/Description/Acceptance Criteria	Due Date
SLP59CM3	Submit ISM PMR Rev 01	01-DEC-2000

Evaluation Criteria (continued)

determine the parameter value

- 6) Alternate conceptual models and alternate interpretations of the available data are documented.
- 7) A discussion of relevant analog information is included and documented.
- 8) All assumptions and their bases are identified and justified
- 9) PMR development must fully address appropriate regulatory requirements and commitments. The PMR will include the following features:
 - a) Common graphics: The graphics will be consistent and, where possible, identical in order to facilitate integration among the analyses and models supporting the PMR. The graphics will be clear and accurate, and reflect the accompanying text descriptions.
 - b) Readability: The text will be clear, simple and concise. Avoid the use of technical jargon and acronyms whenever possible and in line with the need for the SR and LA presentation needs.
 - c) Full M&O Management Review: The final document submitted for DOE review and acceptance shall have received a full M&O management review.
 - d) Project generated data cited in deliverable in the format of graphics, tables, figures, parameter values, and maps must include the Data Tracking Number for the cited data. DTNs cited in the body of the text should be included in the reference section of the document. The data cited by DTN must be resident in the TDMS. Data or information from other sources must have appropriate Technical Information Management System identifiers (e.g. TIC or RIS number) and be accessible through the TMS.

Completion Criteria

This deliverable is complete when it is submitted to the DOE in accordance with YAP-30.63, Submittal, Review and Acceptance of Deliverables.

SLP58CM3	Submit ISM PMR Rev 00	29-OCT-1999
----------	-----------------------	-------------

Description

This Process Model Report will address the following aspects related to the model:

- Description of the model and submodels
- Abstraction of the model into TSPA
- Relevant data and data uncertainties
- Assumptions and bases
- Model results (outputs)
- Information on code verification/model validation
- Opposing views
- Information necessary to support regulatory evaluations

This Process Model Report will be a synthesis report. This report will primarily reference supporting analyses and modeling documentation, documents developed outside the Project, and other key documents (e.g., Topical Reports and other Process Model Reports). Each of the analyses and models that are related to the Process Model Report will be documented in accordance with AP-3.10Q Analyses and Models. This documentation will be summarized in the Process Model Report, but will not be physically part of the report. The Process Model Report itself will be developed using procedure AP-3.11Q, Technical Reports.

In developing this Process Model Report, and the supporting analyses and models, the subject matter

WBS Planning Sheet																			
Date:																			
Revision:																			
Element	1.2.21.3.1	Title:	Integrated Site Process Model Report																
SubProduct	1.2.21.3	Title:	Suitability Criteria Compliance Evaluation																
Product	1.2.21	Title:	Site Recommendation (SR)																
Element Team Leader (DOE)	TYNAN M	Element Manager	LUGO M																
SubProduct Team Leader (DOE)	SULLIVAN T	SubProduct Manager	HANSON G																
Product Manager (DOE)	BROCOUM S	Product Manager	KING J																
Deliverables (continued)																			
ID	Title/Description/Acceptance Criteria		Due Date																
SLP58CM3	Submit ISM PMR Rev 00		29-OCT-1999																
<table border="1"> <thead> <tr> <th colspan="4">Description (continued)</th> </tr> </thead> <tbody> <tr> <td colspan="4">experts will be cognizant of existing documentation (internal and external) that is related to the process model to ensure that the depth and breadth of the available technical information has been adequately considered.</td> </tr> <tr> <th colspan="4">Evaluation Criteria</th> </tr> <tr> <td colspan="4"> <p>1) The technical content of the PMR meets the requirements identified in the scope of work definition and is complete, clearly written, defensible, and traceable to the supporting AMRs so that independent reviewers can understand and verify how data sets were used in AMRs, PMRs and the abstractions that support TSPA-SR.</p> <p>2) The qualification status of at least 50% of those data used as input to the PMR and its supporting AMRs will be verified (i.e., their Q status will have been determined). These data inputs will be identified in the Document Input Reference Sheets (DIRS) for the PMR and AMRs. At least 40% of those data needed to be qualified and used as input to the PMR and its supporting AMRs will be qualified. The PMR will be reviewed and evaluated to verify that, for the technical data (as defined in AP-SIII.3Q) in the deliverable:</p> <p>a) For data that have completed the verification process, the data cited in the PMR and supporting AMRs are labeled or referenced as qualified, accepted, or unqualified in accordance with the AP-SIII.3Q, AP-3.15Q, and AP-SIII.2Q. Unqualified data supporting the postclosure safety case requiring qualification will be identified or referenced</p> <p>b) Priority in the verification/qualification process has been given to data that supports the safety case, as identified in the Repository Safety Strategy Rev. 3. It is anticipated that some data sets will be determined to be unqualified and the PMR may identify results of analyses supporting the postclosure safety case that utilize, in whole or in part, unqualified data</p> <p>c) Within the PMR or a cover letter provide a complete list of DTNs and Q-status for data, analyses, model input and output, and software used directly in the PMR and in the supporting AMRs or other supporting analyses.</p> <p>Using an approach that was documented in qualification plans per AP-SIII.2Q, developed inputs and selected acquired data are being prepared for the ISM PMR. This will establish the basis for this model to provide qualified inputs to other process models.</p> <p>3) At least 40% of software code used in development and/or control of resulting models or manipulation of data presented in the PMR, supporting AMRs, and other supporting analyses will be qualified and maintained in accordance with AP-SI.1Q controlled by the M&O. For software that is not qualified, the qualification status is identified or referenced. A listing of the location of software and status for the PMR and supporting AMRs and other supporting analyses will be provided in the PMR or as a cover letter. All PMRs will be reviewed and evaluated to verify that:</p> <p>a) The software codes used in development of models that are documented in the deliverable have been assigned a unique identifier and are maintained in accordance with AP-SI.1Q</p> <p>b) The software codes used to develop or manipulate the data presented in the deliverable have been assigned a unique identifier and are maintained in accordance with AP-SI.1Q</p> <p>c) The software code is retrievable and usable, and the results reported in the deliverable are reproducible.</p> <p>4) At least 40% of the models used in the development of the PMR and supporting AMRs will be validated and maintained in accordance with AP-3.10Q and AP-3.15Q. For models that are not validated, the validation status is identified or referenced.</p> </td> </tr> </tbody> </table>				Description (continued)				experts will be cognizant of existing documentation (internal and external) that is related to the process model to ensure that the depth and breadth of the available technical information has been adequately considered.				Evaluation Criteria				<p>1) The technical content of the PMR meets the requirements identified in the scope of work definition and is complete, clearly written, defensible, and traceable to the supporting AMRs so that independent reviewers can understand and verify how data sets were used in AMRs, PMRs and the abstractions that support TSPA-SR.</p> <p>2) The qualification status of at least 50% of those data used as input to the PMR and its supporting AMRs will be verified (i.e., their Q status will have been determined). These data inputs will be identified in the Document Input Reference Sheets (DIRS) for the PMR and AMRs. At least 40% of those data needed to be qualified and used as input to the PMR and its supporting AMRs will be qualified. The PMR will be reviewed and evaluated to verify that, for the technical data (as defined in AP-SIII.3Q) in the deliverable:</p> <p>a) For data that have completed the verification process, the data cited in the PMR and supporting AMRs are labeled or referenced as qualified, accepted, or unqualified in accordance with the AP-SIII.3Q, AP-3.15Q, and AP-SIII.2Q. Unqualified data supporting the postclosure safety case requiring qualification will be identified or referenced</p> <p>b) Priority in the verification/qualification process has been given to data that supports the safety case, as identified in the Repository Safety Strategy Rev. 3. It is anticipated that some data sets will be determined to be unqualified and the PMR may identify results of analyses supporting the postclosure safety case that utilize, in whole or in part, unqualified data</p> <p>c) Within the PMR or a cover letter provide a complete list of DTNs and Q-status for data, analyses, model input and output, and software used directly in the PMR and in the supporting AMRs or other supporting analyses.</p> <p>Using an approach that was documented in qualification plans per AP-SIII.2Q, developed inputs and selected acquired data are being prepared for the ISM PMR. This will establish the basis for this model to provide qualified inputs to other process models.</p> <p>3) At least 40% of software code used in development and/or control of resulting models or manipulation of data presented in the PMR, supporting AMRs, and other supporting analyses will be qualified and maintained in accordance with AP-SI.1Q controlled by the M&O. For software that is not qualified, the qualification status is identified or referenced. A listing of the location of software and status for the PMR and supporting AMRs and other supporting analyses will be provided in the PMR or as a cover letter. All PMRs will be reviewed and evaluated to verify that:</p> <p>a) The software codes used in development of models that are documented in the deliverable have been assigned a unique identifier and are maintained in accordance with AP-SI.1Q</p> <p>b) The software codes used to develop or manipulate the data presented in the deliverable have been assigned a unique identifier and are maintained in accordance with AP-SI.1Q</p> <p>c) The software code is retrievable and usable, and the results reported in the deliverable are reproducible.</p> <p>4) At least 40% of the models used in the development of the PMR and supporting AMRs will be validated and maintained in accordance with AP-3.10Q and AP-3.15Q. For models that are not validated, the validation status is identified or referenced.</p>			
Description (continued)																			
experts will be cognizant of existing documentation (internal and external) that is related to the process model to ensure that the depth and breadth of the available technical information has been adequately considered.																			
Evaluation Criteria																			
<p>1) The technical content of the PMR meets the requirements identified in the scope of work definition and is complete, clearly written, defensible, and traceable to the supporting AMRs so that independent reviewers can understand and verify how data sets were used in AMRs, PMRs and the abstractions that support TSPA-SR.</p> <p>2) The qualification status of at least 50% of those data used as input to the PMR and its supporting AMRs will be verified (i.e., their Q status will have been determined). These data inputs will be identified in the Document Input Reference Sheets (DIRS) for the PMR and AMRs. At least 40% of those data needed to be qualified and used as input to the PMR and its supporting AMRs will be qualified. The PMR will be reviewed and evaluated to verify that, for the technical data (as defined in AP-SIII.3Q) in the deliverable:</p> <p>a) For data that have completed the verification process, the data cited in the PMR and supporting AMRs are labeled or referenced as qualified, accepted, or unqualified in accordance with the AP-SIII.3Q, AP-3.15Q, and AP-SIII.2Q. Unqualified data supporting the postclosure safety case requiring qualification will be identified or referenced</p> <p>b) Priority in the verification/qualification process has been given to data that supports the safety case, as identified in the Repository Safety Strategy Rev. 3. It is anticipated that some data sets will be determined to be unqualified and the PMR may identify results of analyses supporting the postclosure safety case that utilize, in whole or in part, unqualified data</p> <p>c) Within the PMR or a cover letter provide a complete list of DTNs and Q-status for data, analyses, model input and output, and software used directly in the PMR and in the supporting AMRs or other supporting analyses.</p> <p>Using an approach that was documented in qualification plans per AP-SIII.2Q, developed inputs and selected acquired data are being prepared for the ISM PMR. This will establish the basis for this model to provide qualified inputs to other process models.</p> <p>3) At least 40% of software code used in development and/or control of resulting models or manipulation of data presented in the PMR, supporting AMRs, and other supporting analyses will be qualified and maintained in accordance with AP-SI.1Q controlled by the M&O. For software that is not qualified, the qualification status is identified or referenced. A listing of the location of software and status for the PMR and supporting AMRs and other supporting analyses will be provided in the PMR or as a cover letter. All PMRs will be reviewed and evaluated to verify that:</p> <p>a) The software codes used in development of models that are documented in the deliverable have been assigned a unique identifier and are maintained in accordance with AP-SI.1Q</p> <p>b) The software codes used to develop or manipulate the data presented in the deliverable have been assigned a unique identifier and are maintained in accordance with AP-SI.1Q</p> <p>c) The software code is retrievable and usable, and the results reported in the deliverable are reproducible.</p> <p>4) At least 40% of the models used in the development of the PMR and supporting AMRs will be validated and maintained in accordance with AP-3.10Q and AP-3.15Q. For models that are not validated, the validation status is identified or referenced.</p>																			

Date:		WBS Planning Sheet	
Revision:			
Element	1.2.21.3.1	Title:	Integrated Site Process Model Report
SubProduct	1.2.21.3	Title:	Suitability Criteria Compliance Evaluation
Product	1.2.21	Title:	Site Recommendation (SR)
Element Team Leader (DOE)	TYNAN M	Element Manager	LUGO M
SubProduct Team Leader (DOE)	SULLIVAN T	SubProduct Manager	HANSON G
Product Manager (DOE)	BROCOUM S	Product Manager	KING J

Deliverables (continued)

ID	Title/Description/Acceptance Criteria	Due Date
SLP58CM3	Submit ISM PMR Rev 00	29-OCT-1999

Evaluation Criteria (continued)

5) Documentation of the following is provided:

- a) the user-defined input parameters (parameter values) that are used to run the codes/software that are used to support TSPA-SR
- b) the actual numerical value/distribution used for each parameter and the rationale for its selection
- c) the source(s) for each parameter value and any intermediate calculations/data manipulations used to determine the parameter value.
- 6) Alternate conceptual models and alternate interpretations of the available data are documented.
- 7) A discussion of relevant analog information is included and documented.


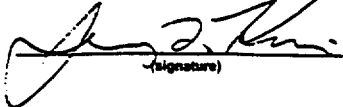
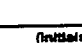

8) All assumptions and their bases are identified and justified.

9) PMR development must fully address appropriate regulatory requirements and commitments. The PMR will include the following features:

- a) Common graphics: The graphics will be consistent and, where possible, identical in order to facilitate integration among the analyses and models supporting the PMR. The graphics will be clear and accurate, and reflect the accompanying text descriptions
- b) Readability: The text will be clear, simple and concise. Avoid the use of technical jargon and acronyms whenever possible and in line with the need for the SR and LA presentation needs
- c) Full M&O Management Review: The final document submitted for DOE review and acceptance shall have received a full M&O management review
- d) Project generated data cited in deliverable in the format of graphics, tables, figures, parameter values, and maps must include the Data Tracking Number for the cited data. DTNs cited in the body of the text should be included in the reference section of the document. The data cited by DTN must be resident in the TDMS. Data or information from other sources must have appropriate Technical Information Management System identifiers (e.g. TIC or RIS number) and be accessible through the TIMS.

Completion Criteria:

This deliverable is complete when it is submitted to the DOE in accordance with YAP-30.63, Submittal, Review, and Acceptance of Deliverables.

 (initials)	SubProduct Manager HANSON G	 (signature)	Product Manager KING J
 (initials)	SubProduct Team Leader (DOE) SULLIVAN T	 (signature)	Product Manager (DOE) BROCOUM S